CHEMISTRY OF ACYL NITRENES IN THE SYNTHESIS OF CARBAMATES AND COMPLEX HETEROCYCLES

By

Cephas Ofoe Afeke

Submitted in Partial Fulfillment of the Requirements

for the Degree of

Master of Science

in the

Chemistry Program

YOUNGSTOWN STATE UNIVERSITY

August 2015

CHEMISTRY OF ACYL NITRENES IN THE SYNTHESIS OF CARBAMATES AND COMPLEX HETEROCYCLES

Cephas Ofoe Afeke

I hereby release this dissertation to the public. I understand that this dissertation will be housed at the Circulation Desk of the University library and will be available for public access. I also authorize the University or other individuals to make copies of this dissertation as needed for scholarly research.

Signature:

_____

Cephas Ofoe Afeke Date

Approvals:

_____

Dr. Peter Norris Date
Thesis Advisor

_____

Dr. John A. Jackson Date
Committee Member

_____

Dr. Sherri Lovelace-Cameron Date
Committee Member

_____

Dr. Sal Sanders Date
Dean of Graduate Studies and Research

Abstract

The synthesis of carbamates via Curtius rearrangement utilizing aryl acyl azides together with a wide range of alcohol-containing complex organic molecules was explored through the use of heat. Additionally, the intramolecular insertion of oxycarbonyl nitrenes generated from thermally decomposed azidoformates was studied with several high and low boiling solvents to observe behavior. The insertion of these thermally generated nitrenes into the solvents used may serve as a new way of functionalizing some stable organic compounds and solvents that may originally appear inert in many reaction systems.

Acknowledgements

I wish to acknowledge the graduate school and express my profound gratitude for the opportunity and funding towards my education over the last two years. I would also like to thank the chemistry department for accepting me into this program as someone coming from outside the United States and for providing excellent research instrumentation facilities for my work.

I would like to thank Dr. Norris for providing interesting research projects and for being a mentor over the years, directing me on what and what not to do, allowing me to hunger for academic success. Many thanks to Dr. Jackson for his mentorship in my teaching and research assignments as well as Dr. Genna for his reviews on presentation skills. I would also like to thank Dr. Howard Mettee for showing belief in me and writing a letter of recommendation for me in that regard, and also Dr. Lovelace-Cameron for her availability and willingness to help whenever approached. I also acknowledge Dr. Zeller for the immense role he has played in my research especially with the identification of new compounds unexpectedly synthesized.

Many thanks to my colleagues with whom I worked in the Norris Group, those who have long moved on to other endeavors, those who are moving on currently and those who have yet to complete their studies.

Finally I wish to God for setting me on this journey, and also my family both home and abroad especially my wife Gloria for the tremendous support and love throughout these years.

Table of Contents

List of Figures

CHEMISTRY OF ACYL NITRENES IN THE SYNTHESIS OF CARBAMATES AND COMPLEX HETEROCYCLES

Introduction

The element nitrogen is essential to life. Considerable attention is thus paid to the development of synthetic methods for its introduction into molecules. Nitrenes, long regarded as highly reactive but poorly selective species, have recently emerged as useful tools for the formation of C-N bonds.[1] Nitrenes belong to a class of organic compounds containing neutral, monovalent nitrogen atoms, while most stable compounds of neutral nitrogen have a valence of three. Thus, most nitrenes, including acyl nitrenes, are very reactive and short-lived reaction intermediates.[2] Research attempts at understanding nitrogen-containing compounds and the development of anti-bacterial agents from these natural products have generated interest in the application of acyl nitrenes in the synthesis of complex carbamates and nitrogen-containing heterocycles which can then be used to synthesize many forms of anti-bacterial agents. [3][4]

Most prominent amongst acyl nitrene precursors are acyl azides.[5] Acyl azides undergo either thermolysis or photolysis to produce highly reactive and unstable acyl nitrene intermediates.[6] These nitrene intermediates from the decomposition of the acyl azides cannot be isolated due to their unstable nature and thus in the absence of "trappers" tend to undergo a concerted Curtius rearrangement to form isocyanates as shown below in **Equation 1**.[7] Isocyanates are also very important intermediates in organic synthesis and are mostly used in accessing carbamates and other polymers of urethane. [6][7]

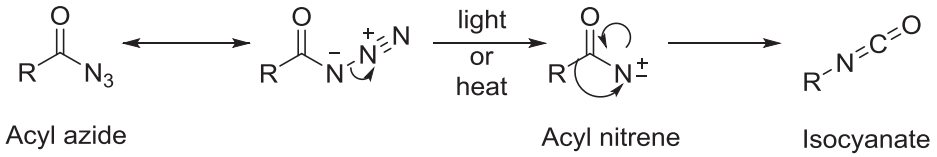

Equation 1: Thermal decomposition of acyl azides into isocyanate intermediates.

Generic Properties and Reactivity of Nitrenes

Many useful reactions are believed to proceed via nitrene intermediates, and the relationship between the spin states of these nitrene intermediates in addition to their reactivity pattern present very interesting problems.[8-10] Yamada and Terashima[10] reported that the oxycarbonyl nitrene II (**Equation 2**), generated from the azidoformate I via thermolysis or photolysis, inserted exclusively at the intramolecular aliphatic C-H bond in its singlet state to yield the oxazolidinone IV through the transition state III with 100% retention of configuration.

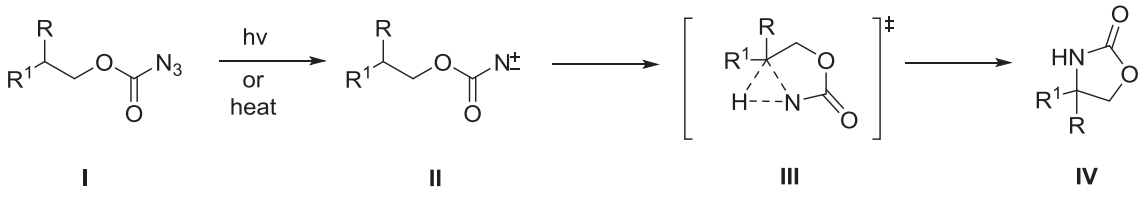

Equation 2: Decomposition of carboxycarbonyl nitrenes.

Lwowski had earlier demonstrated this phenomenon.[5] However, Anastassiou and Fargher *et al*. have individually posited that nitrene species, which are formed from

thermal and photochemical decomposition of phenyl and cyanogen azides, also insert at aliphatic C-H positions in both their singlet and triplet state.[11-12]

Nitrenes have a relatively short lifetime (only several microseconds) and undergo stabilization by the following reactions; isomerization to imines, dimerization to azo compounds, hydrogen abstraction followed by ring-closure to heterocyclic compounds, bimolecular insertion into C-H bonds to secondary amines, addition to solvent yielding ylids, and addition to unsaturated systems yielding heterocyclic compounds.[2][3] In other words in addition to the concerted Curtius rearrangement to yield isocyanate intermediates, molecular acyl nitrenes are capable of being trapped in other molecules present in the reaction environment. These insertion processes are most often applied in cyclization reactions for the synthesis of heterocycles.

It is a commonly accepted view, presented in many reviews, [7] that the addition to olefins and the insertion into the C-H, O-H, and N-H bonds are typical reactions of singlet nitrenes. However, characteristic products of the bimolecular addition and insertion reactions have been almost exclusively isolated for acyl nitrenes and perfluoro-substituted aryl nitrenes as well.[6] Yamada and co-workers determined the spin state of acyl nitrenes to be the singlet state by subjecting an acyl azide species to photochemical decomposition for which they observed intramolecular aliphatic C-H insertion with 98% retention in stereochemistry. Although thermolysis of aryl and alkyl acyl azides proceed via nitrene (Curtius) rearrangement to isocyanate intermediates, as opposed to photolysis generating the nitrenes and leading to insertion reactions exclusively.[13] Alkoxycarbonyl nitrenes are known to not undergo any form of rearrangement and hence do not form

species resembling isocyanates making them perfect precursors for insertion under both thermal and photolytic conditions.[14-17]

Previous Applications of Nitrene Chemistry

Some pioneering applications of acyl nitrenes in synthesis involve the trapping of isocyanates through the Curtius rearrangement to synthesize amine derivatives. Migawa and Swayze[18] reported an efficient method for trapping isocyanates, generated from the Curtius rearrangement, with resin-bound amines (**Equation 3**). A commercially available carboxylic acid was treated with diphenylphosphoryl azide, followed by thermal rearrangement, cooling, and trapping in one pot. Cleavage from the resin gave an *N,N*-disubstituted urea in excellent purity.

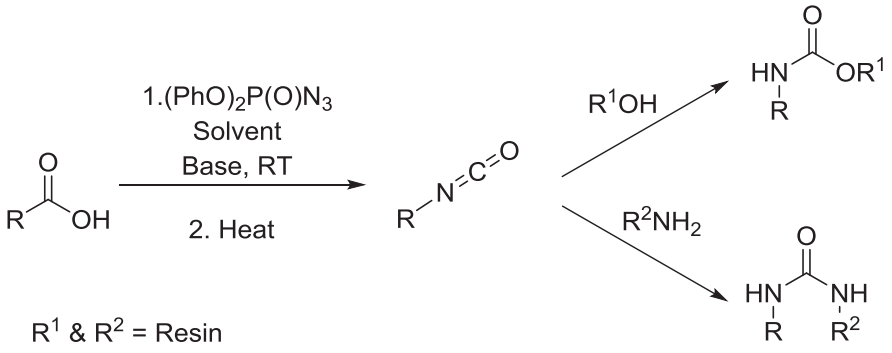

Equation 3: Trapping of isocyanates with resin-bound alcohols and amines.

Lebel and Leogane[19] described a one-pot synthetic approach in which the reaction of a carboxylic acid with di-*tert*-butyl dicarbonate and sodium azide allowed the formation of an acyl azide intermediate, which underwent a Curtius rearrangement in the presence of tetra-*n*-butyl ammonium bromide and zinc(II) triflate (**Equation 4**). The

trapping of the isocyanate derivative in the reaction mixture led to the desired *tert*-butyl carbamate product in high yields at low temperature. These reaction conditions were compatible with a variety of substrates, including malonate derivatives, which provide access to protected amino acids.

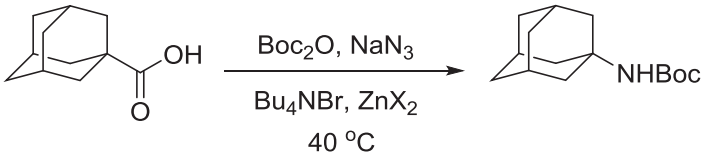

Equation 4: Synthesis of Boc-protected amine from carboxylic acid via Curtius rearrangement.

A simple and convenient approach for the synthesis of asymmetric urea derivatives which contain other functional groups has also been reported by Groszek.[20] The approach involved the Curtius rearrangement of derivatives of aromatic acyl azides via acyl nitrene and the reaction of the resultant aromatic isocyanate with an amine to access high yields of urea compounds (**Equation 5**).

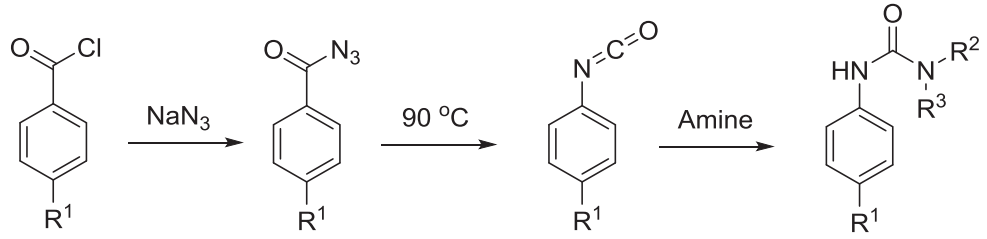

Equation 5: Synthesis of asymmetric urea derivatives.

In addition to synthetic applications of acyl nitrenes via the Curtius rearrangement, many researchers have also studied insertion reactions of acyl nitrenes to synthesize some amine derivatives and heterocycles. Brown *et al*. [21] reported a synthetic

addition of acyl nitrenes to olefinic double bonds. For example, photolysis of cycloheptene-5-carbonyl azide, *endo*-norbornene-5-carbonyl azide (**Equation 6**) and *o*-vinylbenzoyl azide gave very reactive acyl aziridines by internal addition of acyl nitrenes to the olefinic double bonds. Derivatives of 6-azabicyclo-[3,2,2]nonane and 1,2-dihydroisoindol-1-one were prepared. *cis*-2-Vinyl cyclopropyl isocyanate prepared photochemically at -78 ^{o}C, underwent Cope rearrangement at room temperature to yield 2,3-dihydro-1H-azepin-2-one.

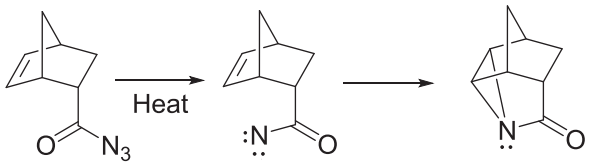

Equation 6: Acyl nitrene addition to olefinic double bond to form a heterocycle.

Wright, Albarella and Lee, as part of their study of acyl nitrene cyclizations in antibiotics synthesis, also applied the insertion reactions of acyl nitrenes to functionalize the branched-chain sugar moiety, garosamine, a component of the antibiotic gentamicin C_2.[22] Contrary to expectations based on intermolecular reactions in simple systems, insertion into the branched-chain methyl group was found to be competitive with insertion into the neighboring methylene group. They also developed successfully a synthetic methodology for the insertion of acyl nitrenes into carbamates using metal catalysts. **Equation 7** illustrates the nature of some of the internal acyl nitrene addition reactions involved.

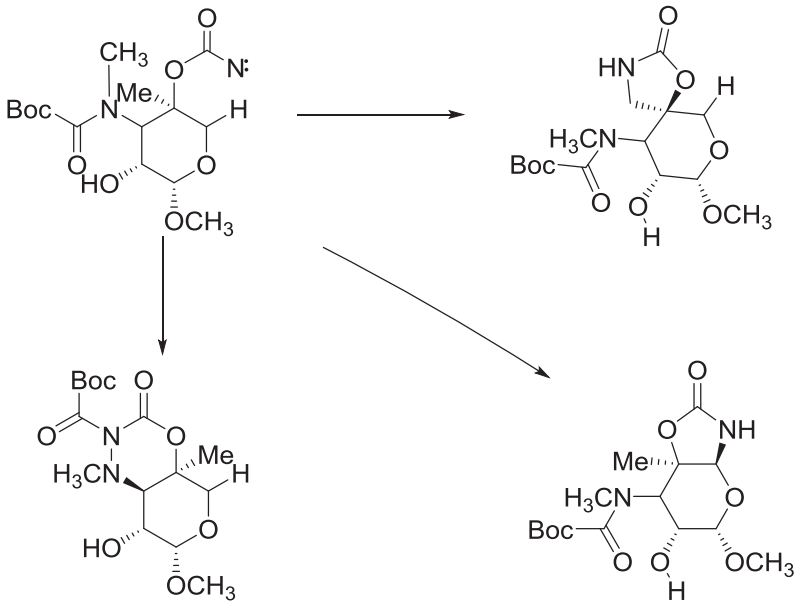

Equation 7: Intramolecular acyl nitrene insertion reactions.

In their efforts to demonstrate the stereo-controlled preparation of complex amino acid derivatives, Williams *et al* showed that acyl nitrenes undergo facile C=C insertions with vinylic ethers (**Equation 8**).[23] Reactions exhibited high diastereofacial selectivity, based upon steric considerations, affording 2,5-dialkoxyoxazolines. Mild hydrolysis of these heterocycles reveals an aldehydic function for further chemical elaboration.

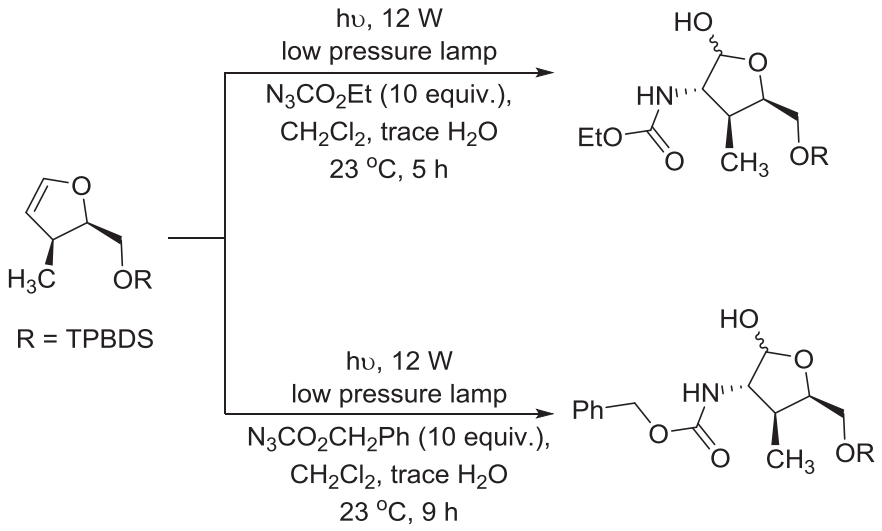

Equation 8: Addition of acyl azide to vinyl ether.

While all of these previous applications prove the efficacy of acyl azides and nitrenes in the synthesis of heterocycles and amide derivatives from many organic molecules, not much work has been done in the application of acyl nitrene chemistry on complex sugars and other complex naturally occurring organic molecules, which could yield complex heterocycles and carbamates that have potential industrial and pharmaceutical applications. Complex organic molecules that contain free -OH groups not only react with isocyanates from the decomposition of acyl azides to form complex carbamates, they also undergo insertion reactions via the highly reactive yet short-lived nitrene intermediates, as earlier shown by Wright *et al* and also by Feuer and Smolinsky.[22][24]

As part of a wider research project being undertaken by the Norris Research Group in the area of carbohydrate and heterocyclic chemistry, this thesis will focus on the synthesis of complex organic molecules (carbamates) and heterocycles. We intend in this

research to go classical by exploring further syntheses of acyl azides and heating these azides up in the presence of nucleophiles which would trap the isocyanates formed via Curtius rearrangement to give carbamates. This approach provides a much more environmentally friendly and less-expensive alternative to the synthesis of carbamates. Berndt [26] in his master's thesis described a procedure where he was able to achieve intramolecular nitrene insertion by use of tetrachloroethane as solvent. Because of the toxic nature of tetrachloroethane we propose in this research to use more benign conditions including solvents that are less toxic and easier to handle. The first part of this research shall involve the syntheses of a wide range of carbamates from the reaction of *meta*- and *para*-substituted nitrobenzoyl azide species with large carbohydrate molecules and some complex organic compounds via the Curtius rearrangement as illustrated in the equation below.

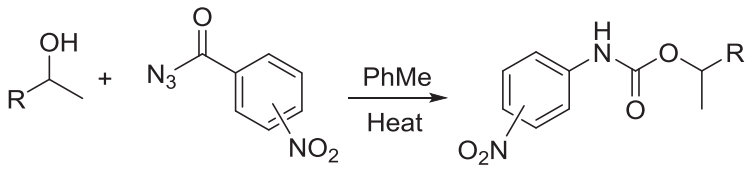

Equation 9: Reaction of aryl acyl azides with free OH containing complex organic molecules.

The research will also involve the synthesis and purification of the aryl acyl azides to be used from their respective acyl chloride precursors at room temperature with NaN_3 in acetone and water (Equation 10).

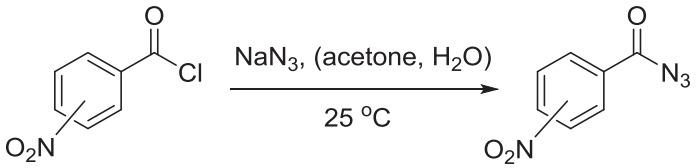

Equation 10: Synthesis of nitro-substituted benzoyl azides.

The second part of this thesis shall delve into the synthesis of cyclic carbamates also known as oxazolidinones, chiral derivative forms of which have been known for asymmetric synthesis and formation of C-C bonds.[25] The synthesis of the heterocyclic carbamates will employ single free hydroxyl-containing organic molecules in the formation of subsequent chloroformates by reaction with triphosgene. The chloroformates will then be converted to azidoformates via reaction with NaN_3.

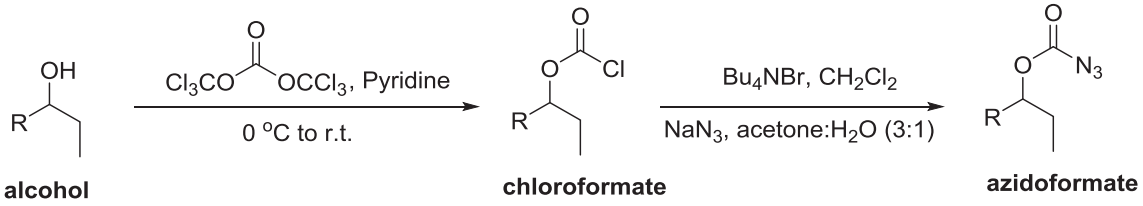

Equation 11: Conversion of alcohol to azidoformate.

The azidoformate is expected to undergo photolysis or thermolysis in a high boiling solvent to yield short-lived singlet nitrenes which will quickly participate in an intramolecular aliphatic C-H insertion to form the oxazolidinone.

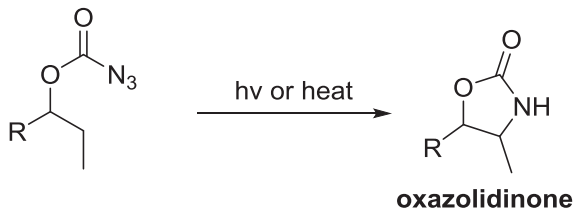

Equation 12: Decomposition of azidoformate to oxazolidinone.

Statement of Problem

Acyl nitrene chemistry on sugars and complex organic molecules will be studied. Previously described synthetic methods for the generation of carbamates will be further investigated using carbohydrate and other complex organic molecules and aryl acyl azides without the use of metal catalysts. Special attention will be paid to variables such as solvents used, equivalent of reagents, heating times, temperature and azide and nucleophile sources. The second part of this research shall involve the study of intramolecular acyl nitrene insertions into adjacent aliphatic C-H bonds on precursor molecules containing single free –OH groups, by converting these molecules with the alcohol functionality to azidoformates and subsequently decomposing them in a variety of solvents to observe their behavior. Attention would be given to reaction times, reaction temperature, solvents used and percentage yield achieved.

Results and Discussion

Project 1

The first part of the research was begun with the synthesis of the azide precursors that would be used in the Curtius rearrangement to yield carbamates. 3-Nitrobenzoyl chloride **(1)** was reacted in acetone and water by pipetting a solution of **1** dissolved in acetone into a round bottom flask containing an excess of sodium azide in water to yield 3-nitrobenzoyl azide **(3)** (**Equation 13**). Pipetting the chloride **(1)** into the reaction mixture was done very slowly to achieve maximum yield as it was observed that pipetting the mixture too quickly into the flask led to prolonged reaction time with very low yields. Room temperature conditions were also observed for this kind of transformation and were applied.

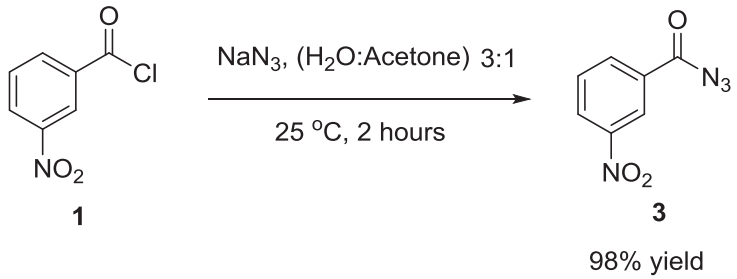

Equation 13: Synthesis of 3-nitrobenzoyl azide **(3)**.

Analysis of spectroscopic data from NMR and IR instruments confirmed the product formed. ^{1}H NMR signals at 7.96 ppm (doublet of doublets), 8.36 ppm (doublet), 8.47 ppm (doublet) and a singlet peak at 8.85 ppm all represent the protons on the

aromatic ring. A look at the ^{13}C NMR spectrum for the product also reveals a slight downward shift at 170.57 ppm representing the chemical shift for the carbonyl group. Six additional signals were found to represent the chemical shift for the aromatic carbons at 124.37 ppm, 128.49 ppm, 129.98 ppm, 132.33 ppm, 134.85 ppm and 148.45ppm. A look at the IR spectrum for the product **(3)** reveals a peak at 2144 cm^{-1} representing the azide functionality and the carbonyl peak at 1706 cm^{-1} in addition to C-H stretching frequency at 2996 cm^{-1}. The azide **(3)** was also found to have a melting point of 55 – 57 ^{o}C.

To synthesize the second precursory azide, 4-nitrobenzoyl azide **(4)**, the procedure from the synthesis of **3** was followed to the letter by reacting 4-nitrobenzoyl chloride **(2)** with sodium azide using acetone and water as solvents in the fashion earlier described (**Equation 14**).

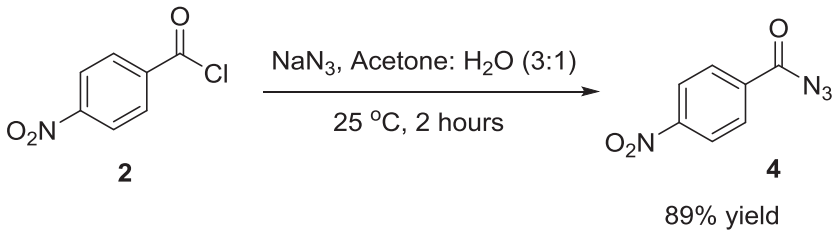

Equation 14: Synthesis of 4-nitrobenzoyl azide **(4)**.

Both NMR and IR spectroscopy were used to confirm the identity of the product. A look at the ^{1}H NMR spectrum reveals two separate doublet signals at 8.21 ppm and 8.30 ppm with both doublet signals having coupling constants (*J* value) of 9.0 Hz. These are the protons found on the aromatic ring. The ^{13}C NMR spectrum gave the expected

five signals with peaks at 123.80 ppm, 130.54 ppm, 135.70 ppm and 151.27 ppm representing the chemical shifts for the aromatic ring carbons. The carbonyl peak was found at 170.84 ppm as expected in addition to IR spectrum peaks at 2138 cm^{-1} representing the azide functionality and the peak at 1702 cm^{-1} representing the carbonyl functional group. C-H stretching frequency at 2974 cm^{-1} was duly observed as well and the azide **4** was found to have a melting point of 60 – 63 ^{o}C in excellent yield.

After synthesizing the precursor azides, we then proceeded with the synthesis of 2,2-dimethyl-5-oxohexahydrofuro-2,3:4,5-furo-2,3-D-1,3-dioxol-6-yl-3-nitrophenyl carbamate **(6)** by reacting D-glucurono-6,3-lactone acetonide **(5)** with **3** in the Curtius fashion at about 90 ^{o}C for six hours (**Equation 15**).

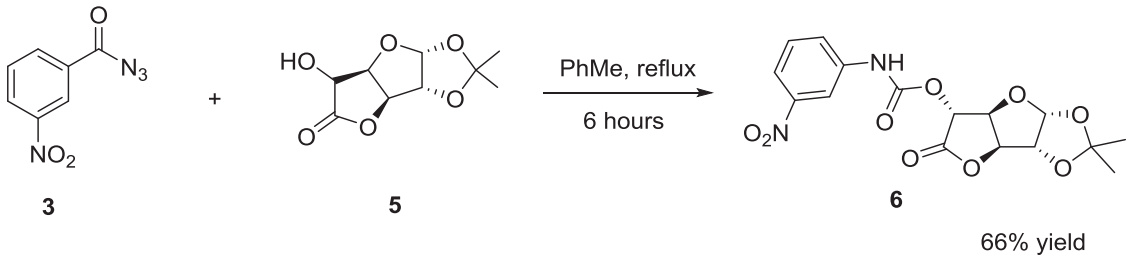

Equation 15: Synthesis of Carbamate **(6)**.

Both ^{1}H and ^{13}C NMR spectra provided enough basis to conclude that carbamate **6** has been synthesized in excellent yield. In all, twelve signals were expected in the ^{1}H NMR spectrum of the product **6** and all twelve were observed. The diagnostic peak at 7.22 ppm represents the N-H proton in addition to the doublet of doublet signal at 7.50 ppm with *J* value of 8.2 Hz which also represents the only proton in the *meta*-position on

the aromatic ring of **6**. The singlet peaks observed at 1.36 ppm and 1.53 ppm integrating to three protons at each signal represent the methyl protons of the sugar moiety. A look at the ^{13}C NMR also reveals chemical shifts for the two carbonyl carbons at 151.20 ppm (carbonyl carbon of the sugar part of the molecule) and 169.39 ppm representing the carbonyl carbon of the carbamate functionality. It is worth noting that performing this reaction in toluene yielded an initial amorphous compound which had to be washed with large quantities of hexane in order to obtain crude crystals via suction filtration. The melting point of carbamate **6** was found to be in the region of 174 – 176 ^{o}C in addition to it being stable on the bench for more than 125 days.

We proceeded in a similar fashion to synthesize the *para*-nitro analogue of the carbamate. In the synthesis of 2,2-dimethyl-5-oxohexahydrofuro-2,3:4,5-furo-2,3-D-1,3-dioxol-6-yl-4-nitrophenyl carbamate **(7)**, **4** was added once again in the Curtius fashion to **5** under reflux conditions in dry toluene and the reaction proceeded for 4 hours (**Equation 16**). Once again the amorphous product was washed with large quantities of hexane to yield yellow crystals which were later purified via recrystallization in hot ethanol.

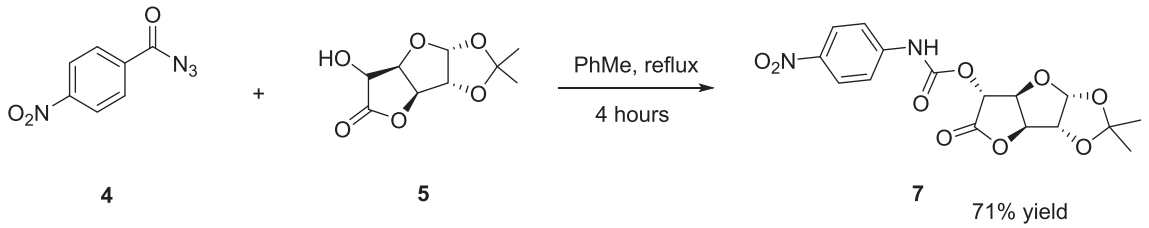

Equation 16: Synthesis of Carbamate **(7)**.

A look at the ^{1}H NMR spectrum of **7** showed chemical shifts at 1.36 ppm and 1.53 ppm representing the methyl protons of the sugar moiety as well as two doublet signals at 7.55 ppm and 8.2 ppm (both having *J* values of 9.2 Hz) representing the chemical shift for the protons on the aromatic ring. The N-H proton signal was found as a slightly broad singlet peak at 7.37 ppm confirming the formation of **7** in good yield. In the ^{13}C NMR spectrum, the chemical shifts at 150.90 ppm as well as 169.32 ppm also confirm the presence of two carbonyl groups on the final molecule **7** which has a melting point of 180 – 183 ^{o}C.

The nucleophilic substrates were then varied with both **3** and **4** to expand the scope of carbamate synthesis via the Curtius rearrangement. The next substrate to be used after **5** was 1,2:5,6-di-*O*-isopropylidene-α-D-glucofuranose **(8)** together with **4** to synthesize 5-(2,2-dimethyl-1,3-dioxolan-4-yl)-2,2-dimethyltetrahydrofuro[2,3-D][1,3]dioxol-6-yl-(4-nitrophenyl) carbamate **(9)** (**Equation 17**). When **4** and **8** were added together and heated up to 9 hours at about 90 ^{o}C, a deep yellow syrup was isolated after purification via column chromatography. Suffice to say that the problem with previously having an initial amorphous compound washed several times with hexane was not encountered in this reaction. After cooling the reaction mixture to room temperature, only rotary evaporation was needed to isolate the crude product from the reaction matrix before purification. Once again both ^{1}H and ^{13}C NMR were used to determine the identity of the final product.

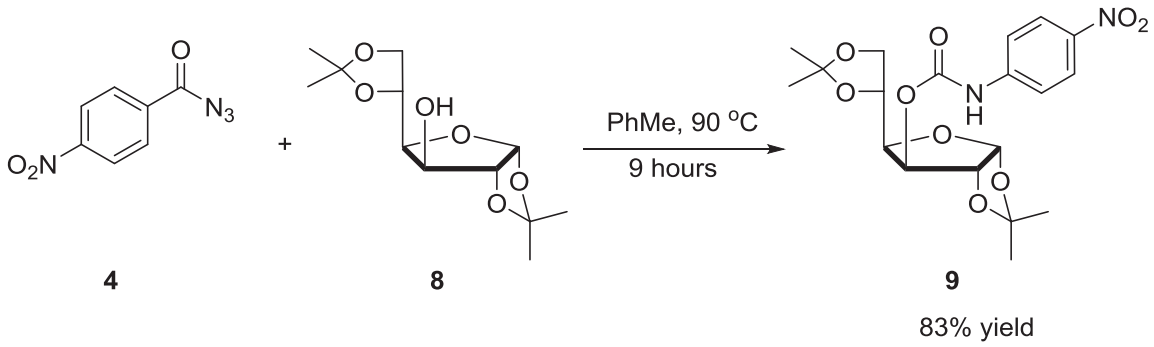

4 **8** **9**

83% yield

Equation 17: Synthesis of Carbamate **(9)**.

In the ^{1}H NMR spectrum, the chemical shift for the N-H proton was found as a singlet peak at 7.83 ppm. The doublets at 7.56 ppm and 8.17 ppm represent the aromatic ring protons with each doublet peak having a coupling constant of 9.2 Hz. Another symptomatic set of signals confirming the coupling of **4** and **8** in the fashion described above are the methyl proton chemical shifts. At 1.33 ppm, a singlet peak integrating to 6 protons confirm the presence of two methyl groups on the sugar moiety in addition to singlet peaks at 1.45 ppm and 1.55 ppm representing the other two methyl groups. All the methyl groups stand out as singlets because they have no coupling partners as suggested by the final structure of **9**. A look at the ^{13}C NMR spectrum for **9** also confirms the presence of carbonyl functionality with the chemical shift at 151.45 ppm representing that functional group. Also, a total of 16 signals were duly observed as suggested by the structure of the compound **9**.

Next was the synthesis of 5-(2,2-dimethyl-1,3-dioxolan-4-yl)-2,2-dimethyltetrahydro-furo-[2,3-D][1,3]dioxol-6-yl-(3-nitrophenyl) carbamate **(10)** from 3-nitrobenzoyl azide **(3)** and 1,2:5,6-di-*O*-isopropylidene-α-D-glucofuranose **(8)** (**Equation**

18). Excess amount of **3** was added to **8** in toluene and heated up for 12 hours at 90 ^{o}C to yield a fair amount of pale yellow syrup identified as **10**. The synthesis of **10** was found to take place in a slightly slower fashion than **9** and the reason for this is unknown at this point.

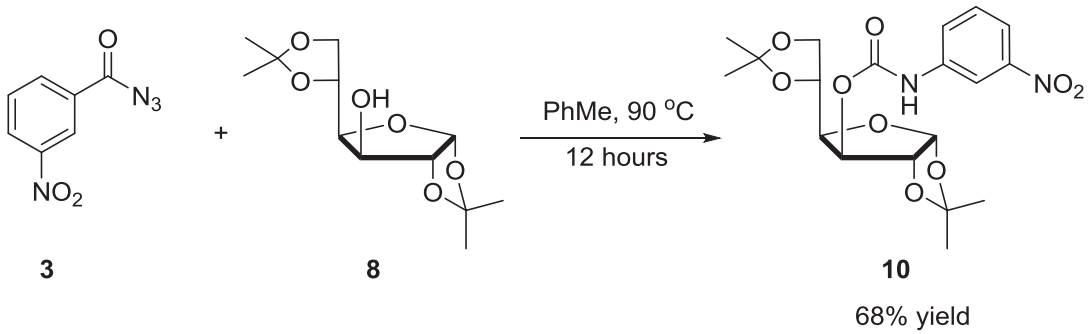

Equation 18: Synthesis of Carbamate **(10)**.

TLC analysis of the product gave a slightly more polar spot than the azide but less than the sugar, which was found in between the R_f of the sugar and the azide. Suffice to say that all the carbamates that were synthesized via the Curtius rearrangement in this thesis had R_f in between the sugar and the azide and upon exposure to UV light, a spot was detected and that spot also burned with the same color as the sugar starting material hence an earlier indication of product formation. After purification of **10**, both ^{1}H and ^{13}C NMR were used to confirm the identity of the product obtained. A look at the proton NMR spectrum revealed four singlet signals at 1.33 ppm, 1.34 ppm, 1.47 ppm and 1.55 ppm all integrating for three protons each representing the methyl protons on the sugar

moiety. The chemical shift for N-H proton was observed at 8.21 ppm in addition to the chemical shifts for the aromatic ring protons at 7.44 ppm (doublet of doublets) with *J* value of 8.2 Hz, a doublet at 7.76 ppm (*J* = 8.1 Hz), another doublet at 7.86 ppm (*J* = 8.2 Hz) and a singlet peak at 8.28 ppm. Analyzing the ^{13}C NMR spectra for the product **10** also confirmed a total of nineteen signals as expected with the chemical shift for the carbonyl carbon peak at 151.95 ppm and the signals for the methyl carbons at 23.26 ppm, 26.15 ppm, 26.71 ppm and 26.88 ppm.

We next embarked on carbamate synthesis using cholesterol **(11)** as the nucleophilic substrate and **3** as the azide counterpart (**Equation 19**). The reaction was carried out overnight in dry toluene at 90 ^{o}C as was done in the previous examples. However, the observation of an amorphous solid product after the reaction was completed and cooled to room temperature was encounted as were in the cases of **6** and **7**. The amorphous solid had to be washed with large amounts of hexane as it became evident that the toluene was locking itself up in the reaction matrix and had to be washed off. Once again success was achieved washing with the hexane and white powdery crude crystals of **12** were obtained in excellent yield for recrystallization.

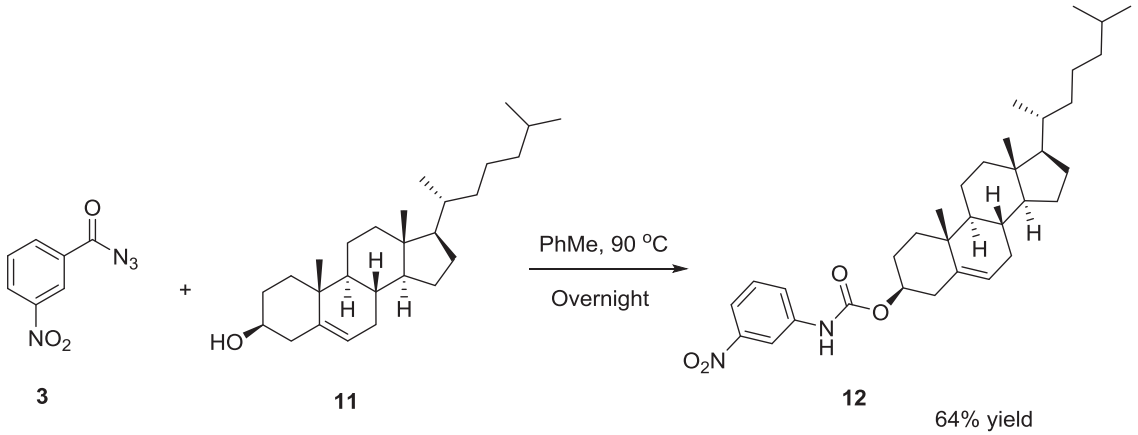

Equation 19: Synthesis of Carbamate **(12)**.

Both ^{1}H and ^{13}C NMR spectra obtained for the product confirmed the identity of the compound as **12**. The series of multiplets ranging from 1.07 ppm to 2.46 ppm represent the methylene protons on the cholesterol moiety as well as singlet peaks at 0.69 ppm integrating to three protons and representing one set of the methyl protons. The N-H signal for the amide proton was noted at 6.80 ppm together with a doublet of doublet signal integrating for the only available *meta*- proton on the aromatic ring at 7.5 ppm with J_1 being equal to J_2 at 8.2 Hz. The other two protons on either *para*- positions to the nitro group on the aromatic ring and the carbonyl group have chemical shifts for doublet peaks each at 7.74 ppm and 7.9 ppm with *J* values at 8.1 Hz and 8.2 Hz respectively. The "land-locked" proton on the aromatic ring with no coupling partner appears at 8.29 ppm as a singlet. The ^{13}C NMR spectrum reveals the carbonyl carbon as having a chemical shift at 152.66 ppm. The aromatic ring carbons have six singlet peaks with chemical shifts between 117.87 ppm and 148.80 ppm in addition to methyl carbon chemical shifts for all the five methyl groups on **12** appearing at 10.12 ppm, 11.86 ppm, 18.72 ppm, 19.31 ppm

and 21.06 ppm. The recrystallized product **12** was also observed to have a melting point of 173 – 180 ^{o}C.

The same nucleophilic substrate **11** was tested with **4** to synthesize the 4-nitro carbamate **13**. Here also the cholesterol **(11)** was added to 4-nitrobenzoyl azide **(4)** and the reaction was heated under reflux overnight, and after cooling to room temperature the crude crystals were separated via suction filtration washing with large amounts of hexane (**Equation 20**). The crude crystals were recrystallised from hot ethanol. This dissolution of product **13** in ethanol takes a longer time and larger quantity of solvent although recrystallization from solution almost immediately occurs when removed from the hot water bath.

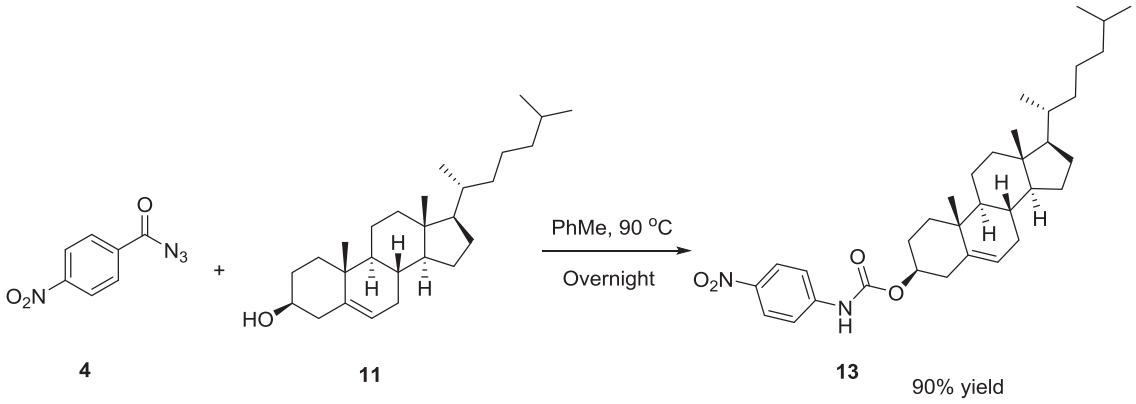

Equation 20: Synthesis of Carbamate **(13)**.

Once again both ^{1}H and ^{13}C NMR spectra confirmed the product **13** in high yield. A look at the ^{1}H NMR spectrum of the product shows a series of multiplet peaks from 1.09 ppm to 5.42 ppm representing the cholesterol part of the carbamate, with the

disappearance of the OH proton signal at 1.62 ppm representing the consumption of **11** and the formation of a new product. The chemical shift for the N-H proton was recorded at 6.87 ppm integrating for one proton hence confirming the N-H group. The protons on the aromatic ring were duly represented by doublet peaks at 7.52 ppm and 8.19 ppm each integrating for two protons with coupling constants of 9.2 Hz in each case. The ^{13}C NMR spectrum showed a chemical shift at 152.45 ppm indicating the presence of a carbonyl group in the product as well as the chemical shifts for the aromatic carbons between 125.22 ppm and 144.05 ppm. The alkene on the cholesterol part of the product also showed ^{13}C NMR shifts at 113.25 ppm and 123.13 ppm confirming the formation of **13**. The IR spectrum for the product also gave further confirmation to the product with peaks at 3429 cm^{-1}, 2950 cm^{-1}, and 1734 cm^{-1} representing the N-H, C-H and C=O functional groups respectively present in the compound **13**. The melting point of the product **13** was also determined to be 187–191 ^{o}C.

The final nucleophilic substrate used in the syntheses of carbamates utilizing **3** and **4** in the Curtius fashion was L-(-)-borneol **(14)**. Upon the reaction of **14** and **4** together in toluene at 90 ^{o}C for about 7 hours, a dense yellow powdery precipitate was observed (**Equation 21**). This precipitate was initially filtered but later proved to be just pigmentation instead of the actual product and hence upon a second try, the crude product was isolated via vacuum evaporation to yield **15 as** a deep yellow syrup which was eventually purified via flash column chromatograpy in a 3:1 hexane - ethyl acetate solvent system.

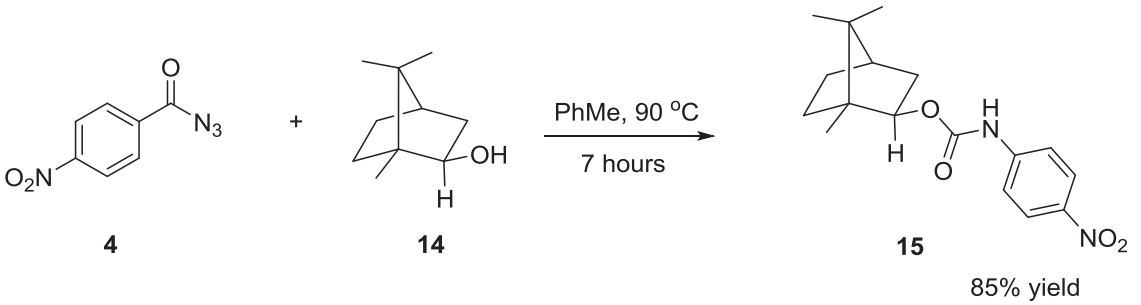

Equation 21: Synthesis of Carbamate **(15)**.

The ^{1}H NMR spectrum of **15** reveals the N-H signal representative of the carbamate functionality at 7.56 ppm as a singlet peak. In addition to that, the two sets of identical protons on the aromatic ring have chemical shifts in the in the form of doublet signals at 7.62 ppm and 8.19 ppm integrating for two protons each with each having a coupling constant *J* of 9.2 Hz. Singlet peaks at 0.88 ppm and 0.92 ppm represent the methyl groups on the bicyclic ring in addition to the series of multiplets from 1.28 ppm to 1.81 ppm representing the methylene protons on the bicyclic ring. The ^{13}C NMR provided further confirmation of the synthesis of **15** with the chemical shift at 153.80 ppm representing the carbonyl group as well as chemical shifts at 124.05 ppm, 129.74 ppm, 139.57 ppm and 148.74 ppm representing the carbon atoms on the aromatic ring. Signals at 18.78 ppm, 19.66 ppm and 27.09 ppm represent the methyl groups on the bicyclic ring also confirm the coupling of the azide **4** with the nucleophilic substrate **14**. Further confirmation of the product **15** came from IR spectroscopic data with the peak at 3428 cm^{-1} representing the N-H stretching frequency of the compound **15**. Other important peaks were observed at 2959 cm^{-1} for the C-H stretching of both the sp^2 and sp^3 groups present in the molecule as well as 1734 cm^{-1} representing the C=O stretching frequency of the carbonyl group.

The final synthetic endeavor embarked on in **Project 1** of this research involving the Curtius rearrangement was the coupling of the azide **3** with **14** to synthesize the 3-nitro analogue **(16)**, of carbamate **15** (**Equation 22**). Similar to the previous synthetic attempts mentioned in this section, L-(-)borneol **(14)** and 3-Nitrobenzoyl azide **(3)** were reacted together for 12 hours under toluene reflux at 90 ^{o}C and the reaction mixture was cooled to room temperature after thin layer chromatography showed the total consumption of both starting materials. The solvent was then evaporated via vacuum on a rotovap and a deep yellow syrup was obtained in good yield (66%) once again upon purification using flash column chromatography.

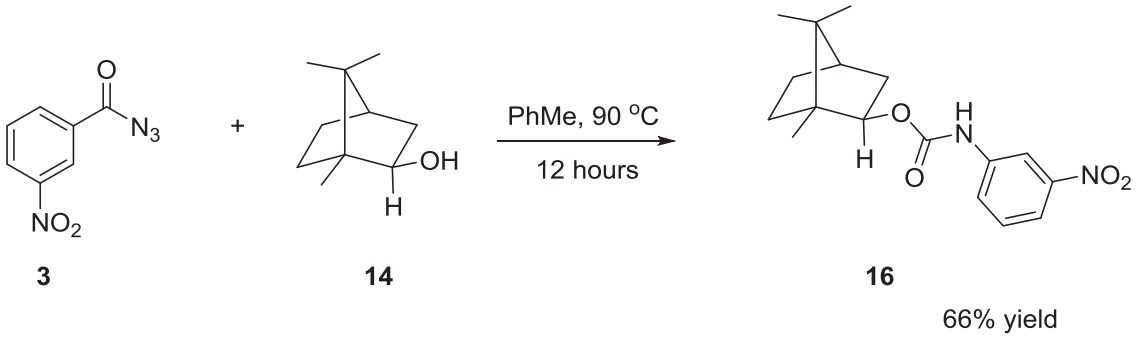

Equation 22: Synthesis of Carbamate **(16)**.

Analysis of spectral information derived from IR and NMR spectroscopic data obtained for the product confirm its identity as **16**. ^{1}H NMR spectral data showed a chemical shift at 7.27 ppm (singlet) representing the chemical shift for the N-H proton signal as well as a doublet of doublet signal (with $J_1 = J_2$) at 7.45 ppm with coupling constant of 8.2 Hz representing the chemical shift of the proton *meta* to both the nitro and the carbonyl groups on the aromatic ring. the doublet of doublet signal integrating for one proton with coupling constant of 3.3 and 9.9 Hz at 4.97 ppm represents the proton

geminal to the carbamate group on **16**. Other proton NMR chemical shifts that confirm the coupling are the singlet peaks at 0.89 ppm and 0.92 ppm representing the methyl groups on the bicyclic ring as well as the doublet signals at 7.77 ppm and 7.89 ppm with coupling constants of 7.8 and 8.2 Hz respectively. The ^{13}C NMR also shows a peak at 153.80 representing the chemical shift of the carbonyl carbon and the aromatic carbons have six singlet peaks between 113.28 ppm and 148.74 ppm. The three methyl carbons on the bicyclic ring have chemical shifts at 18.78 ppm, 19.66 ppm and 27.09 ppm with the rest of the signals representing the methylene, tertiary and quaternary carbons. Spectroscopic information from the IR spectrum showed the N-H stretching at 3432 cm^{-1}, the C-H stretching frequency at 2959 cm^{-1} and the C=O stretching for the carbonyl functional group at 1730 cm^{-1} all confirming the identity of the carbamate product **(16)**.

Project 2

The next phase of the research, which sought to explore intramolecular reactions of acyl nitrenes, involved the syntheses of azidoformates or carbonyl azides from free single -OH containing organic compounds and then decomposing these azides in a variety of solvents via thermolysis to observe their behavior in terms of intramolecular insertion in adjacent C-H bonds. To synthesize the azides, the alcohol containing compounds would first be reacted with triphosgene to yield the chloroformates (carbonyl chlorides) and then these carbonyl chlorides would be transformed into azidoformates.

The first of such organic molecules containing a single free –OH group that was studied in this project was diacetone glucose **(8)** which was previously used in the Curtius rearrangement in **Project 1.**

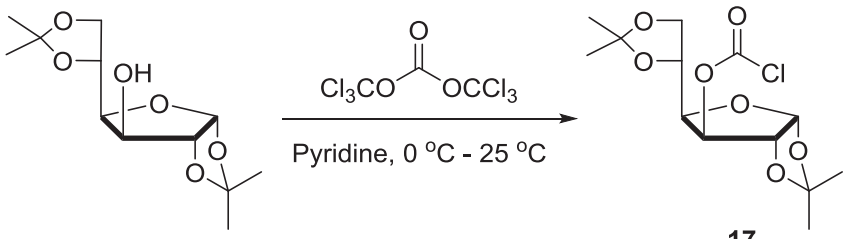

Equation 23: Synthesis of chloroacyl sugar **17**.

Compound **8** and a third of the molar equivalence of triphosgene were weighed into a round bottom flask and purged under inert conditions for the first trial. The reaction was carried out on a 1 mmol scale to test its success before scaling up. The reaction was run in CH_2Cl_2 with a stoichiometric amount of anhydrous pyridine with respect to **8** added to the mixture in an ice bath, and the temperature was gradually elevated towards room temperature as the ice melted. After 6 hours, TLC showed an elevated spot above the sugar indicating the formation of a slightly non-polar compound suspected to be **17** (**Equation 23**). However, after the reaction was left to run overnight if was observed that the starting material could not be consumed completely leading to the decision to use a stoichiometric amount of triphosgene in the next trial. The use of the stoichiometric amount of triphosgene also led to incomplete consumption of the starting sugar.

Next on the agenda was to vary the amount of the base catalyst (pyridine) used. The initial stoichiometric amount of pyridine used was cut down to half and the reaction

was allowed to proceed in similar reaction conditions as before and the results improved. There was barely any starting material left in the reaction mixture as evidenced by TLC. A wide variety of solvents were also tried and the best solvent for this transformation was found to be THF although the reaction also proceeded in *N,N*-dimethylformamide (DMF) and toluene with some significant results. Hence compound **17** was formed in THF with a stoichiometric equivalent of triphosgene and catalytic amount of the base at 0 ^{o}C warming up to room temperature.

Spectroscopic data from both the NMR and IR instruments confirm the formation of the carbonyl chloride **17** in excellent yield. A look at the ^{1}H NMR spectrum for **17** confirmed the disappearance of the singlet peak at 1.80 ppm in the original spectrum for diacetone glucose **8**. The anomeric proton also shifted slightly downfield from about 4.6 ppm to 5.35 ppm with the incorporation of the carbonyl group on the molecule. The changed nature of the two singlet peaks for two of the methyl protons originally at 1.32 ppm and 1.36 ppm merging into just one singlet peak at 1.31 integrating for six protons tells of a transformation.

The ^{13}C NMR spectrum for the starting material **8** shows no peak beyond 140.00 ppm which is an indication of the absence of a carbonyl group in the compound. However, a look at the ^{13}C NMR spectrum for the crude product **17** shows a strong signal at 159.43 ppm indicative of the presence of a carbonyl group on the compound **17**. The methyl carbons show chemical shifts at 25.03 ppm, 26.05 ppm, 26.55 ppm and 26.71 ppm with the remaining carbons having strong signals with chemical shifts between 67.16 ppm and 112.20 ppm. The IR spectrum for the product **17** shows the disappearance

of the broad O-H stretching peak at 3000 cm^{-1} and the presence of the C=O functional group with the peak at 1664 cm^{-1} being an indication of product formation.

Next we set out to transform **17** into its corresponding azidoformate **(18)** (**Equation 24**). Catalytic amounts of tetrabutyl ammonium bromide were added to the **17** in its crude form and methylene chloride added to reflux at room temperature after adding a large excess of sodium azide solution. The use of tetrabutyl ammonium bromide was important because of the need for a phase transfer catalyst to force the reaction between **17** that was dissolved in methylene chloride and the sodium azide that was dissolved in aqueous acetone. After allowing the reaction to run overnight with the magnetic stirrer running at about 600 rpm, a much elevated spot was observed above the R_f of the chloride **17** under UV and upon staining with 5% concentrated H_2SO_4 in methanol, the spot observed under the UV light also burned into a dark color indicative of another transformation.

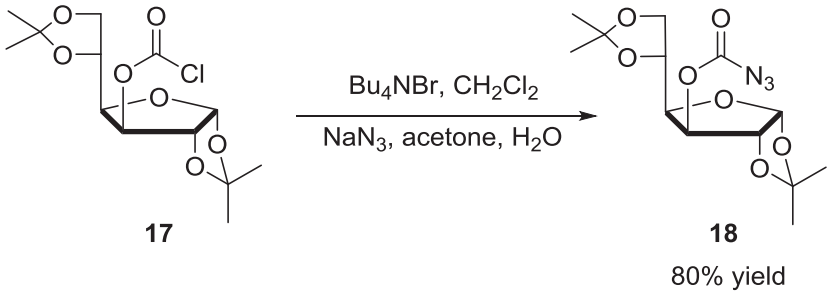

Equation 24: Synthesis of azidoacyl sugar **18**.

After purification of the product via flash column chromatograpy, spectral information gathered from the NMR and IR instruments once again confirmed the

formation of the product **18**. The ^{1}H and ^{13}C NMR signals were similar to the acyl chloride **17** with the only clear difference being the restoration of the two singlets previously merged together at 1.31 ppm in the spectrum of **17** to two individual singlets integrating for three protons each at 1.32 ppm amd 1.33 ppm. Again the chemical shift for the O-H proton initially found at 1.81 ppm in the sugar **8** was not present and the proton at the anomeric position has shifted slightly upfield to 5.23 ppm. The ^{13}C NMR spectrum placed the chemical shift for the carbonyl carbon at 156.7 ppm and the methyl carbons have chemical shifts at 25.13 ppm, 26.15 ppm, 26.63 ppm and 26.85 ppm.

The IR spectrum provided a heavy influence in determining whether the actual transformation to **18** took place. Without the IR information, it could be argued that there was no transformation since the NMR spectra for **17** and **18** were not so different. The symptomatic azide peak at 2119.97 cm^{-1} in addition to the C=O frequency at 1090 cm^{-1} was a clear indication of the presence of an azidoacyl group on the molecule hence the confirmation of the synthesis of 3-*O*-(azidoacyl)-1,2:5,6-di-*O*-isopropylidene-α-D-glucofuranose **(18)**.

Next, we embarked on the journey to synthesize a few other azidoformates via the chloroformate route before proceeding to decompose the azides to observe whether or not the nitrenes generated from the decomposition of these azides would partake in any form of intramolecular C-H insertion reactions.

2-Indanol **(19)** was reacted with triphosgene in the same fashion as described for the synthesis of **17** with catalytic amounts of pyridine to yield **20** (**Equation 25**)**.** After filtering off the precipitate that formed during the reaction, the filtrate was evaporated to

yield initial brown syrup which almost immediately crystallized. The crude product was not purified in order to optimize yield in the subsequent reactions.

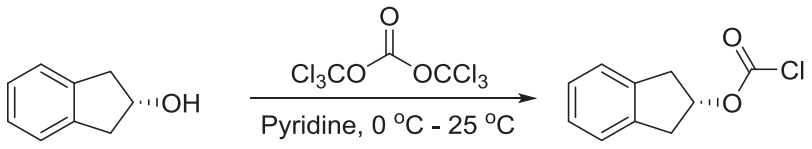

19 **20**

80% yield

Equation 25: Synthesis of acyl chloride **20**.

Spectroscopic information was obtained for the product **20**. Both IR and NMR spectroscopic data confirm the formation of the chloride **20** in excellent yield. A look at the ^{1}H NMR spectrum for **20** shows the disappearance of the O-H proton signal of **19** at 2.14 ppm indicating the complete consumption of the starting material. The chemical shift in the form of doublet of doublet signal with J_1 of 2.8 Hz and J_2 of 6.1 Hz at 5.60 ppm in the spectrum of **20** represents the proton at β position. The methylene protons have a chemical shift at 3.16 ppm and 3.35 ppm whereas the aromatic ring protons have a multiplet of peaks at 7.18-7.85 integrating for four protons.

The ^{13}C NMR spectrum for the chloride **20** shows the chemical shift for the carbonyl carbon at 150.49 ppm in addition to the chemical shifts for the aromatic ring carbons at 124.70 ppm, 127.22 ppm and 139.23 ppm. The methylene carbons recorded a singlet at 83.87 ppm in addition to the signal for the β carbon at 39.31 ppm. IR spectrum for the product **19** showed the presence of a carbonyl group at 1768 cm^{-1} in addition to C-H stretching frequency at 2963 cm^{-1} and C-O stretching frequency at 1161 cm^{-1} to confirm the compound as **20.**

Reaction of the chloride **20** with sodium azide dissolved in a mixture of acetone and water (3:1) in methylene chloride using tetrabutylammonium bromide as a phase transfer catalyst yielded compound **21** in excellent yield (**Equation 26**).

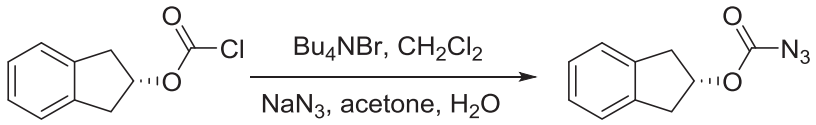

20 **21**

94% yield

Equation 26: Synthesis of acyl azide **21**.

Analysis of the ^{1}H NMR spectrum of the product shows a slight upfield shift for all the signals with the *β* proton shifted from 5.60 ppm in the spectrum of **20** to 5.52 ppm in the spectrum of **21**. The multiplet of peaks for the aromatic ring protons have also shifted slightly upfield from 7.18-7.85 ppm to 7.17-7.23 ppm an indication of substitution from the chloride to a functional group that provides slight shielding to the protons. The ^{13}C NMR spectrum of the compound **20** also shows a further downfield shift at 157.42 ppm from 150 ppm, also an indication of the acyl substitution from the chloride **20** to the azide **21**. The IR spectrum once again played a major role here in the determination of whether indeed the substitute group is an azide. The signal at 2137 cm^{-1} is indicative of the presence of an azido group in addition to the C=O stretching at 1716 cm^{-1} and the C-O stretching frequency at 1091 cm^{-1}, hence confirming the synthesis of the compound **21**.

We decided next to synthesize the L(-)-borneol derivative of both chlorides and azides as done for the previous two substrates. We wanted to test all these substrates in

the various decomposition solvents since they all have different structures although very similar reaction sites for the expected outcome which is the intramolecular insertion.

L(-)-Borneol **14** previously used in the Curtius processes was reacted with triphosgene in the same manner as 2-indanol and diacetone glucose to form the bicyclic acyl chloride **22** (**Equation 27**). The crude product that was isolated after filtering off the pyridinium chloride precipitate and then evaporating off the filtrate under vacuum was a brown oil that is very stable in air and does not harden at room temperature.

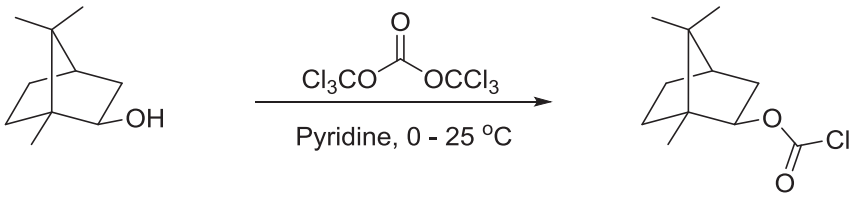

14 **22**

93% yield

Equation 27: Synthesis of acyl chloride **22**.

After isolation of the crude product **22**, NMR and IR spectroscopic information was obtained to elucidate the structure of the compound formed. It was observed that the initial O-H proton signal at 1.56 ppm for **14** had disappeared in the spectrum for **22**, an indication that the compound present is no longer L-(-)borneol. However, three singlet peaks were observed at 0.85, 0.86 and 0.87 ppm representing the three methyl groups on the bicyclic ring in addition to multiplets of peaks at 1.26-1.39 ppm, 1.73-1.95 ppm and 2.36-2.44 representing the methylene and tertiary protons. The proton at the C-1 position appears as a doublet at 4.99 ppm with a coupling constant of 9.4 Hz. The ^{13}C NMR spectrum of **22** also shows an additional peak at 150.53 ppm indicative of the presence of

a carbonyl group. The IR spectrum of the chloride **22** shows the disappearance of the broad O-H peak at 3300 cm^{-1} and the presence of a carbonyl signal at 1770 cm^{-1} confirming the formation of **22**.

When the crude compound **22** was reacted with sodium azide as done for the other substrates, a deep yellow oily compound **23** was isolated after flash column chromatography using a 3:1 hexane:ethyl acetate solvent system and evaporating off the solvent at low pressure. To a very small extent when the conversion from chloride to azide was performed longer than a day, a second spot which was later found to be the starting material **14** (borneol) was isolated (**Equation 28**). This could be attributed to the hydrolysis of the acyl chloride **22** over time since there is water in the reaction mixture enough to carry out that kind of side reaction.

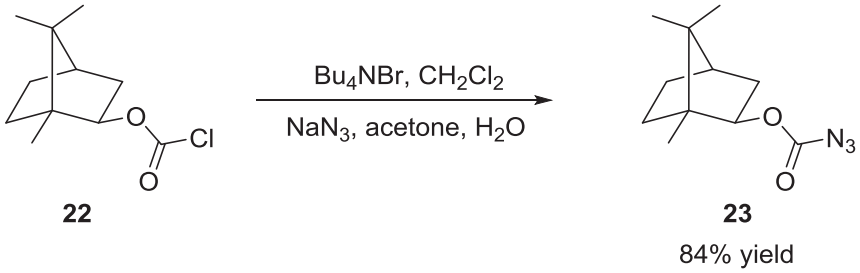

Equation 28: Synthesis of acyl azide **23**.

Spectral information for the isolated product gives confirmation of the formation of compound **23**. The ^{1}H NMR spectrum for the product maintains the chemical shifts for the three methyl groups on the bicyclic ring as singlets at 0.88, 0.9 and 0.91 ppm as well as the proton at C-1 shifting slightly upfield from 4.99 ppm to 4.90 ppm with all the other series of multiplets maintained at their earlier positions. Analysis of the ^{13}C NMR

spectrum shows a downfield shift of the signal for the carbonyl carbon at 157 ppm from 150 ppm an indication of the attachment of a new substituent with some effect of deshielding. Again the IR spectrum provided the final piece to the puzzle with the signal at 2137 cm^{-1} confirming the presence of an azido group and hence the formation of **23**.

The final alcohol substrate we employed once again was cholesterol **(11)**. When **11** was reacted with stoichiometric amounts of triphosgene in dry THF, white crude crystals of **24** were isolated and left in their crude state without purification in order to maximize yield in the subsequent reactions (**Equation 29**).

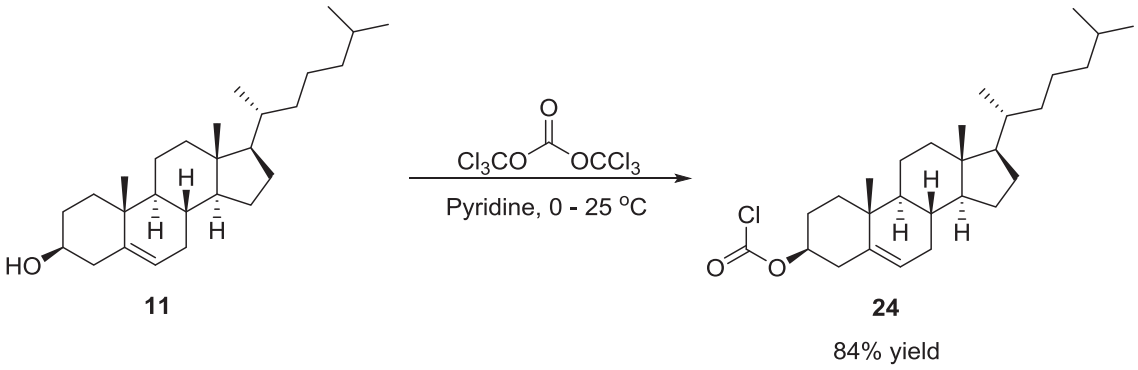

Equation 29: Synthesis of acyl chloride **24**.

Analysis of the product isolated by NMR and IR spectroscopy confirms the synthesis of **24** indeed. A look at the ^{1}H NMR spectrum shows the disappearance of the O-H chemical shift originally at 1.65 ppm. This is an indication that the starting material has been consumed and a new product has been formed. The chemical shift for the proton at C-1 shifted downfield from 3.5 ppm to 3.75 ppm indicating the presence of the acyl group. Also the peaks at 0.68, 0.87, 0.91 and 1.02 ppm integrate for the methyl protons on the cholesterol framework. Analysis of the ^{13}C NMR spectrum also shows a new peak

at 149.68 ppm corresponding to the carbonyl carbon in addition to all the 26 signals expected. The IR spectroscopy also gave further confirmation of the incorporation of the carbonyl group by showing a symptomatic peak at 1769.36 cm^{-1} to confirm **24**.

When **24** was treated with sodium azide together with the phase transfer catalyst with methylene chloride as the reaction solvent, white solid crystals were once again obtained in good yield and purified using hot ethanol to give very nice-looking spiky but small-sized crystals. The crystal structure of the final azide **25** was obtained by the use of the X-ray crystallographic instrument. Spectral information obtained for product in addition to the X-ray crystal structure confirms the formation of **25** (**Equation 30**).

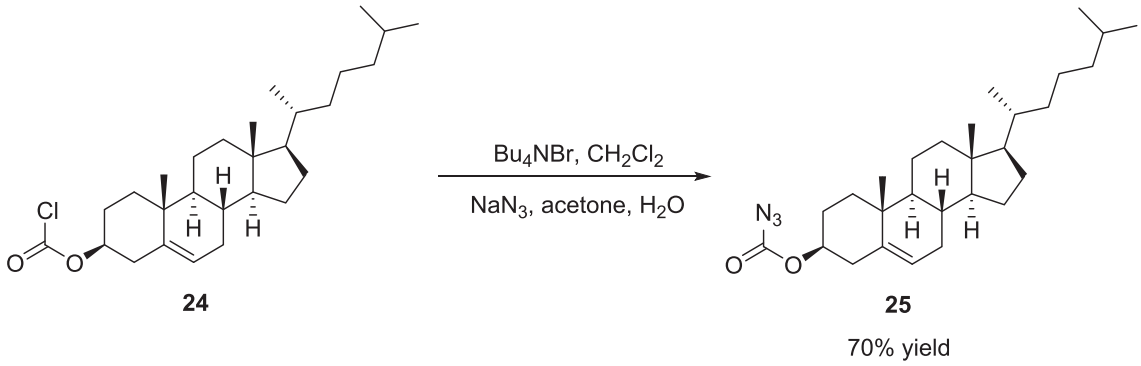

Equation 30: Synthesis of acyl azide **25**.

Here again the signal looks similar to **24** for both the ^{1}H and ^{13}C NMR spectra of **25**. However, the downward shift of the proton at C-1 from 3.75 ppm to the region of 4.56-4.64 ppm is an indication of the replacement of the chloride with a more deshielding group hinting at the formation of the azide. Also TLC showed an elevated spot above the chloride spot which can be seen under the UV light and which burns with the same color as the chloride **25**. A look at the ^{13}C NMR for **25** confirms the downward shift of the carbonyl carbon from 149 ppm to 157 ppm in addition to IR data showing the peak for

the azide functional group at 2126 cm^{-1}. As mentioned earlier the X-ray crystal structure obtained for this product solves the mystery and gives absolute confirmation to the identity of the product isolated as **25**. A look at the crystal structure **(Figure 1)** shows the cholesterol skeleton in addition to the carbonyl carbon and the sp^3 oxygen attached to the carbonyl carbon. It also shows the azido group and three nitrogen atoms bonded linearly to each other.

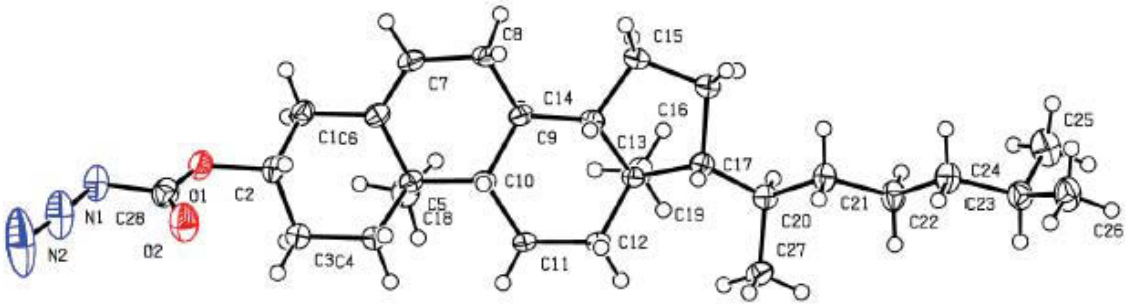

Figure 1: X-ray crystal structure of azide **25**.

We then proceeded to thermally and photochemically decompose the carbonyl azides synthesized from the precursory alcohol containing groups. The decision was made in the course of the research that since diacetone glucose **8** has TLC properties that made it easier to analyze, its azidoformate **18** would be used to do the initial screening of reaction conditions to see which conditions best allow for the intramolecular insertion processes leading to the formation of the desired oxazolidinone final product.

When **18** was thermally and photochemically decomposed in methylene chloride, toluene, DMF and *p*-xylene, results obtained including spectroscopic data showed no

formation of the oxazolidinone as the signal for the N-H proton expected was not observed. In the case of methylene chloride and toluene, there was no reaction as NMR data shows chemical shift in the exact same positions as the azidoformate **18**. For DMF and *p*-xylene the single spot on the TLC identified and isolated resulted in spectroscopic data that looked like several compounds in just one spot. Moving on from here, we decided to try the decomposition of **18** in cyclohexane as was previously done by Edwards and Brown[27] in their photolysis of a variety acyl azides with a few minor modifications such as not using a vycor flask but rather running these reaction in the normal borosilicate glassware. To our surprise, after 72 hours of running the reaction (thermolysis) and monitoring for the consumption of **18** and the formation of a slightly more polar spot, we did not observe any form of intramolecular insertion in the results obtained. Instead, we isolated in significant amounts what looks like an intermolecular nitrene insertion product **(26)** with the solvent (**Equation 31**).

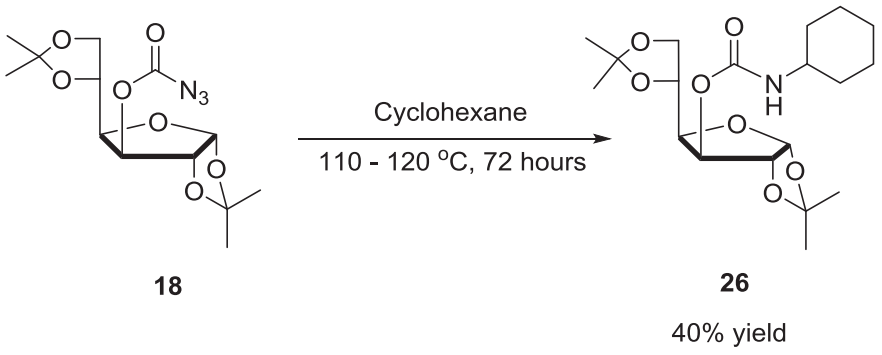

Equation 31: Synthesis of acyl carbamate **26**.

Once again, spectroscopic data in addition to the X-ray crystal structure confirm the formation of **26**. A look at the ^{1}H NMR spectrum reveals the notable peak for the N-H proton at 3.50 ppm integrating for one proton. The multiplet of peaks found at 1.60-1.63

ppm represents the proton at the cyclohexyl C-1 position. The quintet chemical shift at 1.15 ppm with coupling constant of 3.1 Hz also integrates for the cyclohexyl C-4 protons. The singlet peaks at 1.30, 1.33, 1.42 and 1.51 ppm, all integrating for three protons each, represent the chemical shifts of the methyl protons on the sugar moiety. A look at the ^{13}C NMR spectrum for the compound also reveals the signal for the carbonyl at 153.95 ppm in addition to the signal for the four methyl carbons on the sugar at 24.73, 25.41, 26.19 and 26.74 ppm. The expected four signals for the carbon atoms on the cyclohexyl ring also appear at 33.30, 50.10, 66.95 and 72.58 ppm. The X-ray crystal structure **(Figure 2)** of the compound provides the absolute basis for confirming the identity of the product as **26**.

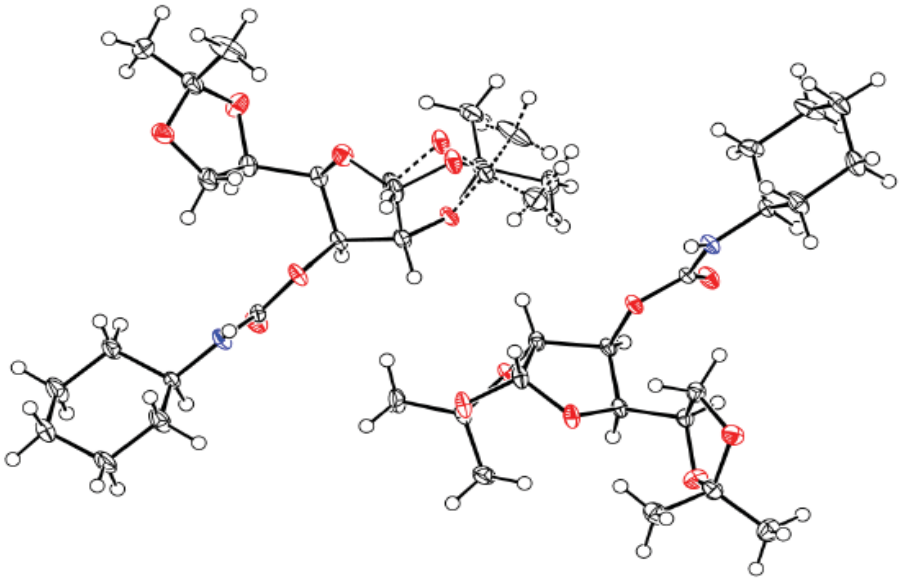

Figure 2: X-ray crystal structure of carbamate **26**.

Since **26** was not the product we desired, we moved on to test our hypothesis on some other higher boiling solvents to see if we could observe intramolecular insertion

products. The next solvent choice we made was mesitylene. When **18** was heated in mesitylene for about 24 hours, three spots immerged on the TLC plate with the upper spot identified as mesitylene and the two lower spots having R_f lower than the azide.

After cooling the reaction mixture to room temperature, flash column chromatography with 5:1 hexane-ethyl acetate solvent system was used to separate the spots. The most polar spot was identified as diacetone glucose which was expected to a small extent because of the ability of our product to hydrolyze. The slightly less polar spot which was isolated in quite a significant amount upon analysis with spectroscopy also did not point towards the formation of an oxazolidinone as expected. We instead observed what looked like another intermolecular insertion to the solvent (**Equation 32**). The isolated product was an amorphous glass that resisted several attempts at recrystallization to yield single crystals for X-ray diffraction. Although the TLC showed a single spot in several solvent systems with various degrees of polarity, spectroscopic information tend to lean towards the instance of having two products within the same fraction, one of which is **27**.

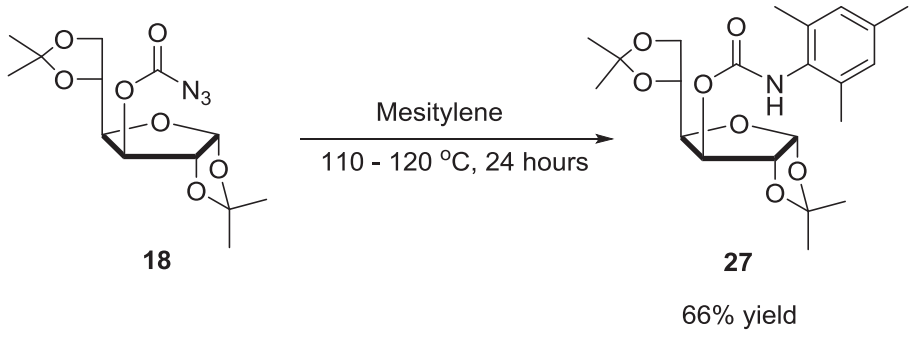

Equation 32: Synthesis of acyl carbamate **27**.

Spectroscopic information allows us to arrive at the conclusion that compound **27** was formed. A look at the ^{1}H NMR spectrum shows the chemical shift for the methyl protons of the sugar moiety at 1.31 ppm integrating for six protons as a singlet, 1.40 ppm for three protons as a singlet and 1.51 ppm for three protons also as a singlet. The methyl protons on the mesityl group have chemical shifts at 2.20, 2.25 and 2.30 ppm all as singlets and integrating for three protons each. The equivalent aromatic ring protons were also found to have a singlet peak with chemical shift of 6.86 ppm integrating for two protons whereas the N-H proton signal was observed at 6.14 ppm. Analysis of the ^{13}C NMR spectrum shows the carbonyl carbon peak at 152.92 ppm in addition to the carbon atoms for the mesityl methyl groups at 18.10 ppm and 20.90 ppm confirming the structure of **27**.

Next we decided to test other substrates with mesitylene to observe whether or not they would behave in a similar manner as **18**. We treated **21** in the same fashion as we did **18** and after 16 hours we isolated a major product based on initial TLC analysis of the cooled reaction mixture.

Upon purification with flash column chromatography it was once again observed that no intramolecular insertion products were isolated. Instead we have another intermolecular insertion between **21** and the solvent mesitylene (**Equation 33**).

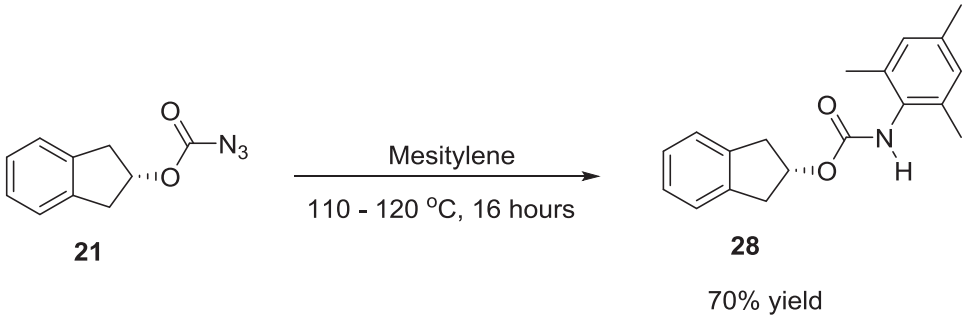

Equation 33: Synthesis of acyl carbamate **28**.

An X-ray crystal structure **(Figure 3)** in addition to spectral information confirmed the formation of **28** in good yield. Analysis of the ^{1}H NMR spectrum for the product revealed the signal for the mesityl protons at 2.20 ppm and 2.25 ppm with the signal at 2.25 ppm integrating for six protons. The aromatic ring protons, which are equivalent and have no coupling partners, were observed together as a singlet at 6.86 ppm. The methylene protons of the indanol were observed as a doublet of doublets signal at 3.08 ppm and 3.33 ppm with coupling constants of 5.9 Hz and 16.7 Hz. The notable signal at 7.25 ppm integrating for one proton was identified as the peak for the N-H proton. ^{13}C NMR spectrum of the product reveals the notable signal for the carbonyl carbon at 154.36 ppm in addition to the signal for the methyl carbons atoms on the aromatic ring at 18.23 ppm and 20.88 ppm. The methylene carbon atoms of the indanol also occur at 39.31 for two equivalent carbon atoms. Below is the X-ray crystal structure of the compound **(28)** isolated.

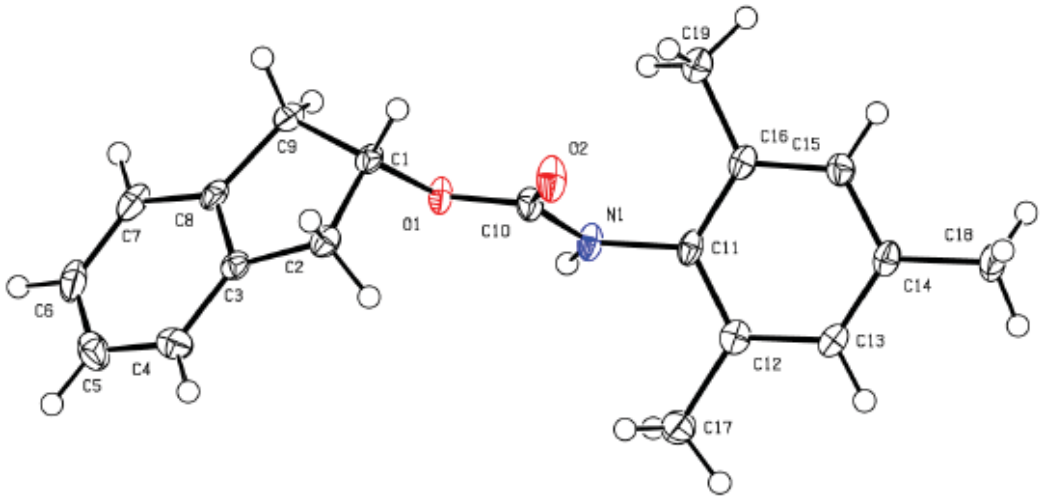

Figure 3: X-ray crystal structure of carbamate **28**.

Treatment of another azide precursor, **23**, with mesitylene also yielded similar results as the first two compounds tested with mesitylene. Although the NMR spectrum for the product isolated had low resolution, even after several purification techniques were employed and the NMR sample concentrated, the integrals derived from the ^{1}H NMR data in addition to the X-ray crystal structure that was obtained from X-ray diffraction instrumentation confirmed the formation of compound **29** (**Equation 34**).

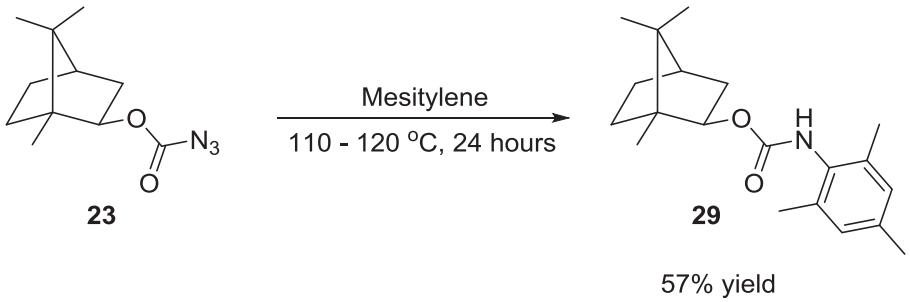

Equation 34: Synthesis of acyl carbamate **29.**

Analysis of the ^{1}H NMR spectrum showed the signal at 0.89 ppm integrating for nine protons representing the methyl groups on the bicyclic ring. The signal at 6.00 ppm was found to be the chemical shift of the N-H proton whereas the methyl protons of the mesityl group had chemical shifts at 2.21 ppm and 2.25 ppm with the equivalent aromatic protons having a singlet peak at 6.86 ppm. The notable carbonyl carbon signal in the ^{13}C NMR spectrum was found at 155.09 ppm and together with the X-ray crystal structure obtained **(Figure 4)**, the identity of **29** was confirmed.

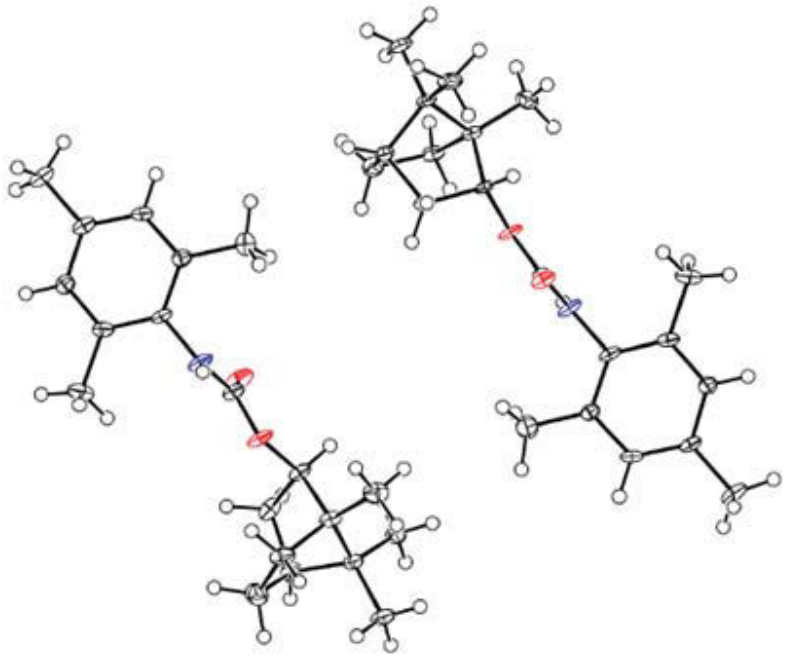

Figure 4: X-ray crystal structure of carbamate **29**.

Because cyclohexane and mesitylene did not yield the expected results, we set-off to use diphenyl ether as was done in 1964 by Smolinsky and Feuer in the decomposition

of azidoformates in their study of thermally generated nitrenes.[24] Azide **21** was decomposed thermally in diphenyl ether at 120 ^{o}C for 6 hours. The reaction mixture turned black after 30 minutes and stayed that way to the end of the reaction. After TLC analysis confirmed the disappearance of the starting azide, the reaction mixture was cooled and flash column chromatography was used to isolate the major product. Analysis of the compound isolated revealed its identity as another intermolecular insertion product. The nitrene has once again inserted to the solvent (**Equation 35**). The product was identified as **30**.

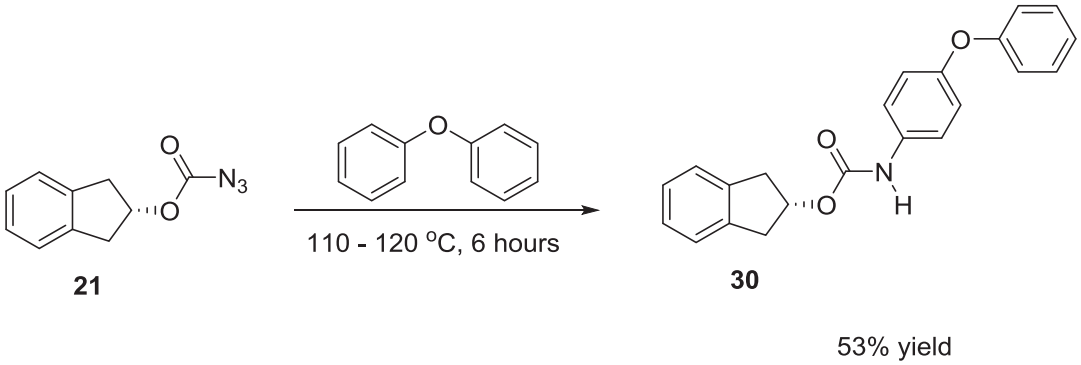

Equation 35: Synthesis of acyl carbamate **30**.

The ^{1}H NMR spectrum shows the nine individual protons of the aromatic ring of the diphenyl ether occuring as a multiplet of peaks from 7.19-7.33 ppm. The notable N-H signal which is symptomatic of the carbamate functionality was observed at 6.50 ppm in addition to the proton at the β position of the product observed as a quintet at 5.58 ppm with coupling constant of 2.7 Hz. The methylene protons of the compound were also observed as doublet of doublets signals at 3.09 ppm integrating for two protons and 3.34

also integrating for two protons with coupling constants of 2.6 Hz and 17.0 Hz and 6.1 Hz and 17.0 Hz respectively.

The ^{13}C NMR spectrum also showed the characterististic carbonyl carbon signal at 157.78 ppm in addition to the aromatic carbons bonded to the oxygen in the diphenyl ether portion of the compound at 152.87 ppm and 153.47 ppm. The X-ray crystal structure **(Figure 5)** of the isolated product in addition to spectral analysis resolves the identity of the product as **30**.

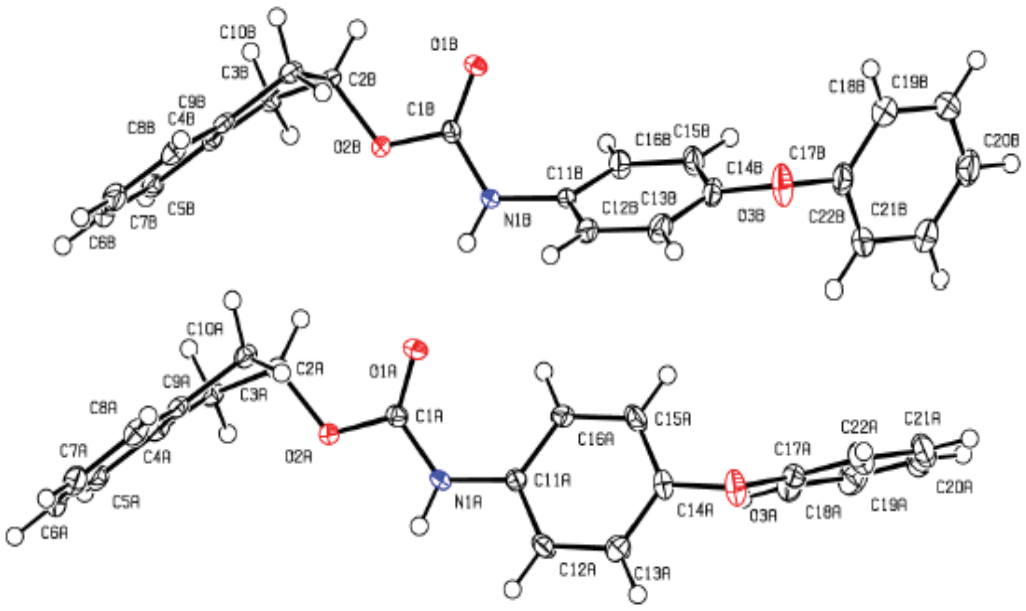

Figure 5: X-ray crystal structure of carbamate **30**.

When azides **18** and **23** were tested with the diphenyl ether, the resultant products could not be isolated with flash column chromatography, which is consistent with the

difficulties in purification faced by Smolinsky and Feuer,[24] for which reason they used gas chromatography to isolate their products. The scope of this research however could not afford us the use of GC and thus we have been unsuccessful in isolating the products in the reaction mixture for the diphenyl ether reaction of **18** and **23**.

Conclusion

The synthesis of carbamates using aryl acyl azides via the Curtius rearrangement has been achieved with a variety of large organic molecules containing a single free OH functionality. The reactions were observed to proceed via a one-pot process where thermally generated acyl nitrenes rearrange into isocyanates and get trapped by surrounding nucleophiles with reasonable reaction time and high yields. The reaction can be adapted to synthesize a wide range of compounds via the Curtius rearrangement varying the nucleophiles involved. Although the intramolecular nitrene insertion reactions were not observed for the azidoformates synthesized, interesting transformations that were not well known to happen with thermally generated oxycarbonyl nitrenes have been explored. Regarded as largely inert solvents in organic synthesis, cyclohexane, mesitylene and diphenyl ether were found to behave differently in the presence of thermally generated oxycarbonyl nitrenes and participate to a great extent in intermolecular coupling with the nitrenes to yield carbamates, hence a new strategy for functionalization of these compounds under moderate reaction conditions.

EXPERIMENTAL

General Procedures

Reactions were monitored and analyzed by TLC on Whatman aluminum-backed plates in solvent systems of various proportions of ethyl acetate and hexane. Nuclear Magnetic Resonance spectra were obtained in $CDCl_3$ or d_6-DMSO using the Bruker Topspin system at a frequency of 400 MHz for ^1H NMR spectra and 100 MHz for ^{13}C spectra. All chemical shifts were recorded in parts per million (ppm) with coupling constants (*J*) recorded in Hertz (Hz). Purification via flash column chromatography employed the use of 20-120 mesh 60-Å silica gel. IR spectroscopic information was obtained from the Thermo IR 200 Spectrometer instrument.

Project 1

Synthesis of 3-Nitrobenzoyl azide (3).

In a 100 mL round bottom flask fitted with a magnetic stirrer 2.275 g (35 mmol) of NaN_3 was added and a rubber septum mounted on the flask. The flask was purged three times with nitrogen gas and 15 mL of water was pipetted into the flask. The reaction mixture was then allowed to stir for an hour under inert conditions. A solution of 3-nitrobenzoyl chloride **(1)** (5.57 g, 30 mmol) in 15 mL of acetone was pipetted slowly into the reaction mixture after which the reaction was allowed to stir for additional 30 minutes under inert conditions. A further 15 mL of H_2O was added to the reaction mixture and the reaction was allowed to stir for another 30 minutes after which the

product was isolated via suction filtration and recrystallized from 20 mL of hot ethanol to yield 5.5 g (98%) of **3** as white solid crystals.

^{1}H NMR ($CDCl_3$): δ 7.69 (1H, dd, J = 8.0), 8.36 (1H, d, J = 7.8), 8.47 (1H, d, J = 8.2), 8.85, (1H, s).

^{13}C NMR ($CDCl_3$): δ 124.37, 128.49, 129.98, 132.33, 134.85, 148.45, 170.57.

IR: 2996 cm^{-1} (C-H), 2144 cm^{-1} (N_3), 1706 cm^{-1} (C=O).

Melting point: 55-57 ^{o}C.

Synthesis of 4-Nitrobenzoyl azide (4).

In a 100 mL round bottom flask fitted with a magnetic stirrer 2.275 g (35 mmol) of NaN_3 was added and a rubber septum mounted on the flask. The flask was purged three times with nitrogen gas and 15 mL of water was pipetted into the flask. The reaction mixture was then allowed to stir for an hour under inert conditions. A solution of 4-nitrobenzoyl chloride **(2)** (5.57 g, 30 mmol) in 15 mL of acetone was pipetted slowly into the reaction mixture after which the reaction was allowed to stir for additional 30 minutes under inert conditions. A further 15 mL of H_2O was added to the reaction mixture and the reaction was allowed to stir for another 30 minutes after which the product was isolated via suction filtration and recrystallized from 20 mL of hot ethanol to yield 5.4 g (89%) of **4** as pale yellow crystals.

^{1}H NMR ($CDCl_3$): δ 8.21 (2H, d, J = 9.0), 8.30 (2H, d, J = 9.0).

^{13}C NMR ($CDCl_3$): δ 123.80, 130.54, 135.70, 151.27, 170.84.

IR: 2974 cm^{-1} (C-H), 2138 cm^{-1} (N_3), 1702 cm^{-1} (C=O).

Melting point: 60-63 ^{o}C.

General procedure for the synthesis of carbamates via Curtius rearrangement.

In a round bottom flask the alcohol was added to the azide in dry toluene and a reflux condenser mounted. The mixture was allowed to heat at 90 ^{o}C while monitoring the consumption of the starting materials via thin layer chromatography. After the complete consumption of the starting materials, the reaction mixture was allowed to cool to room temperature and the product isolated either by suction filtration and subsequent recrystallization from hot isopropyl alcohol or ethanol, or via flash column chromatography using a 3:1 hexane-ethyl acetate solvent system.

Synthesis of 2,2-dimethyl-5-oxohexahydrofuro-2,3:4,5-furo-2,3-D-1,3-dioxol-6-yl-3-nitro-phenyl carbamate (6) from 3-nitrobenzoyl azide (3) and D-glucurono-6,3-lactone acetonide (5) via Curtius Rearrangement.

Following the general procedure described above for the synthesis of carbamates via the Curtius rearrangement, D-glucurono-6,3-lactone acetonide **(5)** (0.648 g, 3.0 mmol) was reacted with **3** (0.576 g, 3.0 mmol) in 20 mL of dry toluene for 6 hours. The crude

product was subsequently recrystallized from hot isopropyl alcohol to yield 0.75 g (65.8%) of **6** as pale yellow crystals.

^{1}H NMR ($CDCl_3$): δ 1.36 (3H, s), 1.53 (3H, s), 4.87 (1H, d, J = 3.6), 4.94 (1H, d, J = 2.8), 5.14 (1H, m), 5.58 (1H, d, J = 4.3), 6.04 (1H, d, J = 3.6), 7.22 (1H, s), 7.50 (1H, dd, J = 8.2), 7.66 (1H, d, J = 8.15), 7.96 (1H, d, J = 8.9), 8.35 (1H, s).

^{13}C NMR ($CDCl_3$): δ 26.52, 26.91, 70.87, 76.67, 77.31, 82.21, 82.58, 107.05, 113.79, 118.93 (2), 130.00, 138.2, 148.86, 151.20, 169.39.

Melting point: 174-176 ^{o}C.

Synthesis of 2,2-dimethyl-5-oxohexahydrofuro-2,3:4,5-furo-2,3-D-1,3-dioxol-6-yl-4-nitro-phenyl carbamate (7) from 4-nitrobenzoyl azide (4) and D-glucurono-6,3-lactone acetonide (5) via Curtius Rearrangement.

Reaction of **5** (0.648 g, 3.0 mmol) with **4** (0.576 g, 3.0 mmol) in 20 mL of dry toluene for 4 hours in the manner as the general procedure produced a crude product that was subsequently recrystallized from hot isopropyl alcohol to yield 0.82 g (71.1%) of **7** as pale yellow crystals.

^{1}H NMR ($CDCl_3$): δ 1.36 (3H, s), 1.53 (3H, s), 4.91 (1H, dd, J = 2.8, 3.6), 5.13 (1H, dd, J = 3.0, 4.2), 5.58 (1H, d, J = 4.3), 6.03 (1H, d, J = 3.6), 7.37 (1H, s), 7.55 (2H, d, J = 9.2), 8.22 (2H, d, J = 9.2).

^{13}C NMR ($CDCl_3$): δ 26.51, 26.89, 29.68, 58.48, 70.92, 77.31, 107.05, 113.80, 118.23 (2), 125.25 (2), 142.70, 143.76, 150.90, 169.32.

Melting point: 180-183 ^{o}C.

Synthesis of 5-(2,2-dimethyl-1,3-dioxolan-4-yl)-2,2-dimethyltetrahydrofuro[2,3-d][1,3]diox-ol-6-yl- (4-nitrophenyl) carbamate (9) from 4-nitrobenzoyl azide (4) and 1,2:5,6-di-*O*-isopropylidene-α-D-glucofuranose (8) via Curtius Rearrangement.

Following the general procedure for the synthesis of carbamates via Curtius rearrangement, **8** (0.780 g, 3.0 mmol) was reacted with **4** (0.576 g, 3.0 mmol) in 30 mL of dry toluene for 9 hours. The crude product obtained was subsequently purified via flash column chromatography to yield 1.05 g (82.5%) of **9** as deep yellow syrup.

^{1}H NMR ($CDCl_3$): δ 1.33 (6H, s), 1.45 (3H, s), 1.55 (3H, s), 4.06 (1H, dd, J = 4.8, 8.9), 4.12 (1H, dd, J = 6.0, 8.8), 4.25 (1H, dd, J = 2.9, 8.5), 4.32-4.37 (1H, m), 4.65 (1H, d, J = 3.7), 5.30 (1H, d, J = 2.9), 5.91 (1H, d, J = 3.70), 7.56 (2H, d, J = 9.2), 7.83 (1H, s), 8.17 (2H, d, J = 9.2).

^{13}C NMR ($CDCl_3$): δ 25.26, 26.17, 26.70, 26.89, 67.47, 72.28, 77.54, 79.70, 83.35, 104.99, 109.90, 112.62, 117.91 (2), 125.17 (2), 143.22, 143.75, 151.45

Synthesis of 5-(2,2-dimethyl-1,3-dioxolan-4-yl)-2,2-dimethyltetrahydrofuro[2,3-d][1,3]diox-ol-6-yl- (3-nitrophenyl) carbamate (10) from 3-nitrobenzoyl azide (3) and 1,2:5,6-di-*O*-isopropylidene-α-D-glucofuranose (8) via Curtius Rearrangement.

In a round bottom flask, **8** (0.78 g, 3.0 mmol) was heated with **3** (0.576 g, 3.0 mmol) in 30 mL of dry toluene for 12 hours following the general procedure described above. Thin layer chromatography was employed to monitor the progress of the reaction and the consumption of the starting materials after which flash column chromatography using hexane:ethyl acetate (3:1) was employed to purify the crude product yielding 0.86 g (67.6%) of **10** as pale yellow syrup.

^{1}H NMR ($CDCl_3$): δ 1.33 (3H, s), 1.34 (3H, s), 1.47 (3H, s), 1.55 (3H, s), 4.07 (1H, dd, J = 4.9, 8.8), 4.11-4.16 (1H, m), 4.28 (1H, dd, J = 2.9, 8.4), 4.37-4.42 (1H, m), 4.69 (1H, d, J = 3.7), 5.31 (1H, d, J = 2.9), 5.93 (1H, d, J = 3.7), 7.44 (1H, dd, J = 8.2), 7.76 (1H, d, J = 8.1), 7.86 (1H, d, J = 8.2), 8.21 (1H, s), 8.28 (1H, s).

^{13}C NMR ($CDCl_3$): δ 23.26, 26.15, 26.71, 26.88. 60.58, 67.40, 72.39, 79.76, 83.43, 105.06, 109.91, 112.52, 113.22, 118.07, 124.10, 129.89, 139.26, 148.61, 151.95.

Synthesis of 10,13-dimethyl-17-(6-methylheptan-2-yl)-2,3,4,7,8,9,10,11,12,13,14,15,16,17-tetradecahydro-1*H*-cyclopenta[a]phenanthren-3-yl-(3-nitrophenyl) carbamate (12) from (3β)-cholesterol (11) and 3-nitrobenzoyl azide (3).

As described in the general procedure, cholesterol **(11)** (1.16 g, 3.0 mmol) was heated **3** (0.576 g, 3.0 mmol) in 30 mL of dry toluene overnight and the product was isolated via suction filtration washing the crude crystals with large amounts of hexane. The crude product was then purified via recrystallization from hot ethanol to yield 1.05 g (63.6 %) of **12** as solid white crystals.

^{1}H NMR ($CDCl_3$): δ 0.69 (3H, s), 0.87 (6H, d, J = 6.6), 0.91 (1H, s), 0.93 (2H, d, J = 2.2), 0.94 (1H, s), 0.96 (1H, s), 1.04 (3H, s), 1.07-1.42 (10H, m), 1.43-1.72 (9H, m), 1.79-2.04 (6H, m), 2.33-2.46 (2H, m), 4.60-4.68 (1H, m), 5.41-5.42 (1H, m), 6.80 (1H, s), 7.45 (1H, dd, J = 8.2), 7.74 (1H, d, J = 8.1), 7.9 (1H, d, J = 8.2), 8.29 (1H, s).

^{13}C NMR ($CDCl_3$): δ 11.86, 18.72, 19.31, 21.06, 22.54, 22.79, 23.84, 24.28, 25.90, 28.00, 28.21, 31.89, 31.91, 35.79, 36.20, 36.58, 36.93, 38.36, 39.52, 39.74, 42.34, 50.03, 56.17, 56.70, 64.71, 75.76, 113.24, 117.87, 123.04, 123.99, 129.80, 139.36, 148.80, 152.66.

Melting Point: 173-180 ^{o}C.

Synthesis of 10,13-dimethyl-17-(6-methylheptan-2-yl)-2,3,4,7,8,9,10,11,12,13,14,15,16,17-tetradecahydro-1*H*-cyclopenta[a]phenanthren-3-yl-(4-nitrophenyl) (13) carbamate from (3β)-cholesterol (11) and 4-nitrobenzoyl azide (4).

Following the general procedure for carbamate synthesis, **11** (1.16 g, 3.0 mmol) was reacted with **4** (0.576 g, 3.0 mmol) in dry toluene (30 mL) overnight in the manner described in the general procedure After heating overnight the reaction was allowed to cool to room temperature and the product was isolated via suction filtration. The crude product was then purified via recrystallization from hot ethanol to yield 1.49 g (90.3%) of **13** as white powdery crystals.

^{1}H NMR ($CDCl_3$): δ 0.69 (3H, s), 0.86 (6H, d, J = 6.6), 0.92 (2H, d, J = 2.2), 1.04 (3H, s), 1.09-1.43 (13H, m), 1.47-1.69 (10H, m), 1.79-2.05 (5H, m), 2.33-2.46 (2H, m), 4.60-4.68 (1H, m), 5.41-5.42 (1H, m), 6.87 (1H, s), 7.54 (2H, d, J = 9.2), 8.19 (2H, d, J = 9.2).

^{13}C NMR ($CDCl_3$): δ 11.86, 18.72, 19.31, 21.06, 22.54, 22.79, 23.84, 24.28, 25.90, 28.00, 28.21, 31.89, 31.91, 35.79, 36.20, 36.58, 36.93, 38.36, 39.52, 39.74, 42.34, 50.03, 56.17, 56.70, 75.95, 113.25, 123.13, 125.22 (2), 129.81 (2), 142.98, 144.05, 152.25.

IR: 3429 cm^{-1} (N-H), 2950 cm^{-1} (C-H), 1734 cm^{-1} (C=O).

Meting Point: 187-191 ^{o}C.

Synthesis of 1,7,7-trimethylbicyclo[2.2.1]heptan-2-yl (4-nitrophenyl) carbamate (15) from L-(-)-borneol (14) and 4-nitrobenzoyl azide (4).

In a 50 mL round bottom flask, **14** (0.46 g, 3.0 mmol) was added to **4** (0.576 g, 3.0 mmol) and heated in 30 mL of dry toluene as described in the general procedure for 7 hours after which the crude product was purified via flash column chromatography using hexane:ethyl acetate (3:1) to yield 0.81 g (85%) of **15** as deep yellow syrup.

^{1}H NMR ($CDCl_3$): δ 0.88 (6H, s), 0.92, (3H, s), 1.25 (1H, dd, J = 3.2, 14.1), 1.28-1.39 (2H, m), 1.70-1.81 (2H, m), 1.91 (1H, ddd, J = 4.2, 9.1, 13.1), 2.36-2.44 (1H, m), 4.96 (1H, dd, J = 3.3, 9.9), 7.56 (1H, s), 7.62 (2H, d, J = 9.2), 8.19 (2H, d, J = 9.2).

^{13}C NMR ($CDCl_3$): δ 18.79, 19.69, 27.08, 28.04, 36.71, 44.83, 47.93, 48.89, 60.56, 81.88, 117.73 (2), 125.20 (2), 142.76, 144.57, 153.52.

IR: 3428 cm^{-1} (N-H), 2959 cm^{-1} (C-H), 1734 cm^{-1} (C=O).

Synthesis of 1,7,7-trimethylbicyclo[2.2.1]heptan-2-yl (3-nitrophenyl) carbamate (16) from L-(-)Borneol (14) and 3-nitrobenzoyl azide (3).

As described in the general procedure, **14** (0.46 g, 3.0 mmol) was reacted with **3** (0.576 g, 3.0 mmol) for 12 hours in 30 mL of dry toluene. The crude product was purified via flash column chromatography using hexane:ethyl acetate (3:1) to yield 0.66 g (69 %) of **16** as deep yellow syrup.

^{1}H NMR ($CDCl_3$): δ 0.89 (6H, s), 0.92, (3H, s), 1.25 (1H, dd, J = 3.2, 14.1), 1.22-1.40 (2H, m), 1.70-1.80 (2H, m), 1.92 (1H, ddd, J = 4.2, 9.1, 13.1), 2.37-2.45 (1H, m), 4.97 (1H, dd, J = 3.3, 9.9), 7.27 (1H, s), 7.45 (1H, dd, J = 8.2), 7.77 (1H, d, J = 7.8), 7.89 (1H, d, J = 8.2), 8.37 (1H, s).

^{13}C NMR ($CDCl_3$): δ 18.78, 19.66, 27.09, 28.02, 36.71, 44.81, 47.89, 48.85, 60.48, 81.69, 113.28, 117.72, 124.05, 129.74, 139.57, 148.74, 153.80.

IR: 3432 cm^{-1} (N-H), 2959 cm^{-1} (C-H), 1730 cm^{-1} (C=O).

Project 2

General procedure for the synthesis of chloroformates.

To a 100 mL round bottom flask containing a stir bar, the alcohol was added to triphosgene and a rubber septum fitted. The reaction vessel was purged three times with nitrogen gas and a balloon containing nitrogen gas fitted into the reaction chamber through the rubber septum. Dry THF was added to the mixture as solvent and while stirring at 0 ^{o}C, anhydrous pyridine was pipetted into the reaction mixture as catalyst. The reaction was allowed to stir for 6 hours while allowing it to slowly warm up to room temperature in the process. TLC was employed to monitor the consumption of the starting material. The mixture was then filtered to obtain the crude product after which the solvent was evaporated off the crude product via vacuum.

Synthesis of 3-*O*-(chloroacyl)-1,2:5,6-di-*O*-isopropylidene-α-D-glucofuranose (17) from 1,2:5,6-di-*O*- isopropylidene -α-D-glucofuranose (8).

1.56 g (6 mmol) of **8** was reacted with 2.079 g (7 mmol) of triphosgene and 0.3 mL (3.7 mmol) of anhydrous pyridine in dry THF (45 mL) as described in the general procedure for the synthesis of chloroformates to yield 1.83 g (95%) of **17** as colorless syrup for the next reaction.

^{1}H NMR ($CDCl_3$): δ 1.31 (6H, s), 1.40 (3H, s), 1.52 (3H, s), 4.00 (1H, dd, J = 4.2, 8.7), 4.07-4.13 (1H, m), 4.17-4.24 (2H, m), 4.54 (1H, d, J = 3.7), 5.35 (1H, d, J = 2.3), 5.89 (1H, d, J = 3.7).

^{13}C NMR ($CDCl_3$): δ 25.03, 26.04, 26.55, 26.71, 67.16, 72.15, 75.61, 79.59, 83.12, 104.96, 109.27, 112.20, 159.42.

IR: 2932.51 cm^{-1} (C-H), 1664.07 cm^{-1} (C=O), 1093.97 cm^{-1} (C-O).

Synthesis of 2,3-dihydro-1*H*-inden-2-yl carbonochloridate (20) from 2-indanol (19).

As described in the chloroformate synthesis procedure above, 0.636 g (6 mmol) of 2-indanol **(19)** was reacted with 2.079 g (7 mmol) of triphosgene in 45 mL of dry THF at 0 ^{o}C adding 0.3 mL (3.7 mmol) of anhydrous pyridine to yield 0.81 g (80.1%) of **20** as brownish crude crystals.

^{1}H NMR ($CDCl_3$): δ 3.16 (2H, dd, J = 2.6, 17.3), 3.35 (2H, dd, J = 6.2, 17.4), 5.60 (1H, dd, J = 2.8, 6.1), 7.18-7.85 (4H, m).

^{13}C NMR ($CDCl_3$): δ 39.31, 83.87, 124.70, 124.22, 139.24, 150.49.

IR: 2963.4 cm^{-1} (C-H), 1768.08 cm^{-1} (C=O), 1161.68 cm^{-1} (C-O).

Synthesis of 1,7,7-trimethylbicyclo[2.2.1]heptan-2-yl carbonochloridate (22) from L-(-)-borneol (14).

In a 100 mL round bottom flask containing a stir bar, 1.54 g (10 mmol) of **14** was reacted with 3.26 g (11 mmol) of triphosgene while adding 0.5 mL (6 mmol) of anhydrous pyridine in 45 mL of dry THF at 0 ^{o}C. The mixture was then filtered to obtain a clear solution of the crude product after which the solvent was evaporated off the crude product under reduced pressure to yield 2.0 g (92.6%) of **22** as brown oil for the next reaction.

^{1}H NMR ($CDCl_3$): δ 0.89 (6H, s), 0.91 (3H, s), 1.18 (1H, dd, J = 3.2, 14.1), 1.26-1.39 (2H, m), 1.73-1.95 (2H, m), 2.36-2.44 (1H, m), 4.99 (1H, d, J = 9.4).

^{13}C NMR (($CDCl_3$): δ 13.31, 18.70, 19.59, 26.78, 27.78, 36.07, 44.66, 48.06, 49.29, 89.29, 150.53.

IR: 2961.03 cm^{-1} (C-H), 1770.37 cm^{-1} (C=O), 1178.18 cm^{-1} (C-O).

Synthesis of 10,13-dimethyl-17-(6-methylheptan-2-yl)-2,3,4,7,8,9,10,11,12,13,14,15,16,17-tetradecahydro-1*H*-cyclopenta[a]phenanthren-3-yl carbonochloridate (24) from cholesterol (11).

Following the procedure for the synthesis of chloroformates 1.935 g (5 mmol) of **11** was added to 2.08 g (7 mmol) of triphosgene and reacted with 0.5 mL of anhydrous pyridine in 45 mL of dry THF at 0 ^{o}C to yield 1.86 g (83%) of **24** as white crystals for the next reaction.

^{1}H NMR ($CDCl_3$): δ 0.68 (3H, s), 0.87 (6H, d, J = 6.4), 0.91 (3H, d, J = 6.4), 1.02 (3H, s), 1.06-1.16 (8H, m), 1.25-1.77 (10H, m), 1.81-2.02 (6H, m), 2.17-2.45 (3H, m), 3.65-3.82 (1H, m), 5.42-5.50 (1H, m).

^{13}C NMR ($CDCl_3$): δ 11.87, 18.73, 19.23, 21.06, 22.57, 22.82, 23.84, 24.28, 27.41, 28.01, 28.21, 31.91, 35.77, 36.20, 36.80, 37.61, 39.53, 39.70, 42.32, 49.97, 56.17, 56.66. 83.06, 123.82, 138.52, 149.68.

IR: 2951.20 cm^{-1} (C-H), 1769.36 cm^{-1} (C=O), 1167.28 cm^{-1} (C-O).

General procedure for the synthesis of azidoformates.

To a 100 mL round bottom flask containing the chloroformate was added 0.2 g of tetrabutylammonium bromide. The mixture was dissolved in of CH_2Cl_2 and a reflux condenser attached. While the reaction stirs at room temperature, sodium azide dissolved in acetone and water (3:1) was pipetted though the condenser into the reaction mixture and reaction was allowed to proceed overnight. TLC was used to monitor the disappearance of the chloroformate and the subsequent formation of the azidoformate. The reaction mixture was then transferred into a separatory funnel and washed three times with 50 mL of water after which the lower organic layer was dried over anhydrous $MgSO_4$ for 15 minutes. The filtrate was evaporated under vacuum and purified via flash

column chromatography using hexane:ethyl acetate (3:1) mixture to yield the purified azidoformate product.

Synthesis of 3-*O*-(azidoacyl)-1,2:5,6-di-*O*-isopropylidene-α-D-glucofuranose (18) from 3-*O*-(chloroacyl)-1,2:5,6-di-*O*-isopropylidene-α-D-glucofuranose (17).

As described in the general procedure for azidoformate synthesis, 1.83 g (5.67 mmol) of the chloroformate **(17)** was reacted with 0.65 g (10 mmol) of sodium azide dissolved in acetone and water (3:1), in 40 mL of methylene chloride to yield 1.49 g (80.1%) of purified product **18**.

^{1}H NMR ($CDCl_3$): δ 1.32 (3H, s), 1.33 (3H, s), 1.42 (3H, s), 1.52 (3H, s), 4.00 (1H, dd, J = 4.2, 8.7), 4.07-4.13 (1H, m), 4.19-4.22 (2H, m), 4.58 (1H, d, J = 3.7), 5.23 (1H, d, J = 2.3), 5.90 (1H, d, J = 3.7).

^{13}C NMR ($CDCl_3$): δ 25.13, 26.15, 26.63, 26.85, 67.26, 72.17, 79.65, 79.95, 82.99, 105.01, 109.50, 112.49, 159.66.

IR: 2937.84 cm^{-1} (C-H), 2119.97 cm^{-1} ($-N_3$), 1681.15 cm^{-1} (C=O), 1090.19 cm^{-1} (C-O).

Synthesis of 2,3-dihydro-1*H*-inden-2-yl carbonazidate (21) from 2,3-dihydro-1*H*-inden-2-yl carbonochloridate (20).

In a 100 mL round bottom flask containing 0.81 g (4.8 mmol) of the chloroformate **20** and 0.1 g of tetrabutylammonium bromide were dissolved in 30 mL of CH_2Cl_2 and reacted with 0.46 g (7 mmol) of sodium azide dissolved in acetone and water (3:1) to yield while solid crystals which were recrystallized from hot isopropyl alcohol for 94% yield (0.79 g) of purified product **(21)**.

^{1}H NMR ($CDCl_3$): δ 3.10 (2H, dd, J = 2.6, 17.3), 3.34 (2H, dd, J = 6.2, 17.4), 5.52 (1H, dd, J = 2.8, 6.1), 7.17-7.23 (4H, m).

^{13}C NMR ($CDCl_3$): δ 39.34, 79.94, 124.66, 127.02, 139.63, 157.41.

IR: 3058.66 cm^{-1} (C-H), 2137.94 cm^{-1} (-N_3), 1716.15 cm^{-1} (C=O), 1091.19 cm^{-1} (C-O).

Synthesis of 1,7,7-trimethylbicyclo[2.2.1]heptan-2-yl carbonazidate (23) from ,7,7-trimethylbicyclo[2.2.1]heptan-2-yl carbonochloridate (22).

Following the general procedure for azidoformate synthesis, 2.0 g (9.3 mmol) of **22** and 0.2 g of tetrabutylammonium bromide were dissolved in 30 mL of CH_2Cl_2 and then reacted with 0.975 g (15 mmol) of sodium azide dissolved in acetone and water (3:1)

to yield yellow oil which was purified with flash column chromatography using hexane:ethyl acetate in a 3:1 ratio for 84% yield (1.73 g) of purified product **(23)**.

^{1}H NMR ($CDCl_3$): δ 0.88 (3H, s), 0.89 (3H, s), 0.91 (3H, s), 1.10 (1H, dd, J = 3.4, 13.9), 1.22-1.36 (2H, m), 1.75-1.81 (2H, m), 2.35-2.43 (1H, m), 4.90 (1H, dd, J = 3.4, 9.4).

^{13}C NMR ($CDCl_3$): δ 13.24, 18.64, 19.50, 26.70, 27.78, 36.23, 44.68, 47.91, 48.96, 84.71, 157.48.

IR: 2961.94 cm^{-1} (C-H), 2137.19 cm^{-1} (N_3), 1714.20 cm^{-1} (C=O).

Synthesis of 10,13-dimethyl-17-(6-methylheptan-2-yl)-2,3,4,7,8,9,10,11,12,13,14,15,16,17-tetradecahydro-1*H*-cyclopenta[a]phenanthren-3-yl carbonazidate (25) from 10,13-dimethyl-17-(6-methylheptan-2-yl)-2,3,4,7,8,9,10,11,12,13,14,15,16,17-tetradecahydro-1H- cyclopenta[a]phenanthren-3-yl carbonochloridate (24).

As described in the general procedure for azidoformate synthesis, 1.86 g (4.1 mmol) of **24** and 0.1 g of tetrabutylammonium bromide were dissolved in 30 mL of CH_2Cl_2 reacted with 0.46 g (7 mmol) of sodium azide dissolved in acetone and water

(3:1) to yield colorless crystals which were recrystallized from hot isopropyl alcohol for 69.5% yield (1.3 g) of purified product **25**.

^{1}H NMR ($CDCl_3$): δ 0.68 (3H, s), 0.86 (6H, d, J = 6.4), 0.92 (3H, d, J = 6.4), 1.02 (3H, s), 1.06-1.16 (8H, m), 1.25-1.77 (10H, m), 1.81-2.02 (6H, m), 2.17-2.45 (3H, m), 4.56-4.64 (1H, m), 5.35-5.45 (1H, m).

^{13}C NMR ($CDCl_3$): δ 11.85, 19.23, 21.04, 22.54, 22.79, 23.83, 24.25, 27.53, 28.00, 31.84, 31.90, 35.78, 36.20, 36.80, 37.81, 39.52, 39.72, 42.33, 50.01, 56.17, 56.69. 78.83, 123.34, 138.94, 156.84.

IR: 2988.02cm^{-1} (C-H), 2126.59 cm^{-1} (-N_3), 1712.76 cm^{-1} (C=O).

Thermal decomposition of 3-*O*-(azidoacyl)-1,2:5,6-di-*O*-isopropylidene-α-D-glucofuranose (18) in cyclohexane to form 26.

To a 50 mL round bottom flask containing a stir bar, 0.5 g (1.5 mmol) of 1**8** was dissolved in 15 mL of cyclohexane and a reflux condenser attached. The reaction was allowed to heat at 100 ^{o}C for 72 hours and TLC with 10:1 hexane-ethyl acetate solvent system was used to monitor the complete consumption of the starting material. After the reaction was completed the crude product was isolated via evaporation of cyclohexane under vacuum. The crude product was then purified using 20 g of 60 Å silica gel and 3:1

hexane:ethyl acetate in flash column chromatograpy to yield 0.2 g (40%) of **26** as colorless syrup which solidified after 24 hours.

^{1}H NMR ($CDCl_3$): δ 1.15 (2H, quintet, J = 3.1) 1.30, (3H, s), 1.33, (3H, s), 1.42, (3H, s), 1.51, (3H, s), 1.60-1.63 (1H, m), 1.68-1.73 (4H, m), 1.93-1.96 (4H, m), 3.50 (1H, s), 3.99-4.11 (2H, m), 4.21-4.23 (1H, m), 4.56-4.62 (1H, m), 5.17 (1H, s), 5.85 (1H, d, J = 3.3).

^{13}C NMR ($CDCl_3$): δ 24.73, 25.42, 26.19, 26.74, 33.25, 50.06 (2), 66.95 (2), 72.58, 76.31, 79.84, 79.92, 81.28, 83.51, 104.95, 109.22, 112.14, 153.96.

Thermal decomposition of 3-*O*-(azidoacyl)-1,2:5,6-di-*O*-isopropylidene-α-D-glucofuranose (18) in mesitylene to form 27.

In a 50 mL round bottom flask containing a stir bar, 0.5 g (1.5 mmol) of **18** was dissolved in 15 mL of mesitylene and a reflux condenser attached. The reaction was heated at 120 ^{o}C for 24 hours and thin layer chromatography was used to monitor the consumption of the starting material using 5:1 hexane-ethyl acetate as eluent. After the reaction was completed, the crude product was isolated via evaporation of mesitylene under reduced pressure. The crude product was then purified using 20 g of 60 Å silica gel

and 5:1 hexane:ethyl acetate in flash column chromatograpy to obtain 0.33 g (66%) of **27** as pale yellow syrup.

^{1}H NMR ($CDCl_3$): δ 1.31 (6H, s), 1.40 (3H, s), 1.51 (3H, s), 2.20 (3H, s), 2.25 (3H, s), 2.30 (3H, s), 4.03 (1H, d, J = 4.6), 4.11 (1H, s), 4.25 (1H, s) 4.59 (1H, d, J = 6.4), 5.36 (1H, s), 6.14 (1H, s), 6.86 (2H, s).

^{13}C NMR ($CDCl_3$): δ 18.10, 20.89, 21.22, 25.28, 26.23, 26.79, 65.25 67.31 (2), 72.68, 76.58, 80.38, 83.72, 105.17, 109.32, 112.27, 124.80, 128.98 (2), 129.15, 135.50, 138.08, 140.95, 152.92.

Thermal decomposition of 2,3-dihydro-1*H*-inden-2-yl carbonazidate (21) in mesitylene to form 28.

Similar to the previous decomposition procedure, 0.83 g (5 mmol) of **21** was heated in 30 mL of mesitylene in a 100 mL round bottom flask at 120 ^{o}C for 16 hours. TLC was used to monitor the complete consumption of the starting material, and after completion, the reaction mixture was allowed to cool to room temperature and purified with hexane:ethyl acetate (3:1) and 20 g of 60 Å silica gel in flash column chromatography to yield 0.58 g (70%) of **28** as brown crystals.

^{1}H NMR ($CDCl_3$): δ 2.20 (3H, s), 2.25 (6H, s), 3.08 (2H, dd, J = 5.9, 16.8), 3.33 (2H, dd, J = 5.9, 16.8), 5.55 (1H, s), 6.86 (2H, s), 7.19 (2H, s), 7.25 (1H, s).

^{13}C NMR ($CDCl_3$): δ 18.23, 20.88, 39.92, 75.99, 124.69, 126.77, 128.92, 130.99, 135.53, 136.80, 140.63, 154.35.

Thermal decomposition of 7,7-trimethylbicyclo[2.2.1]heptan-2-yl carbonazidate (23) in mesitylene to form 29.

As described for the synthesis of **28**, **23** (1.73 g, 7.8 mmol) was heated in 30 mL of mesitylene at 120 ^{o}C for 24 hours. After which the reaction mixture was allowed to cool to room temperature and purified with hexane:ethyl acetate (3:1) and 20 g of 60 Å silica gel in flash column chromatography to yield 0.86 g (57% yield) of product **29**.

^{1}H NMR ($CDCl_3$): δ 0.89 (9H, s), 0.96-1.05 (2H, m), 1.26-1.43 (2H, m), 1.65-1.80 (2H, m), 1.99-2.09 (1H, m), 2.21 (6H, s), 2.25 (3H, s), 4.81-5.09 (1H, m), 6.00 (1H, s), 6.86 (2H, s).

^{13}C NMR ($CDCl_3$): δ 13.49, 18.18, 18.87, 20.89, 21.21, 27.11, 28.11, 36.84, 44.91, 47.78, 47.85, 48.78, 48.90, 80.28, 128.80, 135.59, 136.60, 155.10.

Thermal decomposition of 2,3-dihydro-1*H*-inden-2-yl carbonazidate (21) in Diphenyl ether to form 30.

To a 50 mL round bottom flask containing a stir bar, 0.79 g (3.9 mmol) of **21** was dissolved in 20 mL of Ph_2O and the reaction was allowed to heat at 120 ^oC for 6 hours. TLC with 10:1 hexane-ethyl acetate eluent was used to monitor the complete consumption of the starting material after which the reaction mixture was allowed to cool at room temperature and then purified with 10:1 hexane:ethyl acetate and 20 g of 60 Å silica gel in flash column chromatography to yield 0.42 g (53%) of **30** as orange-brown crystals.

^{1}H NMR ($CDCl_3$): δ 3.09 (2H, dd, J = 2.6, 17.0), 3.34 (2H, dd, J = 6.2, 17.0), 5.58 (1H, quintet, J = 2.7), 6.50 (1H, s), 6.95 (2H, s), 6.97 (2H, s), 7.19-7.33 (9H, m).

^{13}C NMR ($CDCl_3$): δ 39.81, 76.38, 118.27, 118.91, 119.91, 120.37, 122.95, 124.74, 126.87, 129.70, 129.73, 133.46, 140.46, 152.87, 153.47, 157.77.

References

1. Dequirez, G.; Pons, V; Dauban, P. *Angew. Chem. Int. Ed.* **2012***, 51*, 7384-7395.
2. Lwowski, W. "Nitrenes", *Wiley*, *New York*, **1970**, pp. 405-419.
3. Wentrup, C. "Reactive Molecules: The Neutral Reactive Intermediates in Organic Chemistry", *Wiley, New York*, **1984**, pp. 220-242.
4. Bayley, H. "Photogenerated Reagents in Biochemistry and Molecular Biology", *Elsevier*, New York, **1983**, pp. 68-94.
5. Uchida, T.; Katsuki, T. *Chem. Rec.*, **2014**, *14*, 117-129.
6. Gritsan, N. P.; Platz, M. S.; Bräse, S.; Banert, K. "Organic Azides: Synthesis and Application", *Wiley*, *Chichester*, **2009**, pp. 311-372.
7. Platz, M. S.; Moss, R. A.; Jons, M. J. "Reactive Intermediate Chemistry. Part 1", *Wiley, Hoboken, NJ*, **2004**, pp. 501-560.
8. Abramovitch, R. A.; Davis, B. A. *Chem. Rev*., **1964**, *64*, 149-185.
9. Lwowski, W. *Ang. Chem*. **1967**, *79*, 922–931.
10. Terashima, S.; Yamada, S. *Chem. Pharm. Bull*., **1968**, *16*, 1953-1971.
11. Fargher, J. M.; Hill, J. W.; Hall, J. H. *J. Am. Chem. Soc*., **1968**, *90*, 5313-5314.
12. Anastassiou, J. G. *J. Am. Chem. Soc.*, **1966**, *88*, 2322-2324.
13. Lwowski, W.; Linke, S.; Tisue, G. T. *J. Am. Chem. Soc.,* **1967**, *89*, 6303-6308.
14. Lwowski W.; DeMauriac, R. *Tetrahedron Lett.,* **1964**, 3285-3288.
15. Lwowski W.; Woerner, F.P. *J. Am. Chem. Soc*. **1965**, *87*, 5491-5492.
16. Breslow, D. S.; Prosser, T. J.; Marcantonio, A. F.; Genge C. A. *J. Am. Chem. Soc*., **1967**, *89*, 2384-2390.

17. McConaghy J. S.; Lwowski, W. *J. Am. Chem. Soc.,* **1967**, *89*, 2357-2364.

18. Migawa, M. T.; Swayze, E. E. *Org. Lett.,* **2000**, *2*, 3309-3311.

19. Lebel, H.; Leogane, O. *Org. Lett.,* **2005**, *7*, 4107-4110.

20. Groszek, G. *Org. Process Res. Dev.,* **2002**, *6,* 759-761.

21. Brown, I.; Edwards, E.; Mcintosh, J. M., Vocelle, D. *Can. J. Chem.*, **1969**, *47*, 2751-2762.

22. Wright, J. J. K.; Albarella, J. A.; Lee, P. *J. Org. Chem.,* **1982***, 47,* 523-527.

23. Williams, D. R.; Rojas, C. M.; Bogen, S. L. *J. Org. Chem.* **1999**, *64,* 736-746.

24. Feuer, B. I.; Smolinsky, G. *J. Am. Chem. Soc.*, **1964**, *86*, 3085-3088.

25. Evans, D. A. *Aldrichim. Acta*, **1982**, *15*, 23-32.

26. Berndt, D. F., *MS Thesis (Chemistry)* – Youngstown State University, **2001**, pp. 31-35.

27. Brown, I., Edwards, E., *Can. J. Chem.*, **1967**, *45*, 2600-2604.

Appendix A

(NMR & IR Spectra)

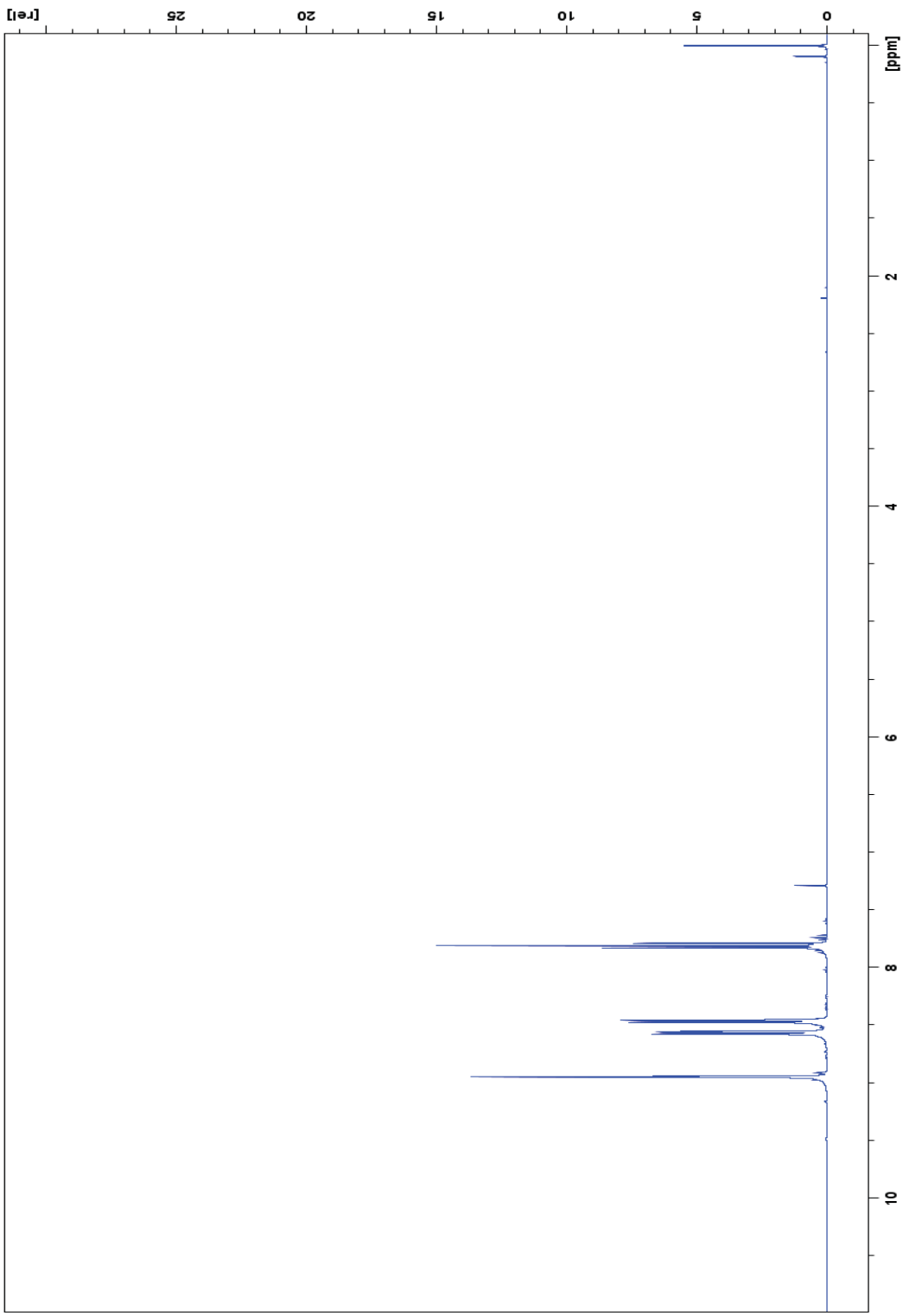

Figure 6: ^{1}H NMR spectrum for compound **1**.

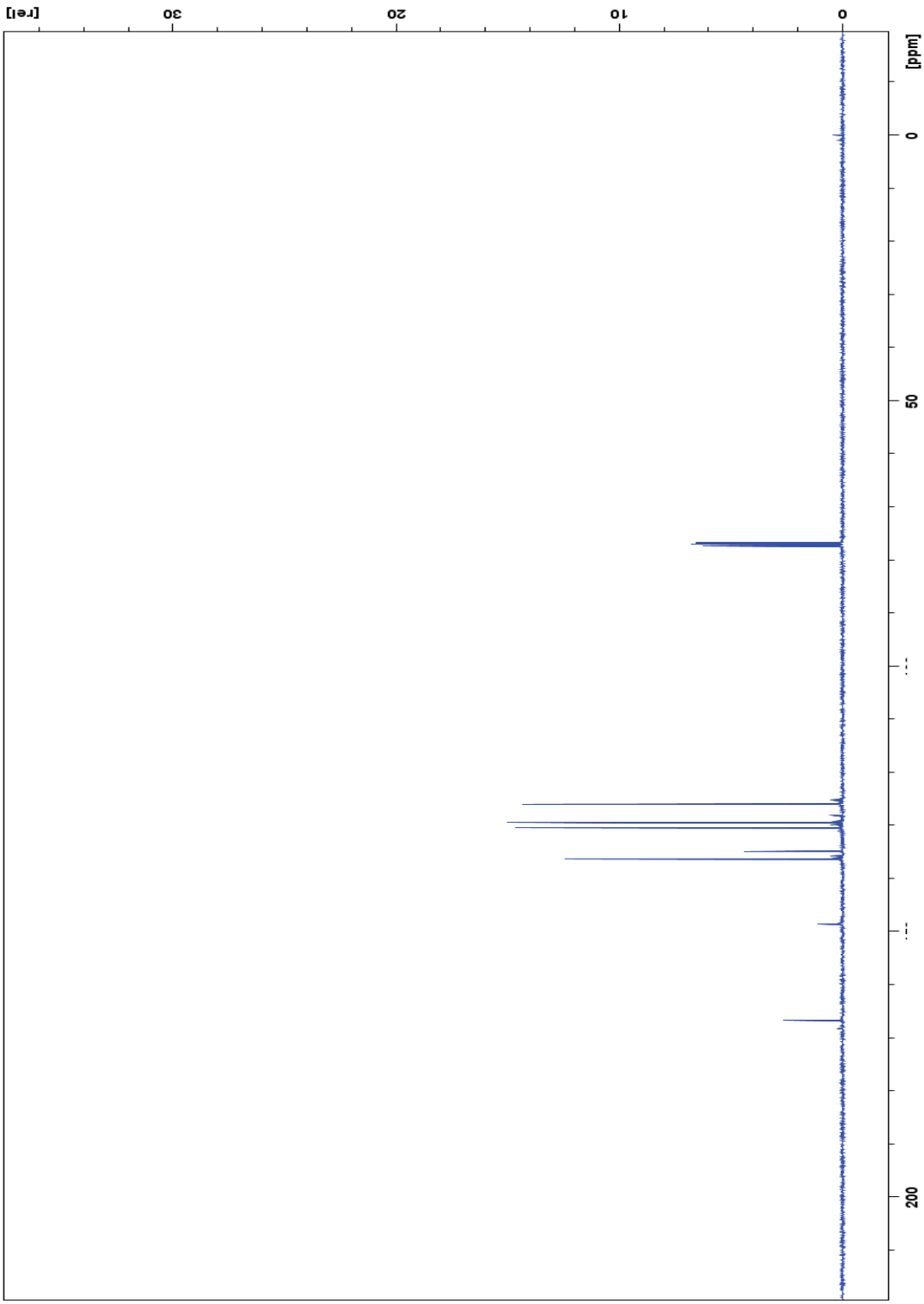

Figure 7: ^{13}C NMR spectrum for compound **1**.

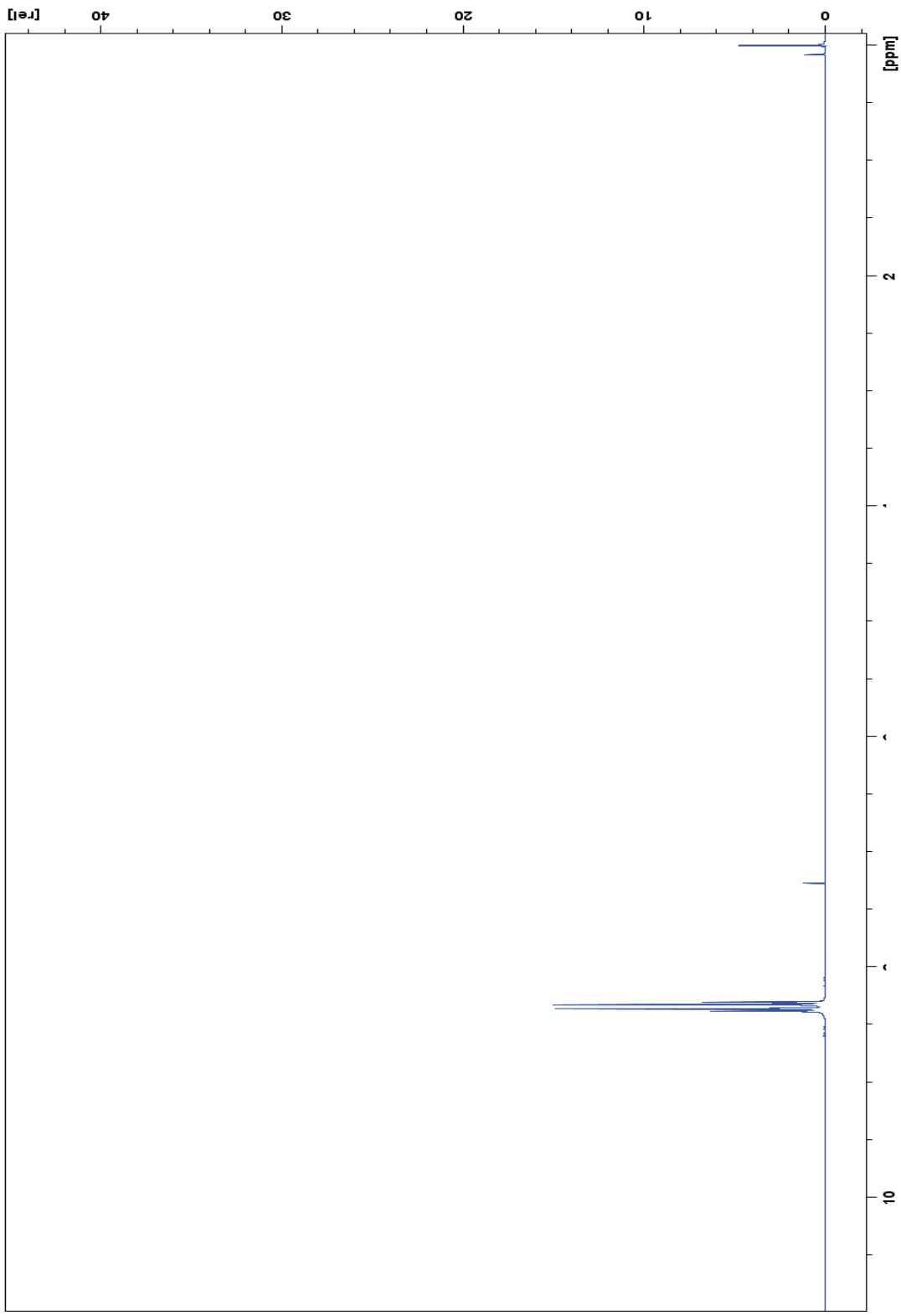

Figure 8: ^{1}H NMR spectrum for compound **2**.

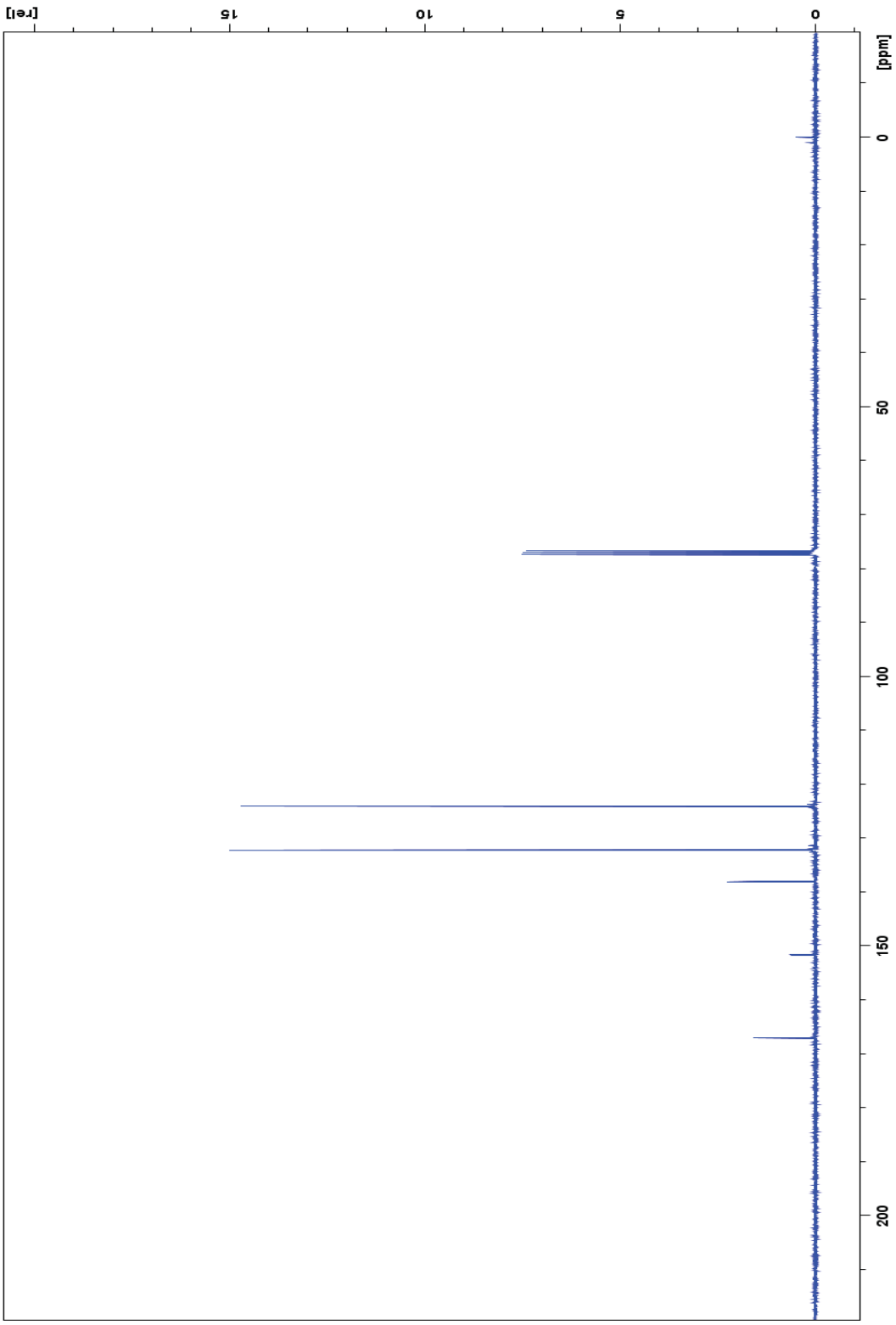

Figure 9: ^{13}C NMR spectrum for compound **2**.

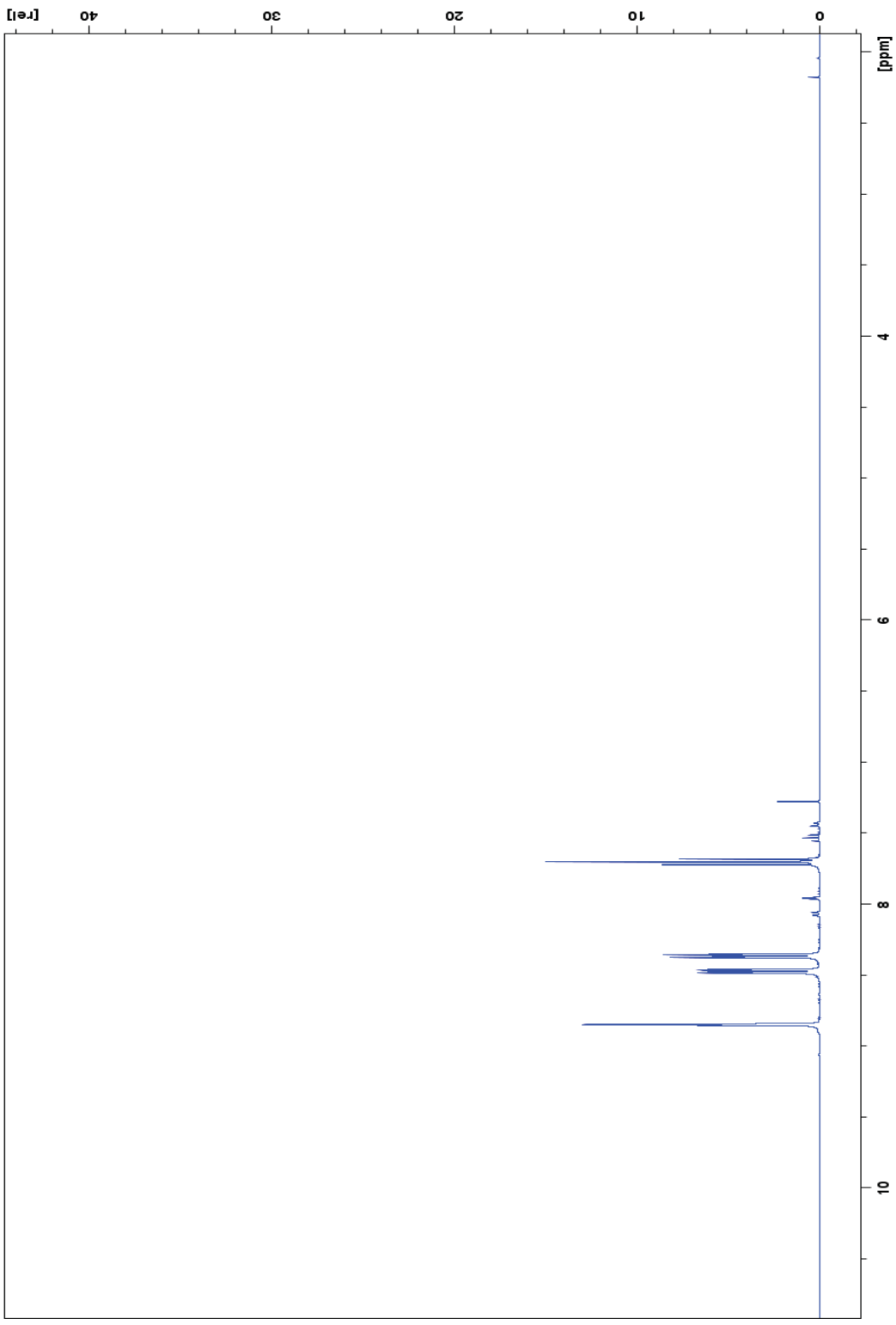

Figure 10: ^{1}H NMR spectrum for compound **3**.

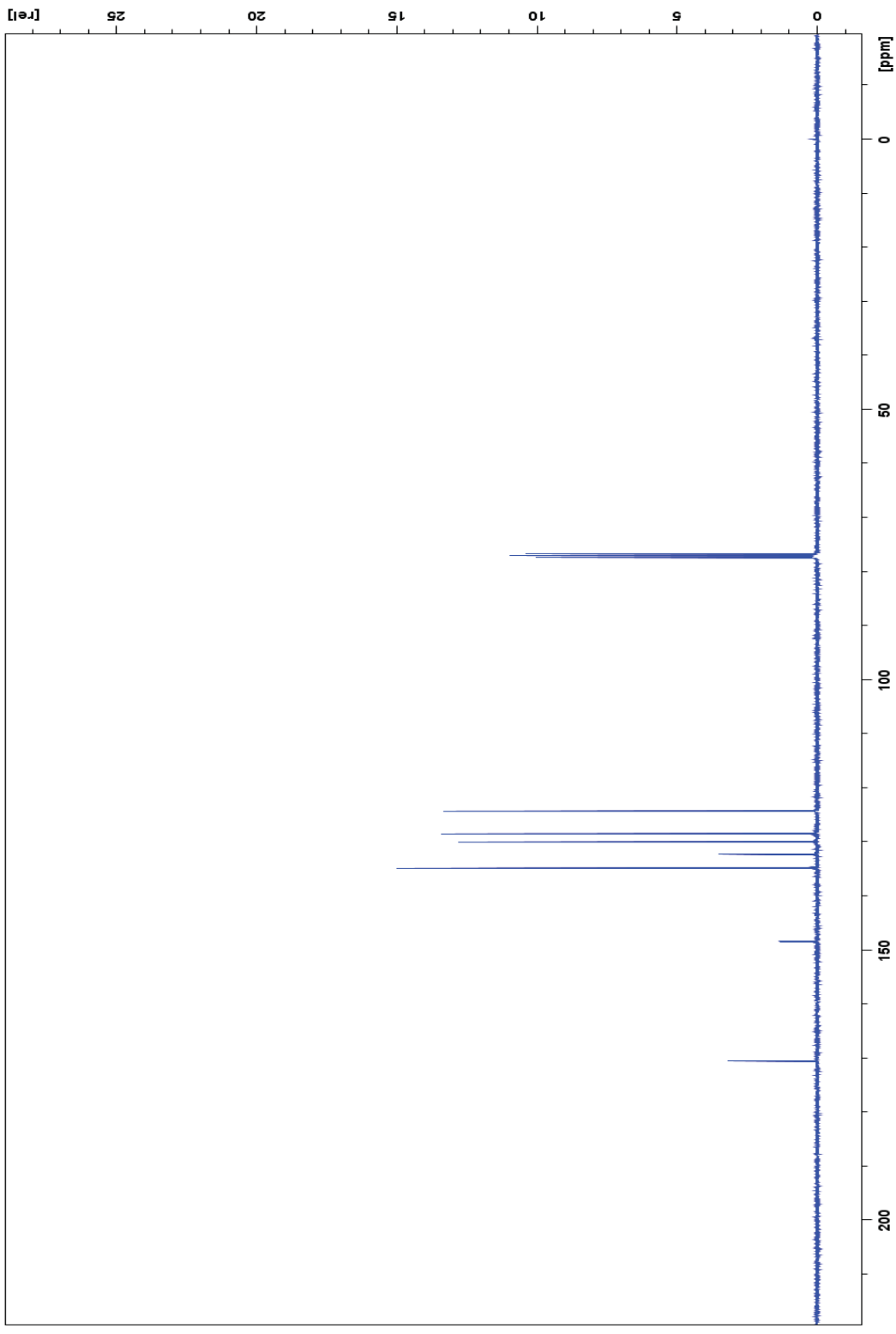

Figure 11: ^{13}C NMR spectrum for compound **3**.

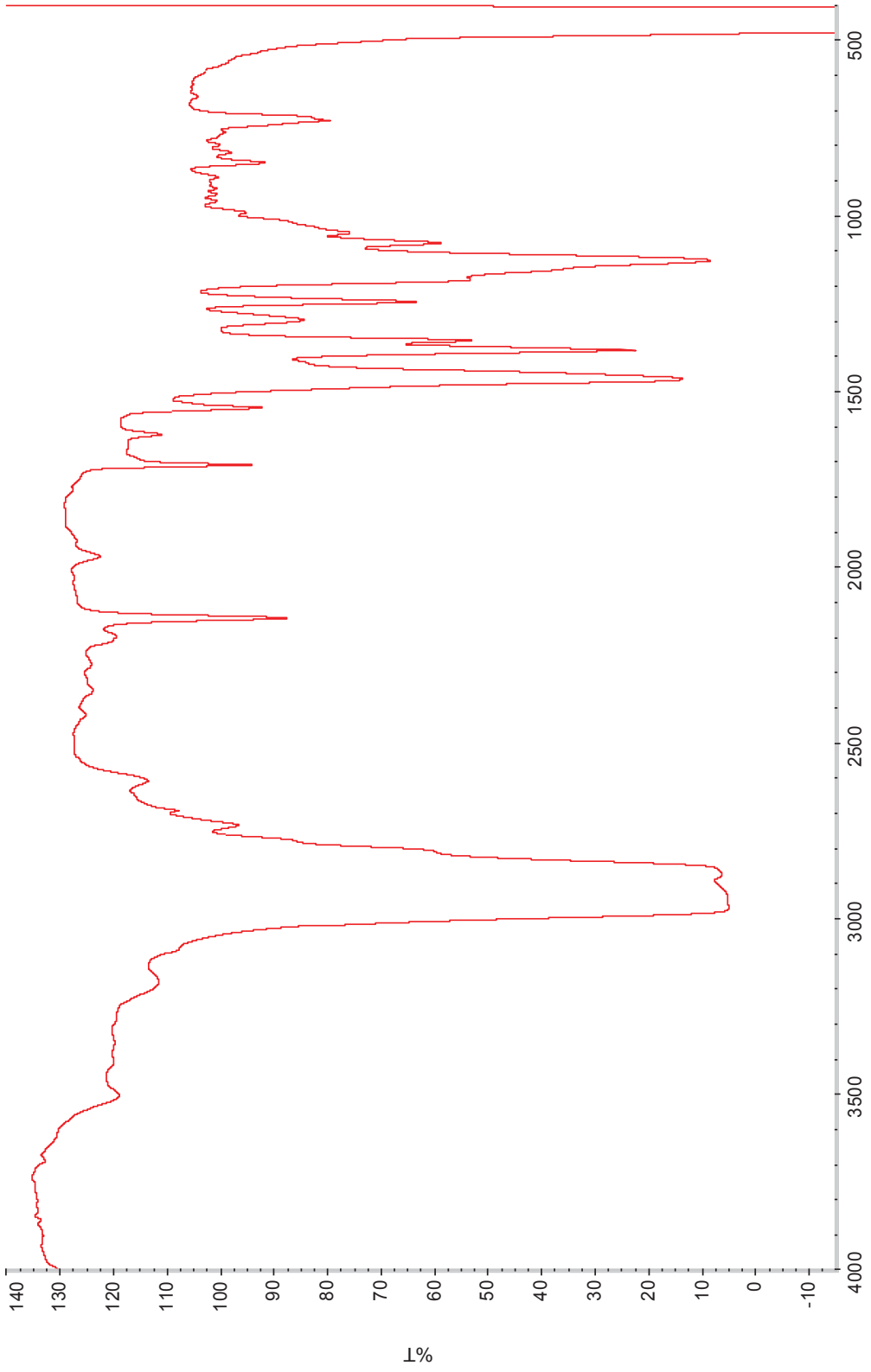

Figure 12: IR spectrum for compound **3**.

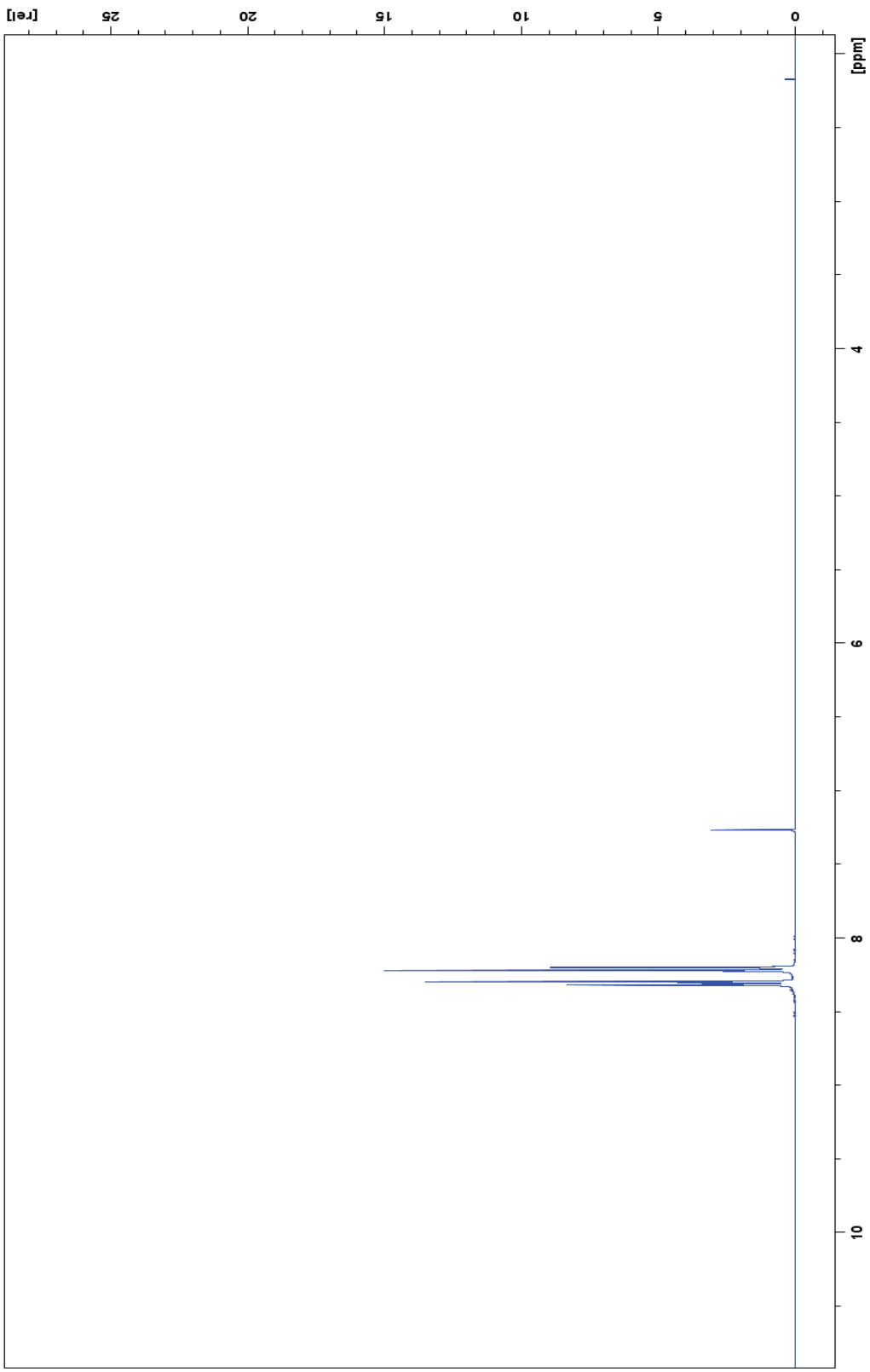

Figure 13: ^{1}H NMR spectrum for compound **4**.

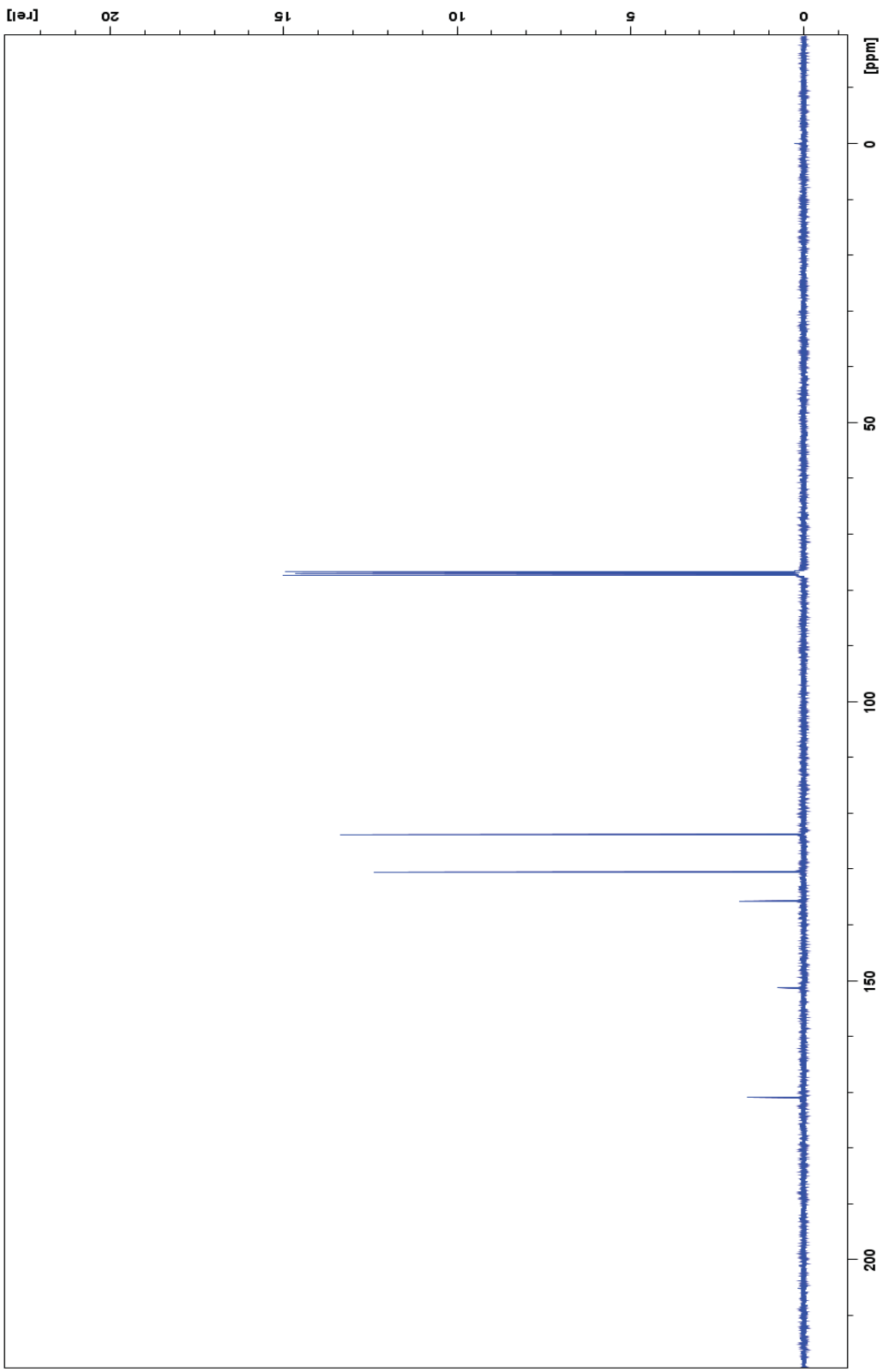

Figure 14: ^{13}C NMR spectrum for compound **4**.

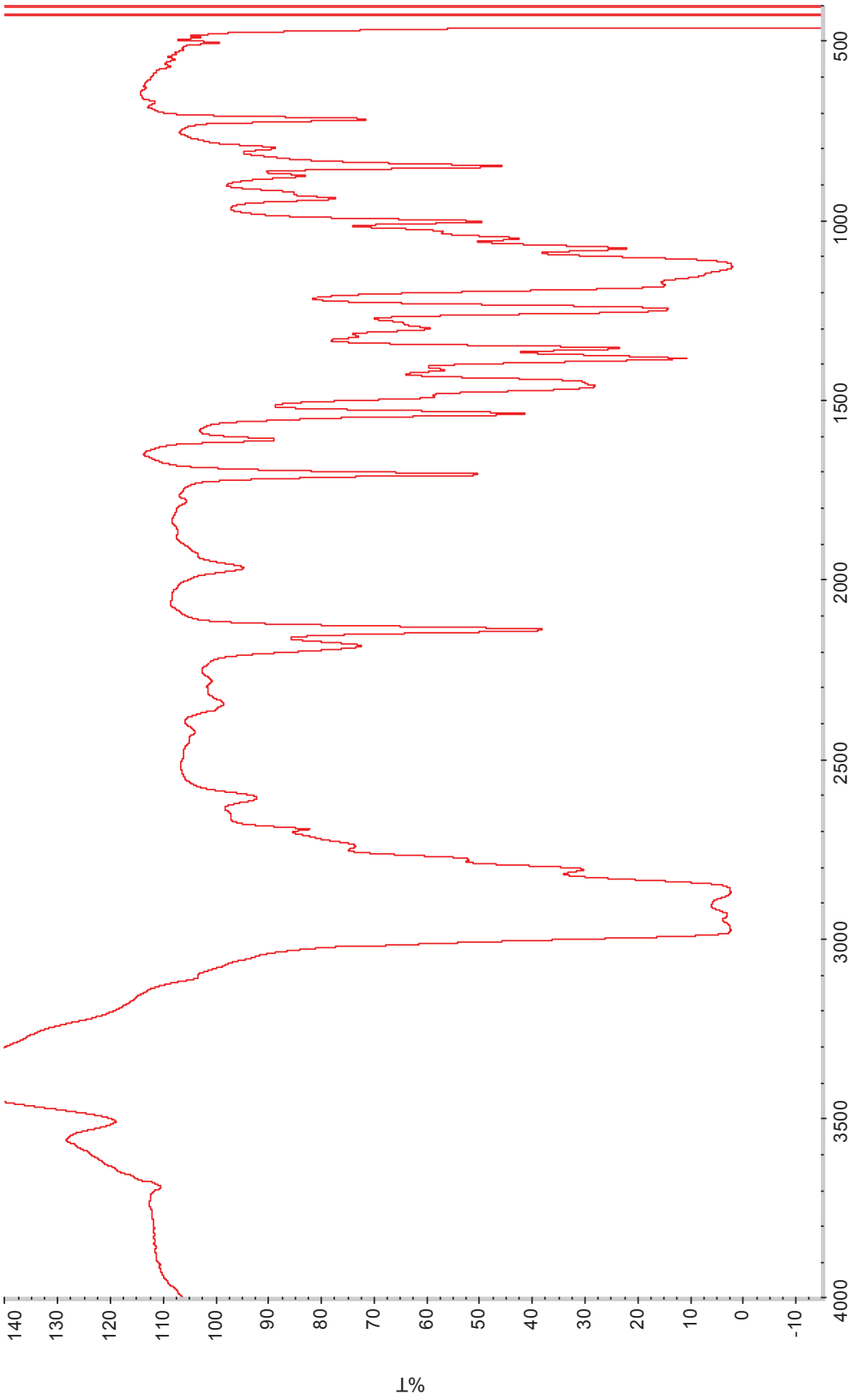

Figure 15: IR spectrum for compound **4**.

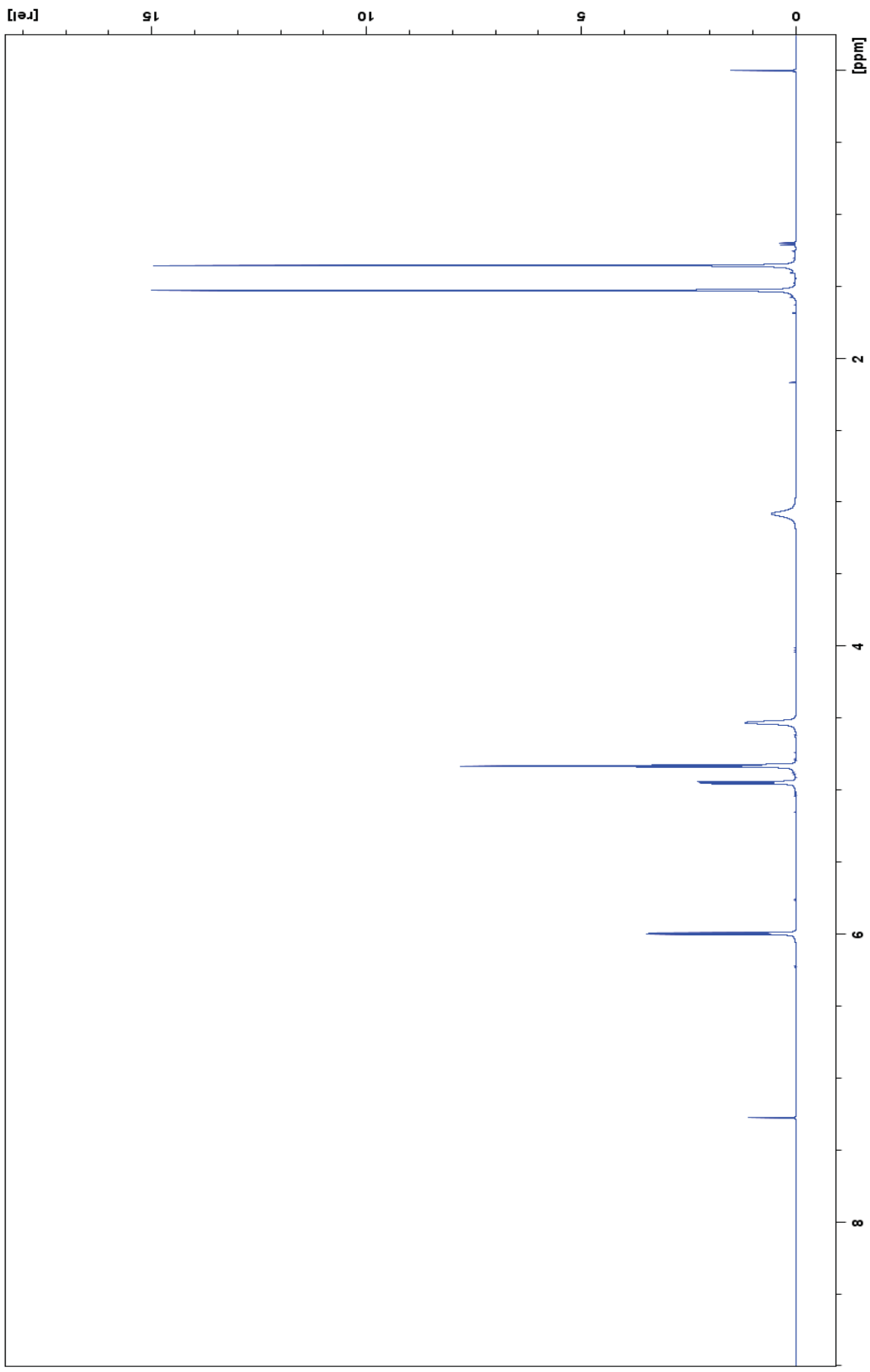

Figure 16: ^{1}H NMR spectrum for compound **5**.

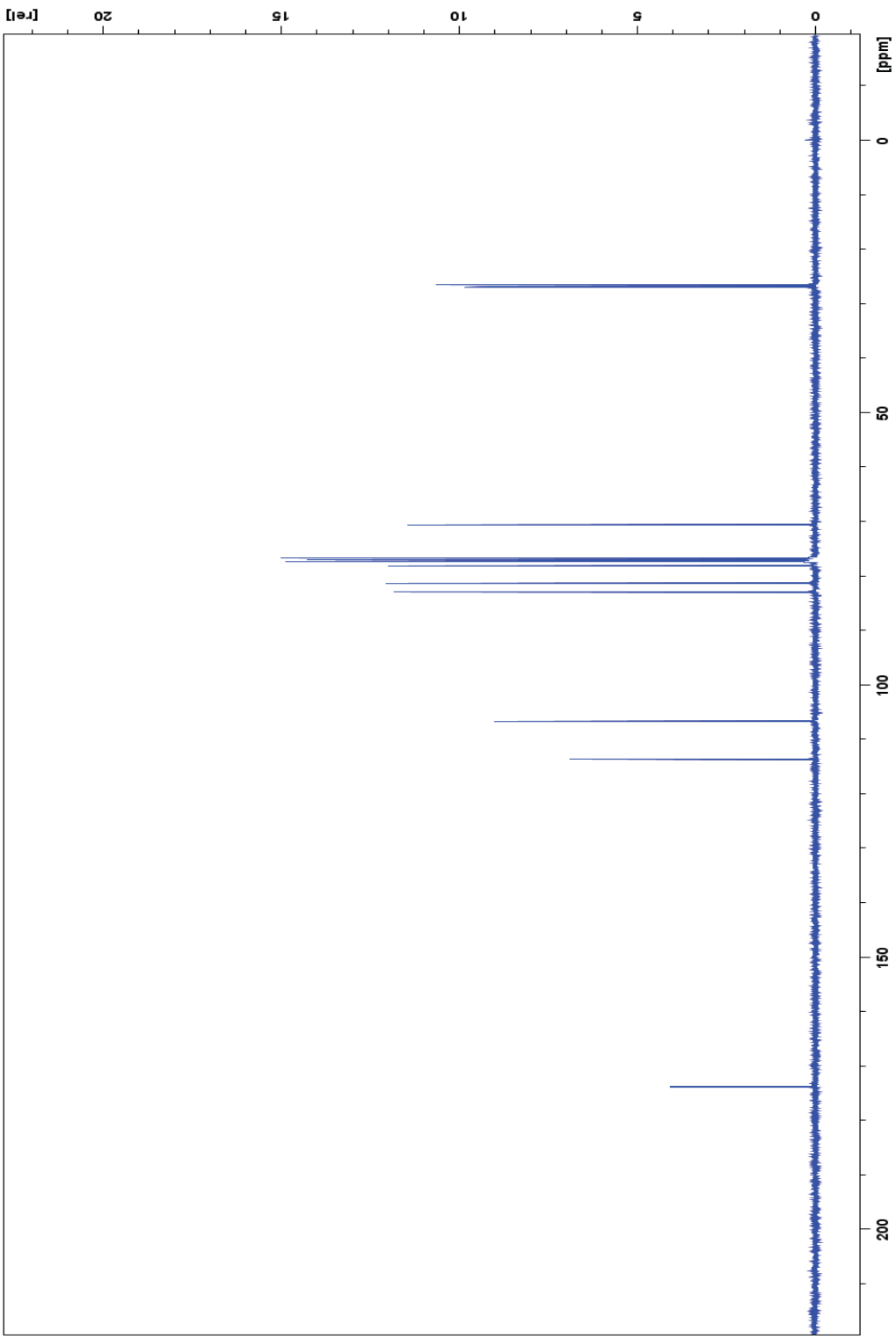

Figure 17: ^{13}C NMR spectrum for compound **5**.

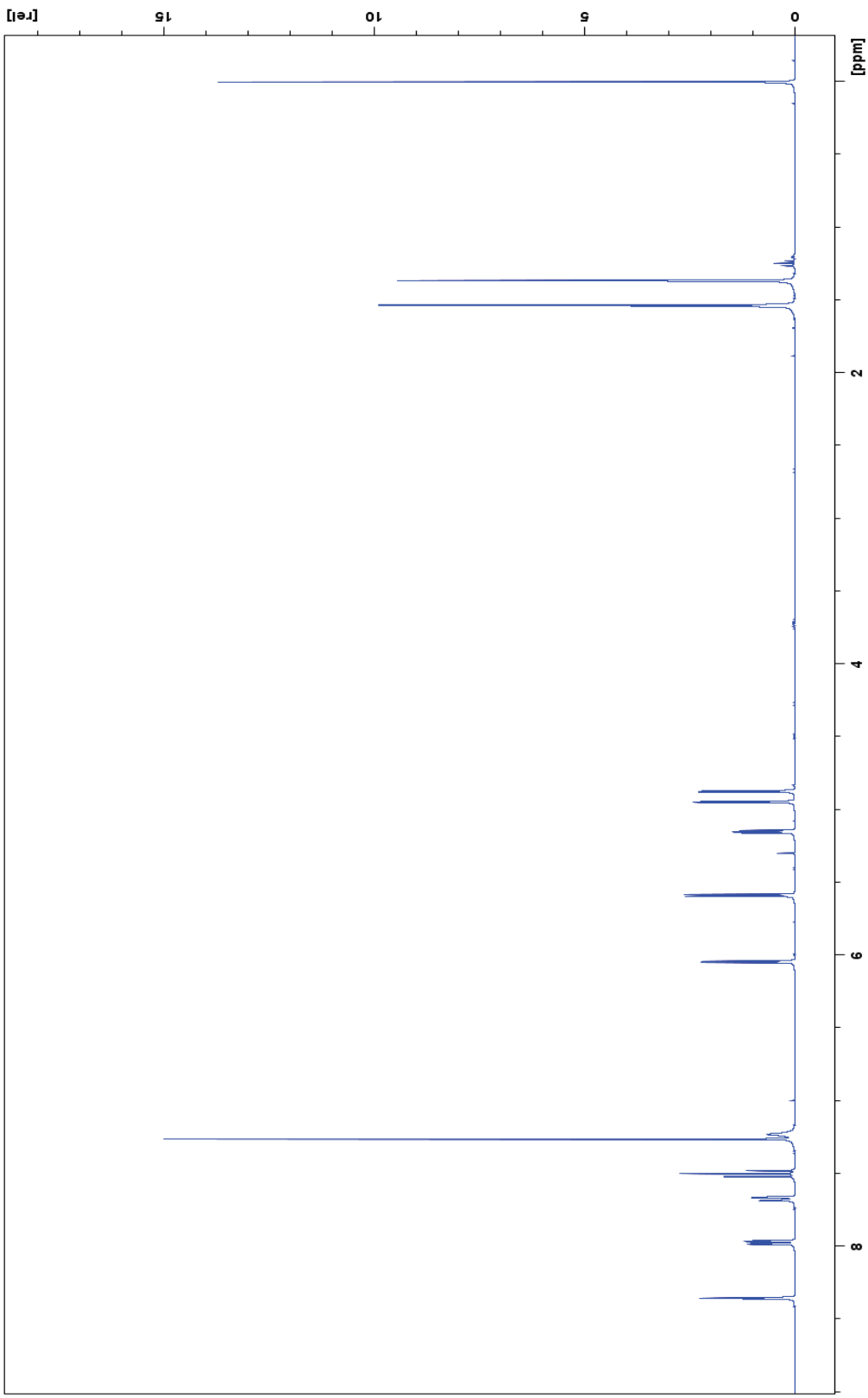

Figure 18: ^{1}H NMR spectrum for compound **6**.

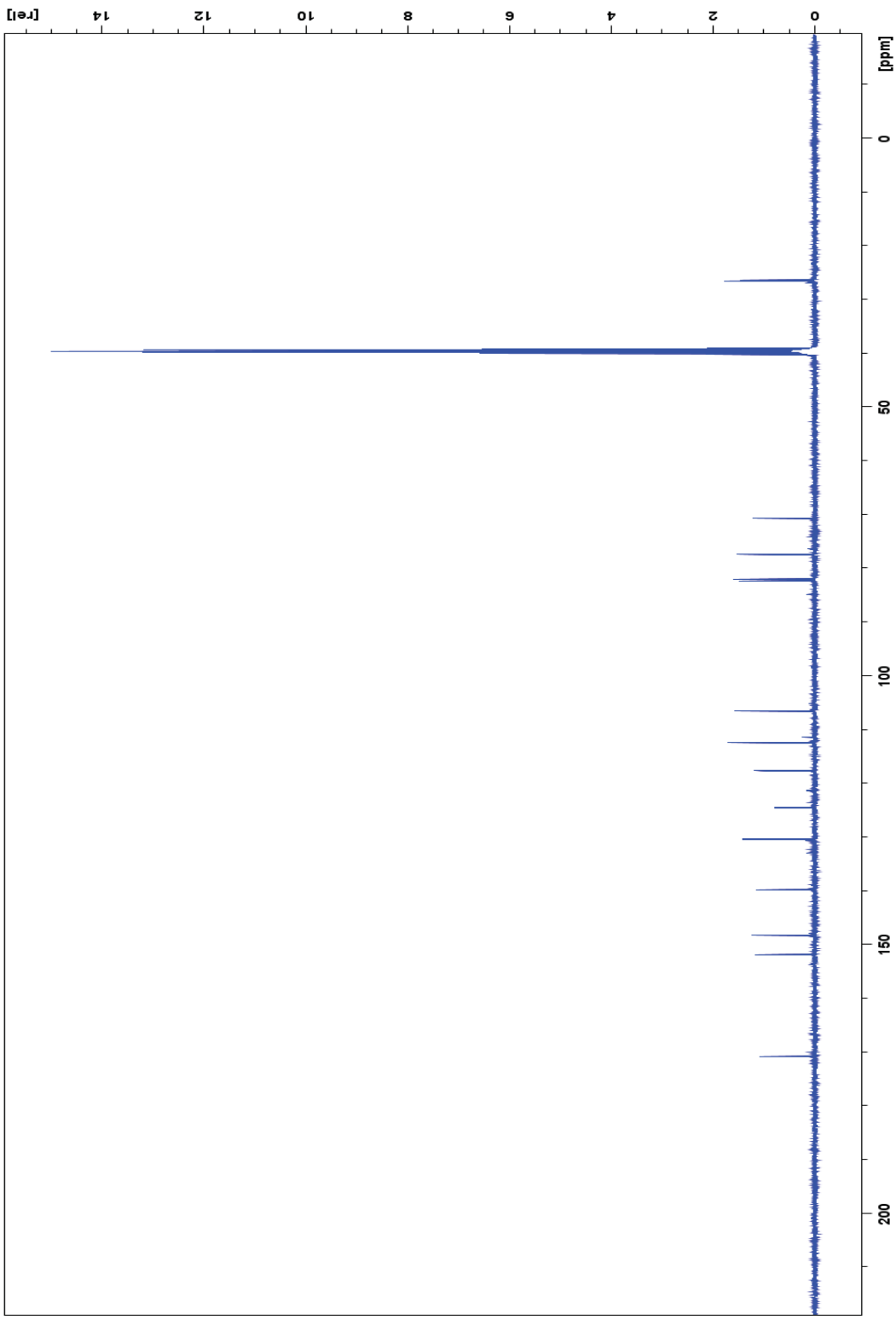

Figure 19: ^{13}C NMR spectrum for compound **6**.

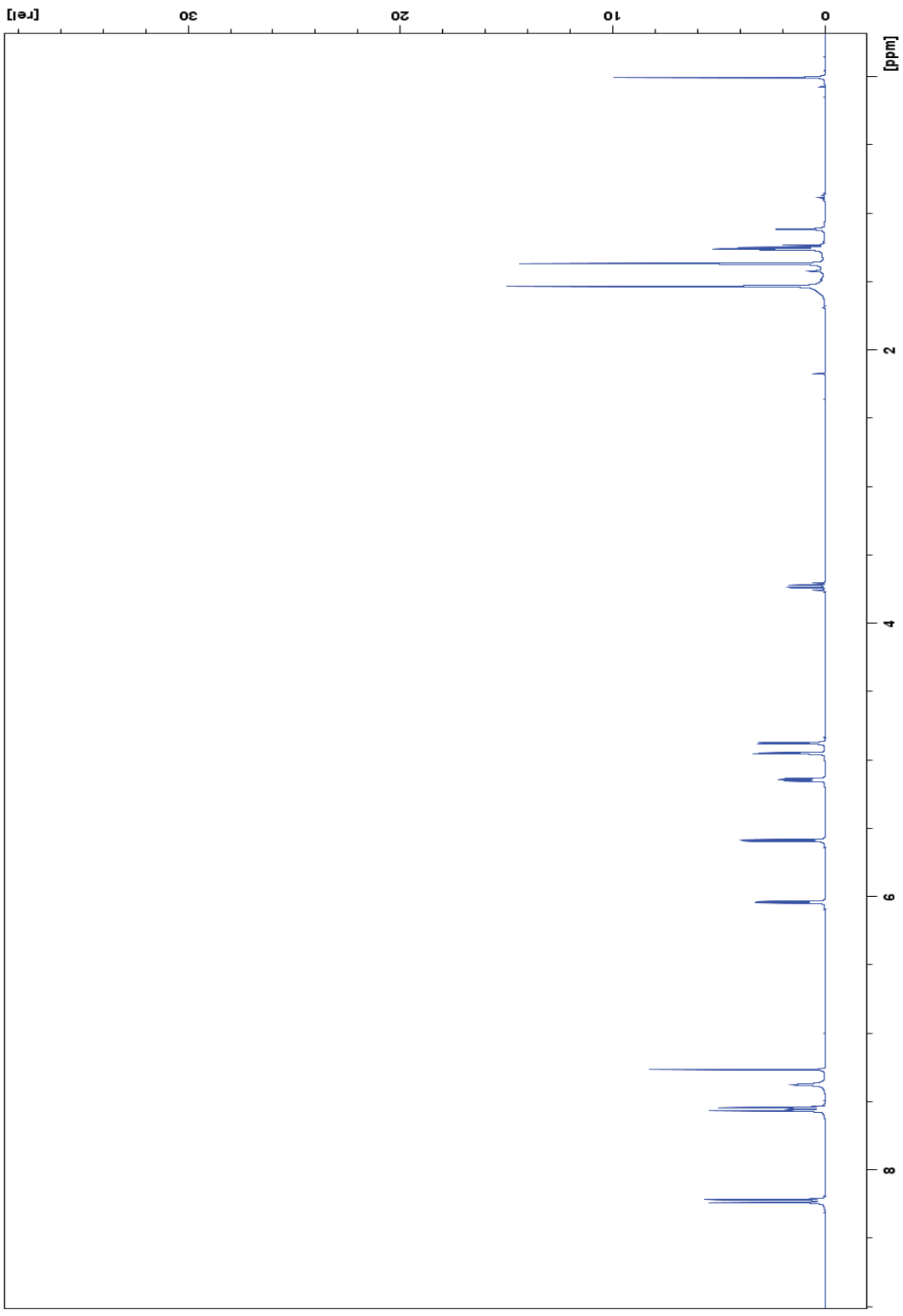

Figure 20: ^{1}H NMR spectrum for compound **7**.

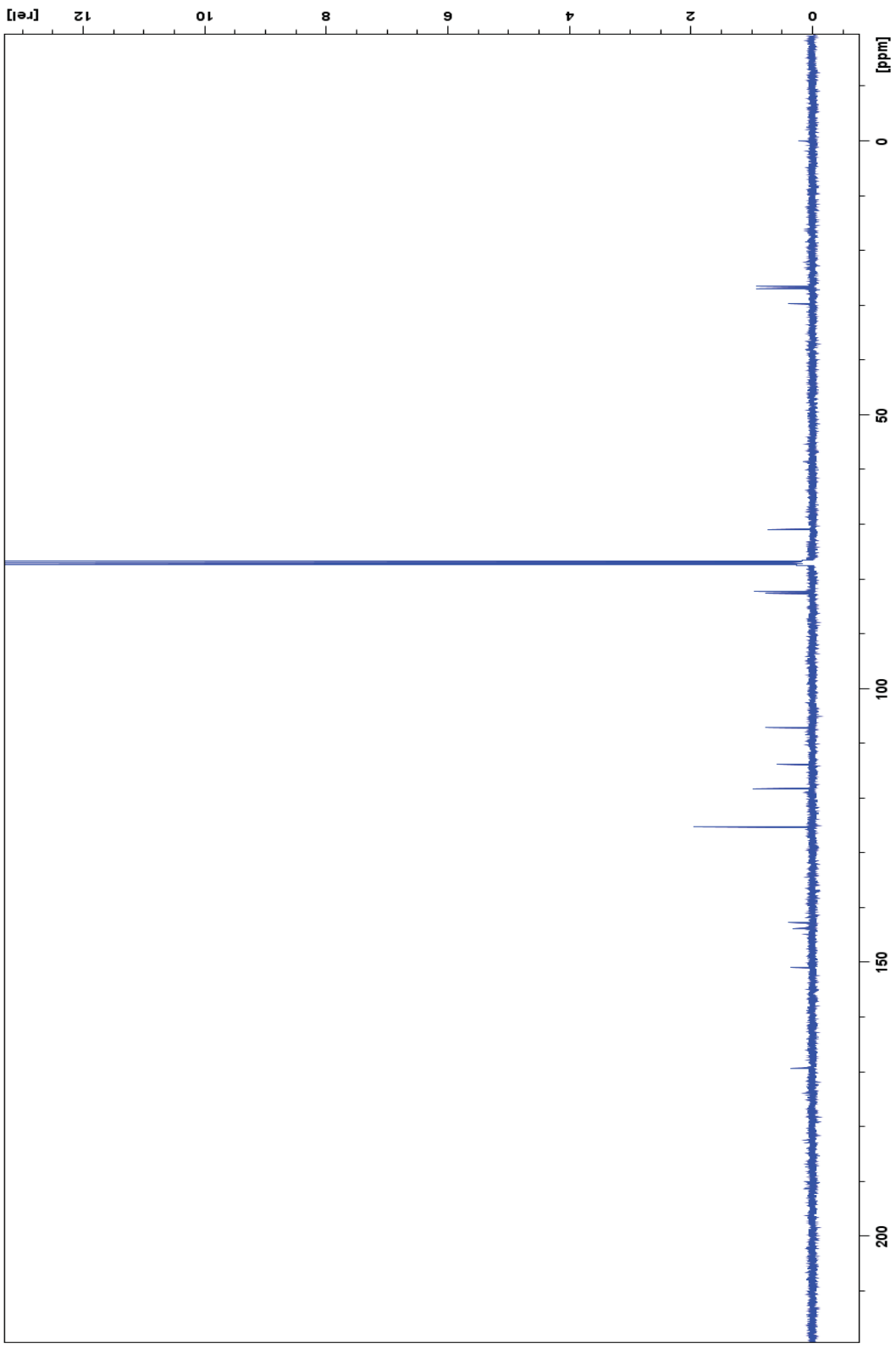

Figure 21: ^{13}C NMR spectrum for compound **7**.

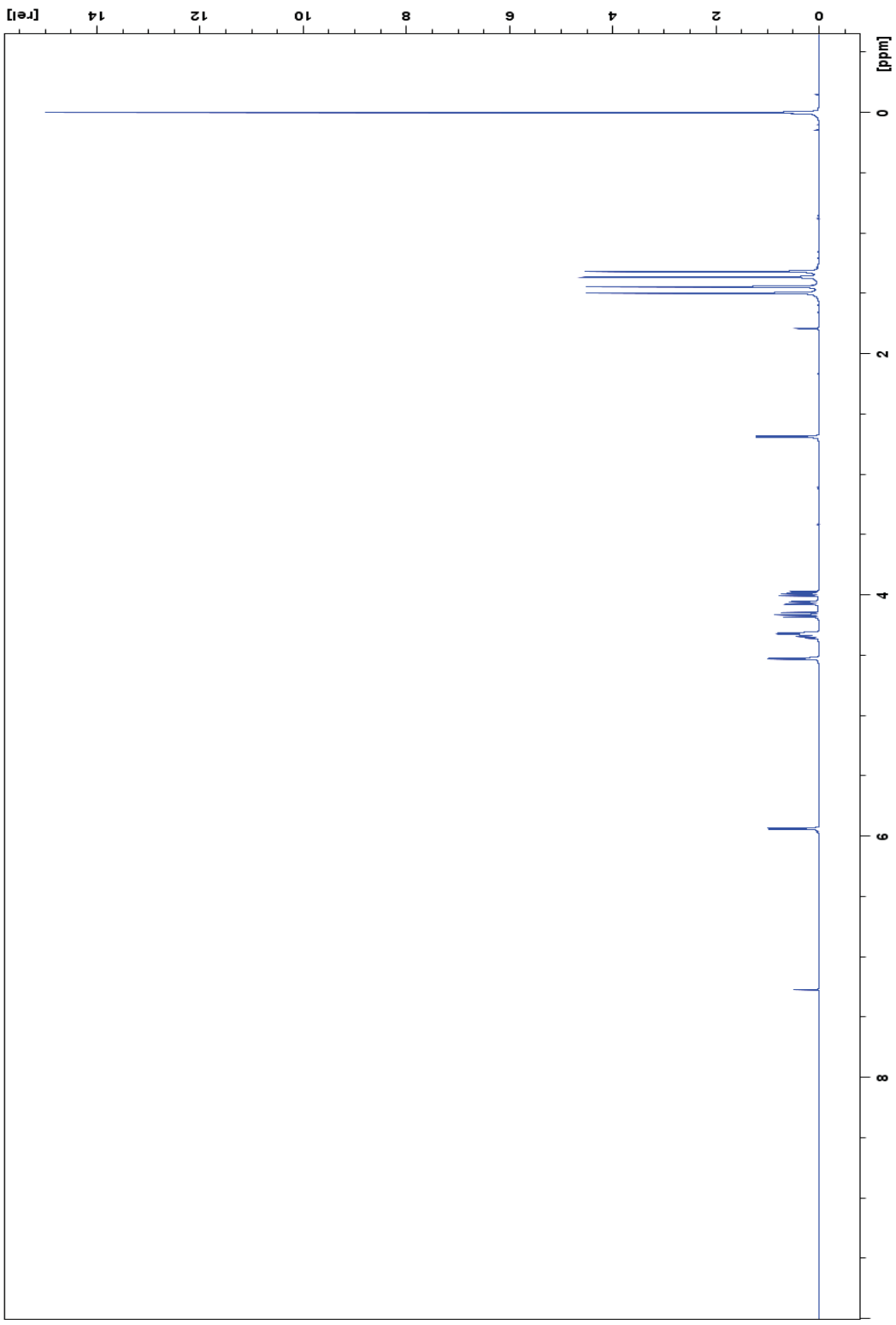

Figure 22: ^{1}H NMR spectrum for compound **8**.

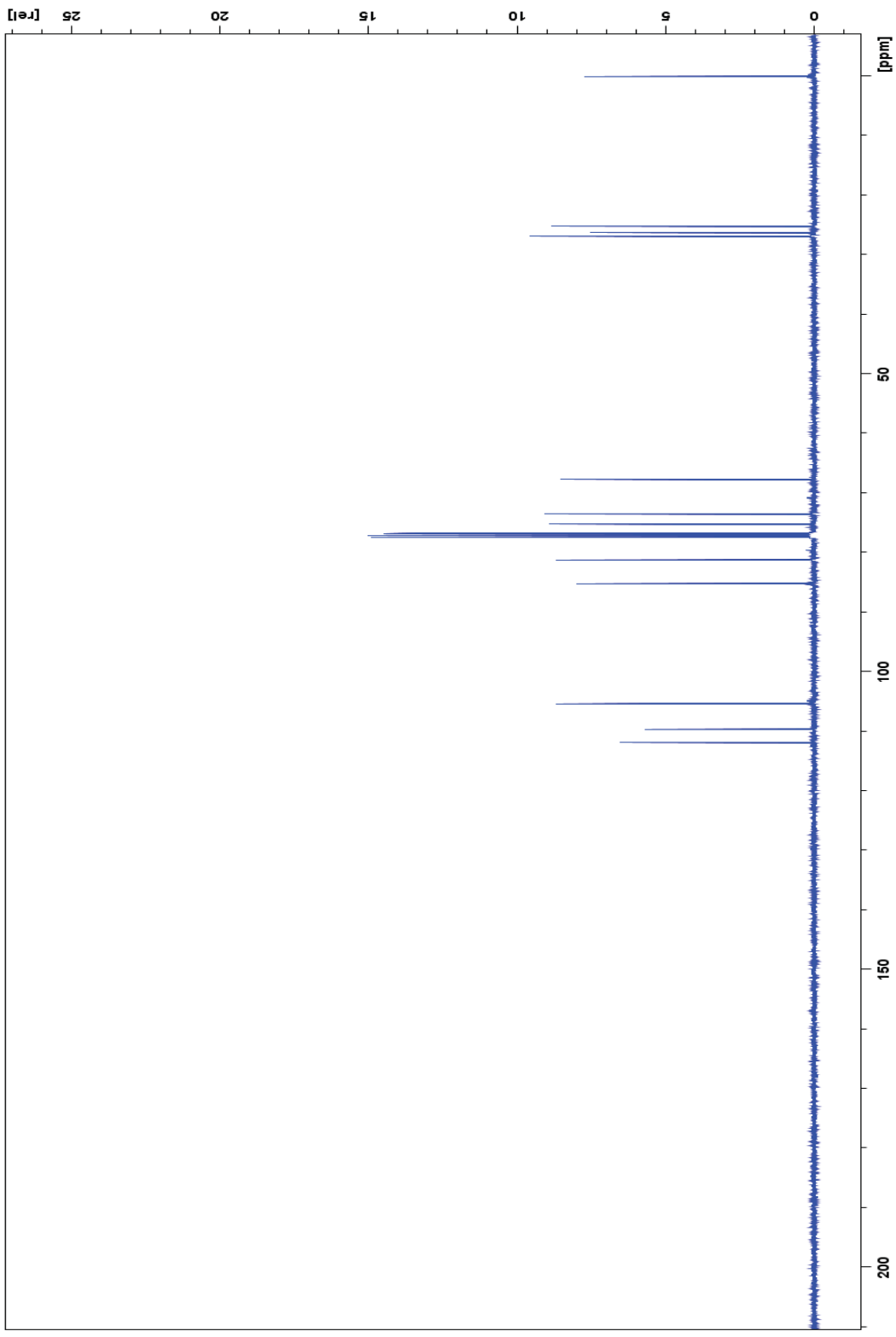

Figure 23: ^{13}C NMR spectrum for compound **8**.

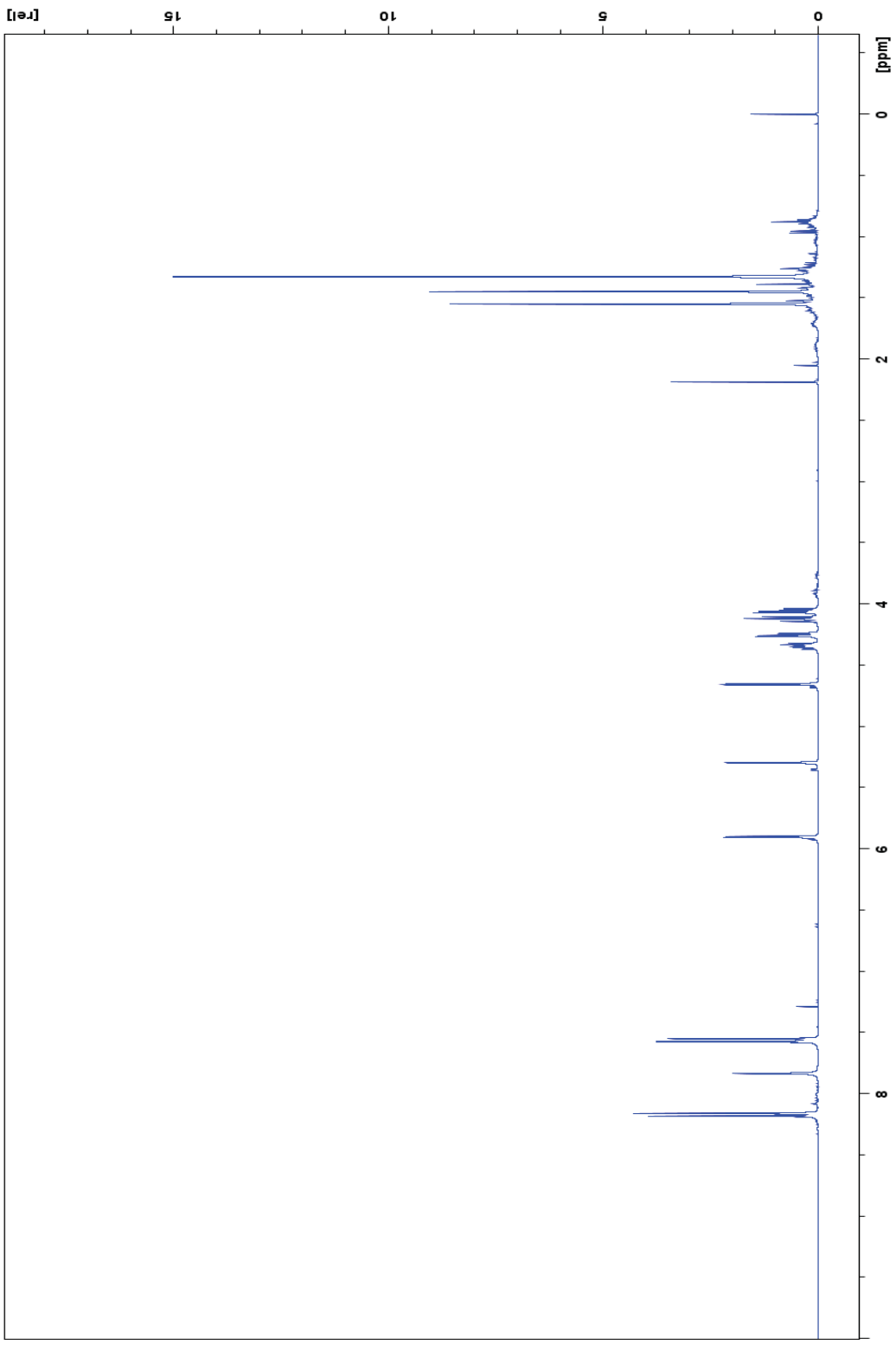

Figure 24: ^{1}H NMR spectrum for compound **9**.

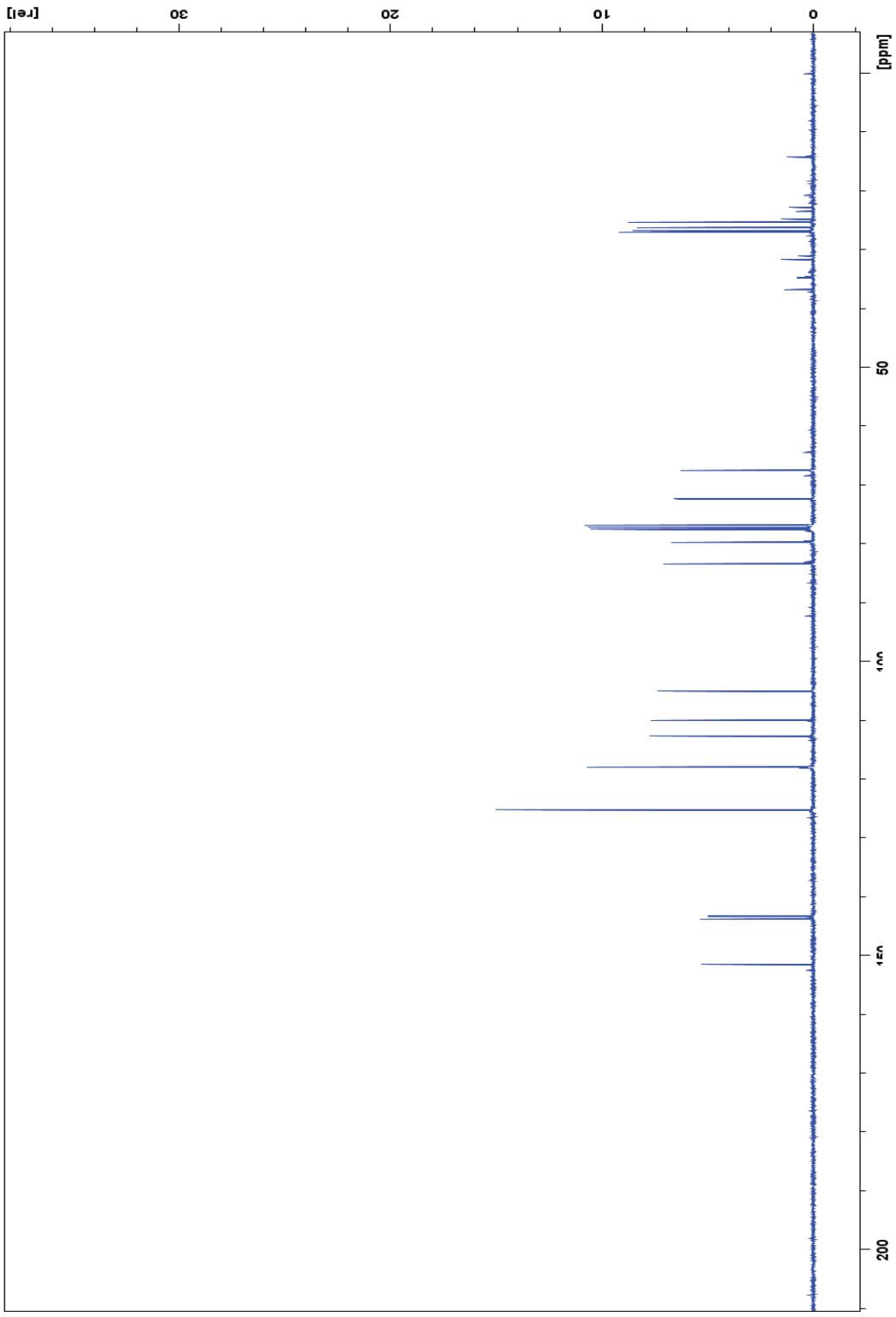

Figure 25: ^{13}C NMR spectrum for compound **9**.

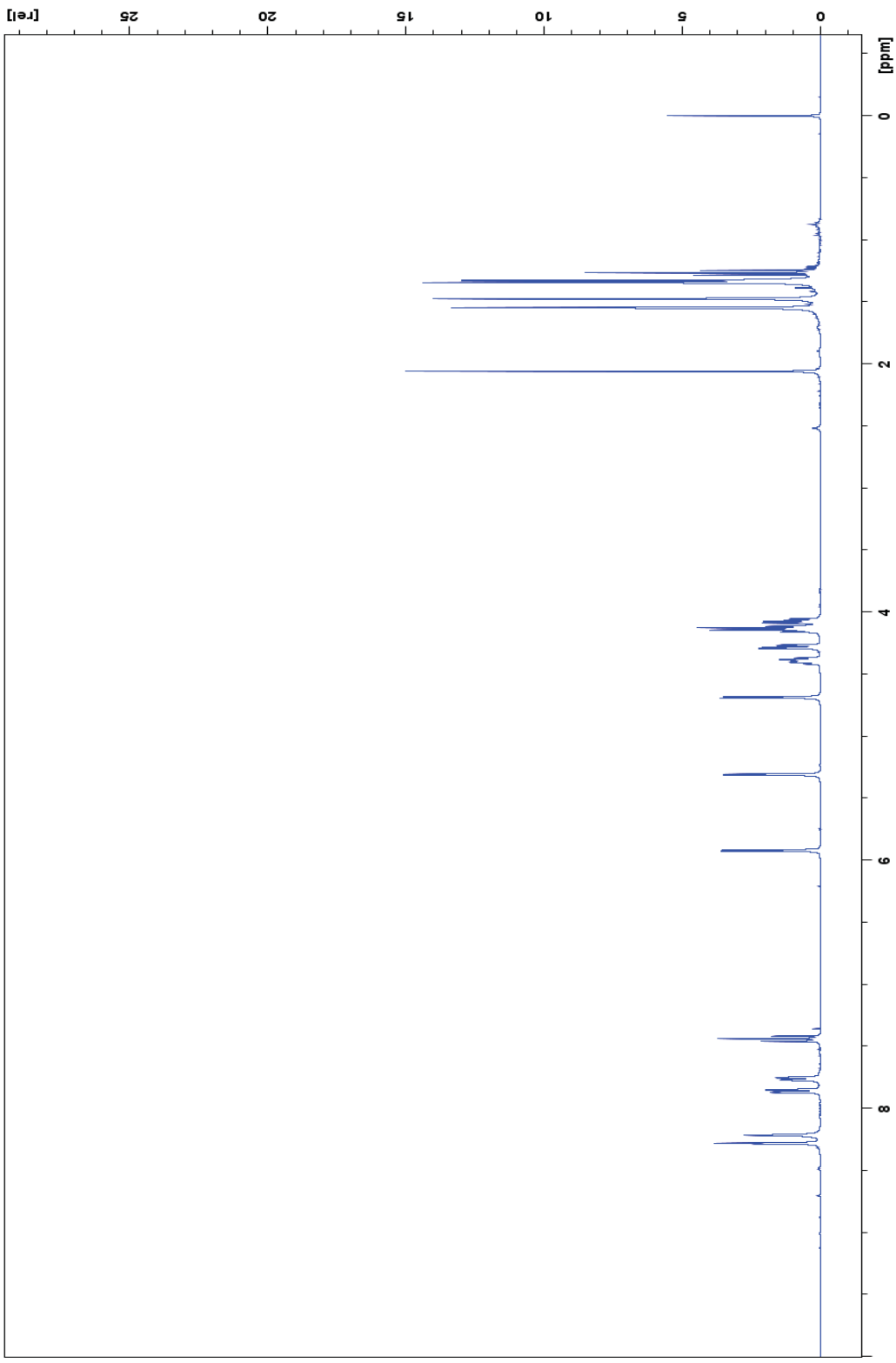

Figure 26: ^{1}H NMR spectrum for compound **10**.

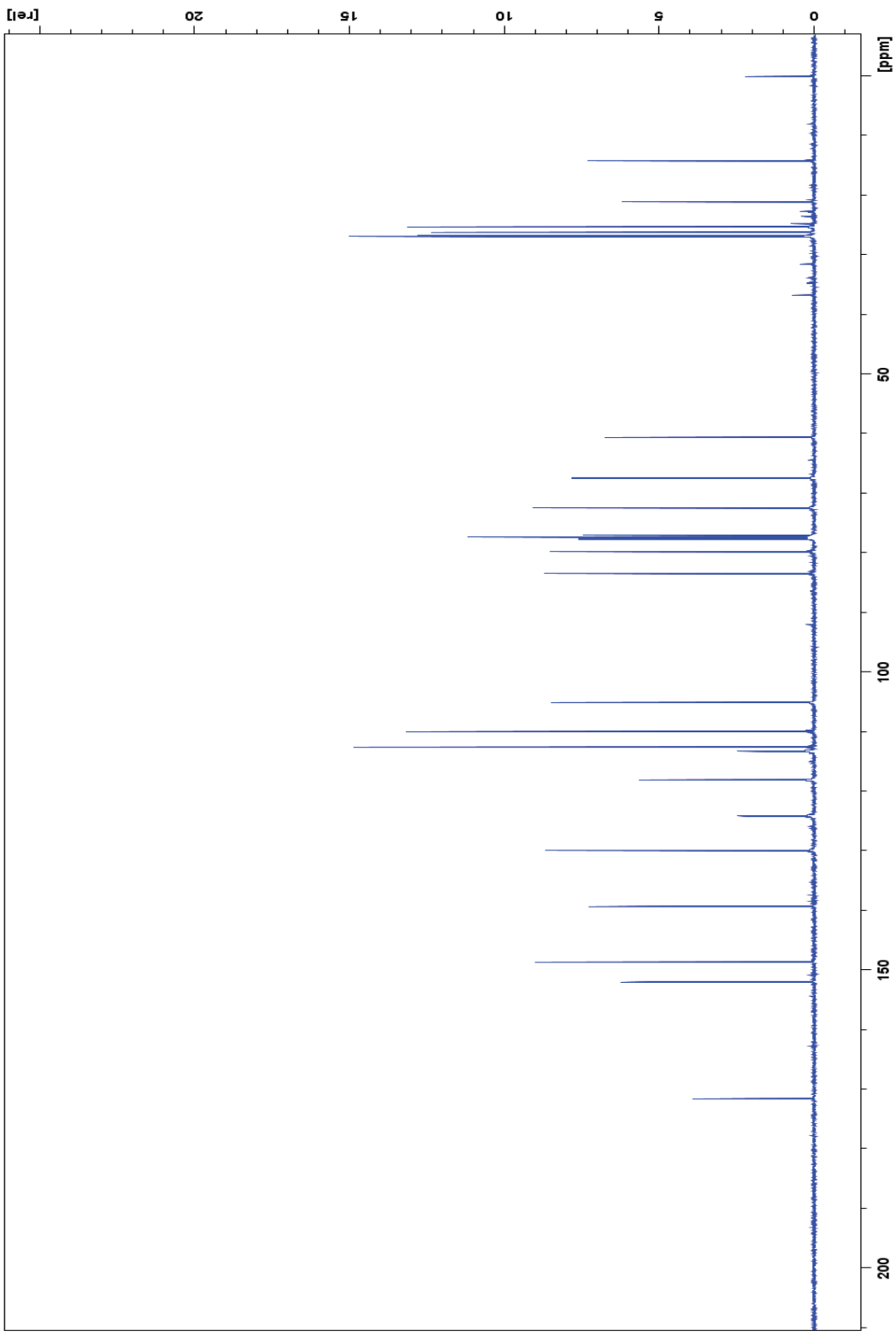

Figure 27: ^{13}C NMR spectrum for compound **10**.

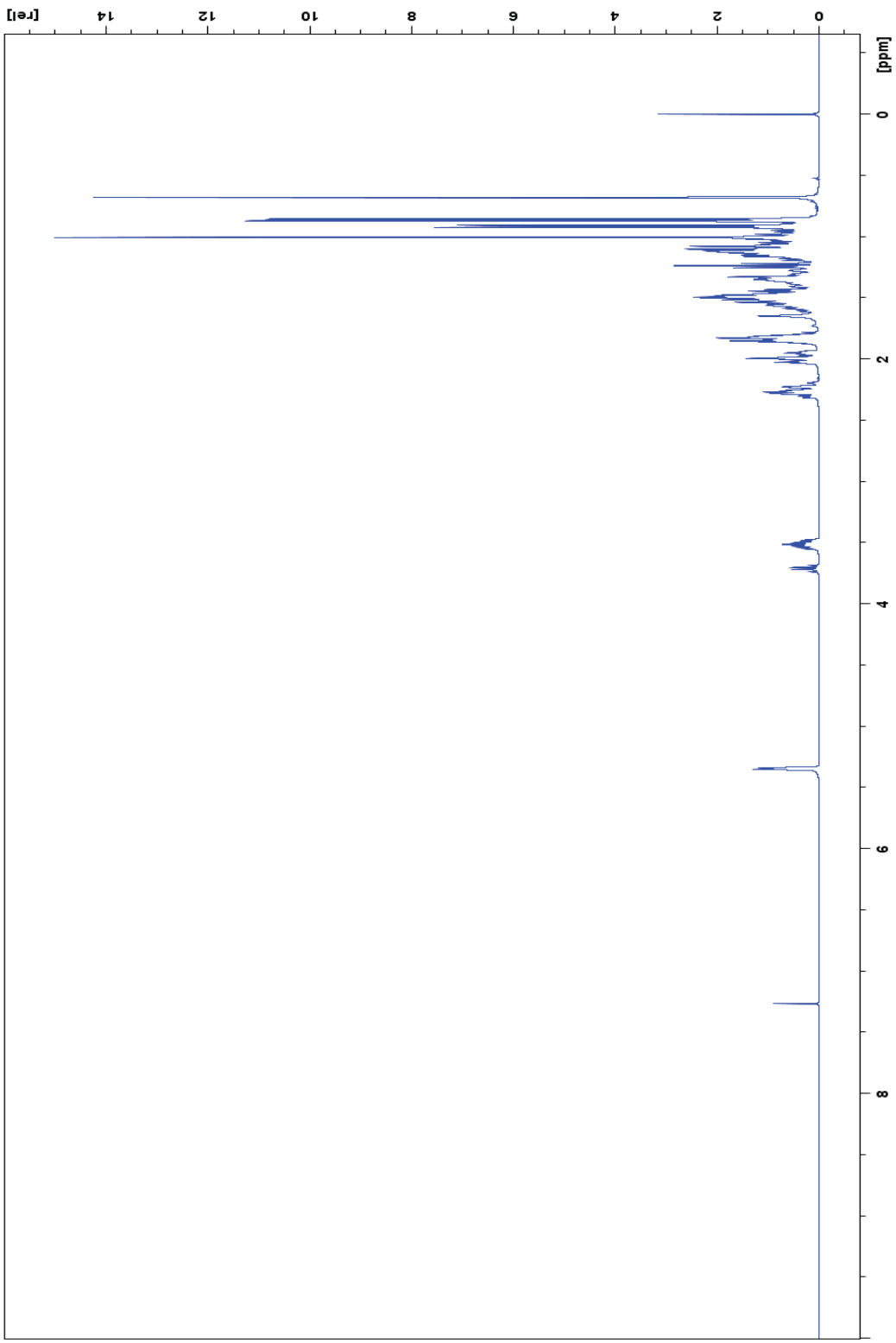

Figure 28: ^{1}H NMR spectrum for compound **11**.

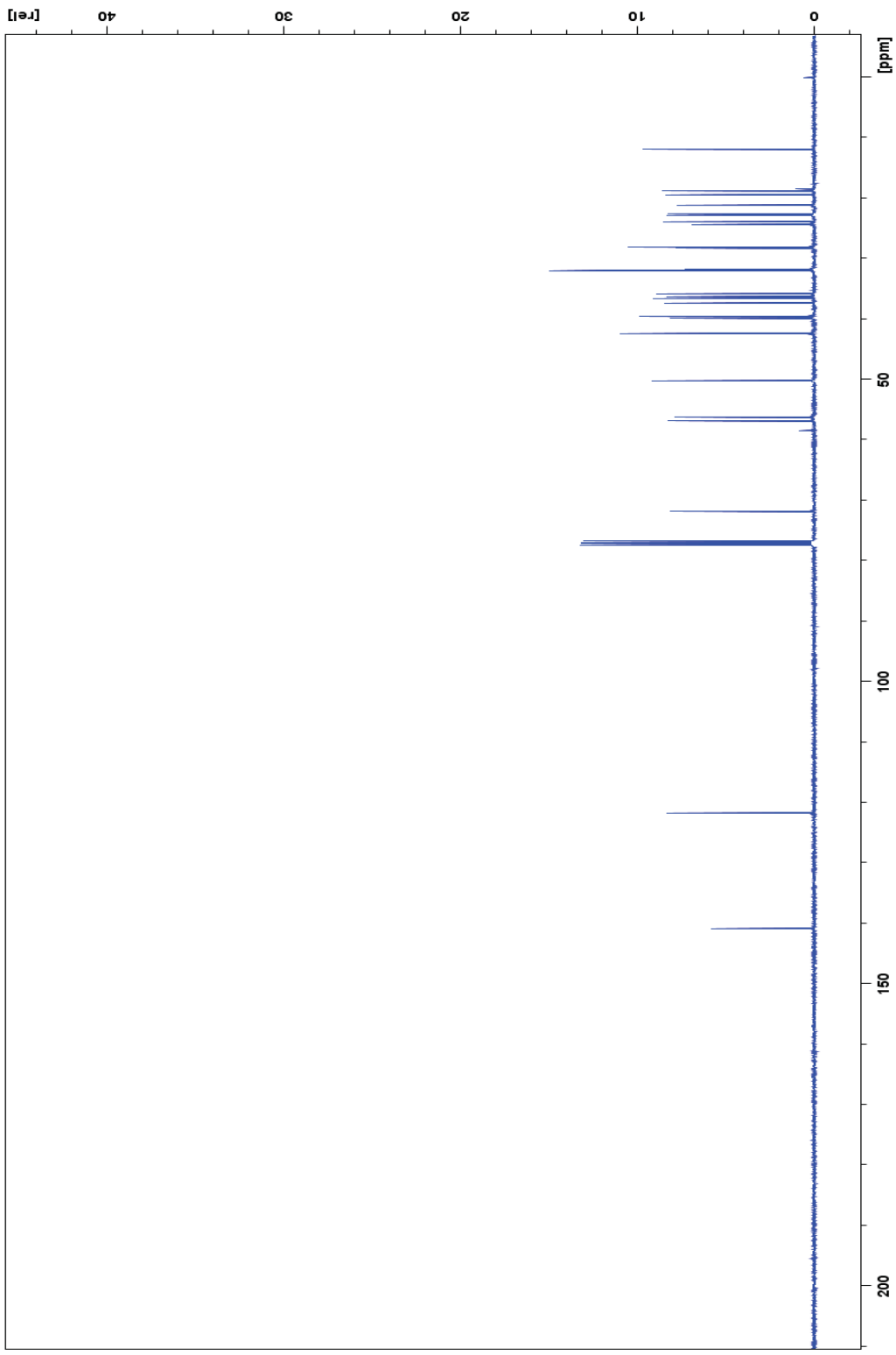

Figure 29: ^{13}C NMR spectrum for compound **11**.

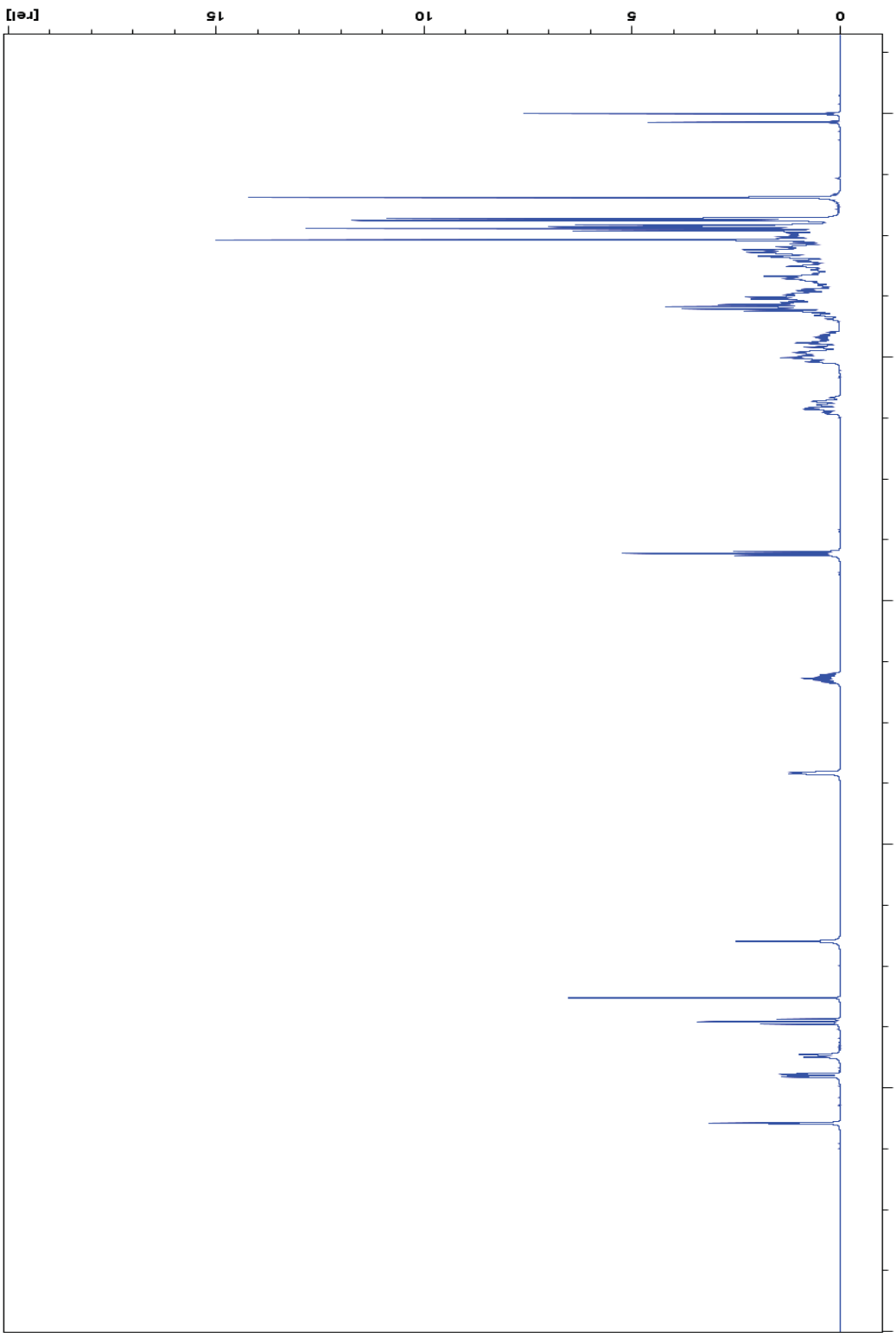

Figure 30: ^{1}H NMR spectrum for compound **12**.

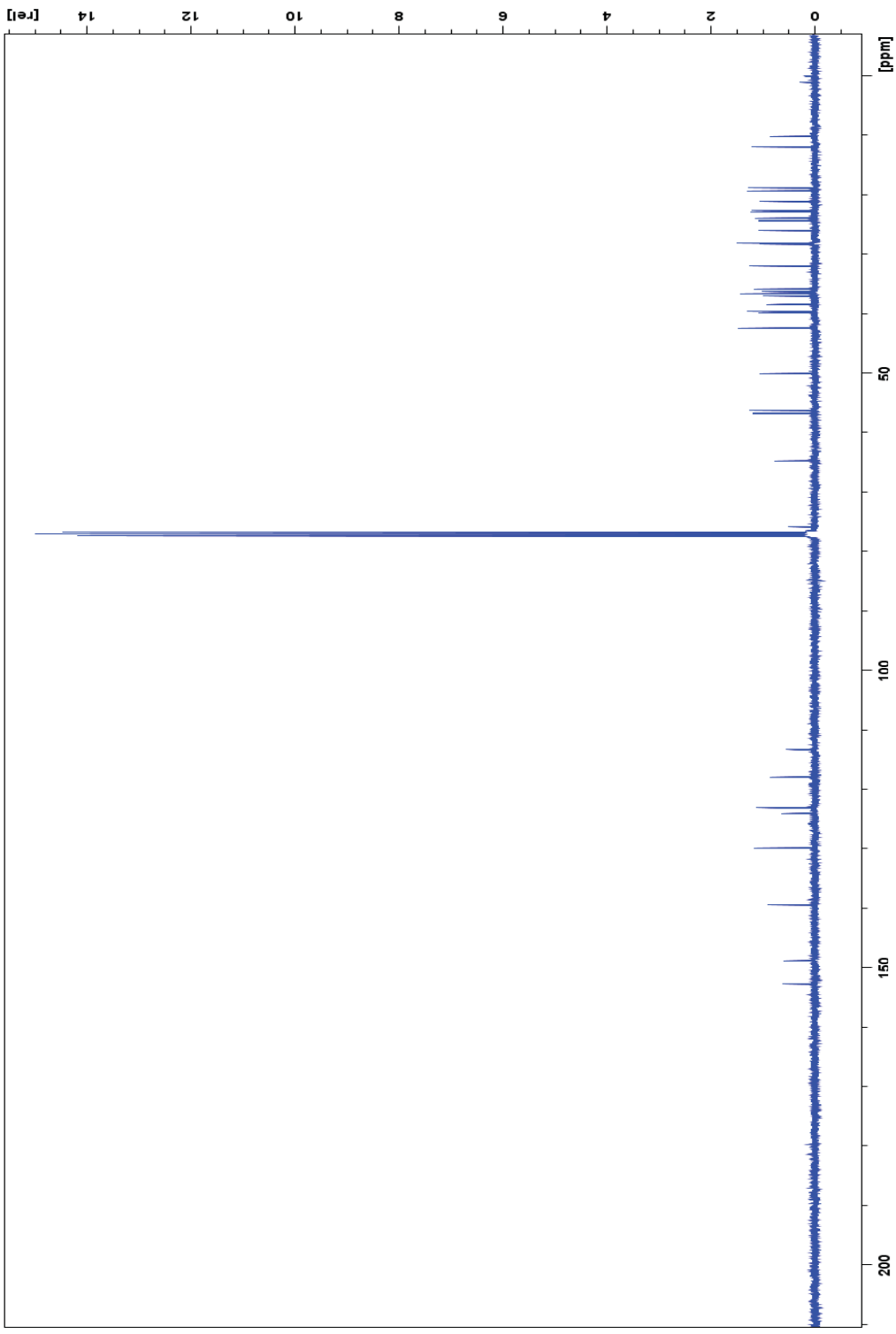

Figure 31: ^{13}C NMR spectrum for compound **12**.

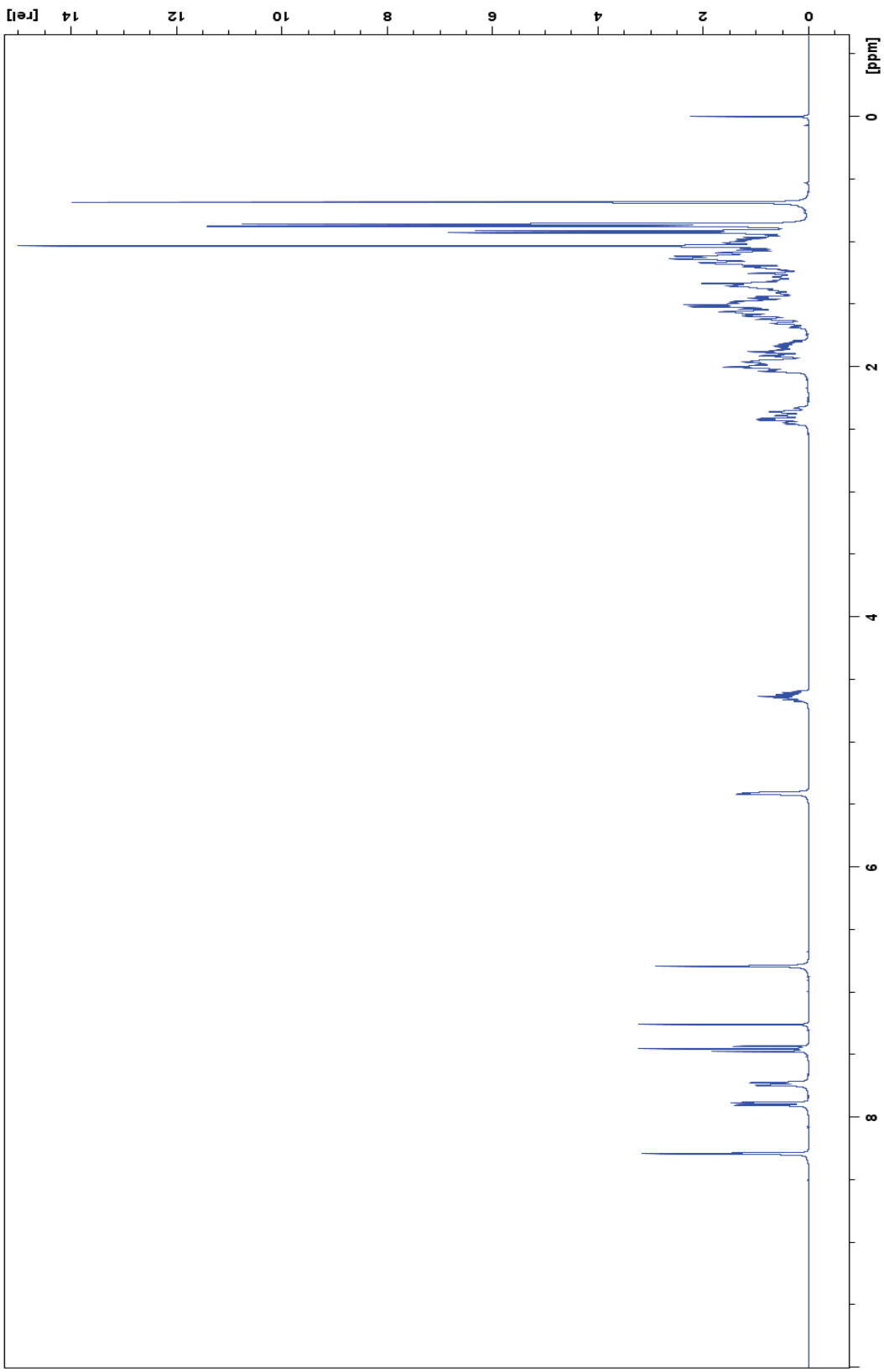

Figure 32: ^{1}H NMR spectrum for compound **13**.

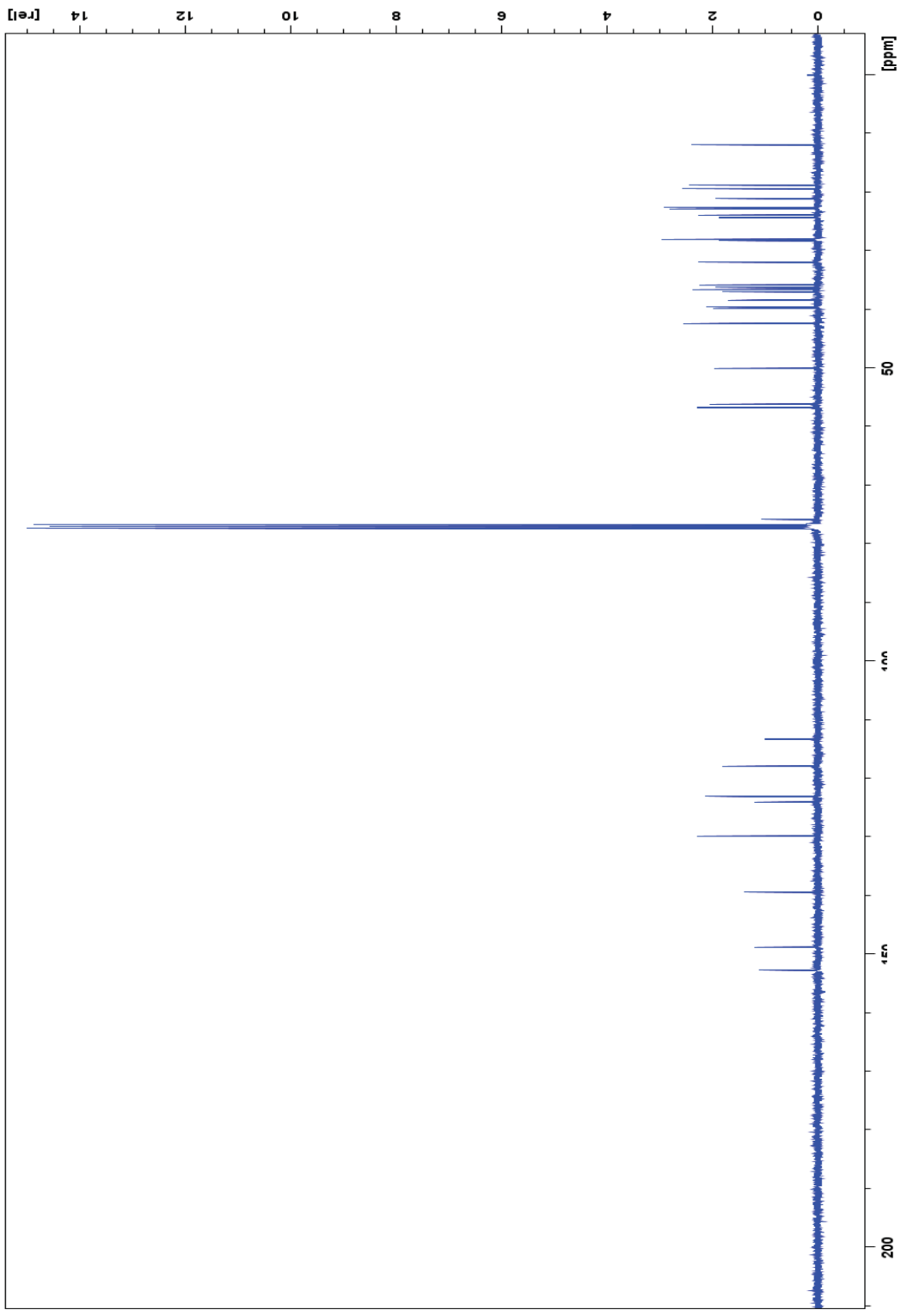

Figure 33: ^{13}C NMR spectrum for compound **13**.

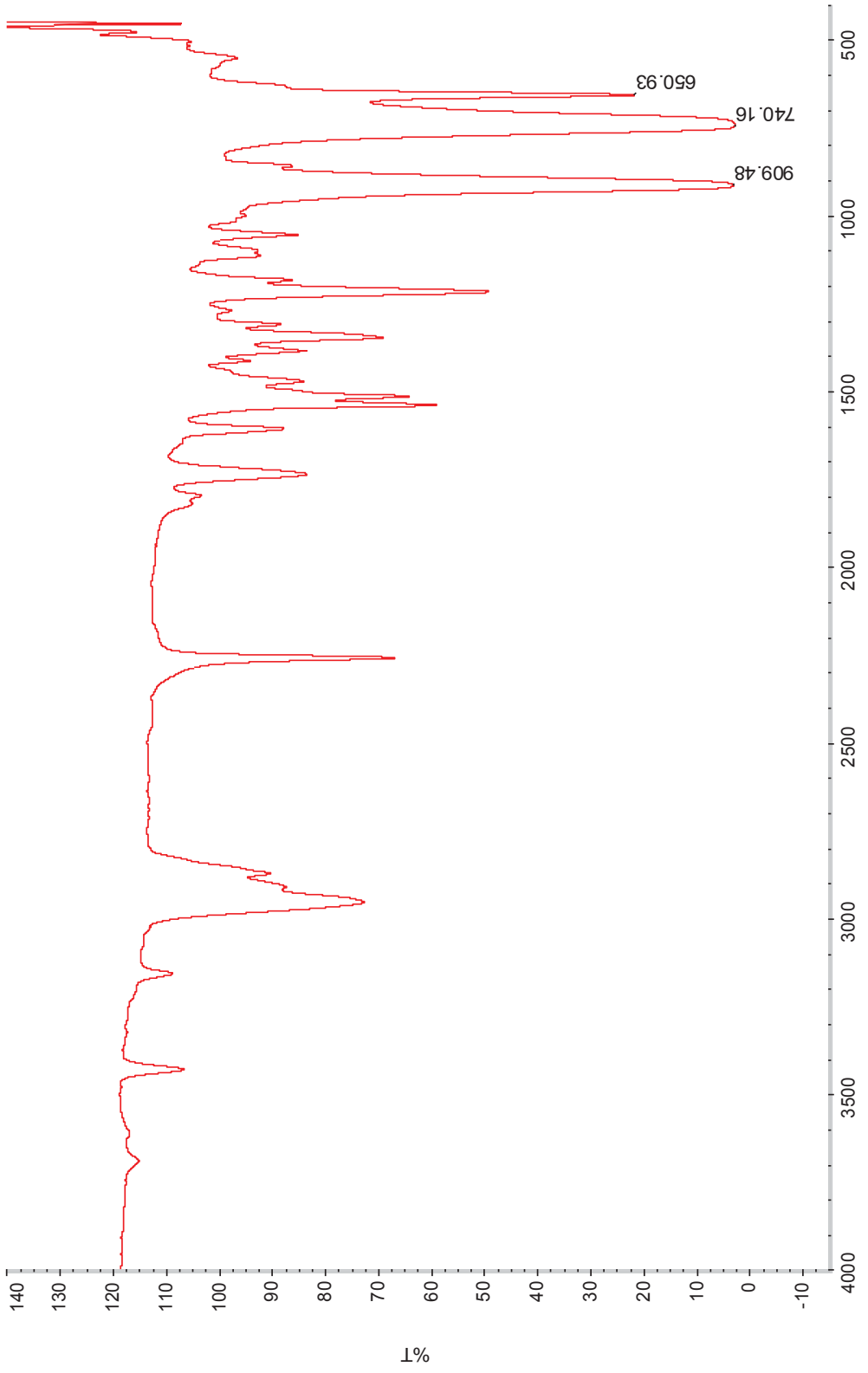

Figure 34: IR spectrum for compound **13**.

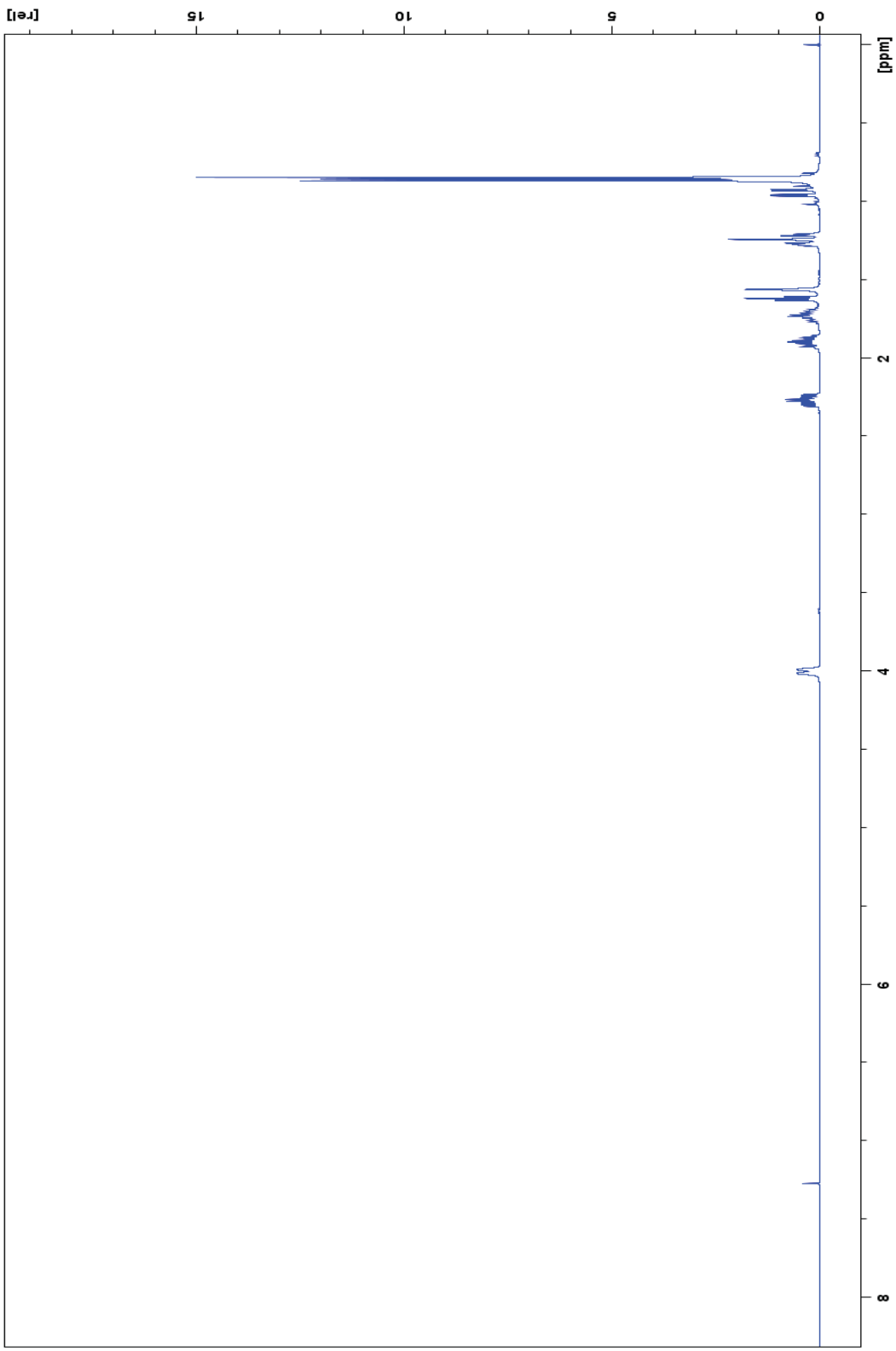

Figure 35: ^{1}H NMR spectrum for compound **14**.

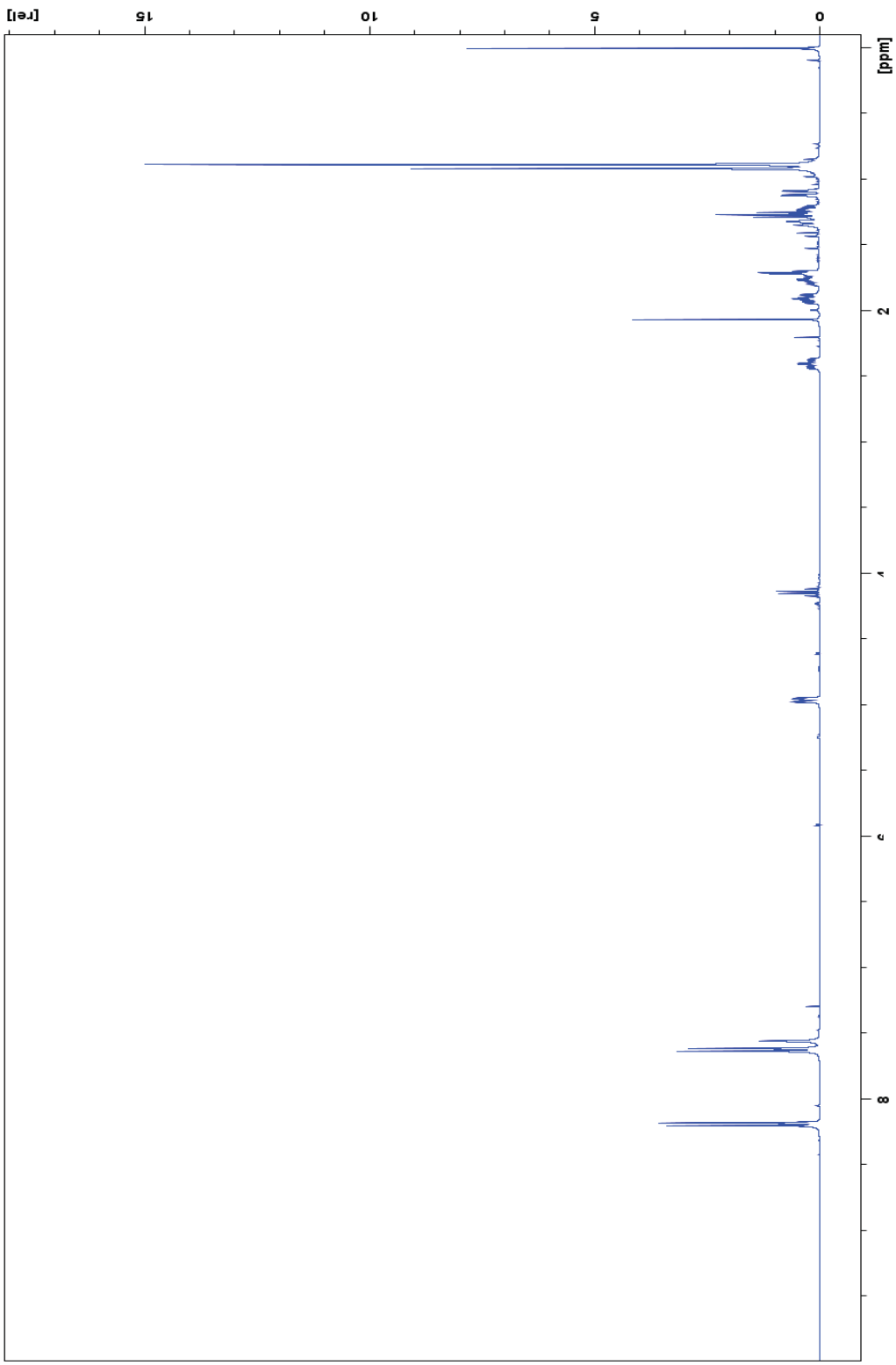

Figure 36: ^{1}H NMR spectrum for compound **15**.

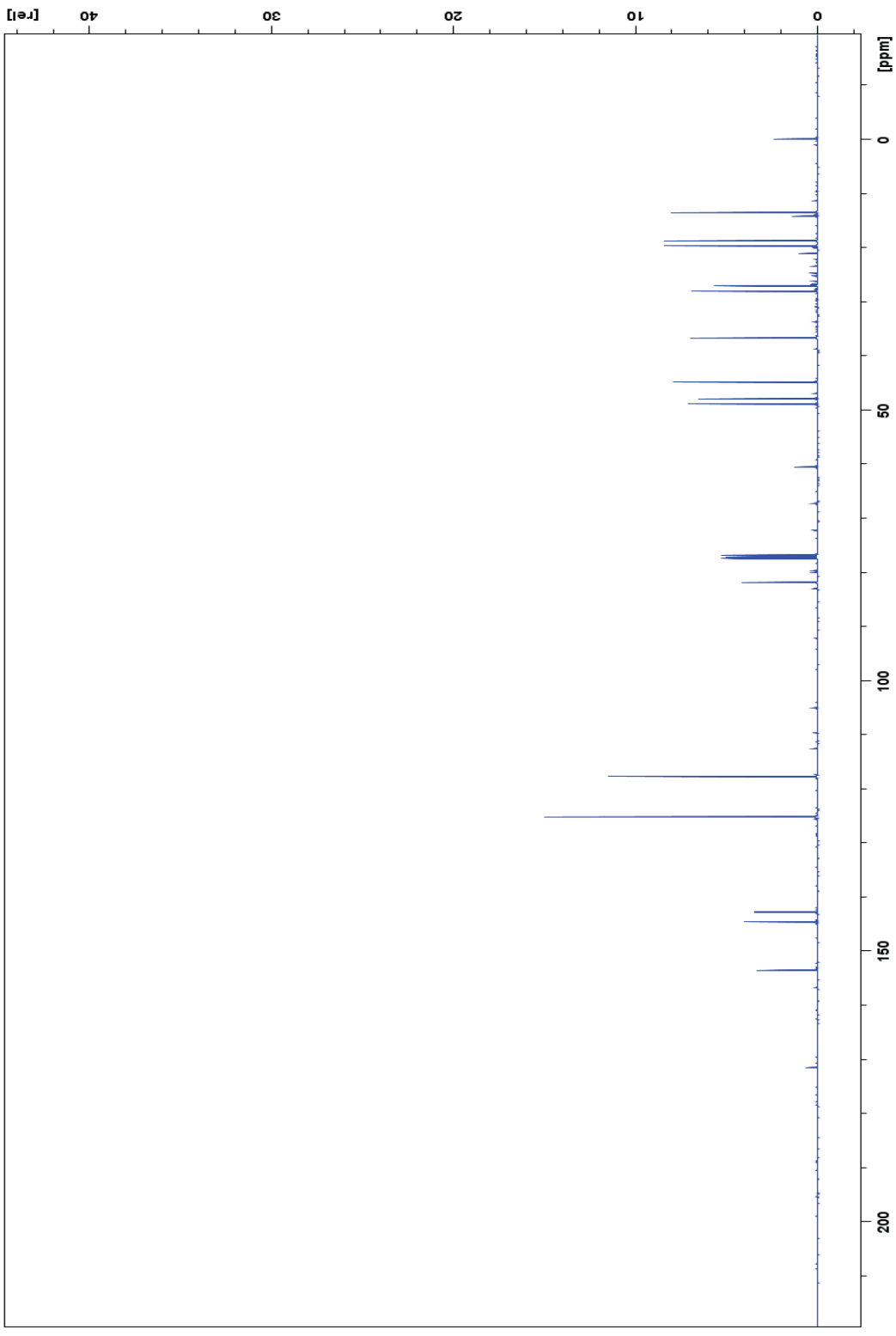

Figure 37: ^{13}C NMR spectrum for compound **15**.

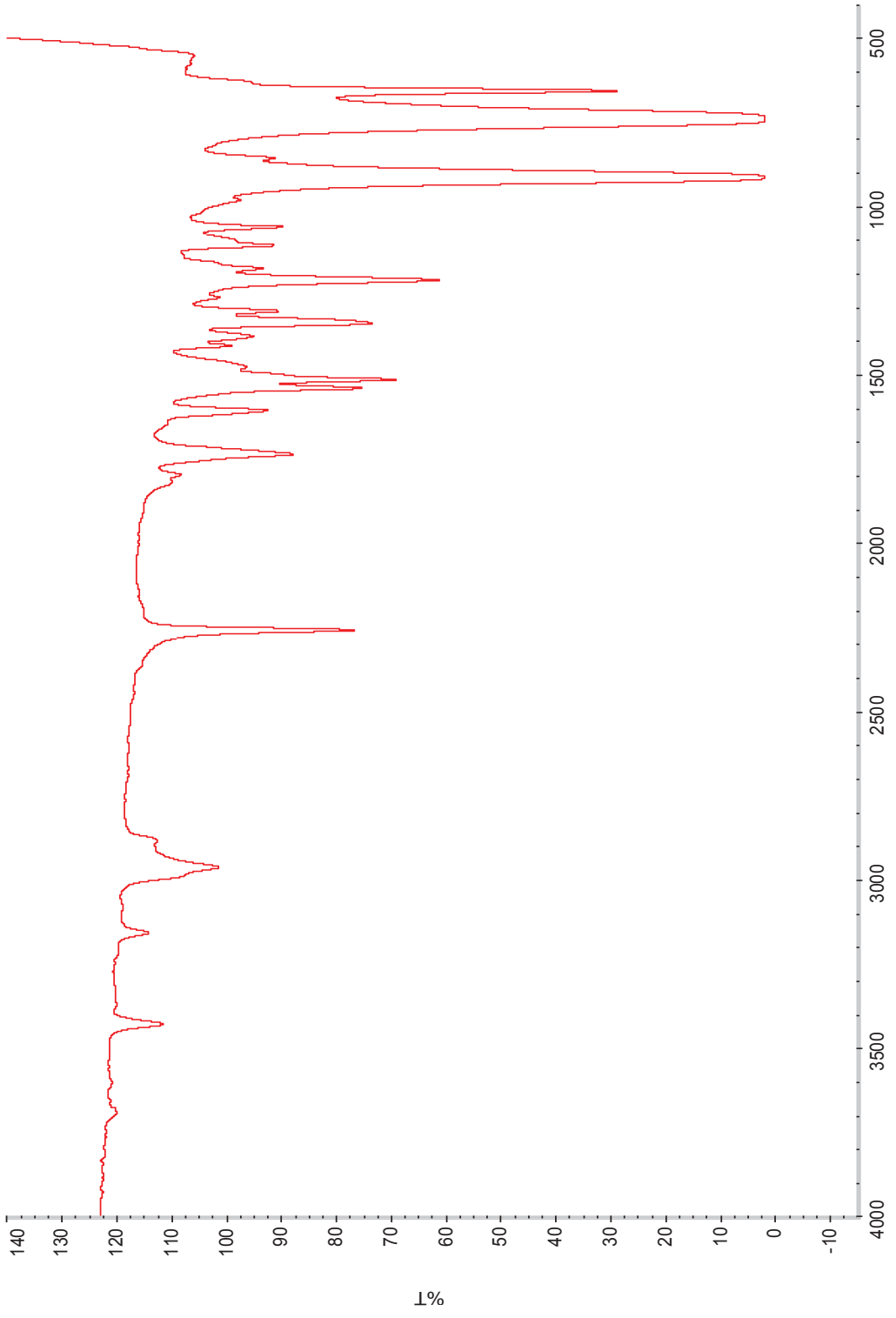

Figure 38: IR spectrum for compound **15**.

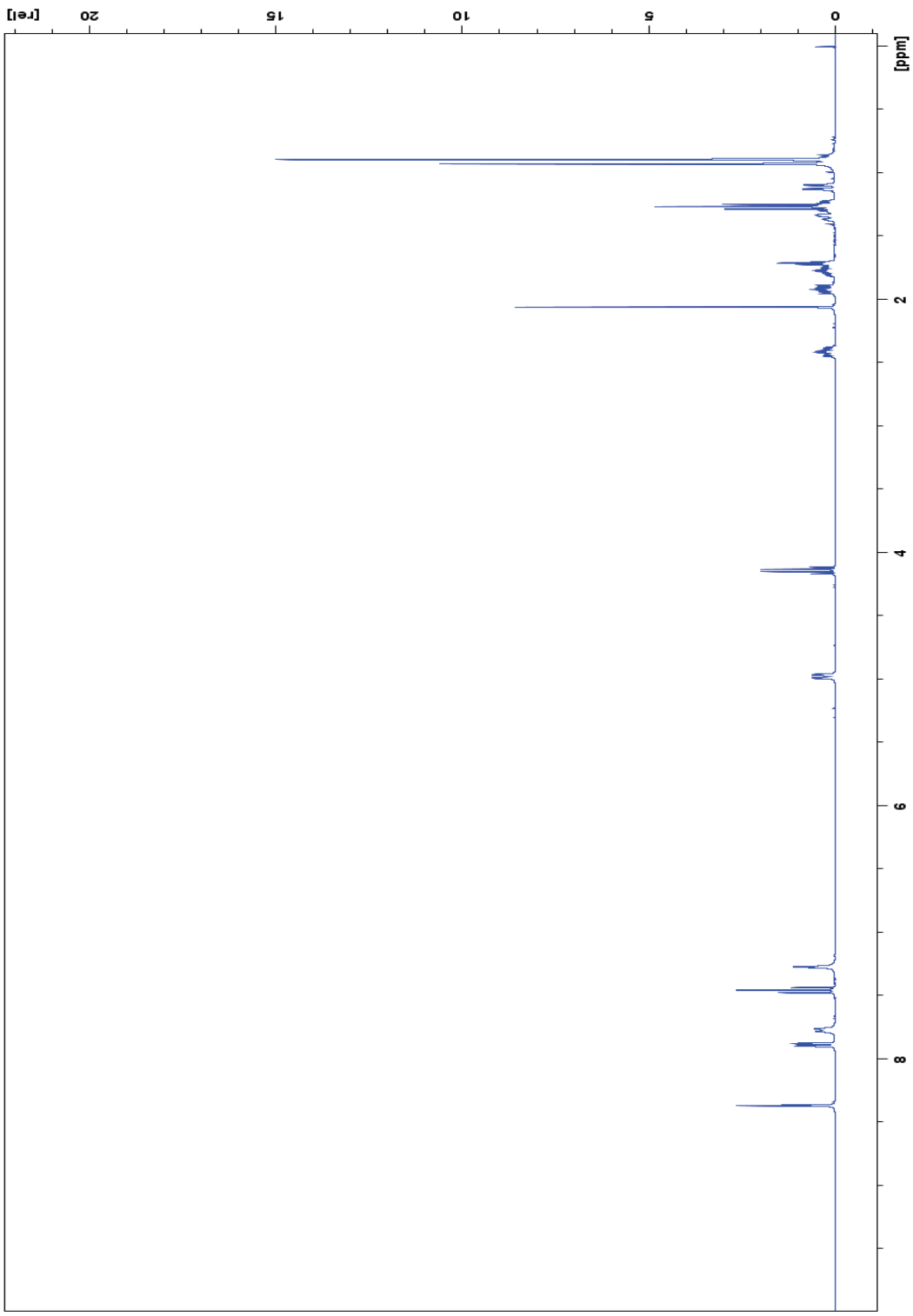

Figure 39: ^{1}H NMR spectrum for compound **16**.

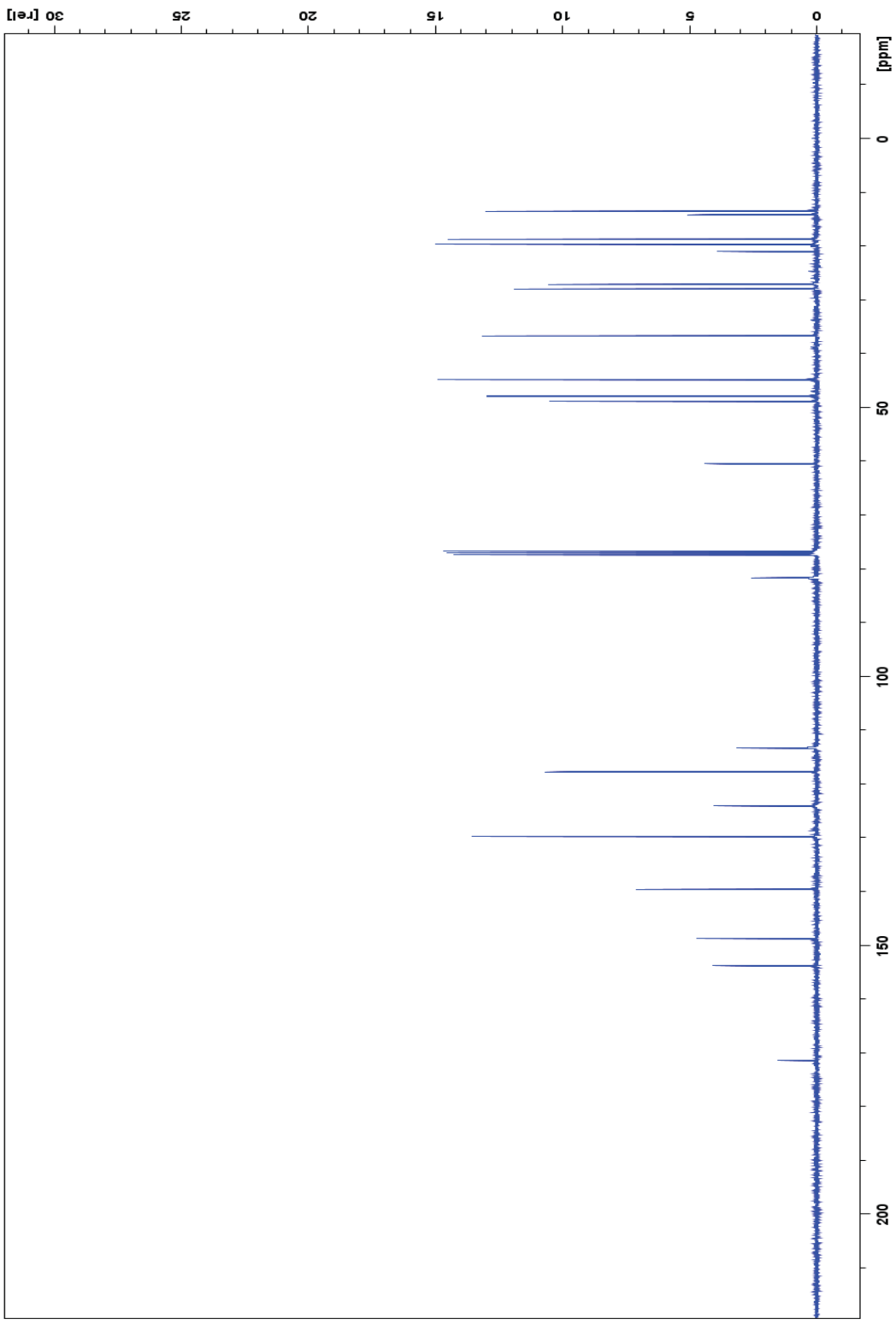

Figure 40: ^{13}C NMR spectrum for compound **16**.

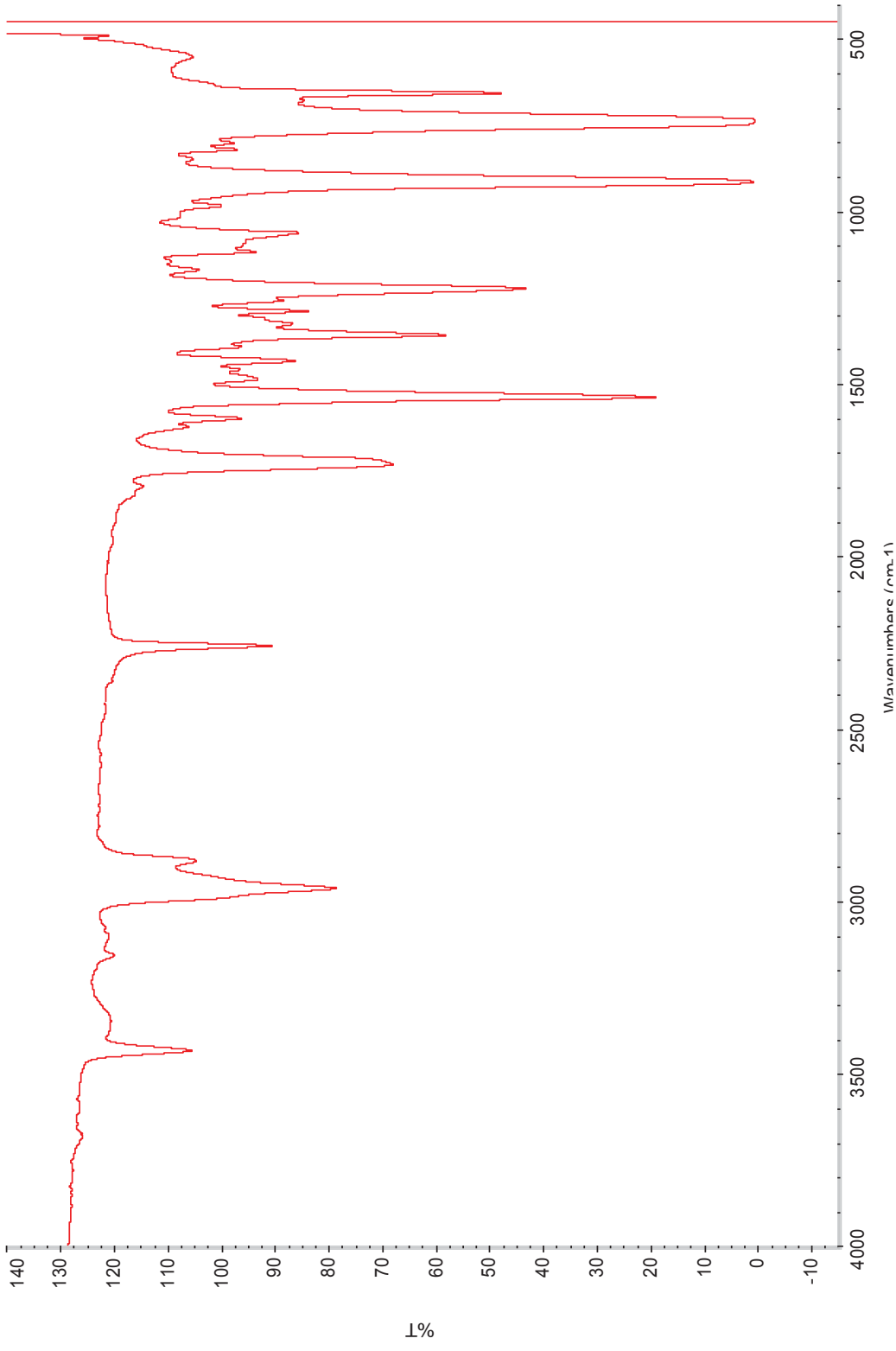

Figure 41: IR spectrum for compound **16**.

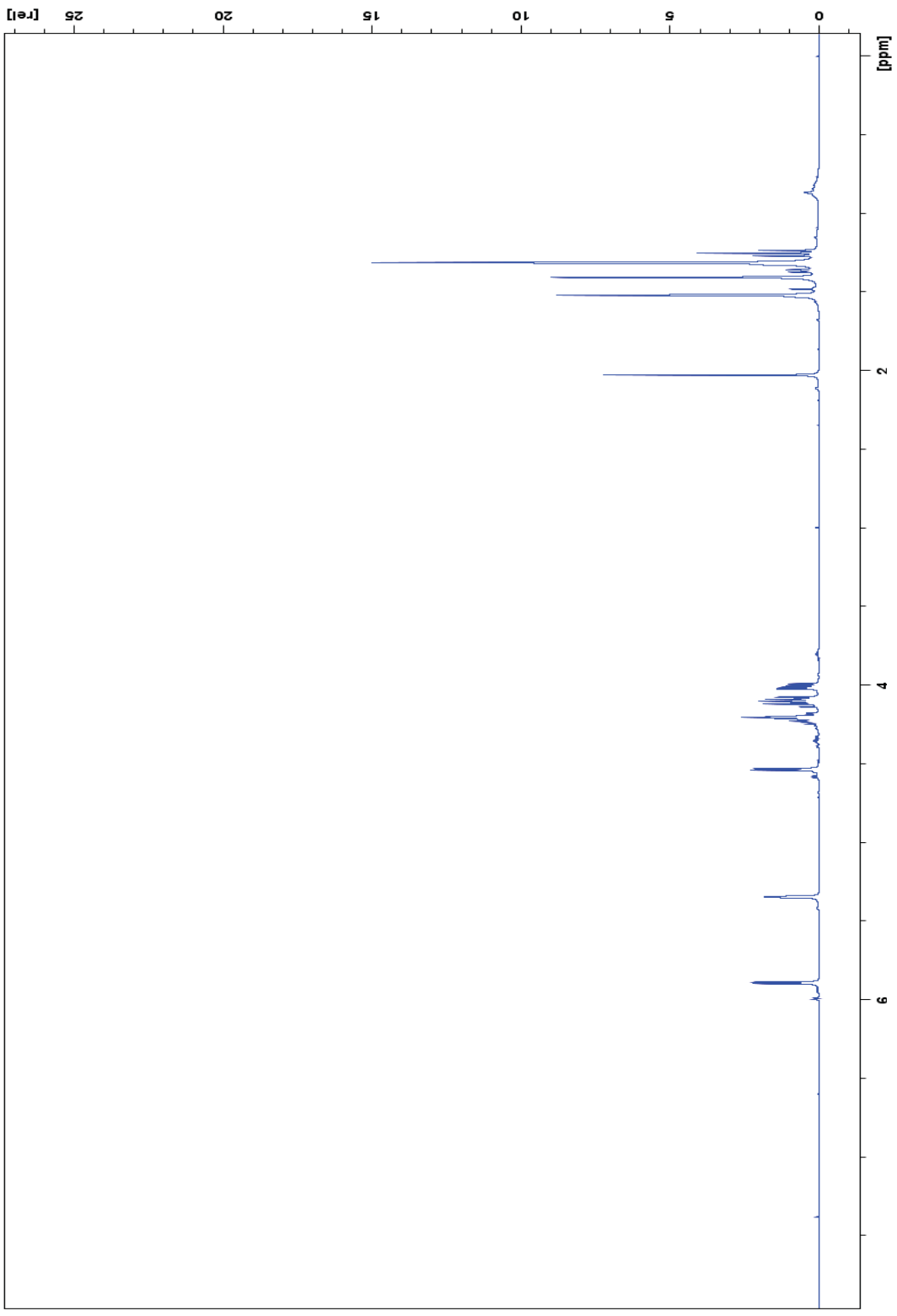

Figure 42: ^{1}H NMR spectrum for compound **17** (crude).

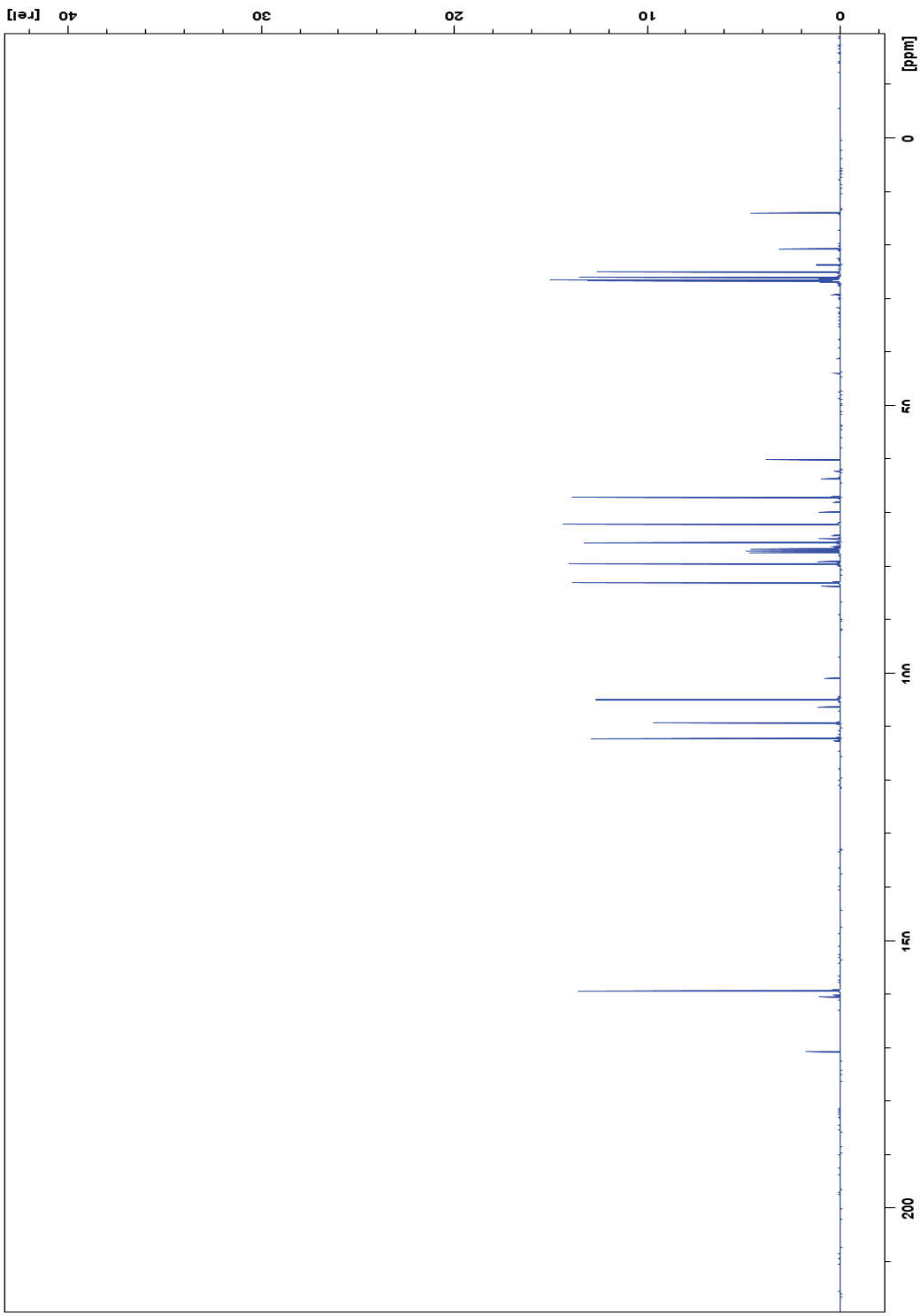

Figure 43: ^{13}C NMR spectrum for compound **17** (crude).

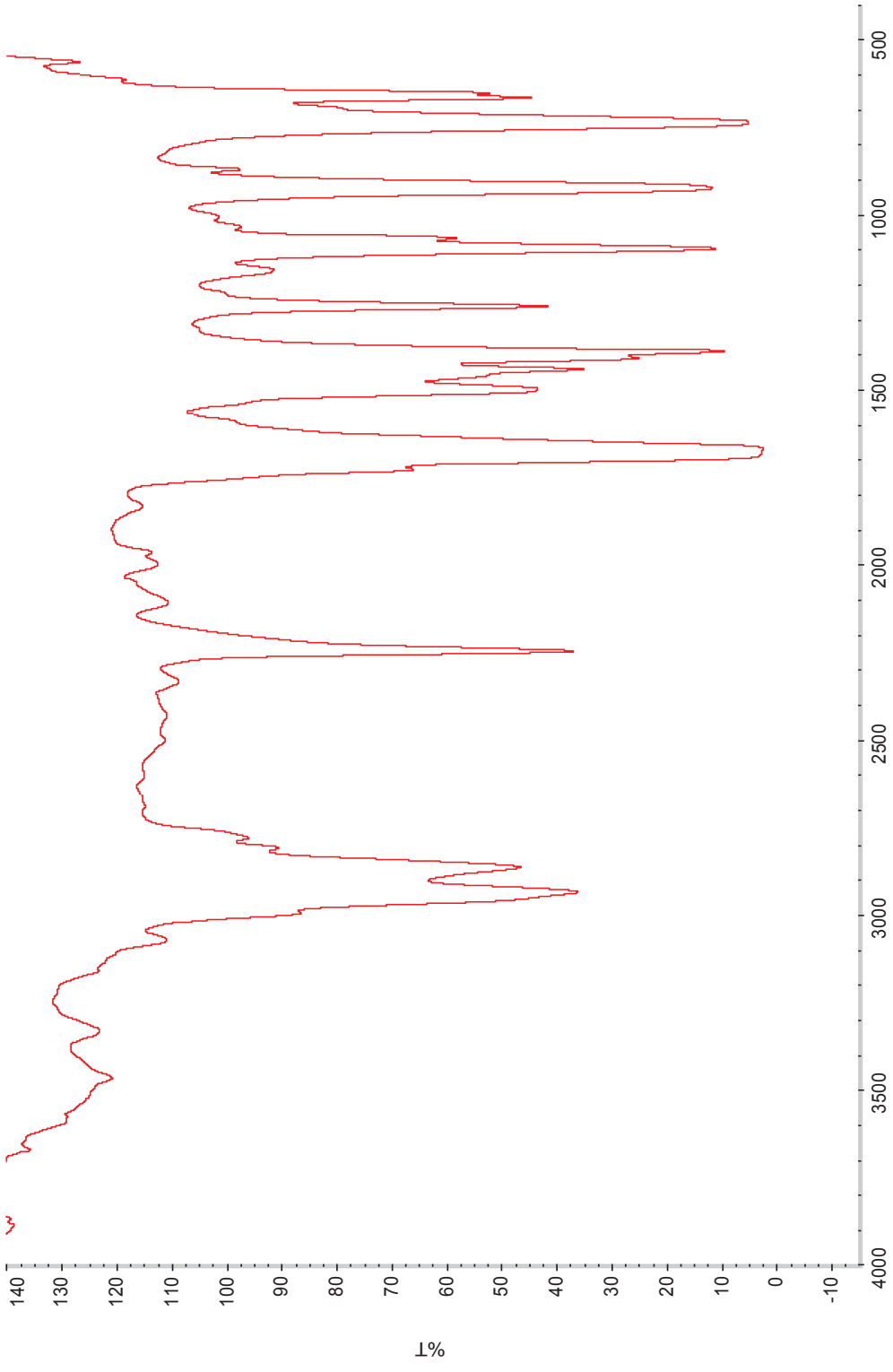

Figure 44: IR spectrum for compound **17** (crude).

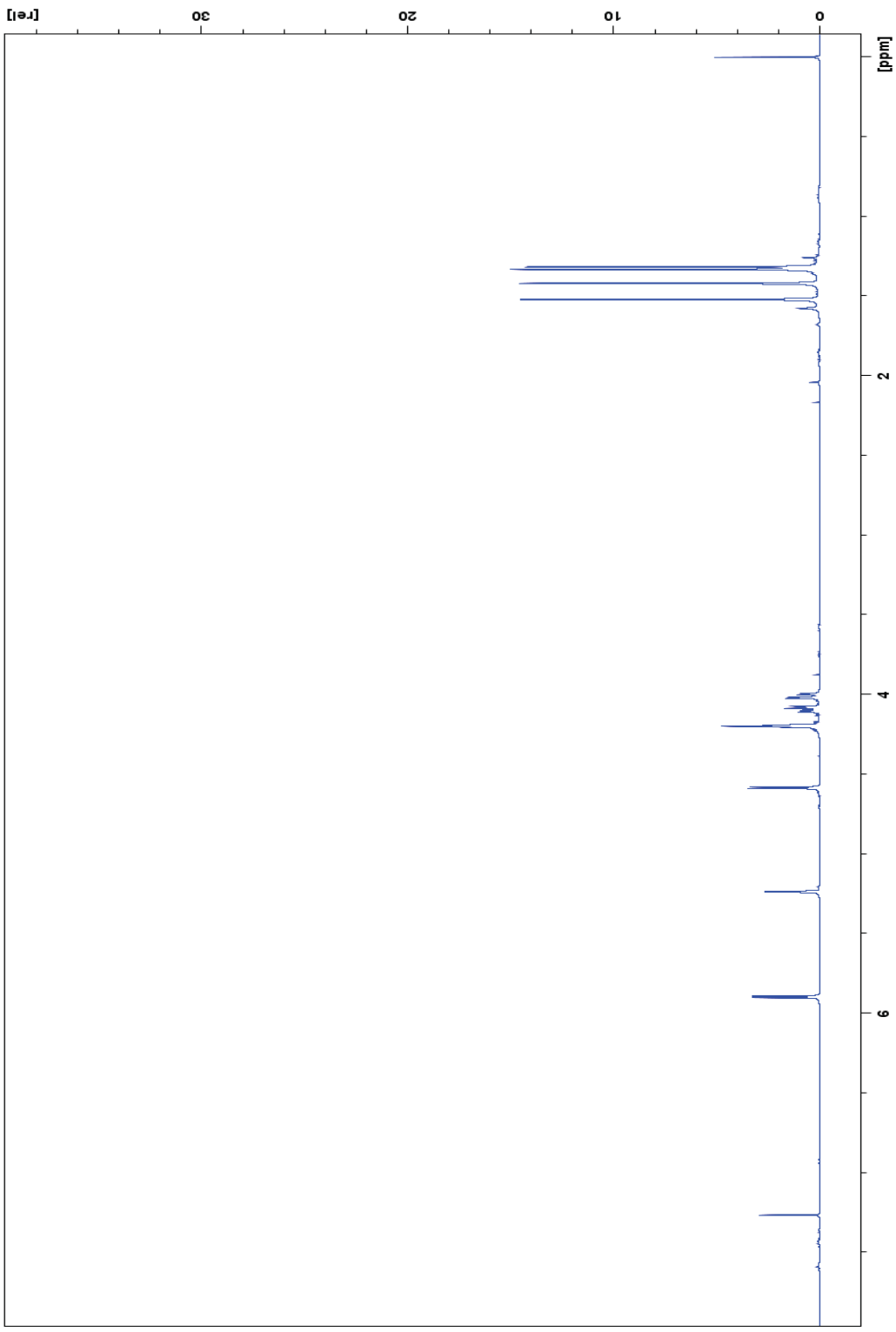

Figure 45: ^{1}H NMR spectrum for compound **18** (crude).

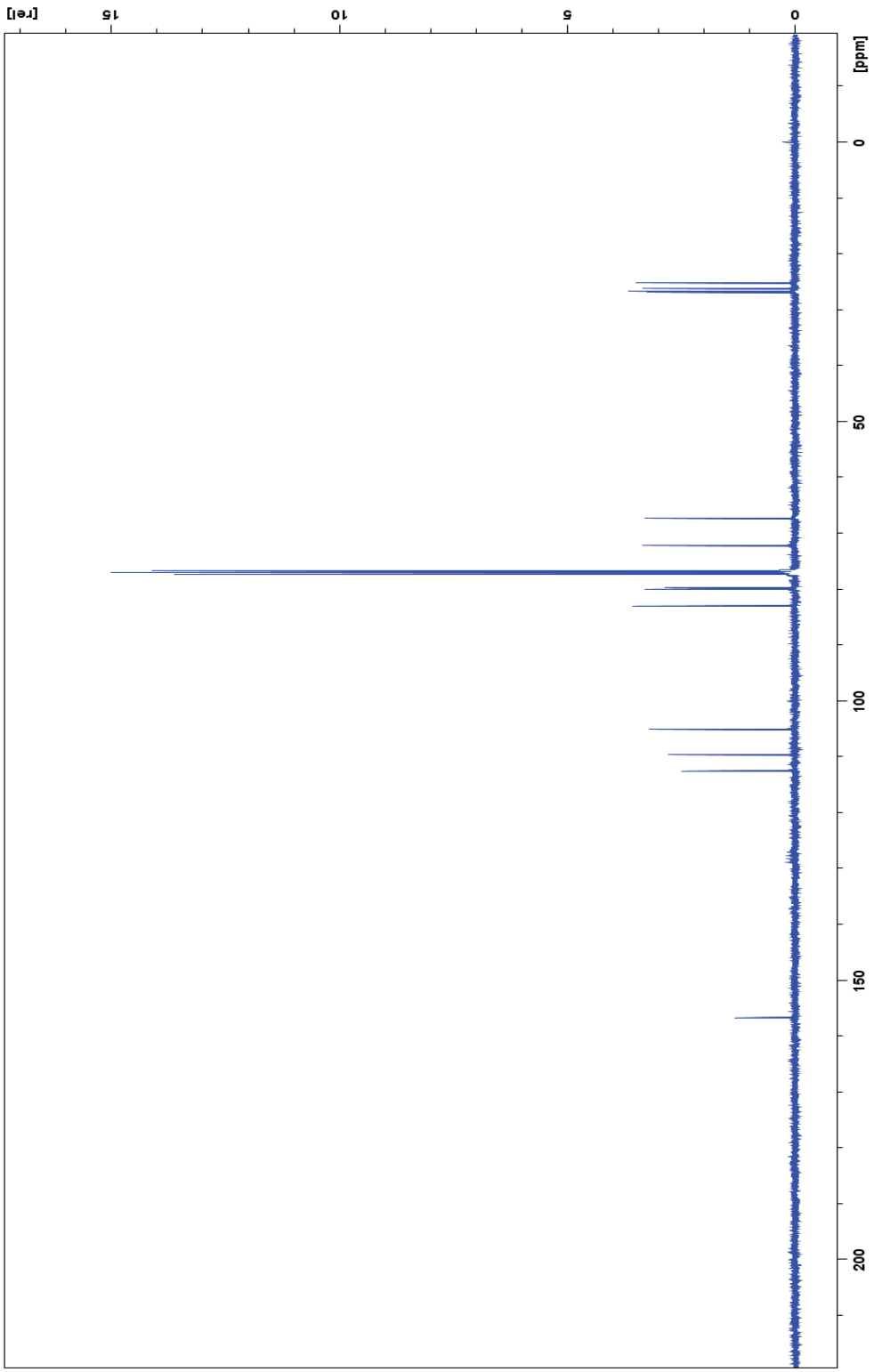

Figure 46: ^{13}C NMR spectrum for compound **18** (crude).

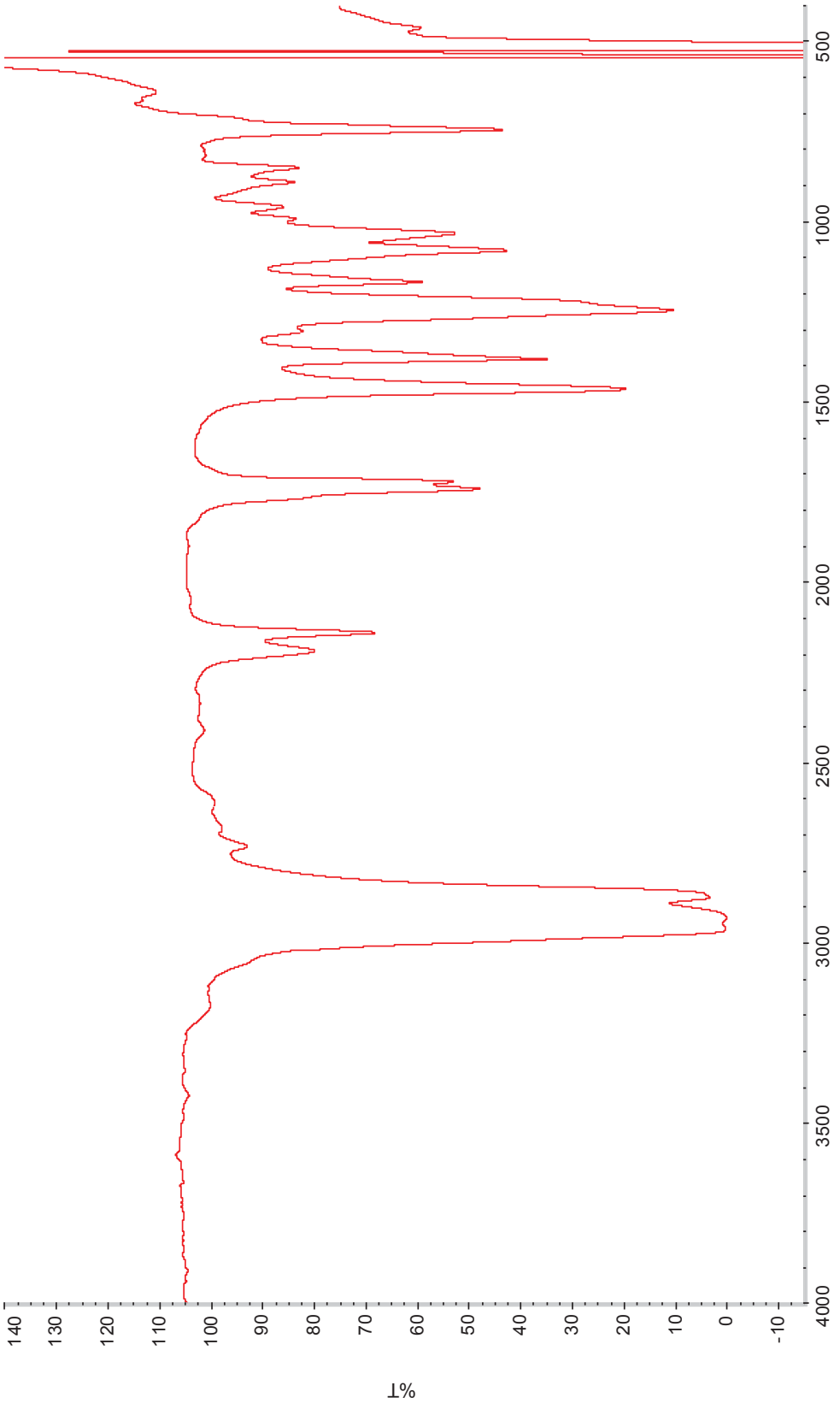

Figure 47: IR spectrum for compound **18** (crude).

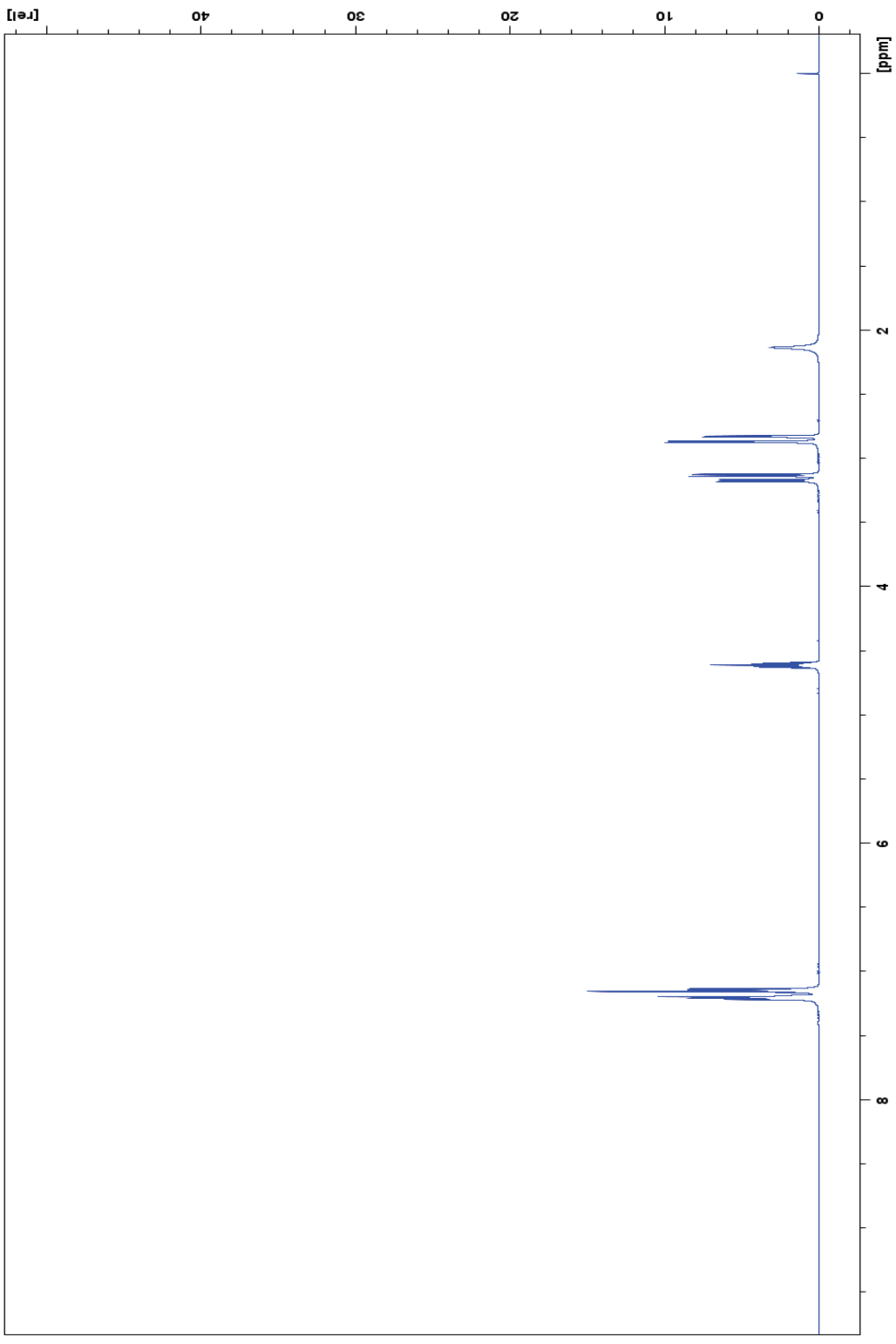

Figure 48: ^{1}H NMR spectrum for compound **19** (crude).

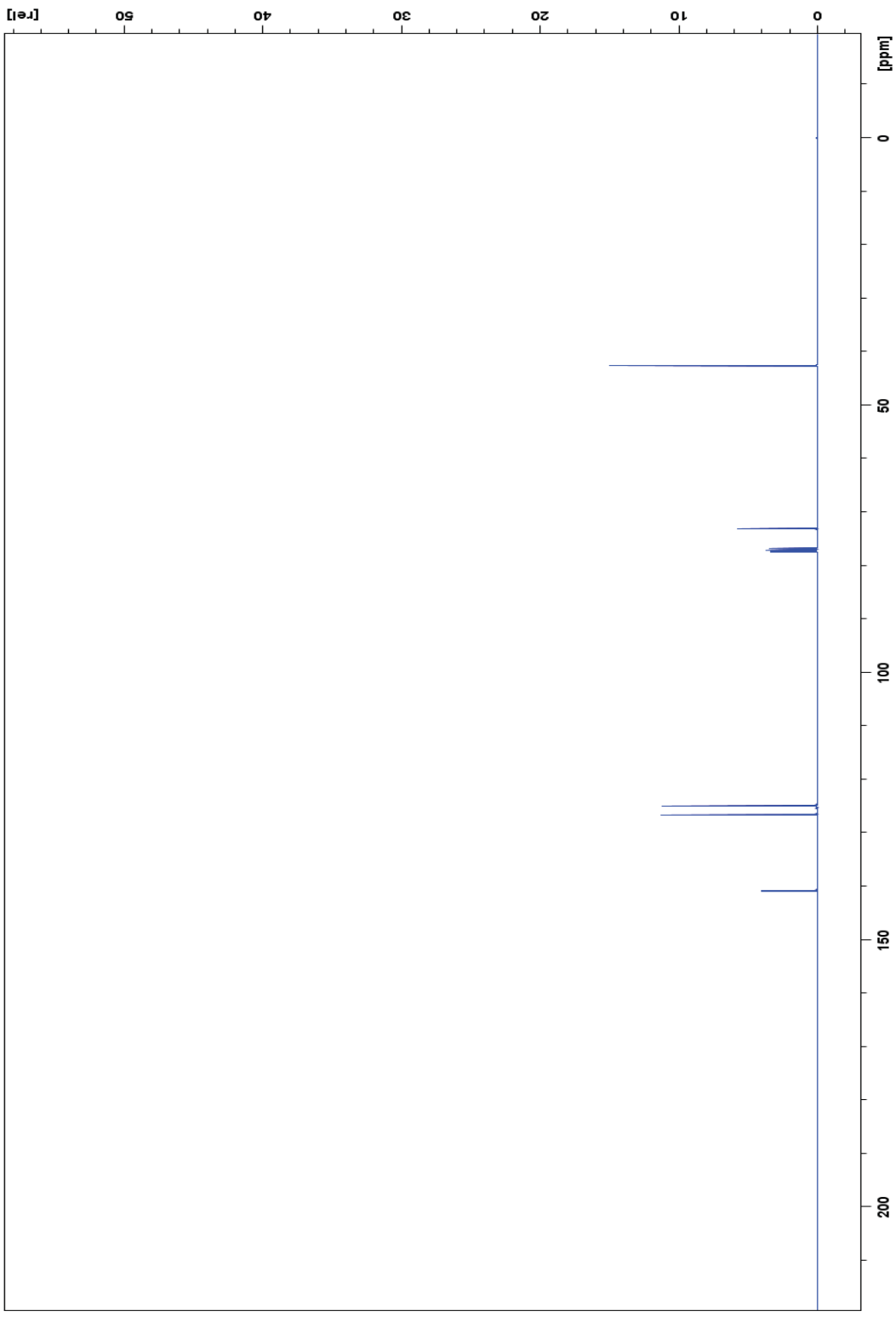

Figure 49: ^{13}C NMR spectrum for compound **19** (crude).

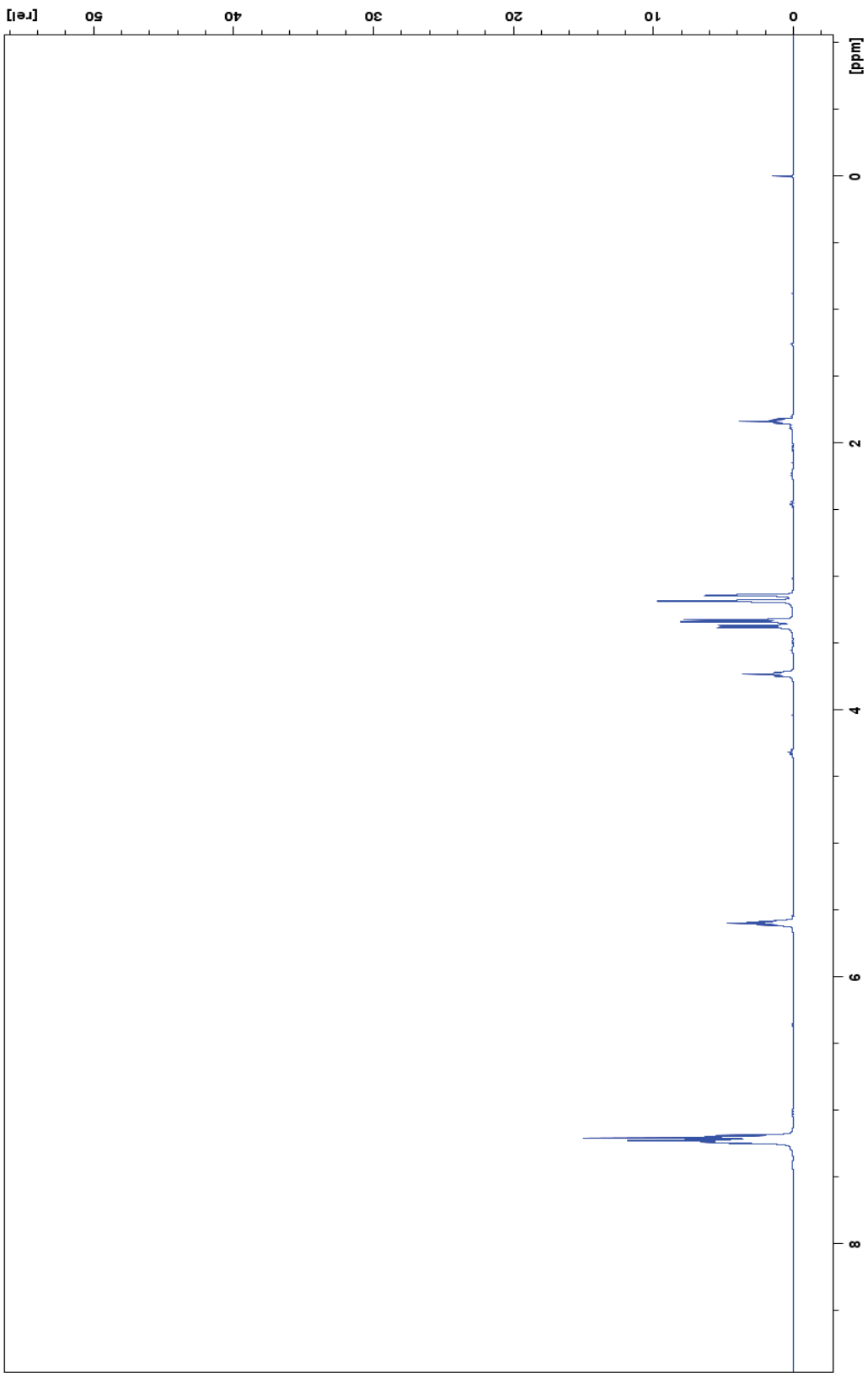

Figure 50: ^{1}H NMR spectrum for compound **20** (crude).

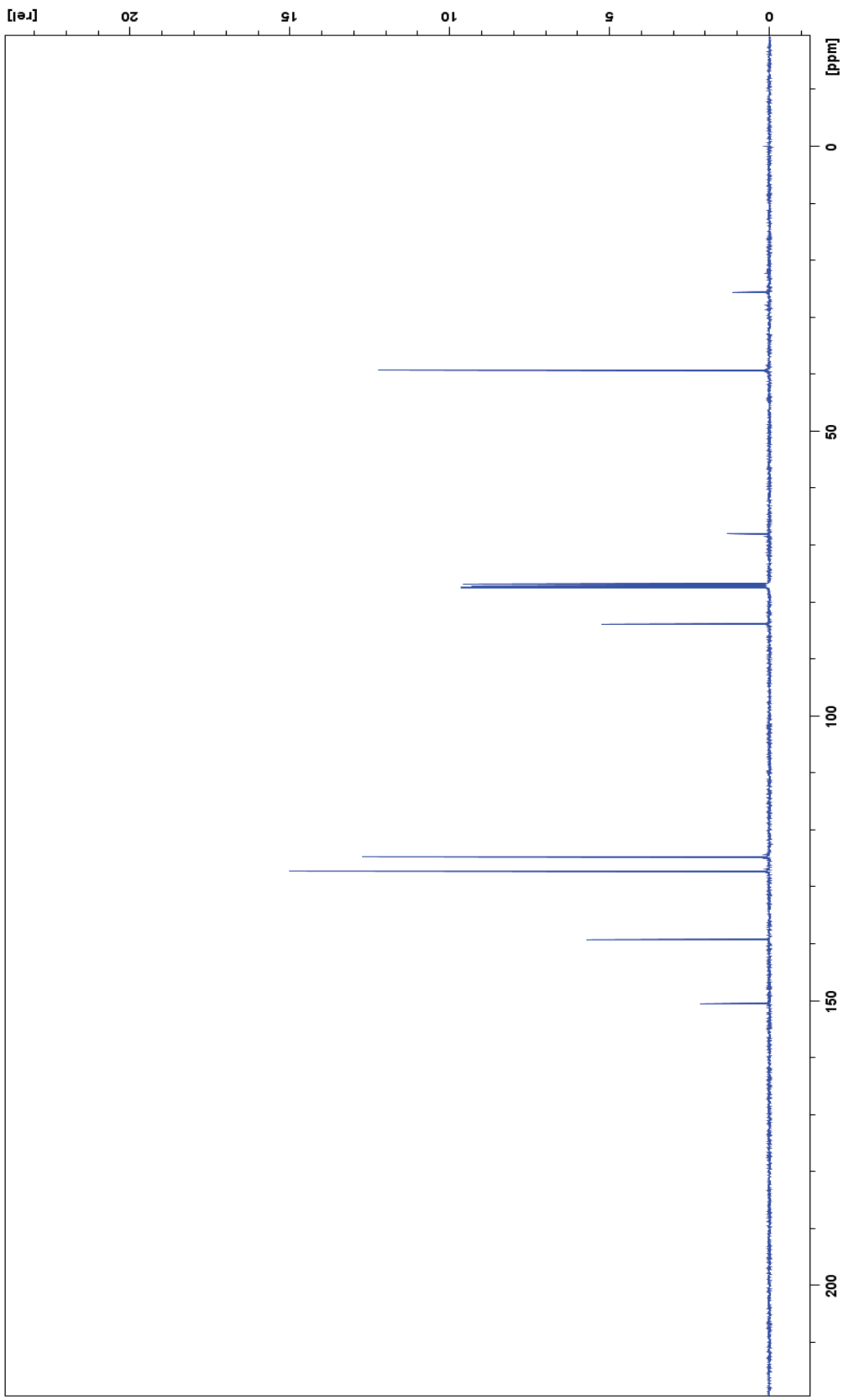

Figure 51: ^{13}C NMR spectrum for compound **20** (crude).

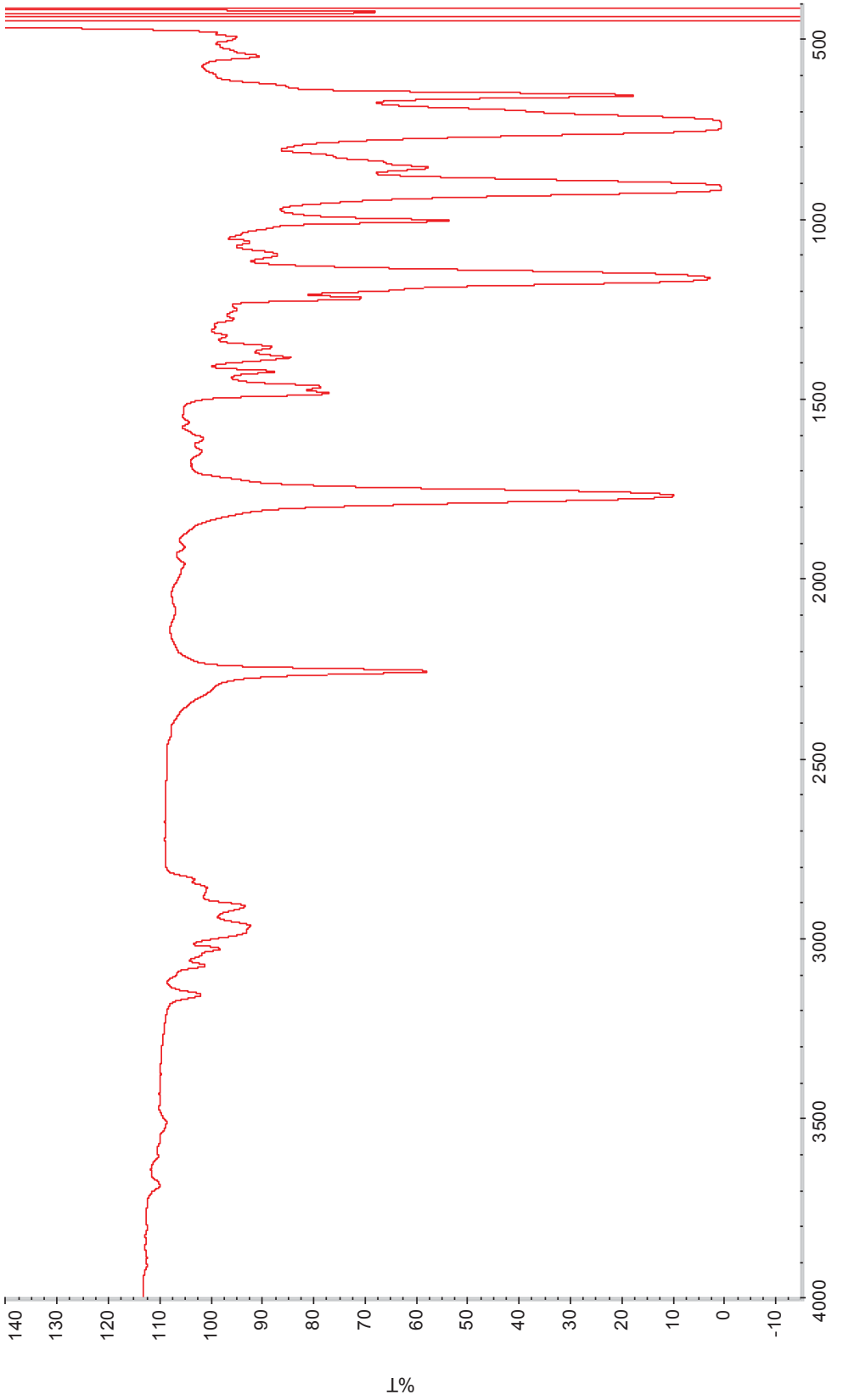

Figure 52: IR spectrum for compound **20** (crude).

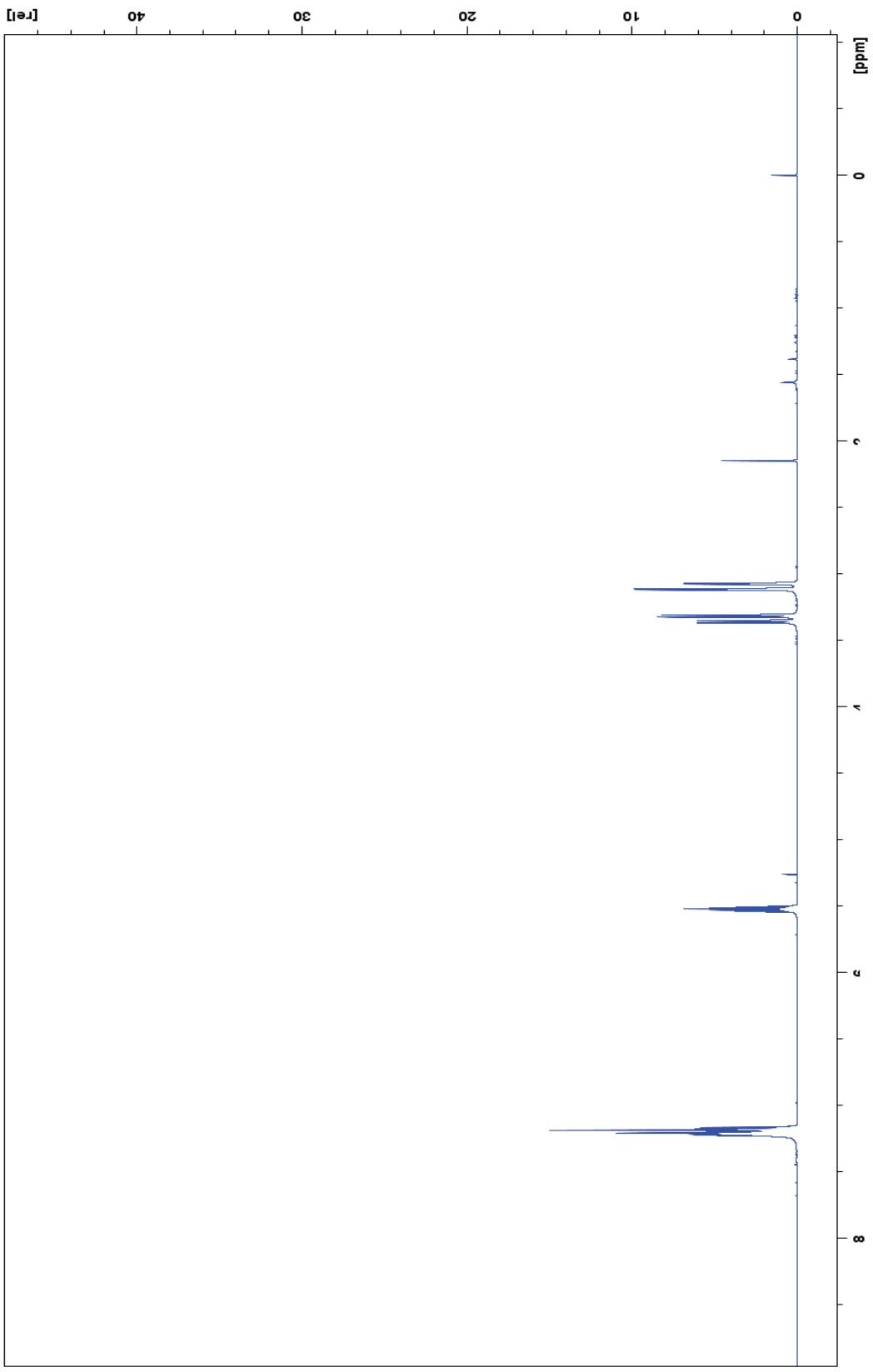

Figure 53: ^{1}H NMR spectrum for compound **21**. (crude).

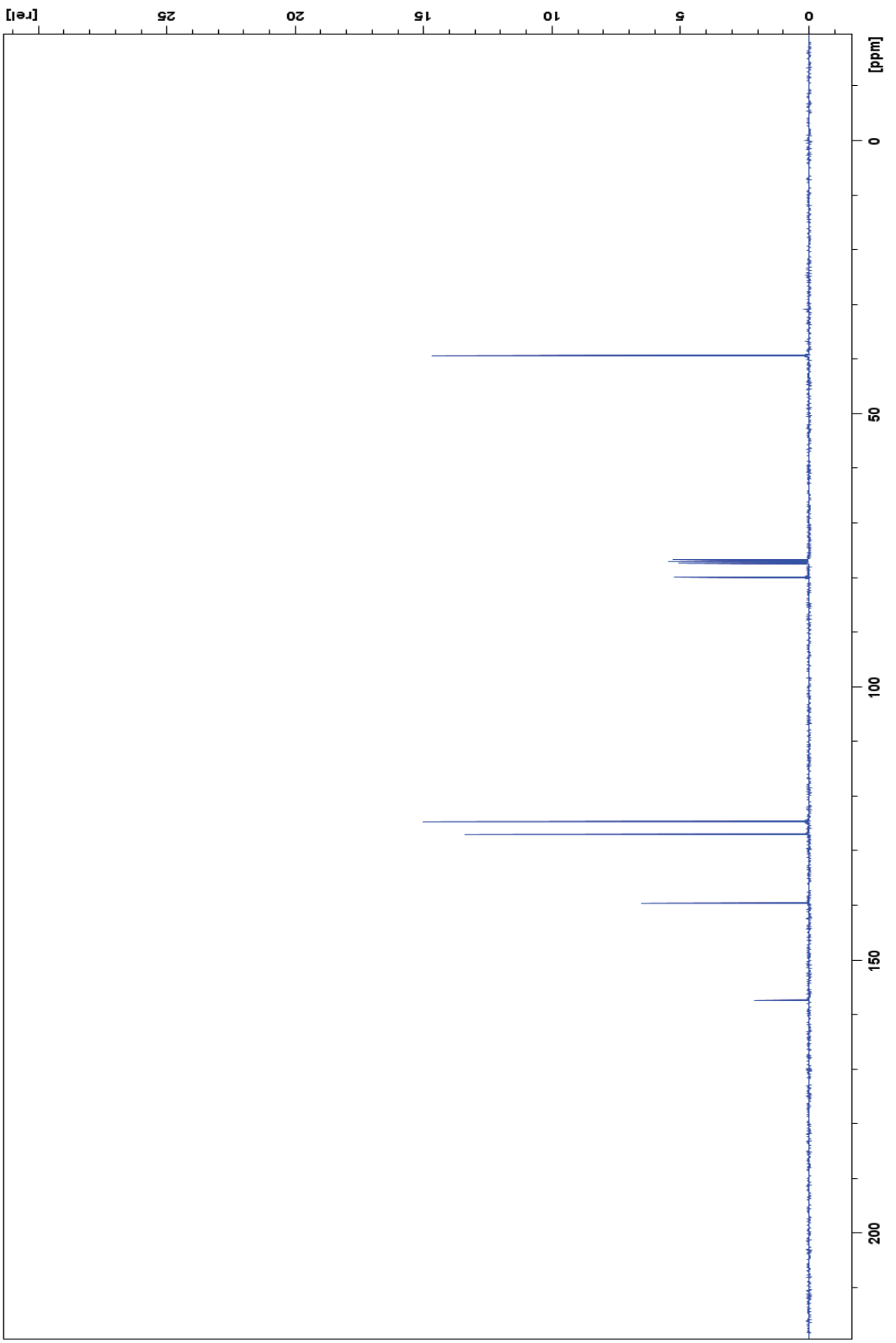

Figure 54: ^{13}C NMR spectrum for compound **21**. (crude).

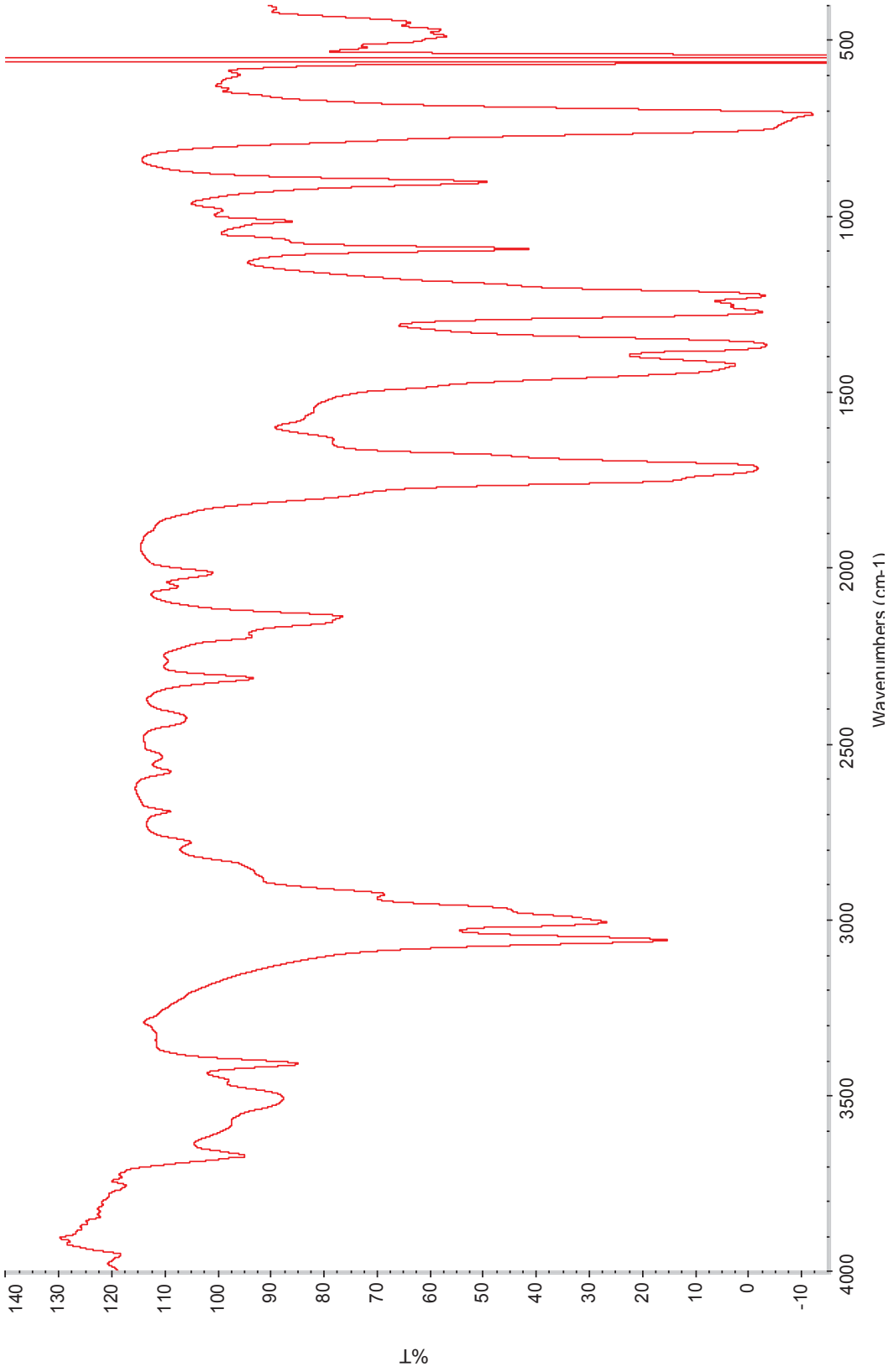

Figure 55: IR spectrum for compound **21**. (crude).

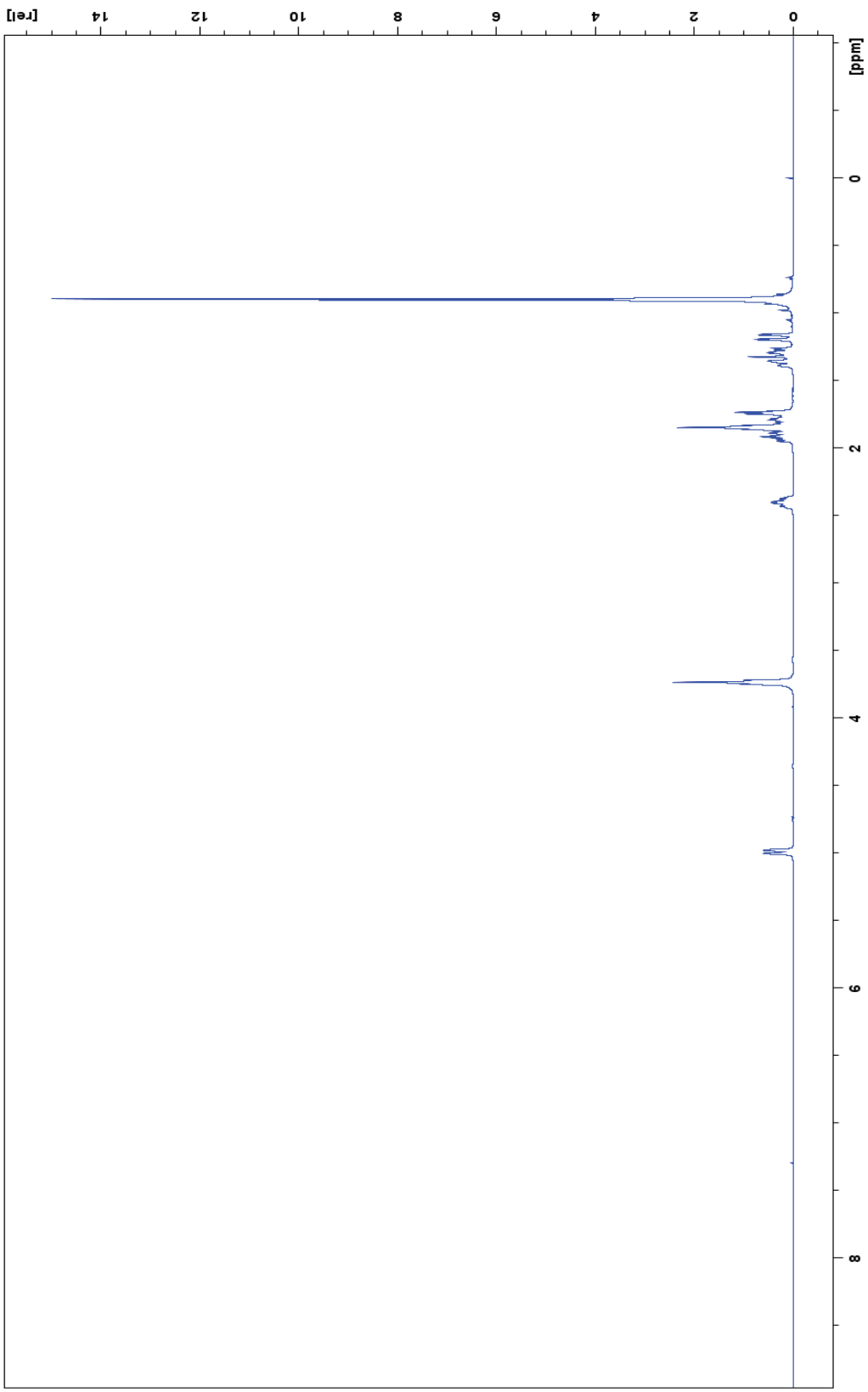

Figure 56: ^{1}H NMR spectrum for compound **22** (crude).

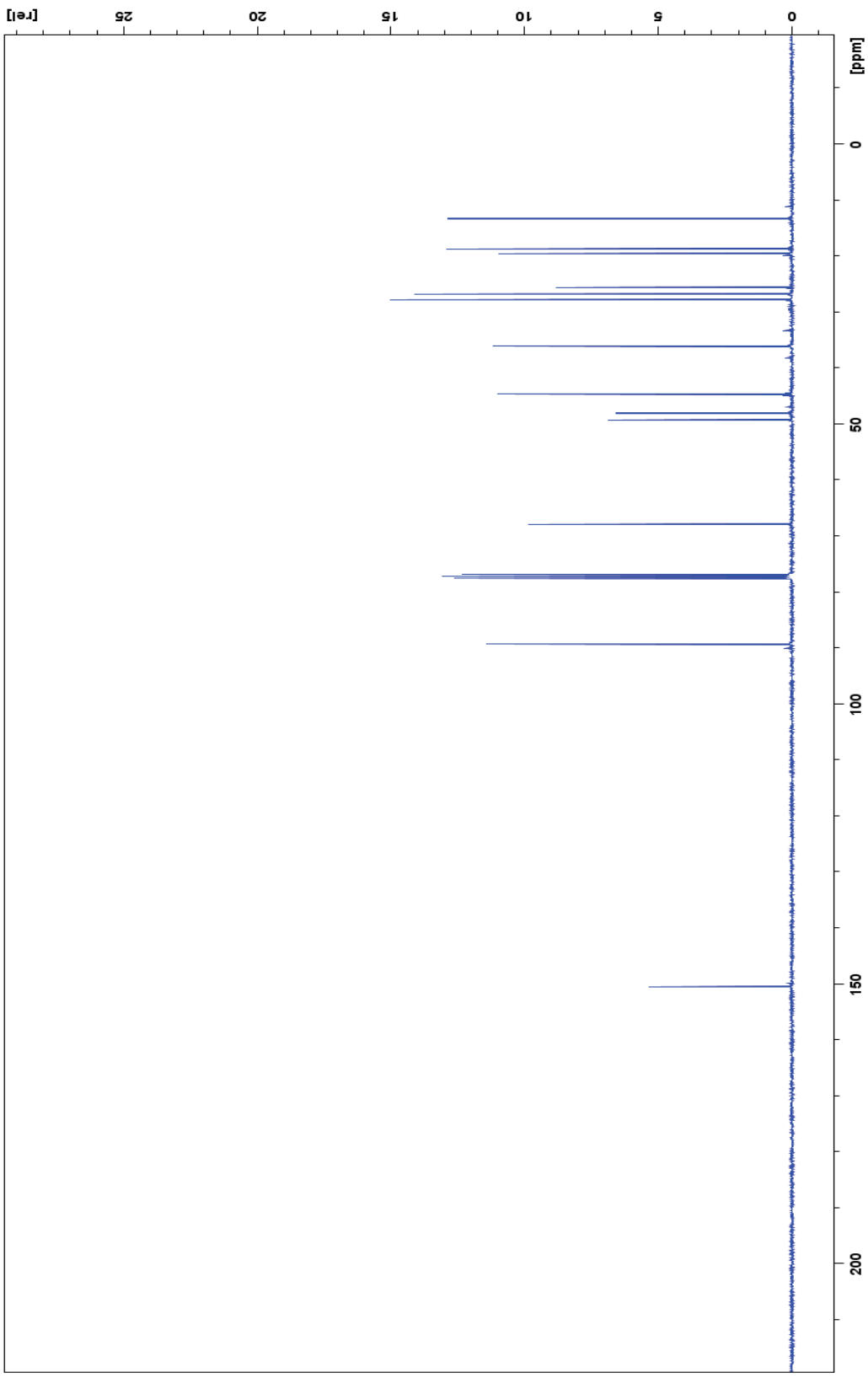

Figure 57: ^{13}C NMR spectrum for compound **22** (crude).

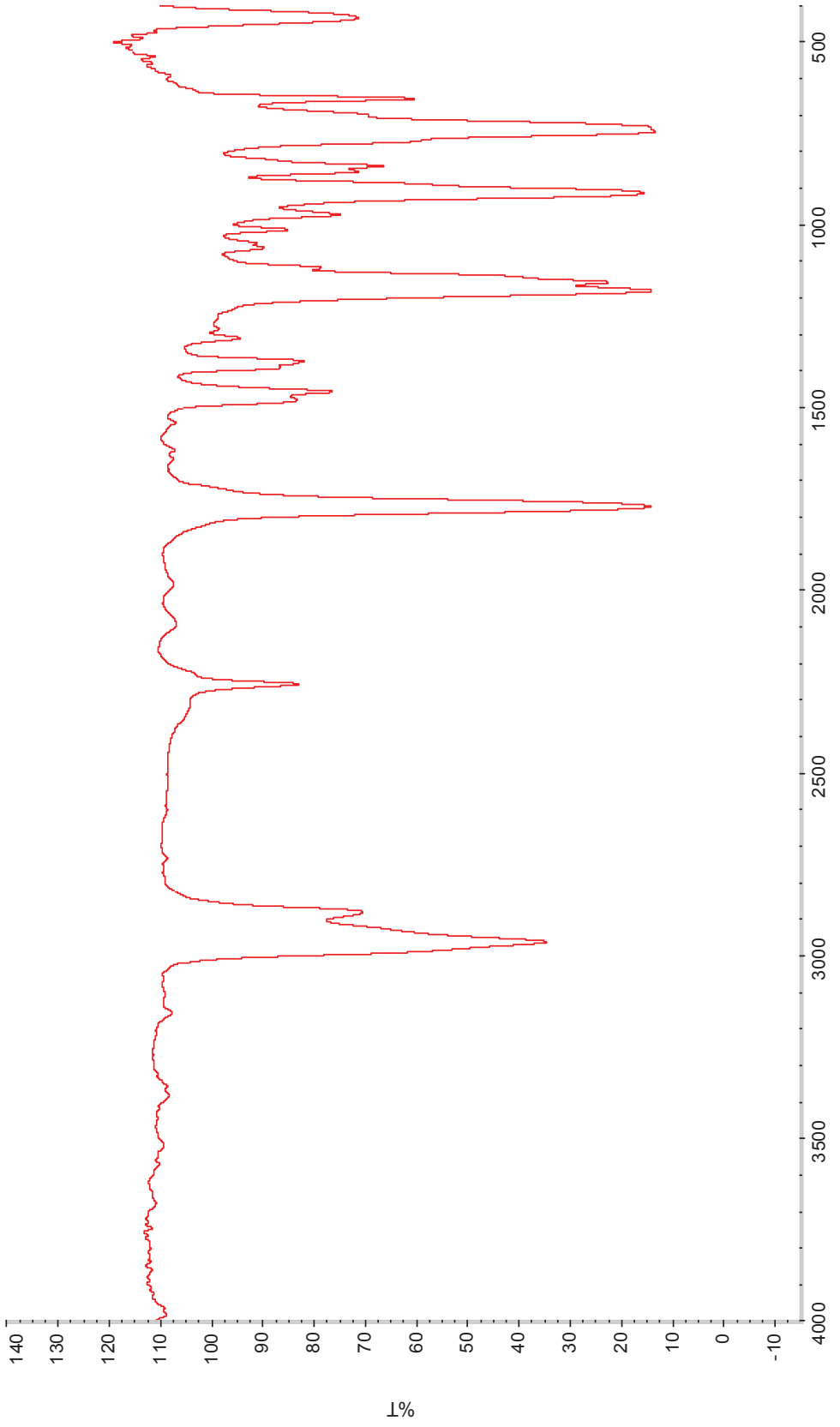

Figure 58: IR spectrum for compound **22** (crude).

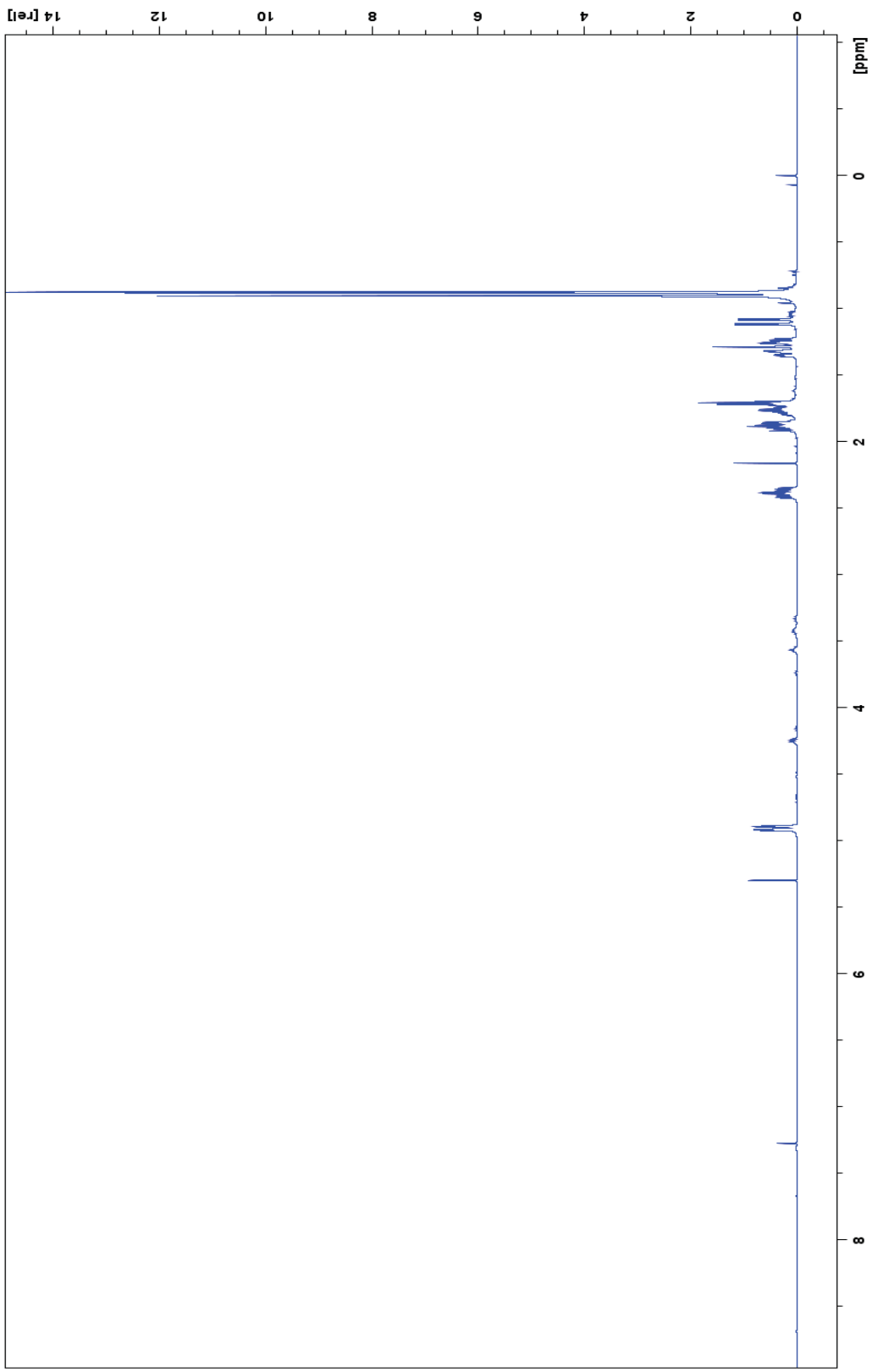

Figure 59: ^{1}H NMR spectrum for compound **23** (crude).

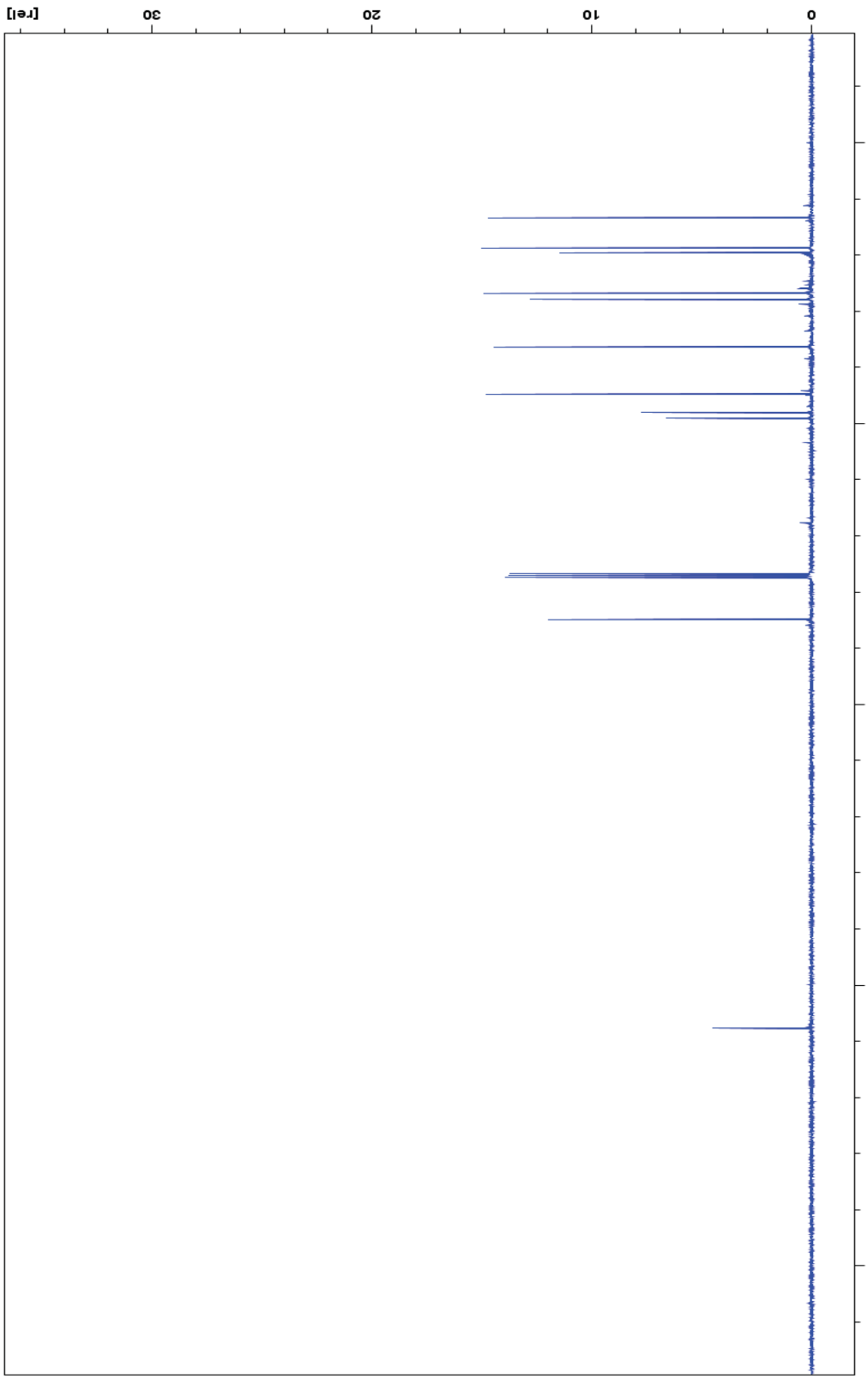

Figure 60: ^{13}C NMR spectrum for compound **23** (crude).

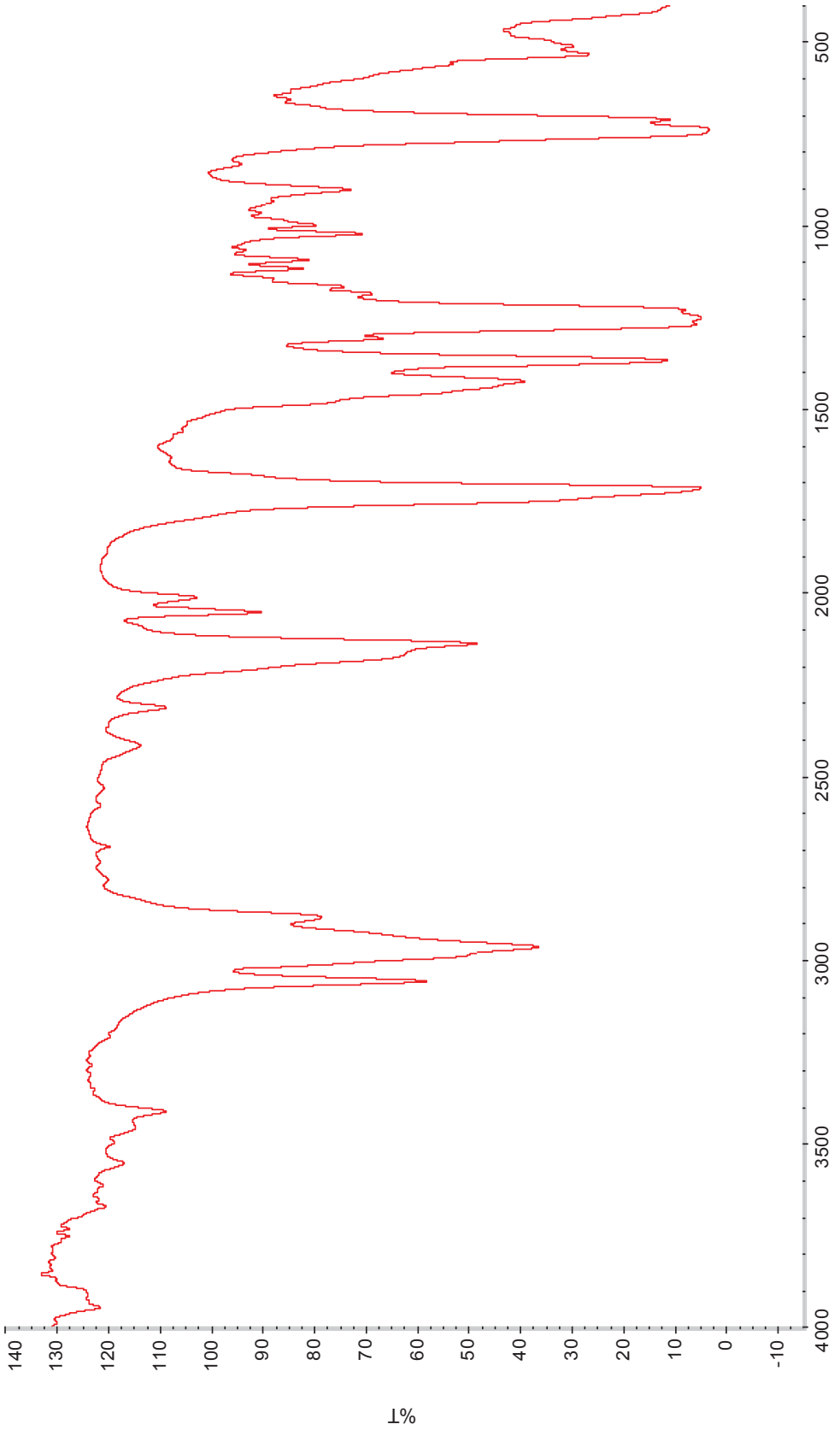

Figure 61: IR spectrum for compound **23** (crude).

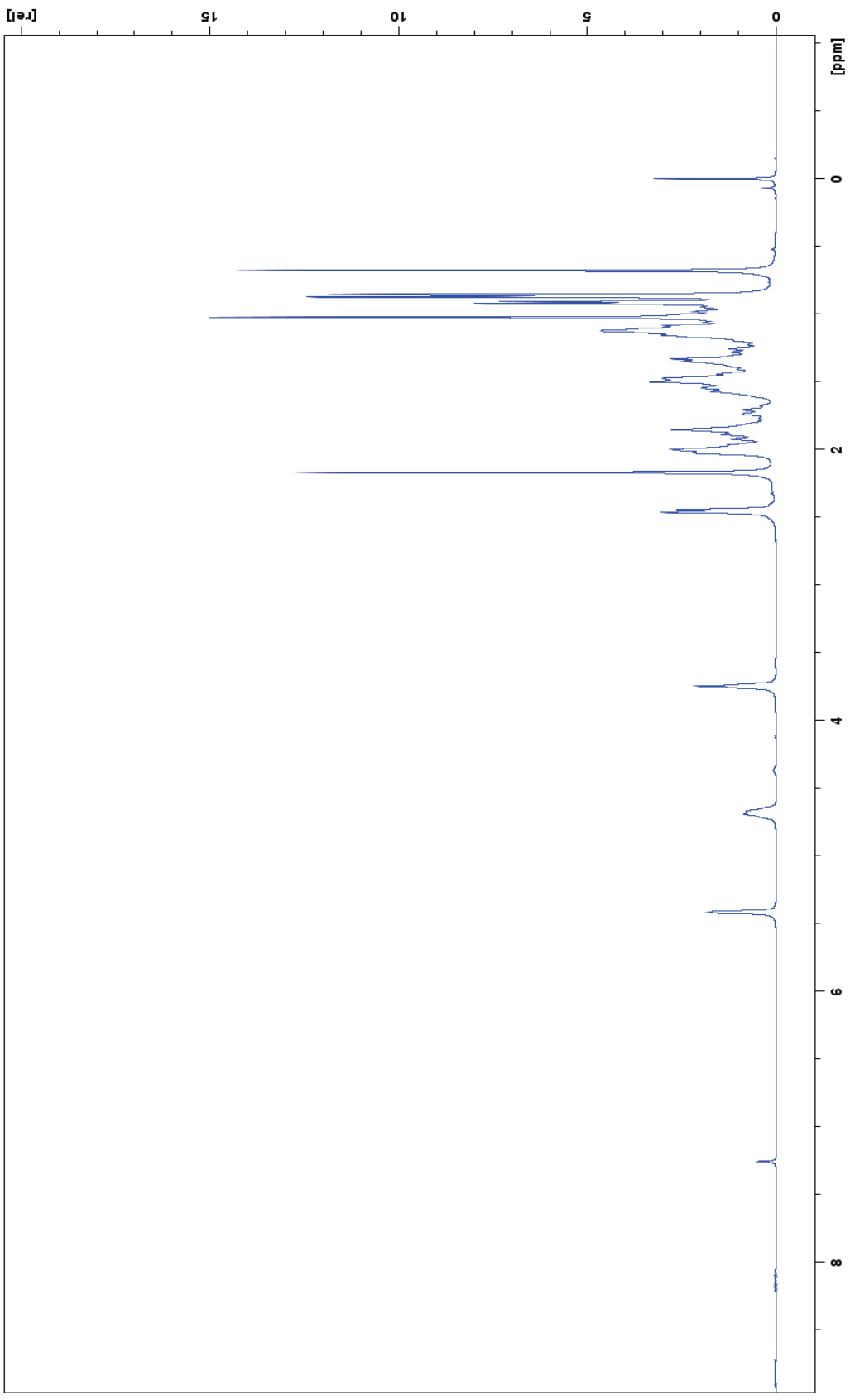

Figure 62: ^{1}H NMR spectrum for compound **24** (crude).

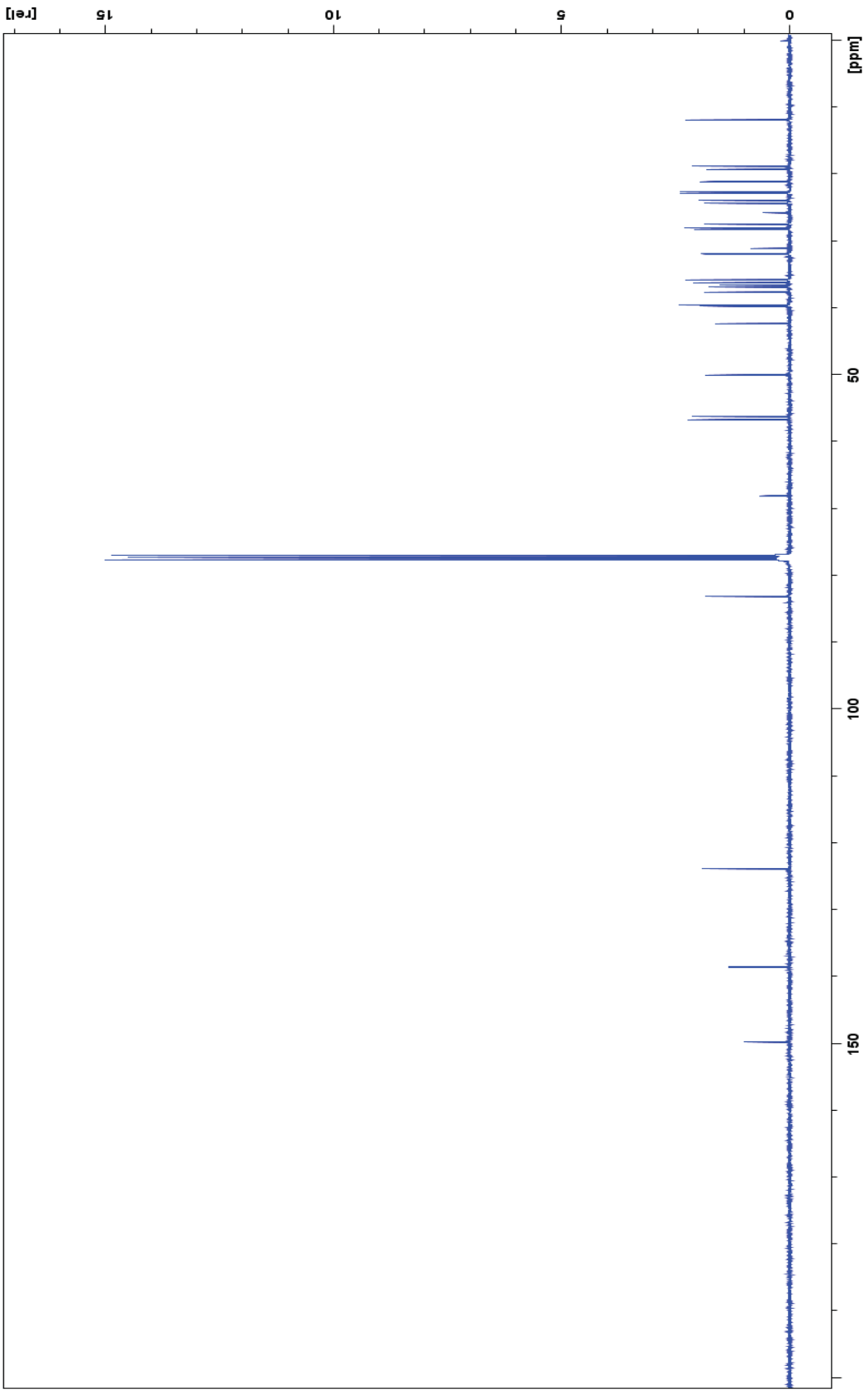

Figure 63: ^{13}C NMR spectrum for compound **24** (crude).

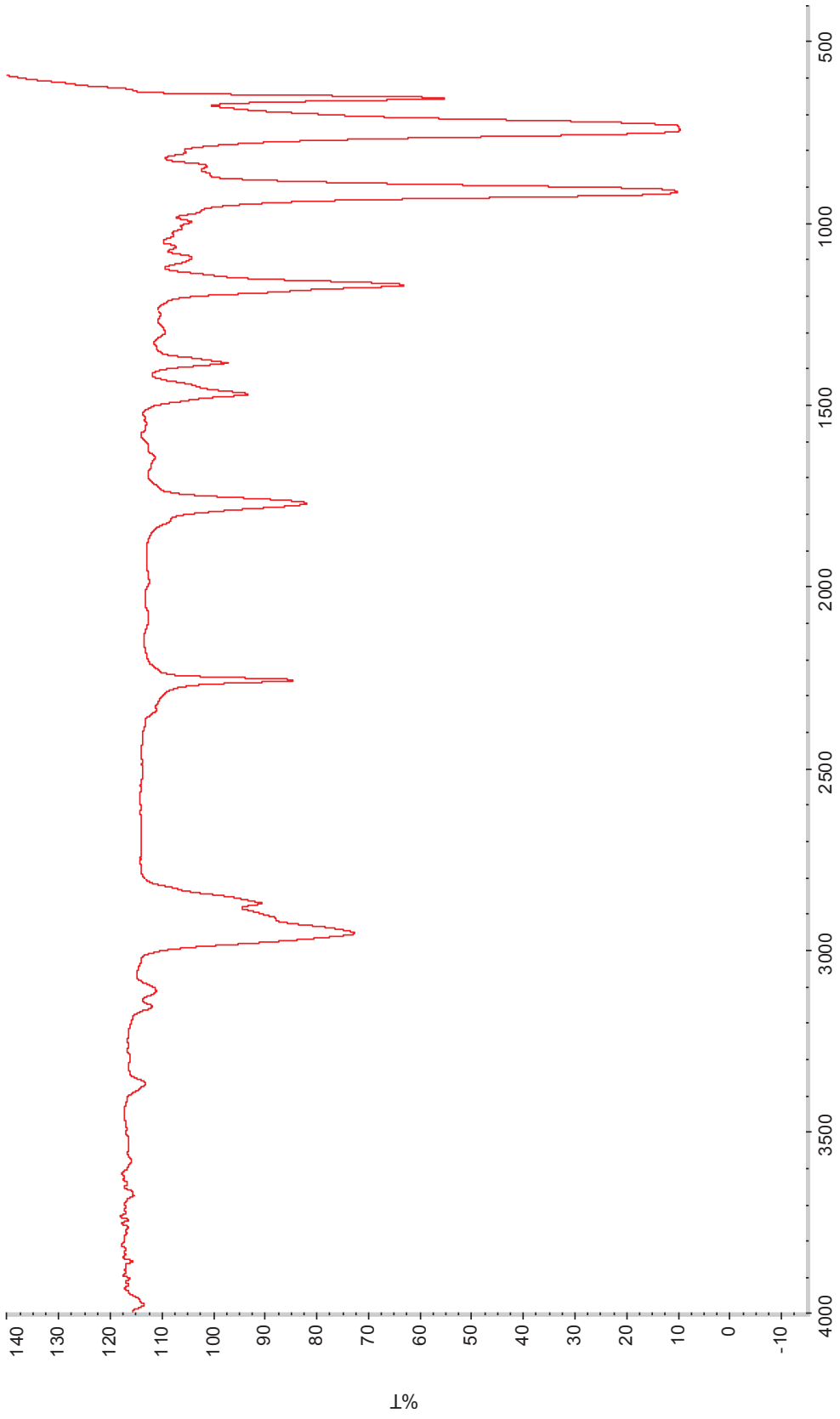

Figure 64: IR spectrum for compound **24** (crude).

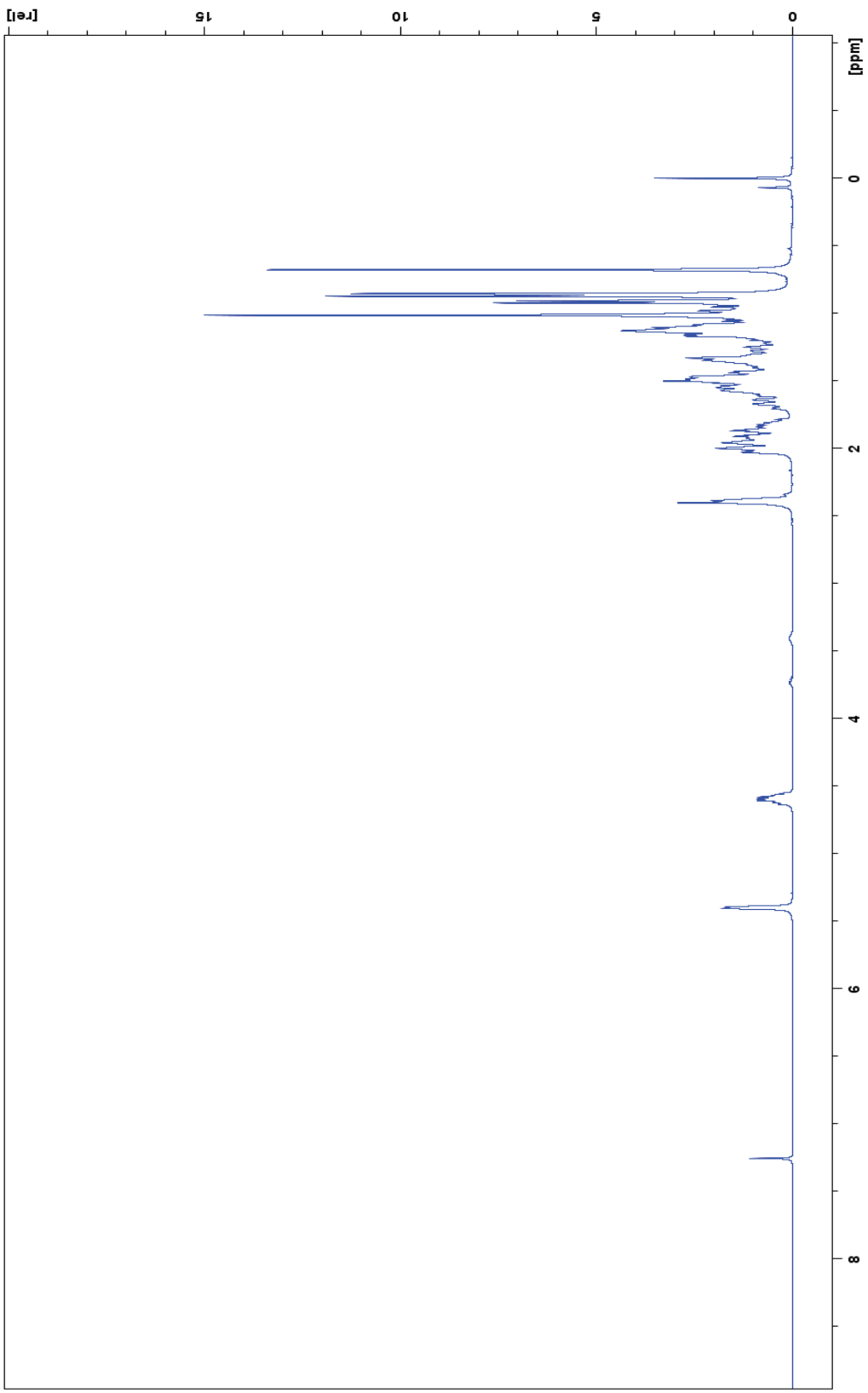

Figure 65: ^{1}H NMR spectrum for compound **25**.

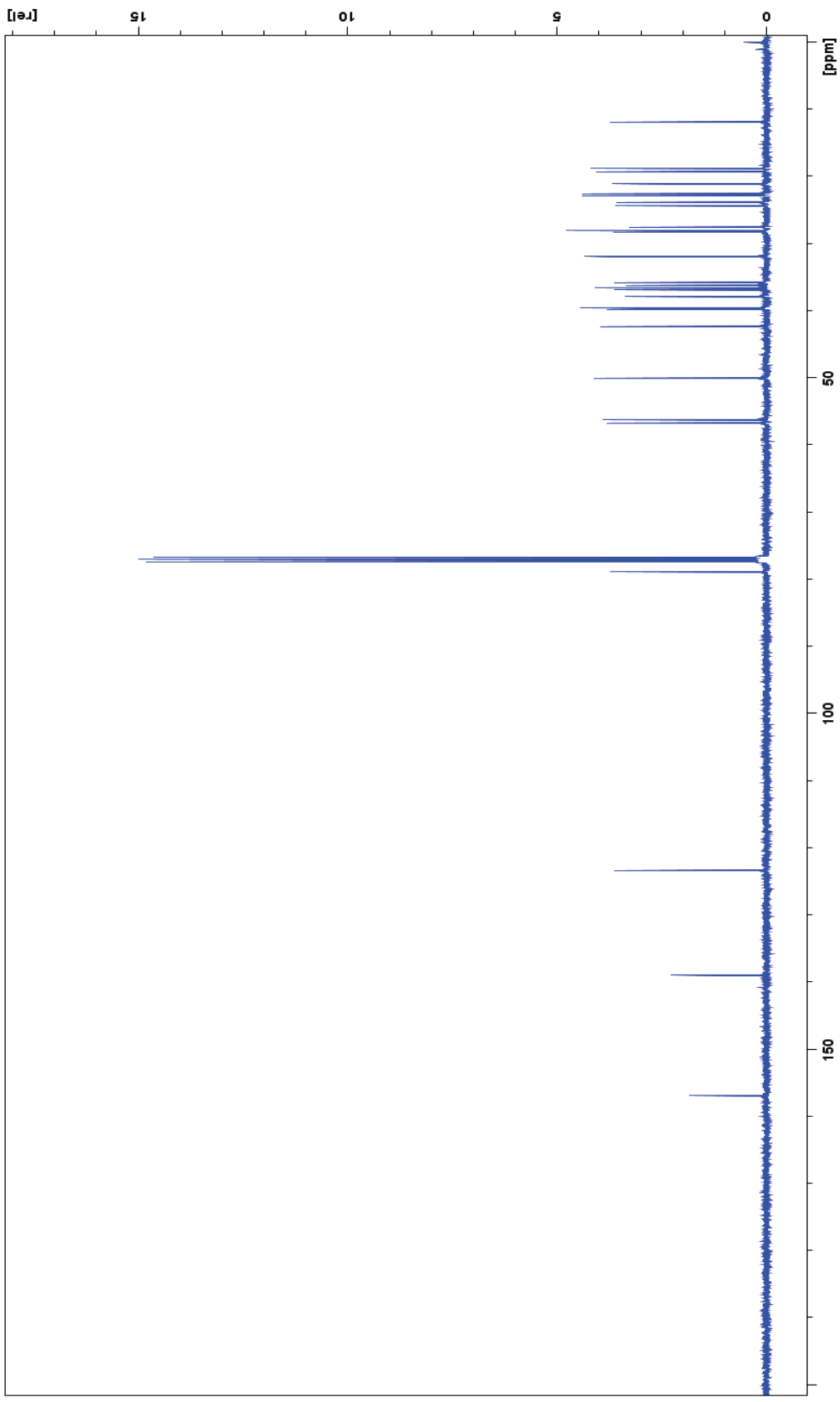

Figure 66: ^{13}C NMR spectrum for compound **25**.

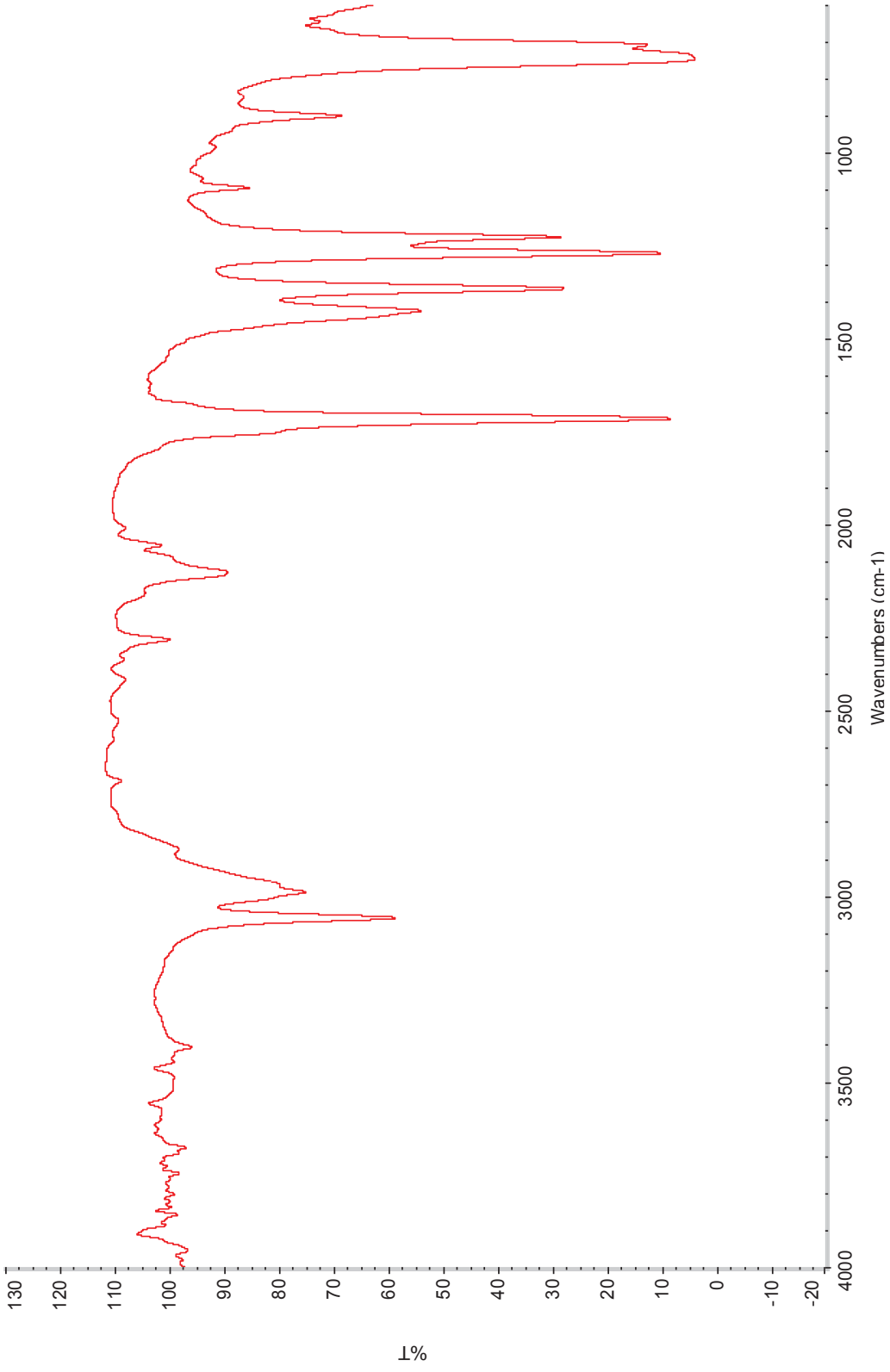

Figure 67: IR spectrum for compound **25**.

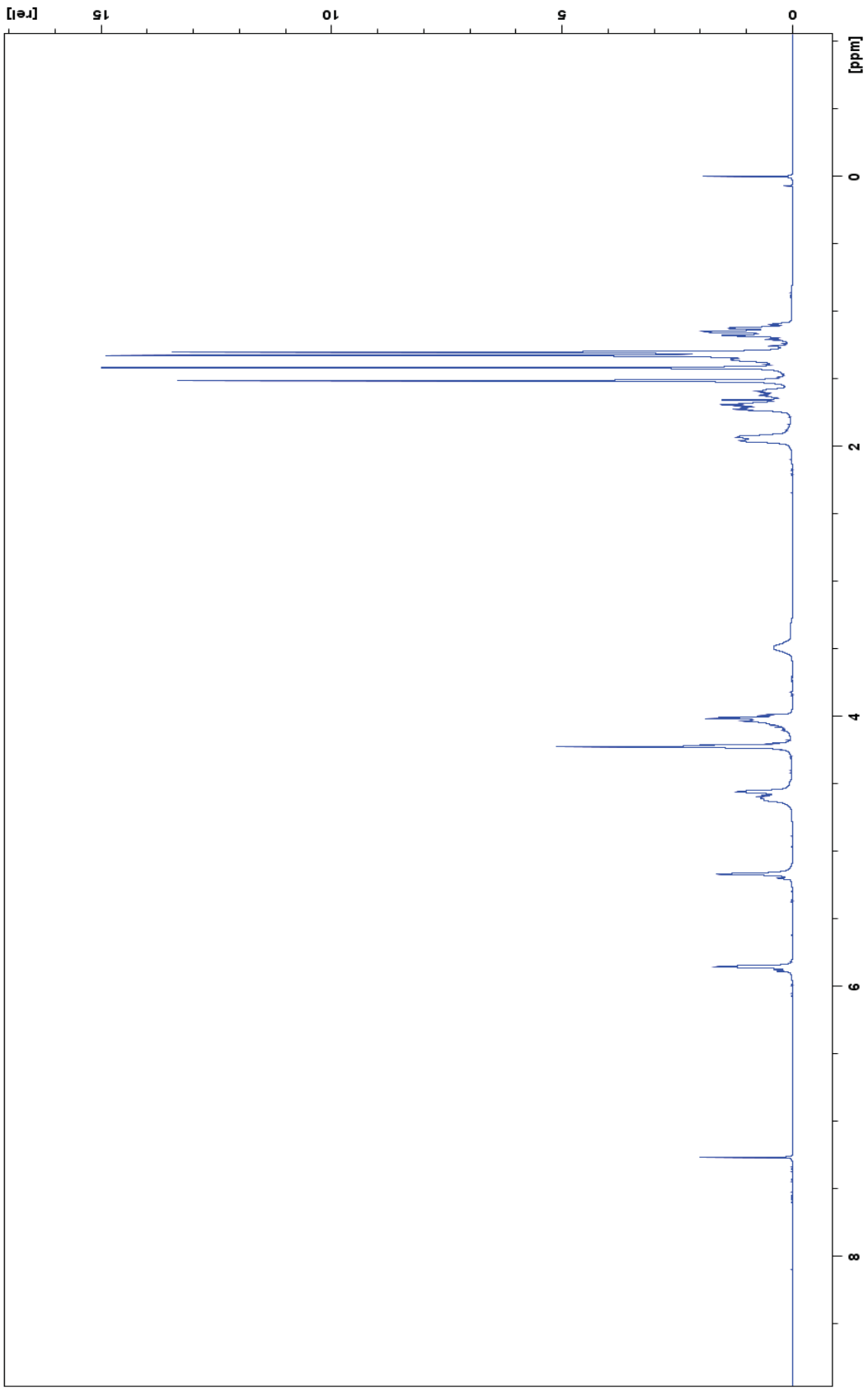

Figure 68: ^{1}H NMR spectrum for compound **26**.

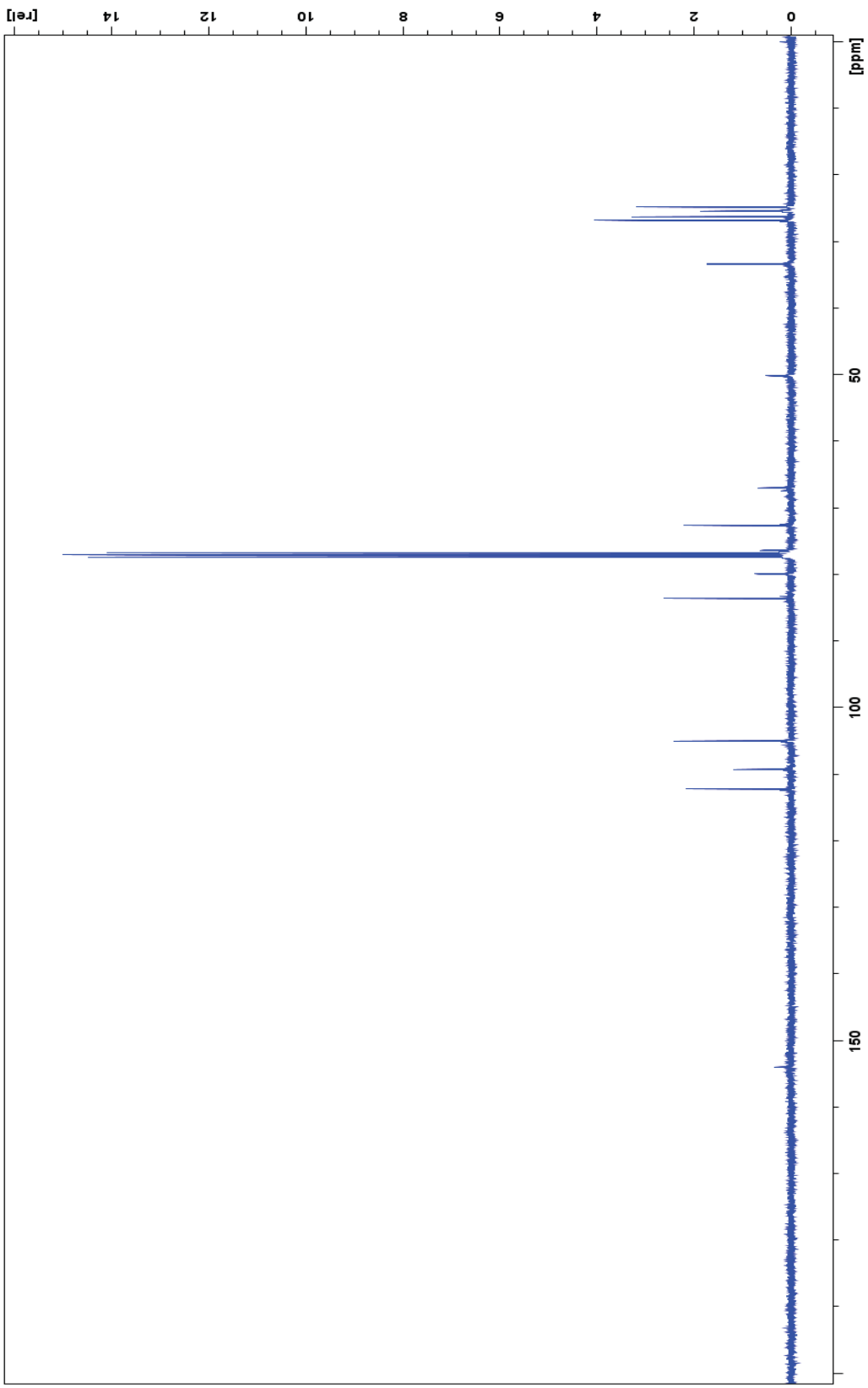

Figure 69: ^{13}C NMR spectrum for compound **26**.

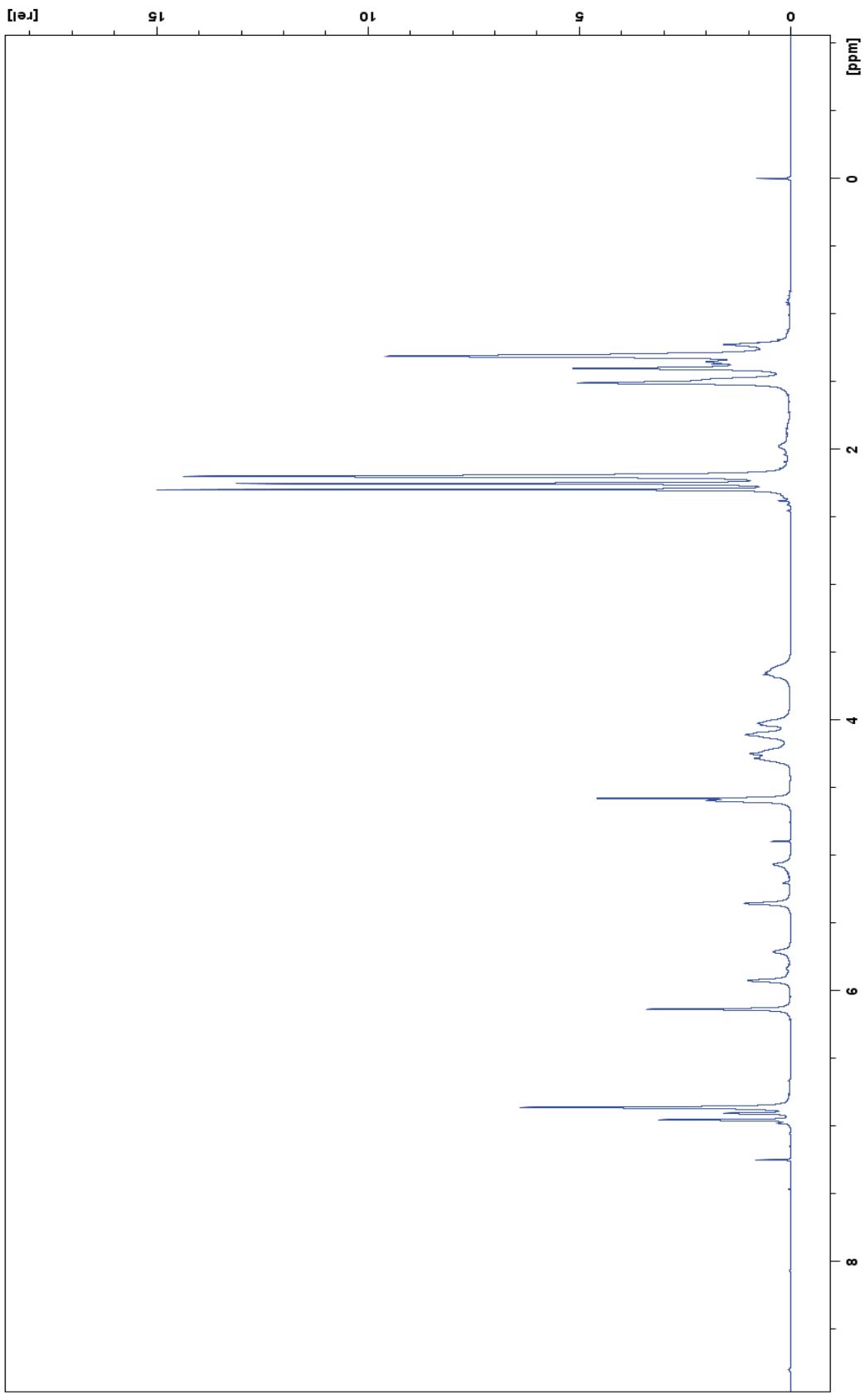

Figure 70: ^{1}H NMR spectrum for compound **27** (crude).

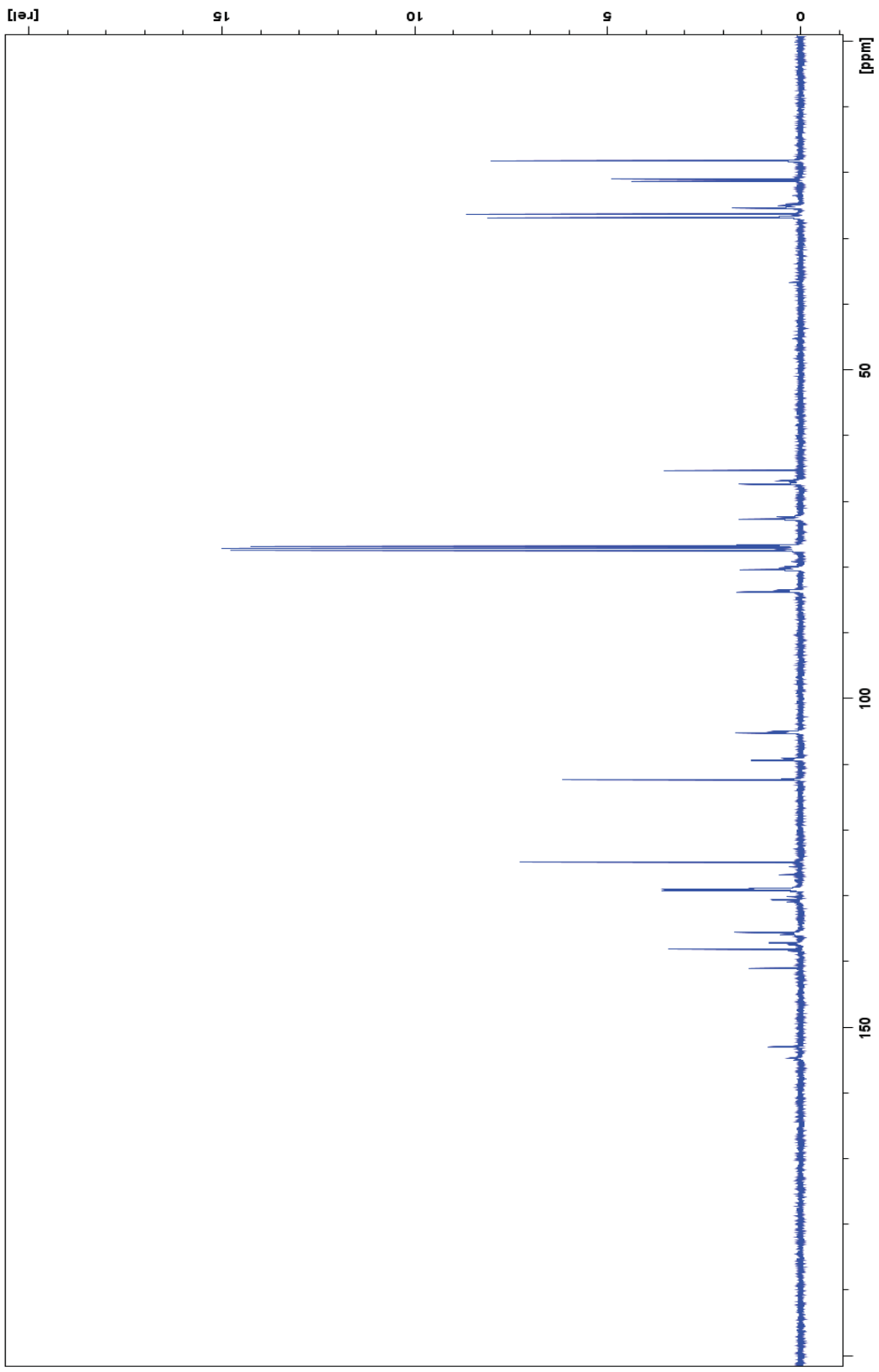

Figure 71: ^{13}C NMR spectrum for compound **27** (crude).

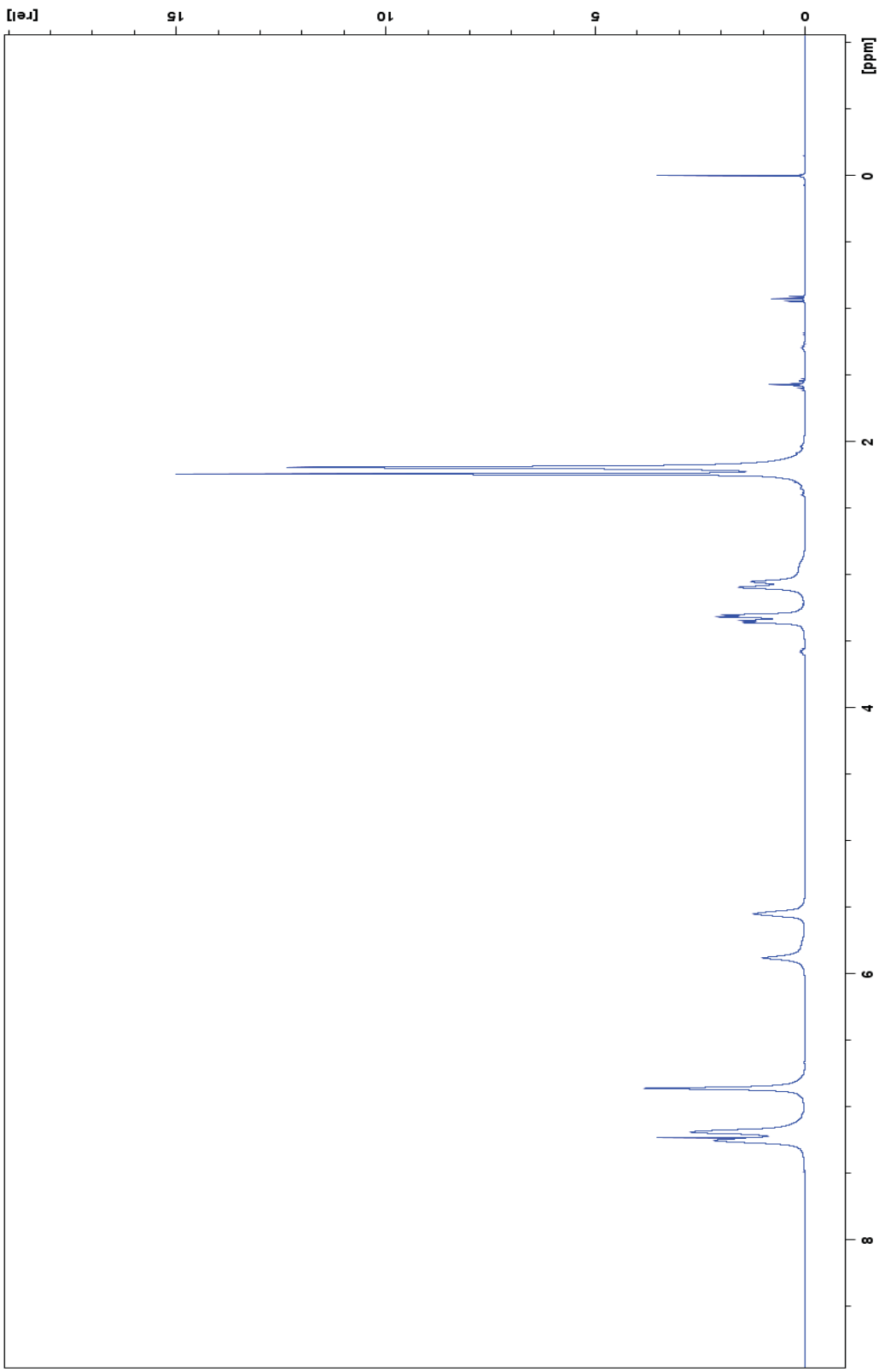

Figure 72: ^{1}H NMR spectrum for compound **28**.

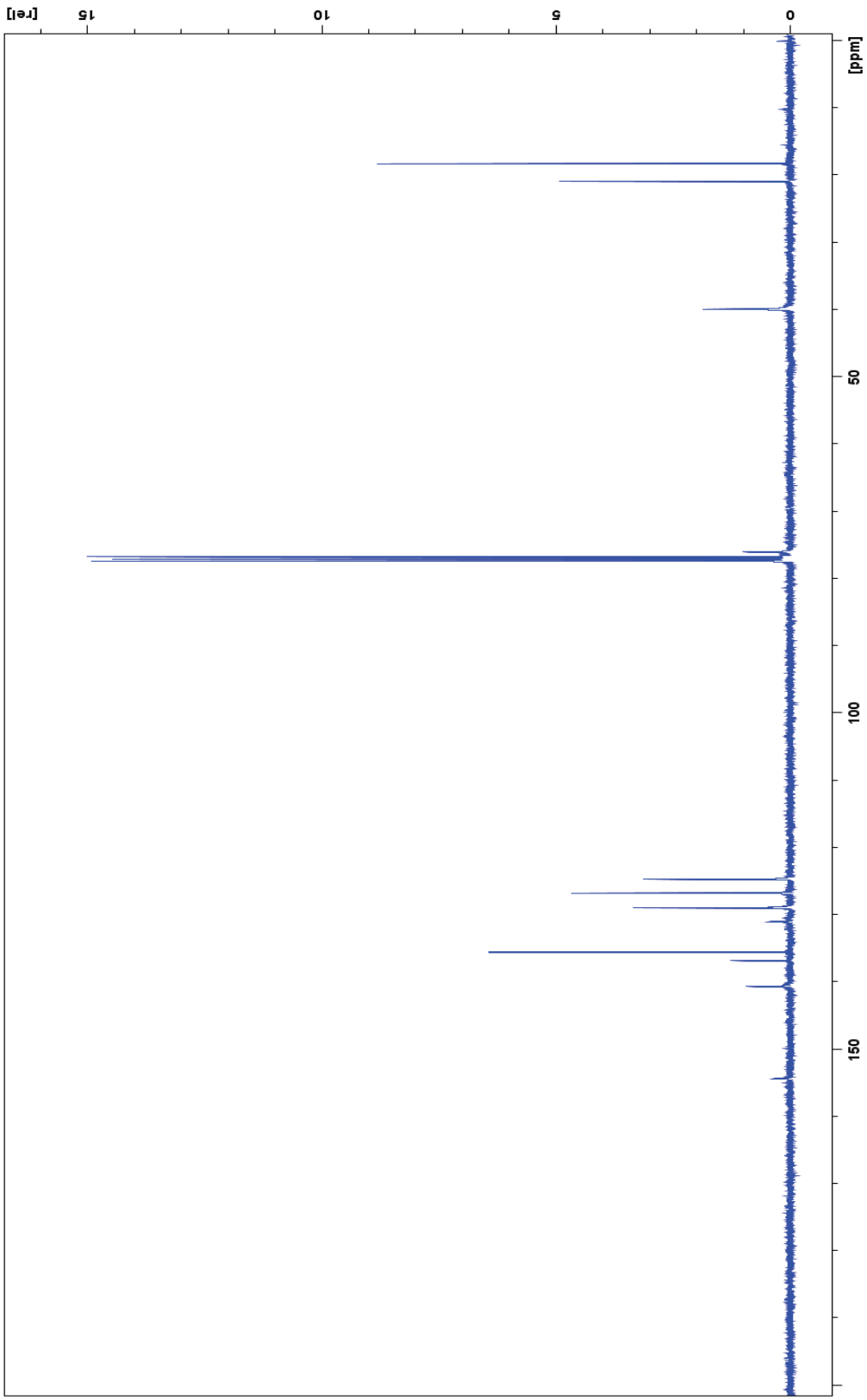

Figure 73: ^{13}C NMR spectrum for compound **28**.

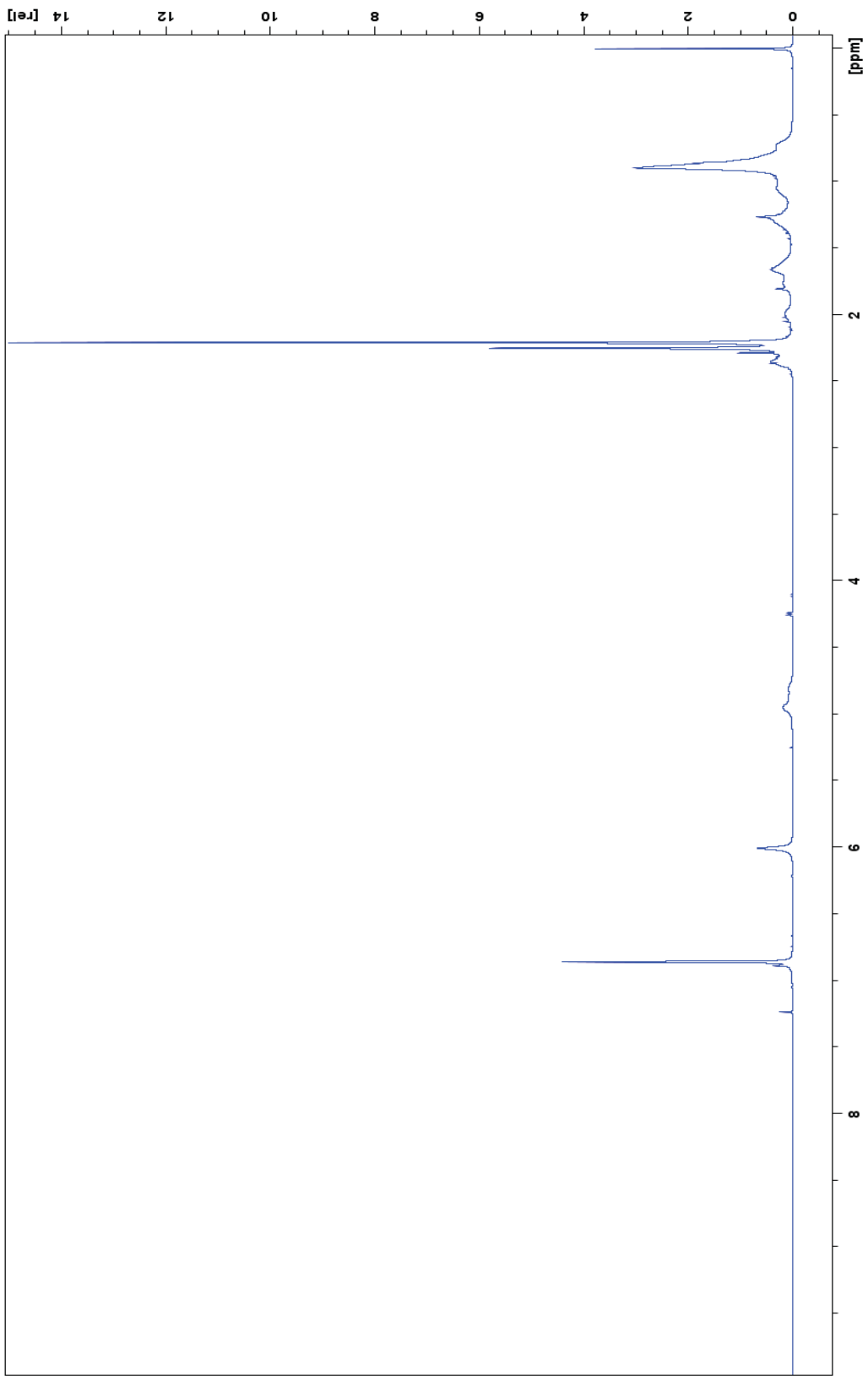

Figure 74: ^{1}H NMR spectrum for compound **29**.

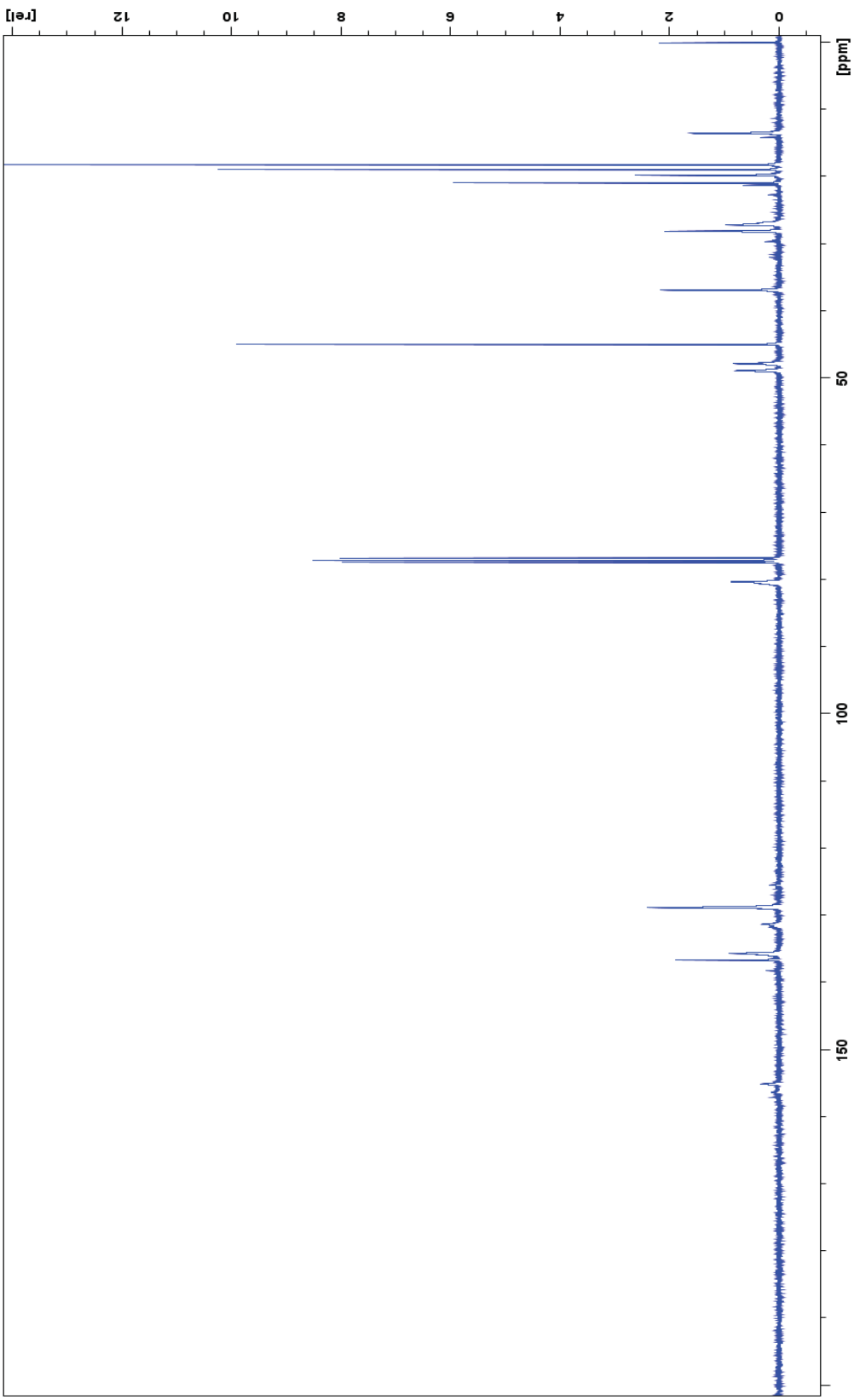

Figure 75: ^{13}C NMR spectrum for compound **29**.

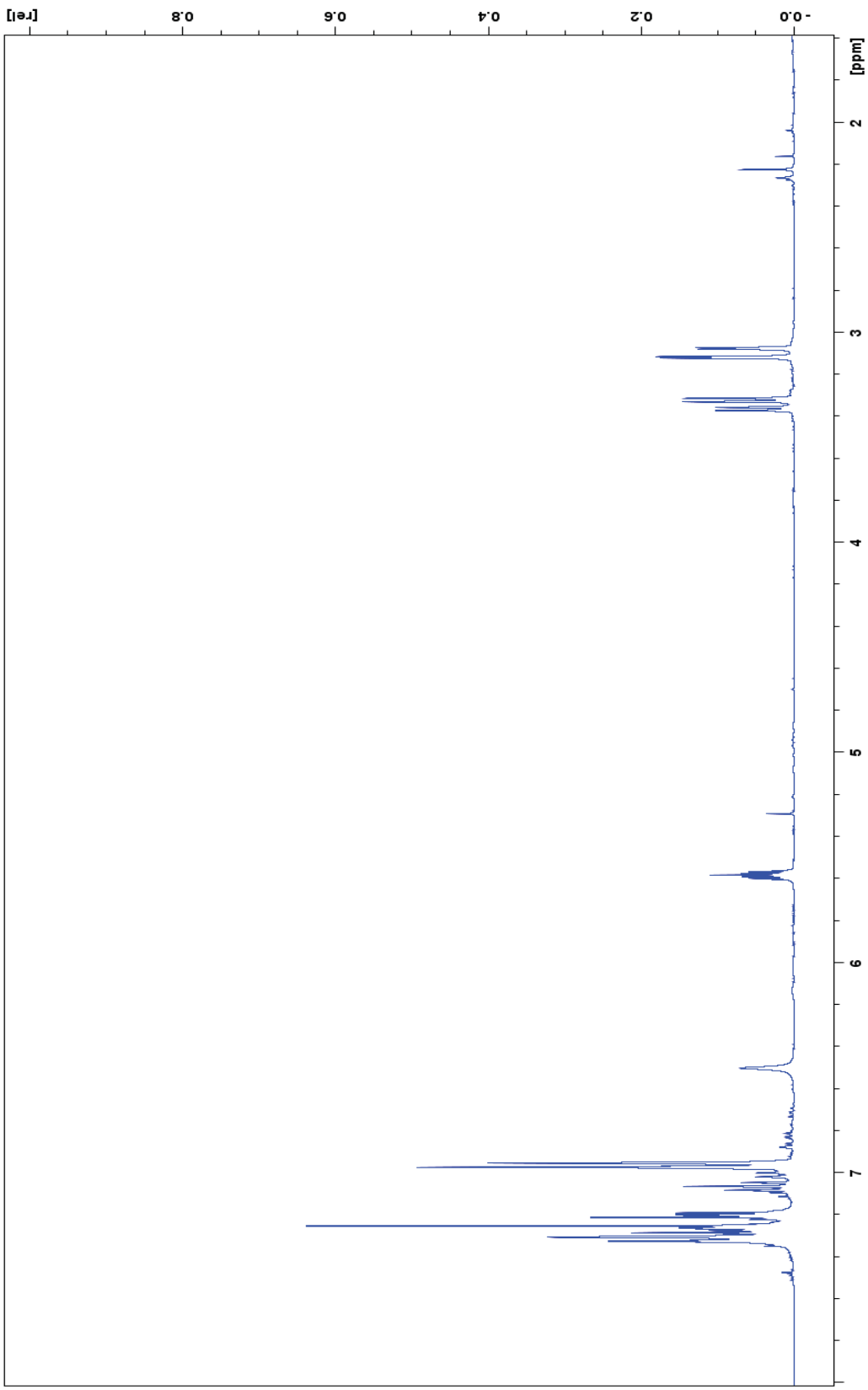

Figure 76: ^{1}H NMR spectrum for compound **30**.

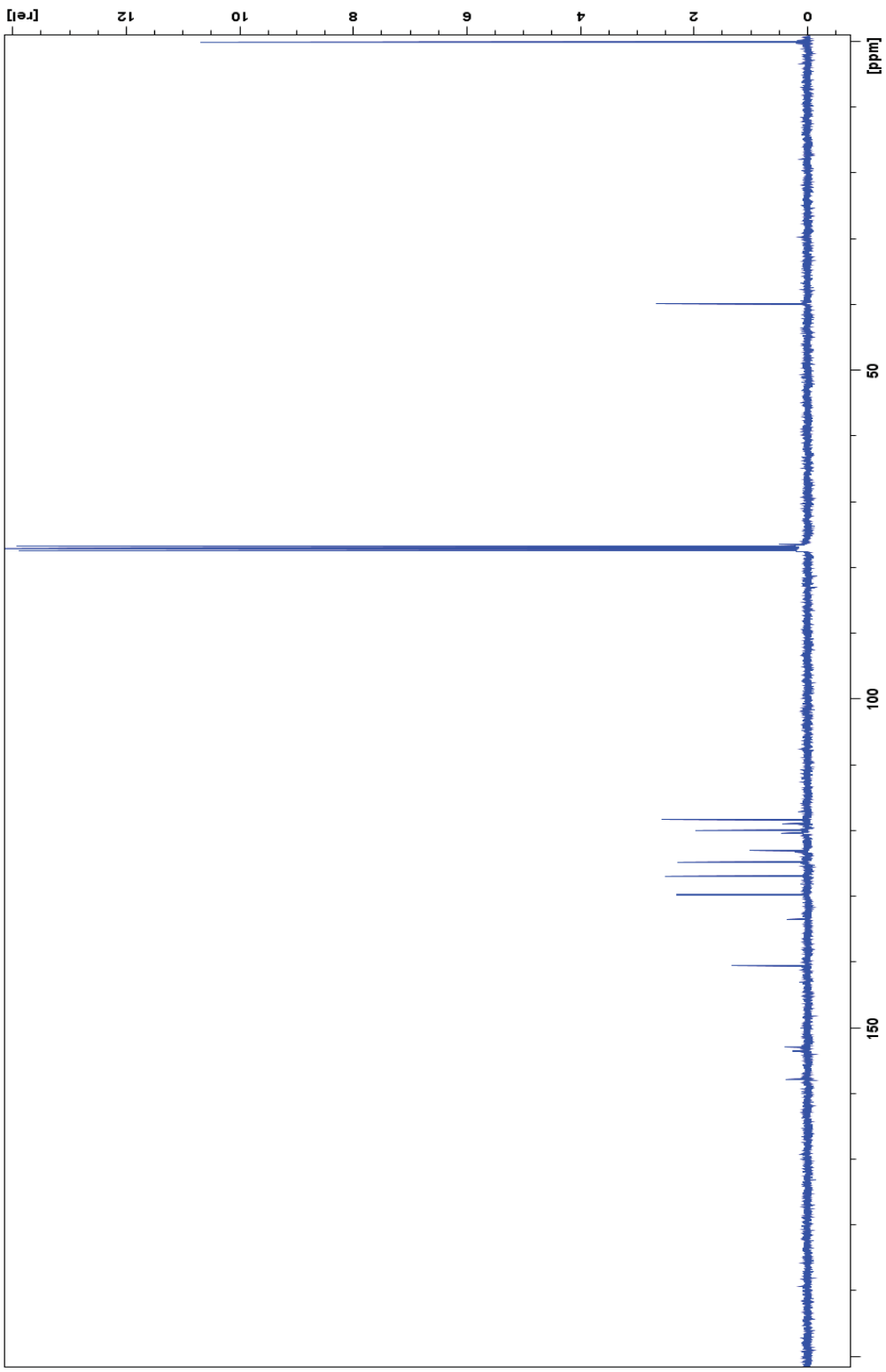

Figure 77: ^{13}C NMR spectrum for compound **30**.

Appendix B

(X-ray Crystallographic Data)

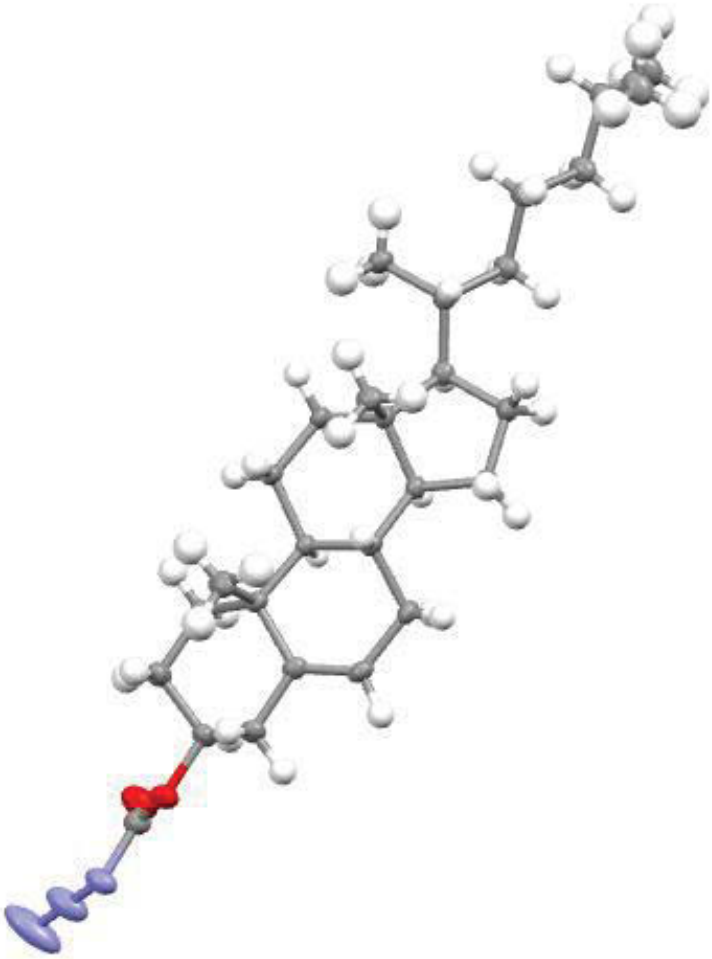

X-ray crystal structure of 10,13-dimethyl-17-(6-methylheptan-2-yl)-2,3,4,7,8,9,10,11,12,13,14,15,16,17-tetradecahydro-1*H*-cyclopenta[a]phenanthren-3-yl carbonazidate (**25**).

Table 1. Experimental details

Crystal data	
Chemical formula	$C_{28}H_{45}N_3O_2$
M_r	455.67
Crystal system, space group	Monoclinic, $P2_1$
Temperature (K)	100
a, *b*, *c* (Å)	10.5157 (17), 7.6584 (12), 16.693 (3)
b (°)	100.659 (7)
V (Å^3)	1321.2 (4)
Z	2
D_x (Mg m^{-3})	1.145
Radiation type	Mo *K*a
No. of reflections for cell measurement	8259
q range (°) for cell measurement	2.9–30.6
m (mm^{-1})	0.07
Crystal shape	Plate
Colour	Colourless
Crystal size (mm)	0.45 × 0.20 × 0.07
Data collection	
Diffractometer	Bruker AXS D8 Quest CMOS diffractometer
Radiation source	I-mu-S microsource X-ray tube

Monochromator	Laterally graded multilayer (Goebel) mirror
Scan method	w and phi scans
Absorption correction	Multi-scan Apex2 v2014.1-1 (Bruker, 2014)
T_{min}, T_{max}	0.532, 0.746
No. of measured, independent and observed [$I > 2s(I)$] reflections	12611, 6078, 4615
R_{int}	0.054
q values (°)	q_{max} = 28.3, q_{min} = 2.1
$(\sin q/l)_{max}$ ($Å^{-1}$)	0.667
Range of *h*, *k*, *l*	*h* = -14-13, *k* = -10-9, *l* = -22®22
Refinement	
Refinement on	F^2
$R[F^2 > 2s(F^2)]$, $wR(F^2)$, *S*	0.059, 0.147, 1.06
No. of reflections	6078
No. of parameters	303
No. of restraints	1
H-atom treatment	H-atom parameters constrained
$\Delta\rho_{max}$, $\Delta\rho_{min}$ (e $Å^{-3}$)	0.27, -0.24
Absolute structure	Flack x determined using 1539 quotients [(I+)-(I-)]/[(I+)+(I-)] (Parsons, Flack and Wagner, Acta Cryst. B69 (2013) 249-259).
Absolute structure parameter	-0.8 (10)

Table 2. Selected geometric parameters (Å)

C1—C6	1.513 (5)	C16—C17	1.574 (4)
C1—C2	1.514 (5)	C16—H16A	0.9900
C1—H1A	0.9900	C16—H16B	0.9900
C1—H1B	0.9900	C17—C20	1.536 (4)
C2—O1	1.476 (4)	C17—H17	1.0000
C2—C3	1.514 (5)	C18—H18A	0.9800
C2—H2	1.0000	C18—H18B	0.9800
C3—C4	1.532 (5)	C18—H18C	0.9800
C3—H3A	0.9900	C19—H19A	0.9800
C3—H3B	0.9900	C19—H19B	0.9800
C4—C5	1.553 (5)	C19—H19C	0.9800
C4—H4A	0.9900	C20—C27	1.538 (5)
C4—H4B	0.9900	C20—C21	1.546 (4)
C5—C6	1.537 (4)	C20—H20	1.0000
C5—C18	1.538 (5)	C21—C22	1.515 (4)
C5—C10	1.549 (4)	C21—H21A	0.9900
C6—C7	1.328 (4)	C21—H21B	0.9900
C7—C8	1.498 (5)	C22—C23	1.522 (5)
C7—H7	0.9500	C22—H22A	0.9900
C8—C9	1.530 (4)	C22—H22B	0.9900
C8—H8A	0.9900	C23—C24	1.529 (5)
C8—H8B	0.9900	C23—H23A	0.9900
C9—C14	1.523 (4)	C23—H23B	0.9900
C9—C10	1.543 (4)	C24—C25	1.514 (5)
C9—H9	1.0000	C24—C26	1.540 (5)
C10—C11	1.542 (4)	C24—H24	1.0000
C10—H10	1.0000	C25—H25A	0.9800
C11—C12	1.537 (5)	C25—H25B	0.9800
C11—H11A	0.9900	C25—H25C	0.9800
C11—H11B	0.9900	C26—H26A	0.9800

C12—C13	1.537 (4)	C26—H26B	0.9800
C12—H12A	0.9900	C26—H26C	0.9800
C12—H12B	0.9900	C27—H27A	0.9800
C13—C14	1.532 (4)	C27—H27B	0.9800
C13—C19	1.540 (5)	C27—H27C	0.9800
C13—C17	1.554 (4)	C28—O2	1.210 (5)
C14—C15	1.523 (4)	C28—O1	1.301 (4)
C14—H14	1.0000	C28—N1	1.440 (5)
C15—C16	1.544 (5)	N1—N2	1.248 (5)
C15—H15A	0.9900	N2—N3	1.130 (6)
C15—H15B	0.9900		

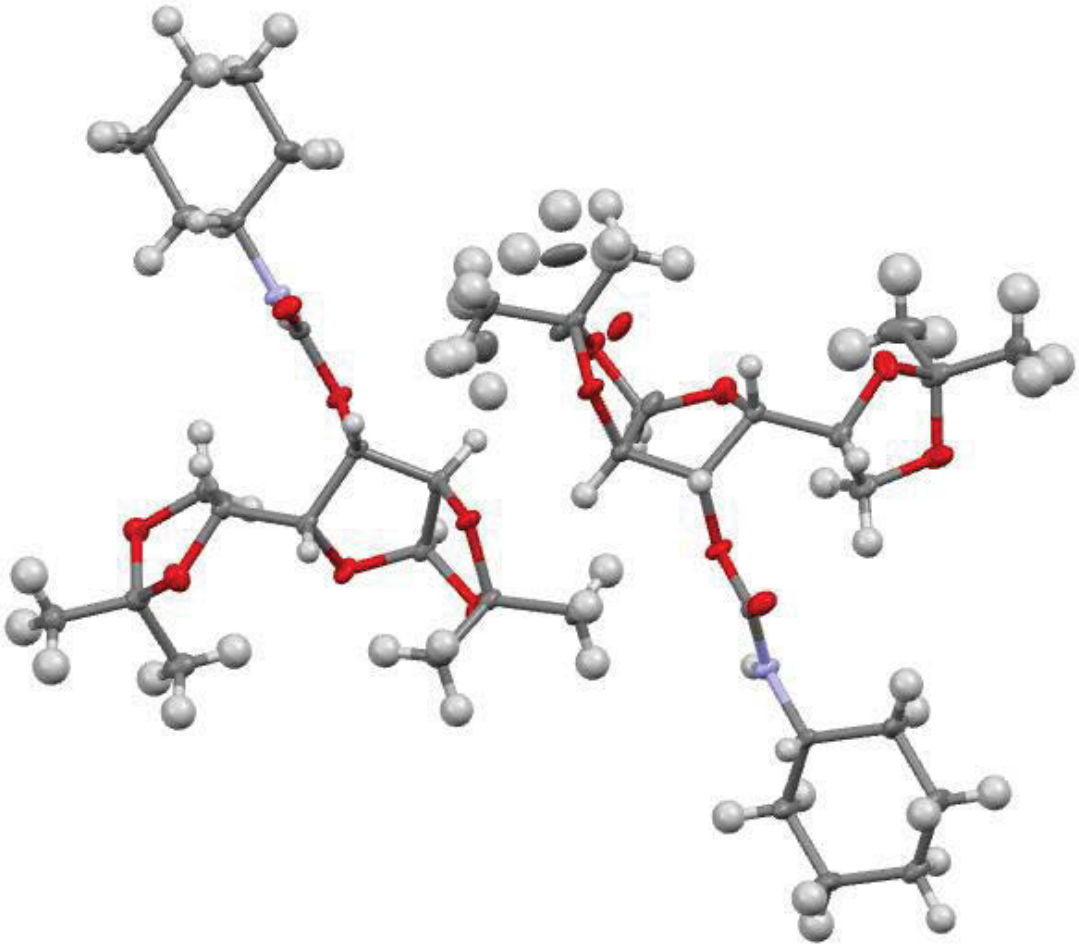

X-ray crystal structure of carbamate (**26**).

Table 1. Experimental details

Crystal data	
Chemical formula	$C_{19}H_{31}NO_7$
M_r	385.45
Crystal system, space group	Monoclinic, *C*2
Temperature (K)	100
a, *b*, *c* (Å)	38.037 (14), 5.285 (2), 22.820 (9)
b (°)	119.504 (5)

V (Å^3)	3992 (3)
Z	8
D_x (Mg m^{-3})	1.283
Radiation type	Mo Ka
No. of reflections for cell measurement	9196
q range (°) for cell measurement	2.5–30.5
m (mm^{-1})	0.10
Crystal shape	Plate
Colour	Colourless
Crystal size (mm)	0.55 × 0.45 × 0.07
Data collection	
Diffractometer	Bruker AXS APEXII CCD diffractometer
Radiation source	fine focus sealed tube
Monochromator	Graphite
Scan method	w and phi scans
Absorption correction	Multi-scan Apex2 v2013.4-1 (Bruker, 2013)
T_{min}, T_{max}	0.644, 0.746
No. of measured, independent and observed [$I > 2s(I)$] reflections	32065, 12059, 10588
R_{int}	0.031
q values (°)	q_{max} = 30.6, q_{min} = 1.8
(sin q/l)$_{max}$ (Å^{-1})	0.716
Range of h, k, l	h = -54-53, k = -7-7, l = -32®32
Refinement	
Refinement on	F^2
$R[F^2 > 2s(F^2)]$, $wR(F^2)$, S	0.044, 0.111, 1.01
No. of reflections	12059
No. of parameters	525

No. of restraints	21
H-atom treatment	H-atom parameters constrained
$\Delta\rho_{max}$, $\Delta\rho_{min}$ (e Å^{-3})	0.41, -0.22
Absolute structure	Flack x determined using 4235 quotients [(I+)-(I-)]/[(I+)+(I-)] (Parsons, Flack and Wagner, Acta Cryst. B69 (2013) 249-259).
Absolute structure parameter	0.2 (3)

Table 2. Selected geometric parameters (Å)

C1B—O2B	1.405 (2)	C3A—H3A	1.0000
C1B—O1B	1.428 (2)	C4A—O1A	1.440 (2)
C1B—C2B	1.527 (3)	C4A—C5A	1.522 (3)
C1B—H1B	1.0000	C4A—H4A	1.0000
C2B—O3B	1.430 (2)	C5A—O5A	1.426 (2)
C2B—C3B	1.524 (2)	C5A—C6A	1.536 (3)
C2B—H2B	1.0000	C5A—H5A	1.0000
C3B—O4B	1.443 (2)	C6A—O6A	1.428 (3)
C3B—C4B	1.528 (2)	C6A—H6AA	0.9900
C3B—H3B	1.0000	C6A—H6AB	0.9900
C4B—O1B	1.443 (2)	C10A—O6A	1.423 (2)
C4B—C5B	1.527 (2)	C10A—O5A	1.436 (2)
C4B—H4B	1.0000	C10A—C11A	1.509 (3)
C5B—O5B	1.433 (2)	C10A—C12A	1.516 (3)
C5B—C6B	1.538 (3)	C11A—H11D	0.9800
C5B—H5B	1.0000	C11A—H11E	0.9800
C6B—O6B	1.427 (2)	C11A—H11F	0.9800
C6B—H6BA	0.9900	C12A—H12D	0.9800
C6B—H6BB	0.9900	C12A—H12E	0.9800
C7B—O2B	1.439 (2)	C12A—H12F	0.9800
C7B—O3B	1.449 (2)	C13A—O7A	1.220 (2)

C7B—C8B	1.513 (3)	C13A—N1A	1.343 (2)
C7B—C9B	1.517 (3)	C13A—O4A	1.370 (2)
C8B—H8BA	0.9800	C14A—N1A	1.463 (2)
C8B—H8BB	0.9800	C14A—C15A	1.518 (3)
C8B—H8BC	0.9800	C14A—C19A	1.518 (3)
C9B—H9BA	0.9800	C14A—H14A	1.0000
C9B—H9BB	0.9800	C15A—C16A	1.532 (3)
C9B—H9BC	0.9800	C15A—H15C	0.9900
C10B—O6B	1.422 (2)	C15A—H15D	0.9900
C10B—O5B	1.436 (2)	C16A—C17A	1.514 (3)
C10B—C12B	1.514 (3)	C16A—H16C	0.9900
C10B—C11B	1.518 (3)	C16A—H16D	0.9900
C11B—H11A	0.9800	C17A—C18A	1.517 (3)
C11B—H11B	0.9800	C17A—H17C	0.9900
C11B—H11C	0.9800	C17A—H17D	0.9900
C12B—H12A	0.9800	C18A—C19A	1.533 (3)
C12B—H12B	0.9800	C18A—H18C	0.9900
C12B—H12C	0.9800	C18A—H18D	0.9900
C13B—O7B	1.219 (2)	C19A—H19C	0.9900
C13B—N1B	1.345 (2)	C19A—H19D	0.9900
C13B—O4B	1.370 (2)	N1A—H1A1	0.8800
C14B—N1B	1.460 (2)	O1A—C1C	1.25 (4)
C14B—C15B	1.524 (2)	O1A—C1A	1.444 (4)
C14B—C19B	1.527 (3)	C1A—O2A	1.401 (3)
C14B—H14B	1.0000	C1A—H1A	1.0000
C15B—C16B	1.537 (3)	O2A—C7A	1.432 (3)
C15B—H15A	0.9900	C7A—O3A	1.446 (3)
C15B—H15B	0.9900	C7A—C8A	1.515 (4)
C16B—C17B	1.526 (3)	C7A—C9A	1.517 (4)
C16B—H16A	0.9900	C8A—H8AA	0.9800
C16B—H16B	0.9900	C8A—H8AB	0.9800
C17B—C18B	1.522 (3)	C8A—H8AC	0.9800

C17B—H17A	0.9900	C9A—H9AA	0.9800
C17B—H17B	0.9900	C9A—H9AB	0.9800
C18B—C19B	1.532 (3)	C9A—H9AC	0.9800
C18B—H18A	0.9900	C1C—O2C	1.44 (2)
C18B—H18B	0.9900	C1C—H1C	1.0000
C19B—H19A	0.9900	O2C—C7C	1.46 (2)
C19B—H19B	0.9900	C7C—O3A	1.50 (2)
N1B—H1B1	0.8800	C7C—C8C	1.50 (2)
C2A—O3A	1.425 (2)	C7C—C9C	1.54 (2)
C2A—C3A	1.526 (2)	C8C—H8C1	0.9800
C2A—C1A	1.527 (4)	C8C—H8C2	0.9800
C2A—C1C	1.56 (2)	C8C—H8C3	0.9800
C2A—H2A	1.0000	C9C—H9C1	0.9800
C3A—O4A	1.442 (2)	C9C—H9C2	0.9800
C3A—C4A	1.526 (3)	C9C—H9C3	0.9800

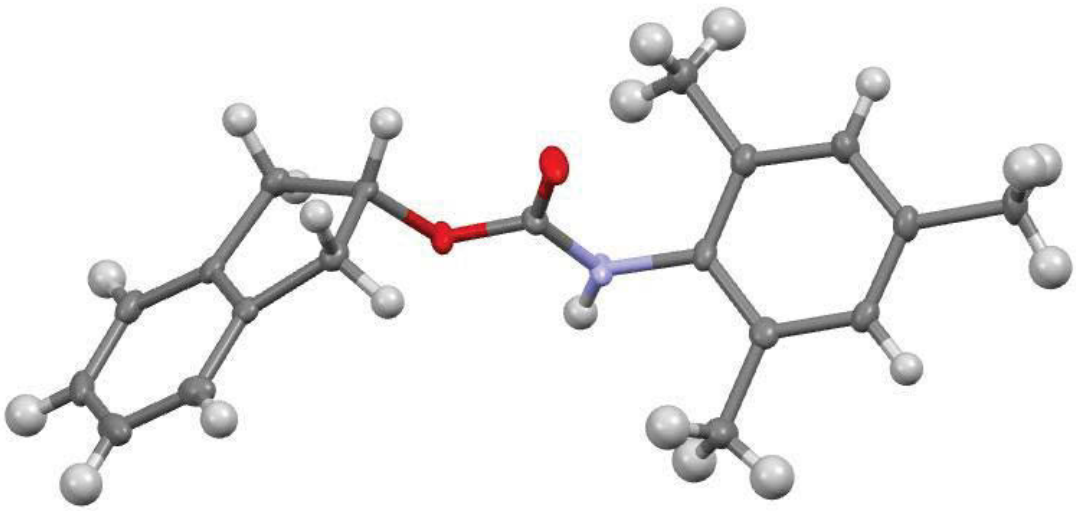

X-ray crystal structure of carbamate (**28**).

Table 1. Experimental details

Crystal data	
Chemical formula	$C_{19}H_{21}NO_2$
M_r	295.37
Crystal system, space group	Monoclinic, $P2_1/n$
Temperature (K)	100
a, b, c (Å)	12.721 (3), 4.751 (1), 26.678 (5)
b (°)	101.40 (3)
V (Å^3)	1580.5 (6)
Z	4
D_x (Mg m^{-3})	1.241
Radiation type	Mo Ka

No. of reflections for cell measurement	6460
q range (°) for cell measurement	3.4–66.5
m (mm^{-1})	0.08
Crystal shape	Plate
Colour	Colourless
Crystal size (mm)	0.14 × 0.11 × 0.05
Data collection	
Diffractometer	Bruker AXS X8 Prospector CCD diffractometer
Radiation source	I-mu-S microsource X-ray tube
Monochromator	Laterally graded multilayer (Goebel) mirror
Scan method	w and phi scans
Absorption correction	Multi-scan TWINABS (Sheldrick, 2012)
T_{min}, T_{max}	0.581, 0.753
No. of measured, independent and observed [$I > 2s(I)$] reflections	13212, 2896, 2802
R_{int}	0.063
q values (°)	q_{max} = 25.0, q_{min} = 1.6
$(\sin q/l)_{max}$ ($Å^{-1}$)	0.595
Range of *h*, *k*, *l*	*h* = -14-14, *k* = 0-5, *l* = 0-31
Refinement	
Refinement on	F^2
$R[F^2 > 2s(F^2)]$, $wR(F^2)$, *S*	0.042, 0.125, 1.13
No. of reflections	2896
No. of parameters	203
No. of restraints	0
H-atom treatment	H-atom parameters constrained
$\Delta\rho_{max}$, $\Delta\rho_{min}$ (e $Å^{-3}$)	0.20, -0.24

Table 2. Selected geometric parameters (Å)

C1—O1	1.461 (2)	C11—C12	1.397 (3)
C1—C2	1.525 (3)	C11—C16	1.404 (3)
C1—C9	1.536 (3)	C11—N1	1.430 (3)
C1—H1	1.0000	C12—C13	1.396 (3)
C2—C3	1.507 (3)	C12—C17	1.503 (3)
C2—H2A	0.9900	C13—C14	1.385 (3)
C2—H2B	0.9900	C13—H13	0.9500
C3—C8	1.388 (3)	C14—C15	1.392 (3)
C3—C4	1.391 (3)	C14—C18	1.513 (3)
C4—C5	1.391 (4)	C15—C16	1.395 (3)
C4—H4	0.9500	C15—H15	0.9500
C5—C6	1.386 (4)	C16—C19	1.499 (3)
C5—H5	0.9500	C17—H17A	0.9800
C6—C7	1.386 (4)	C17—H17B	0.9800
C6—H6	0.9500	C17—H17C	0.9800
C7—C8	1.393 (3)	C18—H18A	0.9800
C7—H7	0.9500	C18—H18B	0.9800
C8—C9	1.504 (3)	C18—H18C	0.9800
C9—H9A	0.9900	C19—H19A	0.9800
C9—H9B	0.9900	C19—H19B	0.9800
C10—O2	1.217 (3)	C19—H19C	0.9800
C10—N1	1.349 (3)	N1—H1A	0.8800
C10—O1	1.354 (2)		

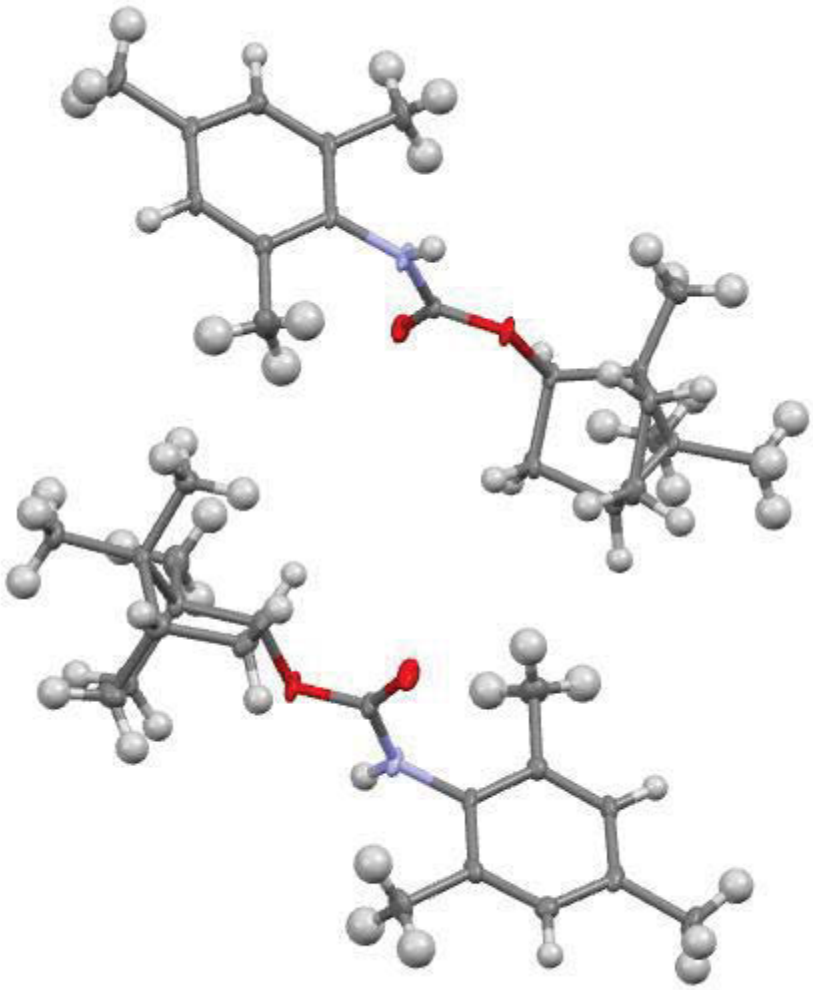

X-ray crystal structure of carbamate (**29**).

Table 1. Experimental details

Crystal data	
Chemical formula	$C_{20}H_{29}NO_2$
M_r	315.44
Crystal system, space group	Monoclinic, $P2_1$
Temperature (K)	100
a, *b*, *c* (Å)	13.2523 (6), 9.9339 (4), 13.9957 (7)

b (°)	94.346 (2)
V (Å^3)	1837.19 (14)
Z	4
D_x (Mg m^{-3})	1.140
Radiation type	Mo Ka
No. of reflections for cell measurement	9393
q range (°) for cell measurement	2.6–30.6
m (mm^{-1})	0.07
Crystal shape	Plate
Colour	Colourless
Crystal size (mm)	0.31 × 0.25 × 0.07
Data collection	
Diffractometer	Bruker AXS D8 Quest CMOS diffractometer
Radiation source	I-mu-S microsource X-ray tube
Monochromator	Laterally graded multilayer (Goebel) mirror
Scan method	w and phi scans
Absorption correction	Multi-scan Apex2 v2014.1-1 (Bruker, 2014)
T_{min}, T_{max}	0.406, 0.746
No. of measured, independent and observed [$I > 2s(I)$] reflections	39790, 8401, 7723
R_{int}	0.082
q values (°)	q_{max} = 27.5, q_{min} = 2.5
(sin q/l)$_{max}$ (Å^{-1})	0.649
Range of h, k, l	h = -17-17, k = -12-12, l = -18-18
Refinement	
Refinement on	F^2
$R[F^2 > 2s(F^2)]$, $wR(F^2)$, S	0.068, 0.177, 1.06
No. of reflections	8401

No. of parameters	427
No. of restraints	1
H-atom treatment	H-atom parameters constrained
$\Delta\rho_{max}$, $\Delta\rho_{min}$ (e Å^{-3})	0.77, -0.46
Absolute structure	Flack x determined using 3395 quotients [(I+)-(I-)]/[(I+)+(I-)] (Parsons, Flack and Wagner, Acta Cryst. B69 (2013) 249-259).
Absolute structure parameter	0.3 (5)

Table 2. Selected geometric parameters (Å)

C1—O1	1.219 (4)	C21—N2	1.348 (3)
C1—N1	1.344 (4)	C21—O4	1.354 (3)
C1—O2	1.361 (3)	C22—O4	1.440 (3)
C2—O2	1.449 (3)	C22—C23	1.532 (4)
C2—C7	1.534 (4)	C22—C27	1.537 (4)
C2—C3	1.544 (4)	C22—H22	1.0000
C2—H2	1.0000	C23—C24	1.547 (4)
C3—C4	1.544 (4)	C23—H23A	0.9900
C3—H3A	0.9900	C23—H23B	0.9900
C3—H3B	0.9900	C24—C25	1.534 (4)
C4—C5	1.543 (5)	C24—C28	1.548 (4)
C4—C8	1.544 (4)	C24—H24	1.0000
C4—H4	1.0000	C25—C26	1.547 (4)
C5—C6	1.549 (5)	C25—H25A	0.9900
C5—H5A	0.9900	C25—H25B	0.9900
C5—H5B	0.9900	C26—C27	1.549 (4)
C6—C7	1.547 (4)	C26—H26A	0.9900
C6—H6A	0.9900	C26—H26B	0.9900
C6—H6B	0.9900	C27—C31	1.520 (4)

C7—C11	1.519 (4)	C27—C28	1.556 (4)
C7—C8	1.567 (4)	C28—C30	1.538 (4)
C8—C10	1.528 (4)	C28—C29	1.538 (4)
C8—C9	1.538 (4)	C29—H29A	0.9800
C9—H9A	0.9800	C29—H29B	0.9800
C9—H9B	0.9800	C29—H29C	0.9800
C9—H9C	0.9800	C30—H30A	0.9800
C10—H10A	0.9800	C30—H30B	0.9800
C10—H10B	0.9800	C30—H30C	0.9800
C10—H10C	0.9800	C31—H31A	0.9800
C11—H11A	0.9800	C31—H31B	0.9800
C11—H11B	0.9800	C31—H31C	0.9800
C11—H11C	0.9800	C32—C37	1.391 (4)
C12—C13	1.389 (4)	C32—C33	1.399 (4)
C12—C17	1.399 (4)	C32—N2	1.440 (3)
C12—N1	1.435 (3)	C33—C34	1.395 (4)
C13—C14	1.395 (4)	C33—C38	1.500 (4)
C13—C18	1.509 (4)	C34—C35	1.383 (4)
C14—C15	1.388 (4)	C34—H34	0.9500
C14—H14	0.9500	C35—C36	1.395 (4)
C15—C16	1.394 (4)	C35—C39	1.508 (4)
C15—C19	1.508 (4)	C36—C37	1.391 (4)
C16—C17	1.393 (4)	C36—H36	0.9500
C16—H16	0.9500	C37—C40	1.512 (4)
C17—C20	1.513 (4)	C38—H38A	0.9800
C18—H18A	0.9800	C38—H38B	0.9800
C18—H18B	0.9800	C38—H38C	0.9800
C18—H18C	0.9800	C39—H39A	0.9800
C19—H19A	0.9800	C39—H39B	0.9800
C19—H19B	0.9800	C39—H39C	0.9800
C19—H19C	0.9800	C40—H40A	0.9800
C20—H20A	0.9800	C40—H40B	0.9800

C20—H20B	0.9800	C40—H40C	0.9800
C20—H20C	0.9800	N1—H1	0.8800
C21—O3	1.211 (4)	N2—H2A	0.8800

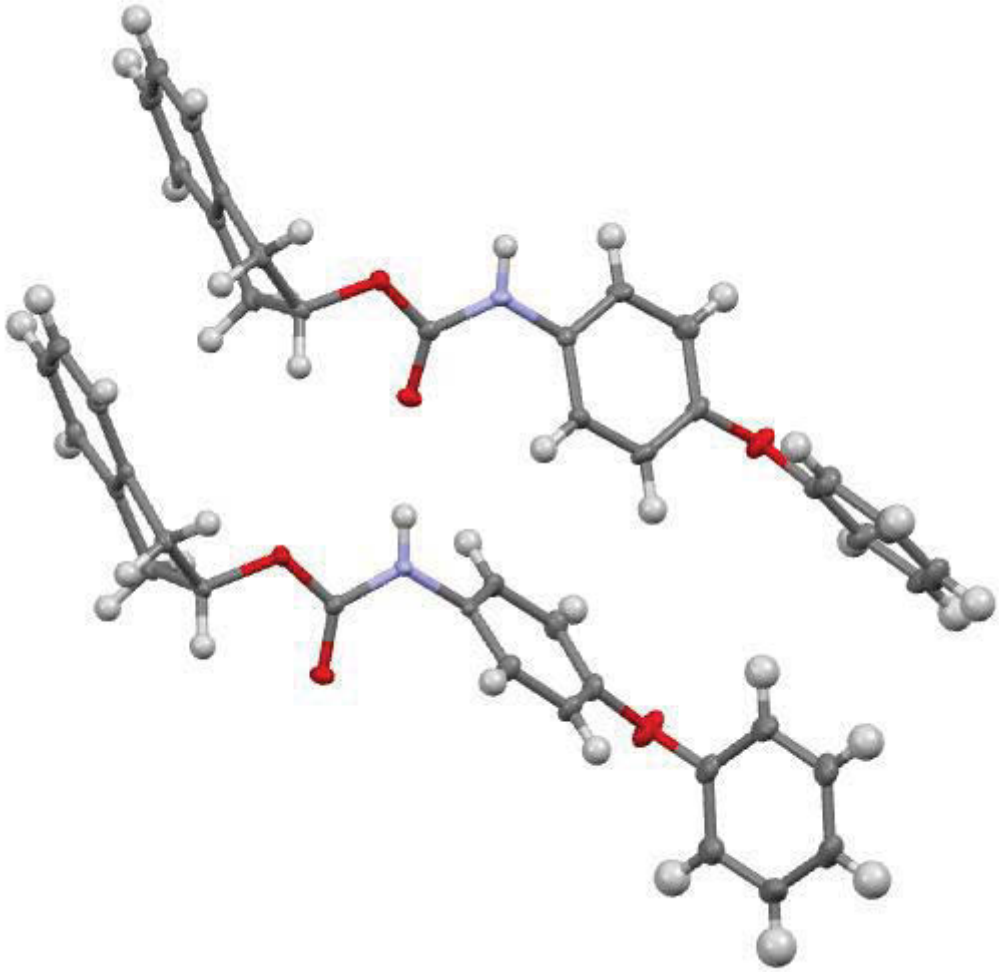

X-ray crystal structure of carbamate (**30**).

Table 1. Experimental details

	Quest15mz206_0m
Crystal data	
Chemical formula	$C_{22}H_{19}NO_3$
M_r	345.38
Crystal system, space group	Monoclinic, $P2_1/c$
Temperature (K)	100

a, *b*, *c* (Å)	9.8522 (7), 36.234 (2), 10.5983 (8)
b (°)	112.079 (3)
V (Å^3)	3506.0 (4)
Z	8
D_x (Mg m^{-3})	1.309
Radiation type	Mo *K*a
No. of reflections for cell measurement	8388
q range (°) for cell measurement	2.4–30.5
m (mm^{-1})	0.09
Crystal shape	Plate
Colour	Colourless
Crystal size (mm)	0.43 × 0.21 × 0.07
Data collection	
Diffractometer	Bruker AXS D8 Quest CMOS diffractometer
Radiation source	I-mu-S microsource X-ray tube
Monochromator	Laterally graded multilayer (Goebel) mirror
Scan method	w and phi scans
Absorption correction	Multi-scan Apex2 v2014.1-1 (Bruker, 2014)
T_{min}, T_{max}	0.409, 0.746
No. of measured, independent and observed [$I > 2s(I)$] reflections	25234, 8520, 6058
R_{int}	0.078
q values (°)	q_{max} = 28.3, q_{min} = 2.3
$(\sin q/l)_{max}$ (Å^{-1})	0.667
Range of *h*, *k*, *l*	*h* = -13-13, *k* = -48-48, *l* = -13-14
Refinement	

Refinement on	F^2
$R[F^2 > 2s(F^2)]$, $wR(F^2)$, S	0.063, 0.143, 1.03
No. of reflections	8520
No. of parameters	475
No. of restraints	2
H-atom treatment	H atoms treated by a mixture of independent and constrained refinement
$\Delta\rho_{max}$, $\Delta\rho_{min}$ (e Å^{-3})	0.36, -0.27

Table 2. Selected geometric parameters (Å)

N1A—C1A	1.346 (2)	N1B—C1B	1.345 (2)
N1A—C11A	1.420 (2)	N1B—C11B	1.435 (2)
N1A—H1A	0.871 (15)	N1B—H1B	0.859 (15)
C1A—O1A	1.225 (2)	C1B—O1B	1.224 (2)
C1A—O2A	1.344 (2)	C1B—O2B	1.344 (2)
C2A—O2A	1.461 (2)	C2B—O2B	1.464 (2)
C2A—C3A	1.530 (2)	C2B—C3B	1.530 (2)
C2A—C10A	1.537 (2)	C2B—C10B	1.533 (3)
C2A—H2A	1.0000	C2B—H2B	1.0000
C3A—C4A	1.516 (3)	C3B—C4B	1.511 (3)
C3A—H3AA	0.9900	C3B—H3BA	0.9900
C3A—H3AB	0.9900	C3B—H3BB	0.9900
O3A—C17A	1.385 (2)	O3B—C14B	1.380 (2)
O3A—C14A	1.393 (2)	O3B—C17B	1.389 (3)
C4A—C5A	1.381 (3)	C4B—C5B	1.386 (3)
C4A—C9A	1.398 (2)	C4B—C9B	1.400 (2)
C5A—C6A	1.394 (3)	C5B—C6B	1.391 (3)
C5A—H5A	0.9500	C5B—H5B	0.9500
C6A—C7A	1.395 (3)	C6B—C7B	1.391 (3)

C6A—H6A	0.9500	C6B—H6B	0.9500
C7A—C8A	1.390 (3)	C7B—C8B	1.390 (3)
C7A—H7A	0.9500	C7B—H7B	0.9500
C8A—C9A	1.392 (3)	C8B—C9B	1.387 (3)
C8A—H8A	0.9500	C8B—H8B	0.9500
C9A—C10A	1.505 (3)	C9B—C10B	1.513 (3)
C10A—H10A	0.9900	C10B—H10C	0.9900
C10A—H10B	0.9900	C10B—H10D	0.9900
C11A—C12A	1.386 (3)	C11B—C16B	1.388 (3)
C11A—C16A	1.399 (3)	C11B—C12B	1.389 (3)
C12A—C13A	1.391 (3)	C12B—C13B	1.389 (3)
C12A—H12A	0.9500	C12B—H12B	0.9500
C13A—C14A	1.386 (3)	C13B—C14B	1.382 (3)
C13A—H13A	0.9500	C13B—H13B	0.9500
C14A—C15A	1.381 (3)	C14B—C15B	1.396 (3)
C15A—C16A	1.384 (3)	C15B—C16B	1.386 (3)
C15A—H15A	0.9500	C15B—H15B	0.9500
C16A—H16A	0.9500	C16B—H16B	0.9500
C17A—C22A	1.382 (3)	C17B—C18B	1.376 (3)
C17A—C18A	1.382 (3)	C17B—C22B	1.379 (3)
C18A—C19A	1.392 (3)	C18B—C19B	1.387 (3)
C18A—H18A	0.9500	C18B—H18B	0.9500
C19A—C20A	1.375 (3)	C19B—C20B	1.375 (4)
C19A—H19A	0.9500	C19B—H19B	0.9500
C20A—C21A	1.380 (3)	C20B—C21B	1.385 (3)
C20A—H20A	0.9500	C20B—H20B	0.9500
C21A—C22A	1.387 (3)	C21B—C22B	1.389 (3)
C21A—H21A	0.9500	C21B—H21B	0.9500

C22A—H22A	0.9500	C22B—H22B	0.9500

Computer programs: Apex2 v2014.1-1 (Bruker, 2014), SAINT V8.34A (Bruker, 2014), SHELXS97 (Sheldrick, 2008), SHELXL2014/7 (Sheldrick, 2014), SHELXLE Rev714 (Hübschle et al., 2011).